United States
Department of
Agriculture

Forest Service

Rocky Mountain
Forest and Range
Experiment Station

Fort Collins,
Colorado 80526

General Technical
Report RM-GTR-288

Analyses of the Temporal Variation of Coarse Bedload Transport and Its Grain Size Distribution
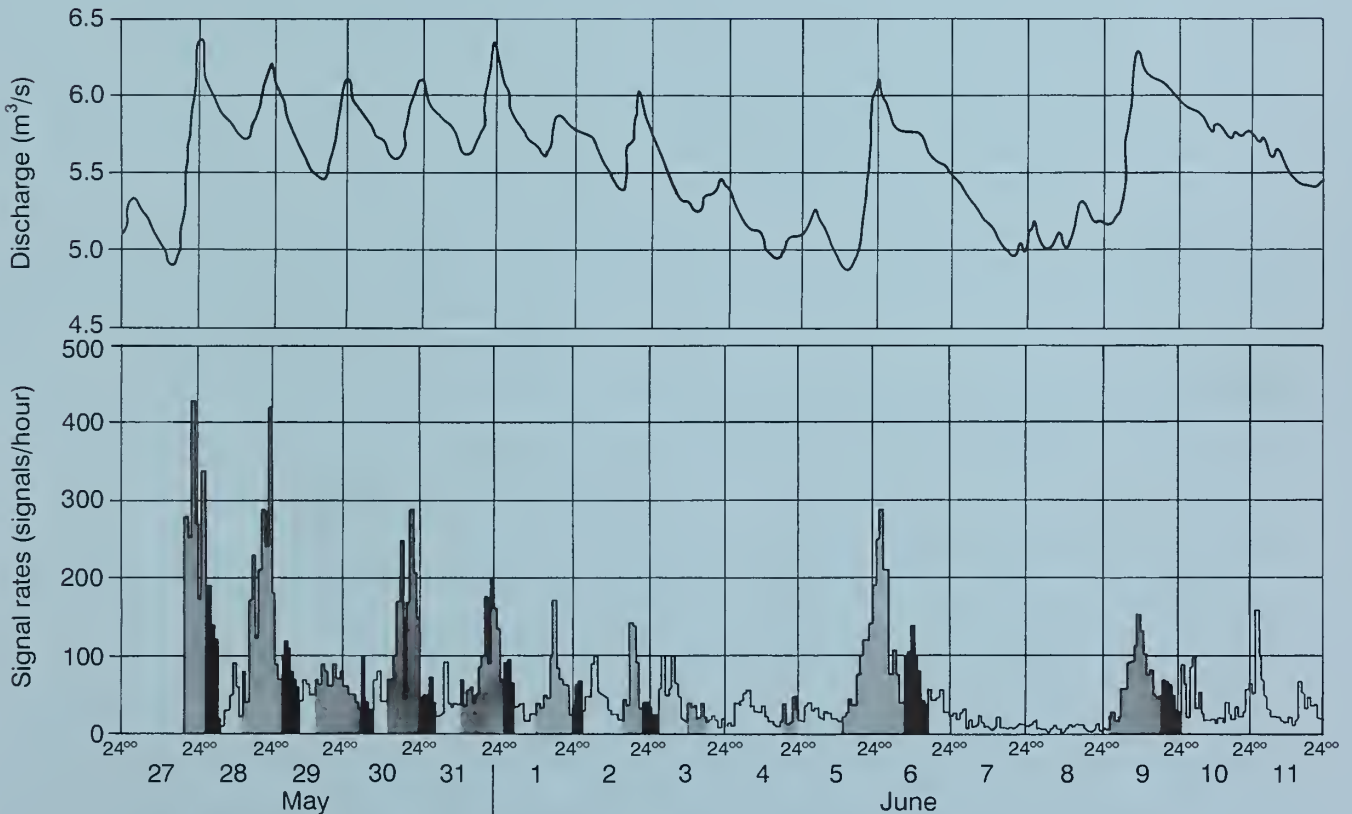
Squaw Creek, Montana, USA

Kristin Bunte

Abstract

A continuous record of coarse material bedload transport was obtained for an entire snowmelt high flow at Squaw Creek, a gravel-bed mountain stream in Montana. The measuring principle, the Magnetic Tracer Technique, makes use of naturally magnetic rocks (andesites) which induce a voltage peak as they pass over a detector log installed across the channel bottom. Signal rates were counted for 1-hour and 5-minute intervals and yielded a 17-day and a 3-day time series. Bedload transport exhibits recurring wave patterns and disintegrates into fluctuating and pulsating transport features as the temporal resolution is increased. The wide scatter in the relationship between bedload transport and discharge indicates that other parameters than flow affect bedload transport as well.

Series of bedload samples were taken during nightly flood waves with a large net-sampler. Its wide (0.3 m by 1.55 m) opening could representatively sample all coarse particles, but the 1 cm mesh width let all smaller particles pass. Bedload transport rates varied with time and grain-size distributions were either wide and symmetrical, or narrow and skewed due to truncation of the coarse, or the fine part. Particle transport rates proved to be a better means of grain-size analysis for these gravel samples than standard procedures of grain-size analyses.

Water surface slope was measured over a riffle area between two points 17.3 m apart. The temporal variation of water surface slope during nightly flood waves seems to indicate the dislocation of bedload on the channel bottom. Together with information regarding the change of the channel bottom micro topography, velocity profiles, and bedload transport, a conceptual model was derived that explains temporally variable amounts and grain-size compositions of gravel transport.

Combining results from various approaches of this study, bedload transport could be explained as adjustment processes between the sedimentary conditions of the river bed and the hydraulics of flow. Given the conditions of ordinary snowmelt high flows which are typically supply-limited, bedload waves cannot result from migrating bedload sheets at Squaw Creek. Grain-size spectra that coarsen and widen with flow during typical snowmelt discharges indicate that bedload transport occurs size-selective. Equal mobility would only be reached during enormous events at Squaw Creek.

Analyses of the Temporal Variation of Coarse Bedload Transport and Its Grain Size Distribution

Squaw Creek, Montana, USA

Kristin Bunte, Fluvial Geomorphologist[1]

Freie Universetät Berlin

[1] *Presently, Research Associate, Colorado State University, Department of Civil Engineering, Engineering Research Center, Fort Collins, Colorado.*

Contents

Preface

This study is based on the research project "Magnetic Pebbles" provided to Professor Ergenzinger by the German Research Council.[1] I have been employed in this project as a research assistant from summer of 1985 until spring of 1988. The aims of the project were the further development of the magnetic tracer technique, its application to field measurements of bedload transport, and the investigation of bedload transport. Field work was carried out during snowmelt high flows in 1986 and 1987 at Squaw Creek in Montana (USA). After funding had stopped in the spring of 1988, field work in 1988 and 1989 was continued with the help and support of friends.

The hydrological and petrological conditions of the Squaw Creek watershed were the most important factors for choosing the measuring site. Snowmelt high flows that can move coarse bed material occur between mid May and late June with a recurrence interval of 1.5 years. The other reason stems from the geology of the catchment: 2/3 of the watershed are underlain by andesite that contains magnetite. These rocks can serve as natural tracers and are appropriate to aid the further development of a measuring technique for coarse bedload thought out and implemented by Ergenzinger (1982), Ergenzinger and Conrady (1983), and Ergenzinger and Custer (1982, 1983).

Last, but not least, good conditions for install-ing a measuring site and its easy accessibility as well as the friendly support of the project by institutes and persons in Montana played an important role in selecting the measurement site. Studies of pebble and cobble bedload transport have been carried out at Squaw Creek, with varying intensity, since 1981.

In the beginning of this study there was no particular path leading to a distant goal. Some results came up without ever having searched for them. Many results grew from a steady but open-minded pursuit and some results for which I searched I never found.

Much of this study was determined by factual circumstances. Apart from financial limitations, the continuation of my work depended on whether a sufficiently large high flow would occur and whether I would find people who would help me with field work that would get tough at times. It was not possible to measure all desirable data. Instruments broke down during the nightly measuring campaigns in a roaring Squaw Creek, or the measurements simply exceeded human strength. These factualities lead to some limitations in this study. However, having the opportunity to work at a mountain stream in Montana (USA) for several years made it possible to learn from previous results and keep final goals flexible. It also gave me the opportunity to get to know a beautiful land and its lovely people.

---

[1] *Deutsche Forschungsgemeinschaft, DFG.*

Acknowledgments

Preface to the English Translation

This text is a translation of a doctoral thesis that was prepared under the guidance of Professor Peter Ergenzinger and submitted in partial fulfillment of the requirements of a doctoral degree at the Freie Universität Berlin in January 1991. Prof. H. Ibbeken from the Department of Geology at the Freie Universität Berlin was the second graduate advisory professor. The field work for this thesis was carried out at Squaw Creek, a mountain stream in Montana, in cooperation with Professor Steve G. Custer from Montana State University in Bozeman.

I would like to express my thanks to the U.S. Forest Service Rocky Mountain Forest and Range Experiment Station, Stream Systems Technology Center in Fort Collins who gave me the opportunity to translate my doctoral thesis, which was originally written in German, into English. Having an English version of my dissertation allows me to reach a much wider audience. I hope that the reader in the United States will find information in this thesis that is useful to the study of current issues of bedload transport phenomena in this country.

Most of this thesis was originally written in 1989 and 1990. Literature published after 1990 has only been incorporated when I had a prepublished manuscript. The English translation follows basically the original text. Any substantial additions to the text or comments hereof are given in footnotes or are identified as additions. Research activities that went on at Squaw Creek after 1989 (1990-1992) are referenced at the respective locations in the text as footnotes. Literature cited in footnotes is included in the list of references.

I would like to inform the reader that the concern about cumulative watershed effects (with respect to coarse sediment) following forestry management in mountainous areas, had until 1990 not become a concern in Germany. Temperate climatic conditions, generally smaller forested areas than in the U.S., frequent small-scale logging operations with light equipment, a 300-year tradition in forest management, long-lasting and maintained logging roads, localized harvest rotations, and single tree harvest ("Plentern") have helped to prevent severe present-day sedimentary effects in the stream systems.

Severe sedimentary cumulative watershed effects will certainly have occurred after initial logging of vast areas in Central Europe during Medieval times. The thicknesses of colluvial deposits that date back to Medieval times are often reported to reach 10 m, while several meters of fine sediment is usually deposited on the floodplains of small and large streams as "Auelehm." However, both the colluvial and alluvial material is usually fine grained (sand and smaller) and has become an integral part of the present day landscape.

Present day sedimentary problems occur in some steep alpine mountain torrents where slopes have been destabilized by construction relating to ski-tourism or modern trans-alpine highways. These sedimentary problems in the creeks are often controlled by check dams that are excavated when filled. The erosional problems directly on the impacted slopes (ski-runs, trails, etc.) are usually more difficult to control.

However, cumulative sedimentary effects may soon become an issue in German forestry, since more and more trees—and even entire forests—are dying from environmental pollution (acid rain-related impacts and tree diseases). This requires felling of the diseased trees or, in severe cases, clear-cutting of a heavily impacted stand—in order to fight pests (pine beetles, etc.) that invade the dying and dead trees and spread to still healthy stands. This problem is especially prominent on westerly facing slopes in the German Central Mountains. Reforestation problems occur where former forests had established in regions close to the ecological altitude border of forests. If the forest dying cannot be controlled, major deforestation will occur, followed by many of the consequences observable in other deforested parts of the world.

—Ft. Collins, August 1994

iii

List of Notations, Abbreviations, and Units

A	cross-sectional area	m²
Cs	suspended bedload concentration	g/l, kg/m³
C	Chezy roughness coefficient ($v/(R{\cdot}S)^{1/2}$)	m$^{1/2}$/s
d	flow depth	m
D	grain size	mm
D_x	xth percentile of the cumulative grain-size distribution	mm
f	Darcy-Weisbach friction factor ($8g{\cdot}R{\cdot}S/v^2$)	-
F	resulting force	kg/m·s²; N/m²
F_D	drag force	kg/m·s²; N/m²
F_F	force of friction	kg/m·s²; N/m²
F_L	lift force	kg/m·s²; N/m²
F_W	gravity	kg/m·s²; N/m²
Fr	Froude number ($v/(g{\cdot}d)^{1/2}$)	-
Fr^*	grain Froude number ($v^{*2}/g{\cdot}D$), equal to Shields mobility number θ	-
g	acceleration due to gravity = 9.81	m/s²
$k3$	the larger of the two differences of three neighboring depths readings	m
n	Manning's roughness coefficient ($(R^{2/3}{\cdot}S^{1/2})/v$)	m$^{-1/3}$/s
Q	water discharge ($v{\cdot}d{\cdot}w$)	m³/s
Q_{crit}	water discharge at the initiation of bedload motion	m³/s
q	unit discharge (Q/w)	m²/s
Qb	bedload transport rate	kg/m·s
r^2	correlation coefficient	-
R	hydraulic radius (A/U)	m
Re	Reynolds number ($d{\cdot}v/v$)	-
Re^*	grain Reynolds number ($D{\cdot}v^*/v$)	-
S	stream gradient	m/m
S_w	water surface slope	m/m
t	time	s; hr; d; a
U	wetted perimeter	m
v	flow velocity	m/s
v_{crit}	flow velocity at the initiation of bedload motion	m/s
v^*	shear velocity ($\tau_o/\rho)^{1/2}$	m/s
w	flow width	m
x, y	variables	*any unit*

α	angle of inclination	°
β	pivot angle	°
δ	increment	-
ε	eddy viscosity	-
ϕ	grain-size unit = $-\log_2 D$ (mm) = $-3.322 \log_{10} D$ (mm)	-
ϕ_x	xth percentile of the cumulative grain-size distribution in ϕ-units	-
η	dynamic viscosity	N·s/m²
v	kinematic viscosity (η/ρ)	m²/s
θ	Shields mobility number ($\tau_o/\rho_s-\rho_w){\cdot}g{\cdot}D$) = dimensionless shear stress = grain Froude number	-
ρ_s	density of sediment	kg/m³
ρ_w	density of water	kg/m³

τ_o	shear stress $(\rho \cdot g \cdot d \cdot S)$ or $(\delta v / \delta d \cdot (\eta + \varepsilon))$		kg/m·s²; N/m²
τ_{crit}	shear stress at the initiation of bedload motion		kg/m·s²; N/m²
τ_o'	grain shear stress		kg/m·s²; N/m²
τ_o''	form shear stress $(\tau_o - \tau_o')$		kg/m·s²; N/m²
Ω	stream power $(Q \cdot \rho \cdot S_w)$		kg/m·s
Ω_{crit}	stream power at the initiation of bedload motion		kg/m·s
ω	unit stream power $(Q/w \cdot \rho \cdot S_w)$		kg/s

Metric Units and Time

g	gram	= 0.001 kg	= 0.0353 ounces
kg	**kilogram**	**= 1,000 g**	**= 2.205 pounds**
t	metric tonne	= 1,000 kg	= 1.103 tons
mm	millimeter	= 0.001 m	= 0.0394 inches
cm	centimeter	= 0.01 m	= 0.394 inches
m	**meter**	**= 3.281 feet**	**= 1.094 yards**
km	kilometer	= 1,000 m	= 0.621 miles
m²	square meter	= 10.764 ft².	= 1.197 square yard
ha	hectare	= 10,000 m²	= 2.471 acres
km²	square km	= 100 ha	= 0.386 square miles
l	liter	= 0.001 m³	= 0.0353 cubic feet
m³	cubic meter	= 1,000 l	= 35.316 cubic feet

s	**second**
min	minute
hr	hour

°C	degree Celsius	= °F·(9/5)+32

1. Introduction

This study investigates several aspects of coarse bedload transport at a Rocky Mountain stream.

Before actual analyses and results are presented, the term "coarse bedload transport" needs to be clarified. Also, it will be demonstrated how the stream carrying coarse bedload have been impacted by man's activities, and it will be explained why it is important to investigate coarse bedload transport. Finally, the introduction will provide a short review of past and present research of bedload transport and point to future tasks in bedload research.

1.1 Explanation of "Coarse Bedload Transport"

Creeks and streams leaving watersheds through the valley systems transport solid materials out of mountain areas. This fluvially transported solid material is distinguished with respect to their modes of transport into suspended transport (transport of suspended matter) and bedload. Bedload is that part of the solid matter load that is transported in direct and indirect contact with the channel bed. Regarding the mode of transport and the frequency of contact with the stream bottom, transport can occur as rolling, sliding, and saltation. Strictly speaking, none of these transport modes is associated with, or confined to, a particular particle size. During small flows only the smallest particles move by rolling or sliding, while during large flows or at waterfalls even the largest boulders can be transported in suspension. Nevertheless, it seems reasonable to differentiate bedload transport according to its grain sizes into

sand transport (which can frequently change its mode of transport) and coarse bedload transport. Due to the limited effects of grain-to-grain interactions, the transport of sand in sand bedded streams is much more hydraulically controlled and predictable from flow hydraulics than bedload transport rates in streams that carry coarse sediment. These streams often exhibit broad grain-size distributions ranging from sand to boulders. Coarse bedload transport refers to the fluvial transport of particles in the range of larger than 2 mm up to boulders that experience frequent contact with other particles on the channel bottom. In contrast to sand transport, which can already be initiated during ordinary, frequently occurring stream flows, coarse bedload transport usually is limited to high flow situations, which occur less frequently.

1.2 Multiple Use of Coarse Bedload Streams

Coarse gravel-bed rivers and their riparian areas have been affected by human impacts for centuries. The impacts of hydraulic engineering can be summarized in these main points:
- regulating stream discharge,
- channelization of streams in their long- and cross-sectional profiles,
- sediment depletion from gravel mining and,
- sediment addition from anthropogenic debris dumping,
- stream aggradation following agricultural, silvicultural [1], recreational, and constructional impacts

Agriculture, vehicle traffic, housing developments, and construction extend into riparian

---

[1] Stream aggradation due to increased sediment yields following roading and logging is not a major issue of concern in Germany. Forestry roads have been put in many decades or even centuries ago. Clear-cutting of old growth forest started about 1,000 years ago with the widespread onset of agriculture in central Europe and reached its largest areal extent in late Medieval and Renaissance times (15th to 16th century). Following the 30-year war (1618-1648) and the great European plague, declined populations allowed forested areas to grow back again. Having experienced poor agricultural performance in the mountainous areas of the German Central Mountains (geologically old mountainous areas reaching up to about 1500m), agriculture retreated to more productive, lower, and less steep areas, while cultivated forests took its place in the higher parts of the watersheds.

Increased sediment yield in mountain torrents due to roading, clear-cutting, and tourist uses is controlled by a multitude of artificial check dams which, if possible, are emptied when filled. Sedimentary cumulative watershed effects due to forestry management in mountainous areas are therefore not a major concern in Germany. However, catastrophic floods can occur, destroying check dams and depositing large amounts of sediments in the stream beds (Schmidt 1994). This is viewed as a one-time catastrophe. The river bed is put back in place with bulldozers if access along the valley is needed.

Since logging in mountainous areas occurs only once or twice per century and seems to be restricted to parts of a watershed only, and also because logging roads are already in place, less sediment might be generated by silvicultural activities in mountainous areas in Germany than during large-scale first-time old-growth logging in the Pacific Northwest. The largest impacts of forestry management on sediment budgets probably already happened during Medieval settlement many centuries ago and are by now indistinctly overgrown and incorporated into the present landscape as ordinary features. Besides, fishing in mountain streams is not as popular in Germany as it is in the U.S. Therefore, there is less environmental concern about the destruction of fish habitat in mountain streams due to the effects of silvicultural activities .

areas. To maintain and guarantee the undisturbed usage of near-stream areas, stream banks are covered with rip rap, in order to decrease channel migration.

Rip rap, check dams, river dams, and weirs are installed in order to decrease the kinetic energy of flow or to transform this energy into usable energy, respectively. The aim of flow energy reduction is to prevent or minimize bedload movement and to keep the stream confined to its actual bed or its designed channel. The flow regime is altered in many watersheds. For example, water is diverted in mountain streams to increase reservoir storage volumes in other catchments for use in irrigation. Reservoirs and dams are used for discharge control and hydroelectric purposes. They are expected to maintain their reservoir functions as long as possible. Therefore, sediment transport is reduced. Water discharge is maintained at relatively even levels, which discourages coarse bedload transport. Streams are depleted of coarse sediment downstream of reservoirs. Last but not least, sediment transport is disturbed by taking gravel out of the streams (gravel mining, navigational dredging) or by disposing of debris by dumping.

Watersheds are no longer natural, but they are impacted in various ways. Various forms of agriculture, local clear-cutting, the dying of entire forests due to environmental pollution, and tourist uses (especially ski areas) lead to areal and linear erosion of fine and coarse sediments, which then get into the stream system.

These watershed impacts often severely disturb the water and sediment budget (Karl et al. 1975; Chang 1987; Knighton 1989; Macklin 1989). Streams respond to these sedimentary and hydraulic changes with cross-sectional and longitudinal changes. Trying to reestablish its energy budget, the stream changes its course, and its bottom grain size (Lewin 1976) incises or deposits sediments (Gölz and Dröge 1989; Scheurmann 1989; Gölz 1990). These stream responses occur both in anthropogenically altered reaches as well as in more or less natural reaches.

Many fish species need a habitat that comprises a variety of stream conditions to find food and shelter (open gravel, aerated water over steps and riffles, pools with various flow velocities in close proximity, shaded banks, boulders, logs, overhanging banks, etc.). Analysis is reduced to determine how the habitat of insects, worms, and fry that live in interstitial spaces are affected by an impaired sediment budget (Ohde et al. 1990; Rehfeld 1990) and especially by channel erosion and stream bed siltation (Milhous 1982; Carling and Hurley 1987). Decision-making agencies as well as the operational units of agencies associated with hydraulic engineering, ecology, biology, fluvial geomorphology, and sedimentology need to understand the development and processes of a fluvial landscape and incorporate the results of bedload transport research into their work.

There is much interest regarding the usage of coarse gravel streams. It is generally expected that streams at all times and in all locations, regardless of natural events of anthropogenic impacts, "behave well". Measures of hydraulic engineering only partially succeeded in satisfying these expectations (Geiger 1989; Karl 1989), because river training measures often lead to an ugly alteration of the stream to an average profile that streams try to adjust or modify during extreme events. Neither hydraulic engineering nor the subject of earth sciences has acquired a sufficiently detailed and comprehensive knowledge of the various processes and interactions occurring in bedload transport: "Until presently there are no sufficiently exact hydrologic and hydraulic calculation of high flows and sediment transport events including debris flows, so that with respect to safety construction work is designed conservatively. This might seem barbaric to those who are environmentally conscious, at least as long as they are not themselves affected by a high flow in a mountain torrent"[2] (Karl 1989: 465).

Human handling of the stream system needs to be done more considerately and carried out with more care regarding the natural equilibrium of the stream system. Some of the recent literature heads in this direction and attempts to apply "river bed stabilization"[3] (Gölz and Dröge 1989) and "integral watershed improvement"[4] (Karl 1989). The larger the impacts and the diversity of

---

[2] Translation of the German citation "So entziehen sich Hochwasserereignisse und Feststofftransporte bis hin zu Muren bis heute ausreichend genauer hydrologischer und hydraulischer Berechnungen, so daß schon aus Sicherheitsgründen die Bauwerke großzügig bemessen werden, wenn auch dies manchem Naturfreund als Barbarei erscheinen mag, zumindest er sich nicht selbst in der Lage eines von einem Wildbachhochwasser Betroffenen befindet."

[3] Translation of the German citation "Sohlstabilisierung"

watershed and stream system uses, the more responsibly water and sediment budgets have to be treated.

1.3 Development of Coarse Bedload Transport Research

Researchers in central Europe started to measure bedload transport using bedload samplers in the 1930's at the Danube (Ehrenberger 1931) and at the Inn (Mühlhofer 1933). Although both researchers already noted that bedload transport is temporally and spatially variable, this aspect of bedload transport was not addressed again until the 1970's. Most of the earlier research interests were focused on river usage and river training. The development of suitable bedload transport measurement techniques was not a primary issue[5].

Also during the 1930's Shields (1936) and Einstein (1937) started to publish their pioneering works regarding bedload transport. While they were working on investigating the details of the water-sediment interactions, other researchers considered bedload transport as spatial and temporal averages. Schoklitsch (1934, 1962) and Meyer-Peter and Müller (1948, 1949) among others developed bedload equations that were based on simple hydraulic and sedimentological parameters or on index numbers. Although it is known that "A universal transport equation is not and may never be available" (Simons and Sentürk 1977: 644 and 1992: 695), this period of empirical bedload equation development still continues today (Zanke 1989; McDowell 1989). Richards (1982: 112) points out that "formulae are applicable to specific environments and circumstances, and errors are inevitable when they are used beyond their appropriate range." Nevertheless, formulas are not even available to reliably predict bedload transport rates for one stream type with its characteristic conditions of flow and sediments. This is partially due to the fact that various forms of particle interaction are not incorporated into the equations, but what is even more neglected in bedload transport prediction are the interactions between flow and sedimentary conditions on the stream bed, sediment availability, and stream bed morphology.

During the 1970's, research of bedload transport began to change: the analyses of sedimentological processes on the river bed received more attention, since it was recognized that a prediction of bedload transport could only stem from a knowledge of the processes involved. Predecessors of this development were Shields (1950) and Einstein (1937, 1950) who incorporated sedimentological processes such as **relative roughness**, **hiding and exposure**, or **particle step lengths** into the development of their bedload equations.

The progress in bedload transport research since the 1980's has been documented in the proceedings volumes of the Gravel-Bed Rivers group, which comes together each five years. The 1982 volume "Gravel-Bed Rivers, Fluvial Processes, Engineering and Management" emphasizes the analyses of hydraulic conditions and their dependency on channel bottom roughness (friction analyses) and channel morphology (spatial variation of hydraulic conditions). A large part of the proceedings contributions refers to advancements in hydraulic engineering. The 1987 volume "Sediment Transport in Gravel-Bed Rivers" features a broad spectrum of phenomena and problems encountered in bedload transport research (e.g., statistical analyses of the temporal variation of bedload transport, methods and problems in representative sampling, application of bedload transport formulae), as well as examples of hydraulic engineering in coarse gravel-bed rivers. The 1992 volume "Dynamics of Gravel-Bed Rivers" focuses on the analyses of the processes and mechanisms of bedload transport. The interactions between single particles and the channel bottom during the initiation of motion and during transport are analyzed in several contribu- tions (e.g., temporal and spatial variation of channel geometry and roughness, hydraulic and sedimentary conditions during incipient motion, and analyses of the grain-size distribution of bedload transport).

Bedload transport research of the 1990's must develop new measuring techniques that allow recording and analyzing the hydraulic, sedimentological, and morphological parameters of the

---

[4] Translation of the German citation "Intergralsanierung"

---

[5] An exception to this are the studies by Hubbell and Sayre (1964) and Sayre and Hubbell (1965) to detect the fluvial transport of radioactively traced sand.

channel bottom. Given these data, the processes that govern bedload transport can be analyzed. It is important that results of different aspects of bedload transport are compared and combined. Various models need to be developed that explain processes of bedload transport, starting at the very local scale and extending to the watershed scale where all processes that are active in a stream system and affect bedload transport act together.

2. Research Problems and Aims of This Study

2.1 Difficulties in Bedload Transport Analyses

Stream systems develop with respect to the conditions of their watersheds (climate, geomorphology, geology, vegetation, and hydrology). The watershed conditions produce typical amounts and durations of flows. These flows can transport typical amounts of the sediments available in the stream system. This causes a certain channel morphology. Stimulated by the studies of Leeder (1983), Hickin (1983), and Ashworth and Ferguson (1986), Figure 2.1 shows a diagram of the interacting processes in a gravel-bed river.

Bedload transport is part of the interactions between flow dynamics, the sedimentological conditions at the stream bottom, and the stream channel geometry. The unsteady flow hydraulics and the mobile channel bottom adjust to each other until a dynamic equilibrium is reached (Yang 1971; Yang et al. 1981). If the river bottom form or grain-size distribution changes during these adjustments, this process is observable as bedload transport. The temporal and spatial variability of the amount and grain-size distribution of bedload transport varies in different stream types in accordance to the flow hydraulics, sedimentological conditions and channel geometry.

Problems in the investigation of coarse bedload transport arise from the complexity of the interactions which, due to a dearth of appropriate measuring techniques and data from natural streams, have only begun to be investigated.

In their pioneering investigations in a Norwegian stream, Ashworth and Ferguson (1986) tried to acknowledge and measure these complex interactions in their temporal and spatial variations and interpret results in terms of a mutual dependency of all parameters. Ashworth and Ferguson (1986: 371) point out that "...more data sets of integrated and intensive field measurements are needed if a better understanding of the functioning of active gravel-bed rivers is to be gained." On the same token, the American Geophysical Union
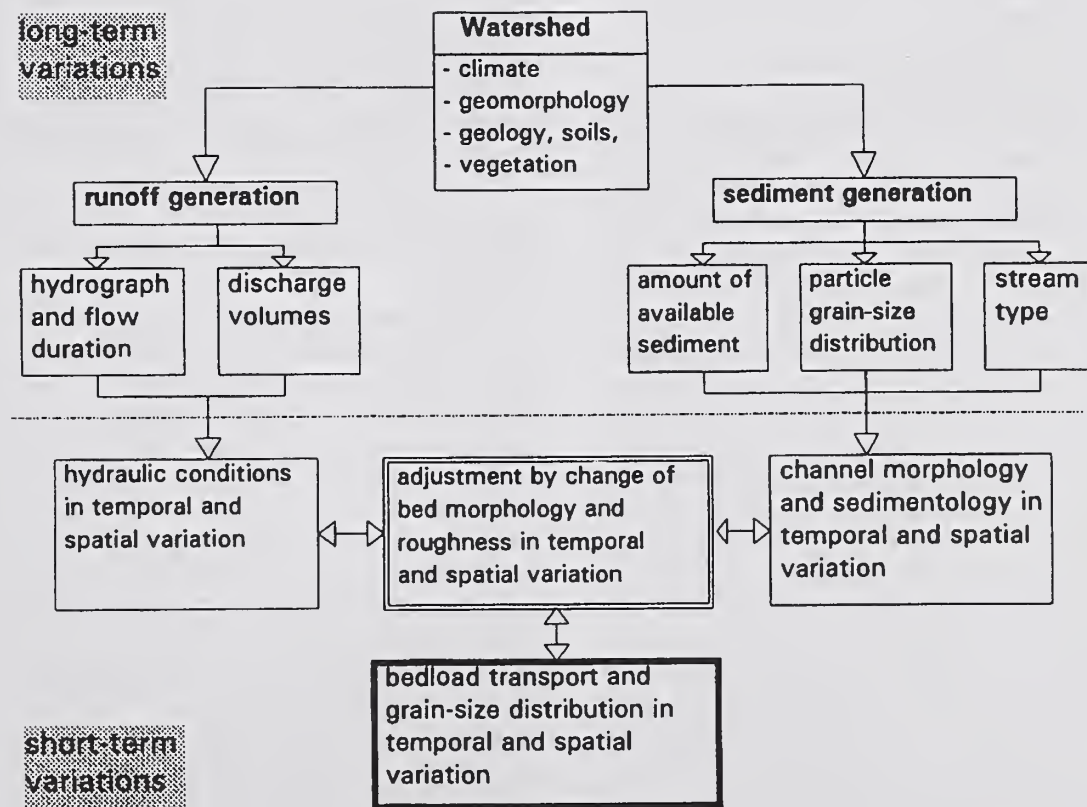
Figure 2.1 – Bedload transport as part of a complex interactive system. Parameters are subjected to short-term and long-term variability.

calls for contributions for the 1989 AGU Fall-Meeting, that analyze and quantify the interactions between the hydraulic, sedimentological and morphological factors which are needed in order to develop predictive models for river bed adjustments to steady and unsteady flows (EOS 1989).

Referring to Figure 2.1, at least the following parameters would have to be measured in order to analyze the interactions:

- watershed conditions that lead to the specific temporal variation of high flows, such as
  - weather (and snow) conditions*[1],
  - processes of runoff generation*,
  - discharge volumes*.
- watershed conditions that lead to the specific sediment availability*, such as
  - slope and stream sediment sources*,
  - stream and near-stream sediment storage*, and
  - travel velocity of stream sediments*.
- high flow measurements of the temporal and spatial variation of
  - coarse and sandy bedload transport and its grain-size distribution,
  - flow hydraulics,
  - cross-sectional geometry, and
  - stream morphology.

Though necessary, such a data base is not available for any natural stream. Data sets on flow and sediment transport are either from laboratory experiments which necessarily are performed under modified and restricted conditions, or if there are data sets from streams they focus on partial sediment transport aspects. The studies describe many bedload transport phenomena, but their interpretation is often difficult. Results obtained from different streams are often contradictory, since flow and stream conditions were not comparable. Drawing analogies is therefore problematic. However, an attempt to understand the complexity of processes involved in bedload transport demands that results from different studies are combined, since one study cannot cover it all.

The grain-size distribution of gravel-bed streams is often very broad, especially in mountainous areas. The steep channel gradients give the flow the competence to occasionally transport even very large clasts. The potential transport of these wide grain-size spectra from sand to cobbles leads to big problems regarding the research of coarse bedload transport: complex interactions take place between particles of different grain sizes and shapes, both during incipient motion, as well as during transport and deposition. These interactions have only been started to be investigated, since techniques capable of measuring the temporal and spatial variation of bedload transport of such different grain sizes are not at hand. The latest publications still point to this immense problem in coarse bedload transport research: "sampling and good data sets are still a problem" (Gomez and Church 1989).

Information gained from the analyses of transport processes in very well sorted sediments (especially those based on the analyses of sand transport in hydraulic engineering), as well as bedload equations derived from these analyses, cannot be used to explain the processes in coarse gravel-bed rivers. The grain size and shape dependent variability in particle stability, and the forces needed for entrainment, greatly affects transport rates and grain-size compositions of bedload transport.

Bedload transport research has still not succeeded in describing all the processes and their interactions involved in bedload transport in its entirety. Given the current techniques, the respective parameters are hardly measurable in their temporal and spatial variability under high flow conditions in natural streams. Therefore, their interactions are not yet describable in a deterministic way. Due to this dearth of appropriate field measuring techniques, and the lack of data, only few theories and models have been developed that help to connect data and theoretical concepts.

Field measurements regarding the temporal and spatial variability of coarse bedload transport and its grain-size distribution, as well as the conditions of flow, channel grain-size distribution, and geometry are indispensable for the analyses of the dynamics of coarse bedload transport. However, field measurements will only be successful, if they are supported by suitable hydrological and sedimentological catchment conditions, and a well equipped and accessible measuring site. The measuring technique has to fit the research question and the conditions encountered. The development of special measuring techniques, their installations at the site, and the performance of the measurements require relatively large financial, personnel and logistic efforts.

---

[1] Items with asterisk were added during translation.

2.2 Aims of the Study and Procedure

As indicated during the last symposium of the *Gravel-Bed Rivers* group in the fall of 1990, much attention is given to the analyses of the **dynamics** of bedload transport. Research focused on how channel grain-size composition and river bed geometry affect flow hydraulics and the transport of particles of various grain sizes. The investigations of this study are closely related to the present research.

In particular, it is the aim of this study to analyze the dynamics of coarse bedload transport by investigating the temporal variation of coarse bedload transport and its grain-size distribution and the associated channel change using Squaw Creek, a mountain stream in Montana as an example. Several measuring techniques were employed in this study. Some of them had to be especially developed for Squaw Creek.

A continuous registration of bedload transport was desired for a long and high temporal resolution data series which could be used to analyze the temporal variation of bedload in various temporal scales. The **magnetic tracer technique** was an adequate tool for the continuous registration of bedload transport for Squaw Creek. Continuous records of various hydraulic parameters are not only useful for establishing a discharge-bedload relationship, but they also offer the opportunity to compare time series of bedload transport and flow hydraulics. Detailed surveys of channel morphology and measurements of the cross-sectional channel geometry with the *"Tausendfüßler (millipede)"* device should render it possible to analyze the interactions between bedload transport and the processes on the channel bottom. The analyses of the temporal variation of the bedload grain-size distribution should permit one to gain insights into the interactions between channel bottom and bedload transport. This can be done with **consecutive and representative bedload sampling** using **appropriate samplers**. Furthermore, detailed grain-size analyses and analyses of clarify particle transport rates should help to elucidate the still controversially discussed question of whether or under which circumstances bedload transport is grain size-selective (**selective transport**) or comprises the entire grain-size spectrum (**equal mobility**).

Since finances, measuring techniques and the number of personnel are always somewhat limited, measurements and investigations were focused on those parameters and relationships which are necessary for an understanding of the causes of a fluctuating bedload transport and its variable grain-size composition.

The majority of the field data collection for this study at Squaw Creek was carried out during snow melt high flow in 1986 and 1988. In 1987 high flows were not sufficient to move coarse bedload. Some supplementary measurements were done in 1989 and 1990.

3. The Measuring Area—Squaw Creek

A suitable measuring site is an important requirement for measurements of coarse bedload transport in natural streams. Since 1981, coarse bedload transport has been measured intermittently at Squaw Creek. This site was chosen for measurements according to the following criteria:

- bedload should contain a high percentage of natural magnetic pebbles and cobbles which can serve as tracers for the magnetic tracer technique which facilitates the continuous measurement of bedload transport,
- high flows with competence for coarse bedload transport should be predictable with a high probability and occur annually,
- the site should be accessible by vehicle. Catwalks, instrumentation shelters, and electricity should be available.

Squaw Creek, a mountain stream in Montana, fulfilled these requirements.

3.1 The Measuring Area

The following section briefly introduces the topographical, geological, morphological, and climatological/hydrological conditions of the Squaw Creek watershed and its measuring site.

The Squaw Creek watershed is situated in southwest Montana in Gallatin County (fig. 3.1). Squaw Creek, a steep Rocky Mountain stream, is a tributary to the Gallatin River in the Missouri headwaters. The measuring site (45° 26' 28" N, 111° 13' 20" W) is 42 km south of Bozeman, about 50 m upstream from the confluence with the Gallatin River. The catchment area is 106 km² and ranges from 1,634 m in elevation at the measuring site to about 3,000 m at its highest parts. The watershed is 20.3 km long, and the Squaw Creek stream length is 22 km. The average stream gradient in the measuring reach is 2%.

The geological conditions of the catchment gave the main reason to chose Squaw Creek for a measuring site. Tertiary volcanic rocks comprise 55% of the watershed area. Widespread lava flows several hundred meters thick were produced by the Laramie orogenesis. The lava flows consist of black to gray-black, dense or intermediate porphyric andesites which contain about 7.4% magnetite (McMannis and

Chadwick 1964). The rest of the basin comprises Precambric gneiss in the northwestern part (20% of the total area), and Paleozoic and Mesozoic sedimentary rocks in the westerns parts (fig. 3.2). Most of the watershed is forested. Between 1960 and 1985, about 8% of the forest has been clear-cut[1]. The West-East valley orientation (WNW to ESE) leads to pronounced climatological, vegetational, and morphological differences between the shaded and the sun-exposed slopes.

3.1.1 The shaded, north-facing slopes

Traces of glacial erosion (cirques) are discernible in the highest parts of the watershed in shaded areas on north-facing slopes. Except for clearcuts in the distant part of the watershed, these slopes are forested from the valley bottom to the watershed (*Picea engelmannii*, *Pseudotsuga menziesii*, *Pinus contorta*). Traces of mass movements are discernible under the forest cover. Owing to the shielded exposition, the snow cover prevails until relatively late in spring.

3.1.2 The sun-exposed, south-facing slopes

The watershed on the south-facing slopes is higher than the southern rim and part of it extends for another 100–200 m above tree line which is at 2800–2900m. While the distal and higher areas of the south-facing slopes are forested, parts of the lower slopes are characterized by rather dry conditions featuring dryland vegetation (*Artemisia tridentata* and *Juniperus*). The dryland vegetation becomes sparse on slopes where the soil cover is thin. This happens especially in the proximal, lower parts of the watershed where Squaw Creek has scoured deeply into Mesozoic and Paleozoic sediments. The scour has lead to the formation of canyonlike walls on the south-facing slopes. Snow melt responds quickly to winter and spring sunshine on these slopes which are almost bare of vegetation.

3.1.3 Valley and stream morphology

In the upper and most distant parts of the catchment, the valley is U-shaped and Squaw

---

[1] Information from a handout provided by M. Story (U.S. Forest Service in Bozeman) at a U.S. Forest Service meeting at Squaw Creek in June 1994. The prelogging forest cover indicated on the 1955 edition of the Garnet Mountain quadrangle map, 15 minute series, 1:62,000, appears to be > 90%. De Jong (1993) gives a 50% forest cover for the Squaw Creek watershed which seems to be somewhat low.
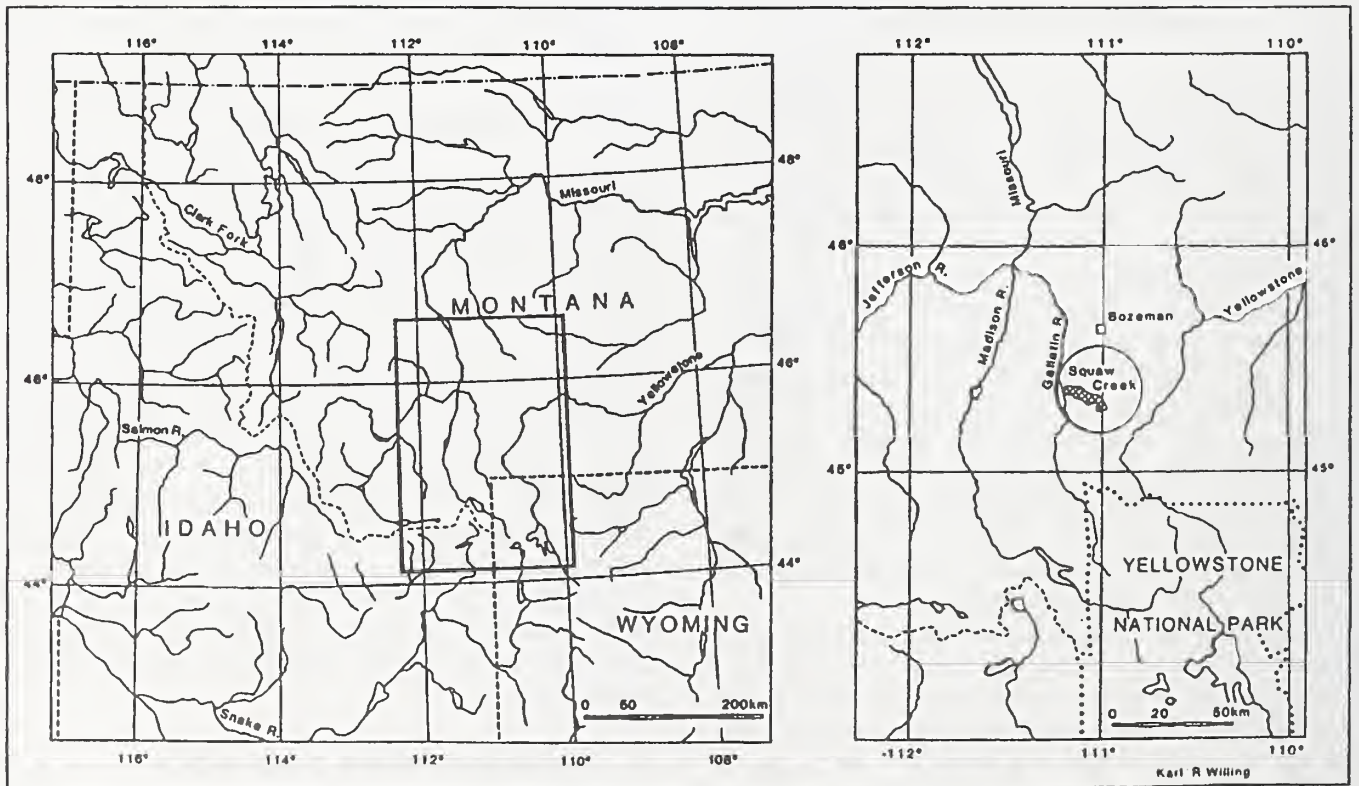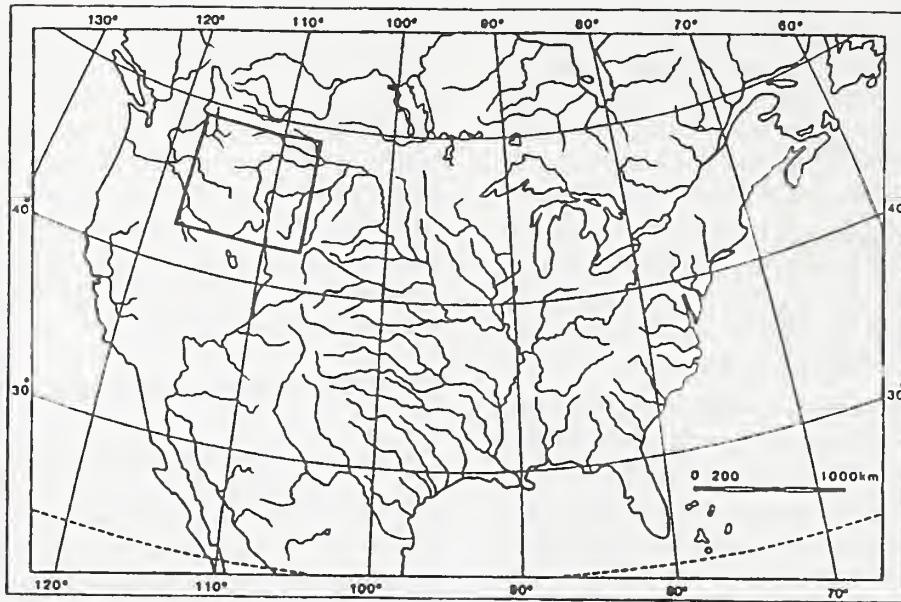
Figure 3.1 – Geographical location of the measuring area.
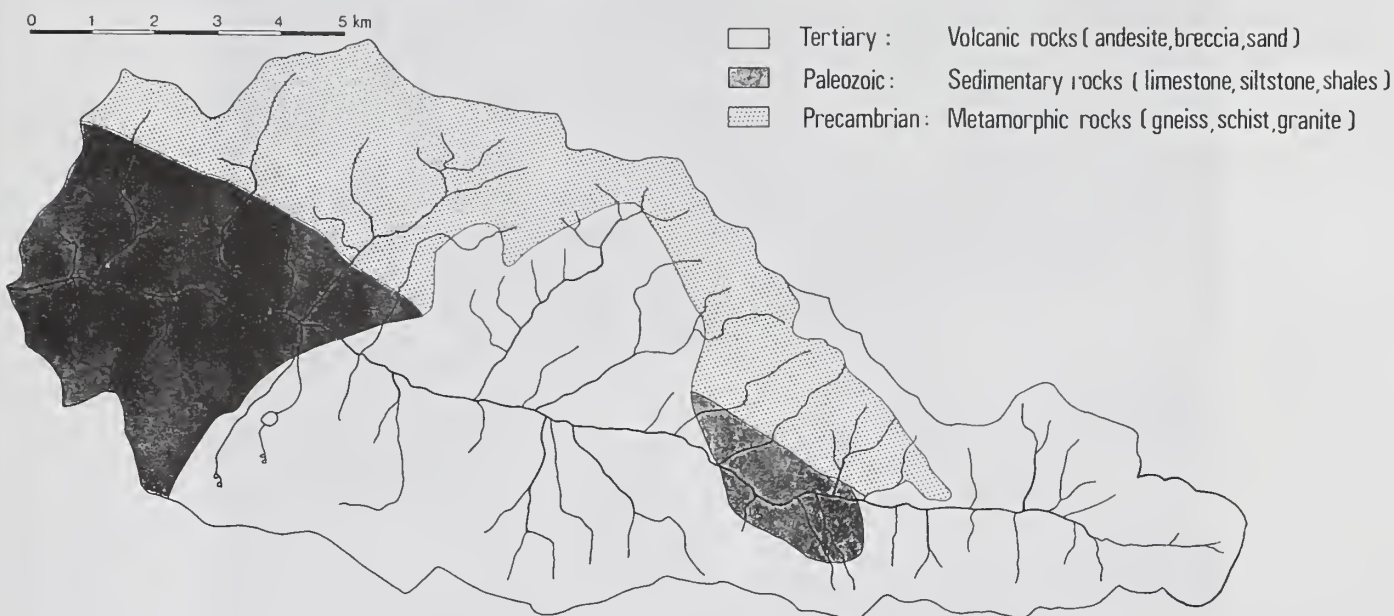
Figure 3.2 – Main geological units of the Squaw Creek watershed.

Creek has a step-pool morphology. In the broader and less steep valley in the central part of the catchment the stream becomes braided[2] (fig. 3.3a). In the sections following below, the stream bed is frequently confined, either by terrace sediments on both stream banks or by steep rock faces on the southern banks (fig. 3.3b). Lateral gravel bars occur mostly in unconfined reaches. Large woody debris affects the stream morphology as well, so that a jumble of stream forms occur, ranging from step-pool to pool-riffle and straight confined channel reaches. In its lowest reach along the measuring site, Squaw Creek follows a slightly meandering course incised into a presumably Pleistocene gravel terrace. Stream morphology is mostly pool-riffle and plane-bed.

3.2 Hydrological Conditions at Squaw Creek

The climate in southwest Montana is continental (Dfb-climate according to the Köppen climate classification): winter in the mountains is long and cold. Spring brings most of the precipitation and summer is short, hot, and dry. Snow cover starts to build up in October. The local climatic conditions in the Squaw Creek basin are affected by its mountainous terrain and its aspect (Section 3.1). Compared to the intramountainous basins (e.g., Bozeman valley), the Squaw Creek watershed is much colder and wetter. Using the data produced by the U.S. Forest Service for 1959 to 1981, Ergenzinger and Custer (1983) calculated the average annual precipitation for the entire watershed to be 813 mm, of which 56.2% is snow. Depending on elevation, snow cover lasts 6 to 9 months. The snow cover is so persistent because weather patterns in winter alternate between low-pressure systems from the northwest, bringing fresh snow, and cold, clear, high-pressure systems from the northeast.

General snow melt starts at Squaw Creek around mid May, not counting small-scale periods of snowmelt in the valley bottom and on south-facing rock faces. The reason for the late snowmelt is that radiation produces enough warmth for snowmelt only around the end of April or beginning of May. Besides, warm and wet frontal systems reach this part of Montana only in May and June.

---

[2]This braided reach has already been identified on prelogging areal photography in 1959 (S. Glasser, pers. com. 1994).

Figure 3.3 – Various channel forms at Squaw Creek:
a)   braided reach in the central part of the watershed.
b)   confined reach less than one km above the measuring reach.

3.2.1 Snowmelt high flows at Squaw Creek

The shape of the snowmelt hydrograph is dependent on the amount and water equivalent of the snow cover and on the temporal and spatial variation of melting rates. A warm spring with frequent sunshine and a generally small snow cover produces low daily melting rates that have already gradually consumed the snow pack before hot weather or spring rain sets in by mid-May, leading to an early and low snowmelt runoff. This happened in the springs of 1985, 1987, and 1990, when discharges never, or not for sufficient periods of time, exceeded the threshold of motion of coarse bedload. However, if a warm frontal precipitation coincides with a good pack of warmed-up snow, this produces discharges that exceed ordinary snowmelt runoff by two or three times. Such a high flow has been observed and partially measured by Ergenzinger and Custer (1983; Section 5.2.1.3).

Usually, spring provides a combination of both weather patterns, and every other year produces a "good" spring high flow that is large enough to cause bedload transport for a period of 2 or 3 weeks. Such high flows with sustained periods of bedload transport were observed and measured in 1986 and 1988[3]. In another 30% of the years, full pebble and cobble transport can be expected for several, individual days of the high flow. In 20% of the years spring high flow is not sufficient to start the transport of pebbles and cobbles[4].

Figure 5.8 (Section 5.3.2) shows a typical example of a snowmelt hydrograph during the runoff season in 1986. The elongated shape of the drainage basin delays the daily discharge response to snowmelt until late afternoon. Peak flows do not occur until late at night or midnight. The hydrograph shows diurnal fluctuations of flow typical of a snowmelt regime. The difference between daily low and daily high flow ranges from 0.5 to 1.5 m³/s and is especially well developed during a rapid and vigorous snowmelt at the onset of high flow (May 27/28, 1986), after hot and sunny days during snowmelt (May 31/June 1, 1986) or when already decreasing snowmelt is reinforced by frontal rain (June 5/6 and June 9, 1986). The change in the rate of flow is usually stronger on the rising limbs than on the falling limb of flow. If snowmelt is mainly due to warm and sunny weather, the rate of snowmelt, and consequently peak flows and daily amplitudes of flow, decrease over time as the snowpack becomes depleted. Finally, when runoff is mainly fed from interflow and groundwater, a "warm" frontal system, or even individual thunderstorms, may produce some peak flows again.

3.2.2 Time series analyses of high flows

If the occurrence, magnitude, and the frequency of high flows is known, occurrence, magnitude and the frequency of flows which produce coarse bedload transport can be calculated. The U.S. Forest Service kept a stream gage at the Squaw Creek measuring site from 1959 to 1986. A 27-year record is therefore available for the analyses of annual maximum flows. The statistical analyses showed that annual peak flows usually occur either in the second part of May or in mid June (fig. 3.4). These peak flows are most often of a magnitude of 5.5 to 6.5 m³/s (fig. 3.5). The recurrence interval for annual peak flows was calculated after Morisawa (1968) and is 1.8 years for peak flows of 6 m³/s (fig. 3.6). According to local experience at Squaw Creek, annual peak flow of 6 m³/s produces at least 1 week of flows larger than 4 m³/s, which is the threshold of motion for coarse bedload transport at Squaw Creek.

The most frequently occurring peak flow (about 6 m³/s) coincides roughly with bankfull flow for which Leopold et al. (1964) give a recurrence interval of 1 to 2 years. Both high flows in 1986 and 1988 fall into this category. They are therefore referred to as "ordinary" high flows that modify the channel morphology but which do not alter the type of the channel morphology. The high flow of 1981 reached a peak discharge of 16 m³/s, which corresponds to a statistical recurrence interval of 10 to 20 years. Such flow events flood the gravel bars and tear up the armor. The stream shifts within its gravel bed. The effects of such a high flow event are described in Section 5.2.1.3.

3.3 Stream Morphology at Squaw Creek in the Measuring Reach

In order to monitor changes within the stream morphology, the stream bed, including its sur-

---

[3] *and in 1991. Snowmelt runoff in 1992 was too low for sustained coarse bedload transport, but a few days of coarse bedload motion set in after the researchers had left already. Spring high flow was excellent for bedload transport in 1993, but no measurements took place.*

[4] *These calculation were done in 1994 and added during the translation.*
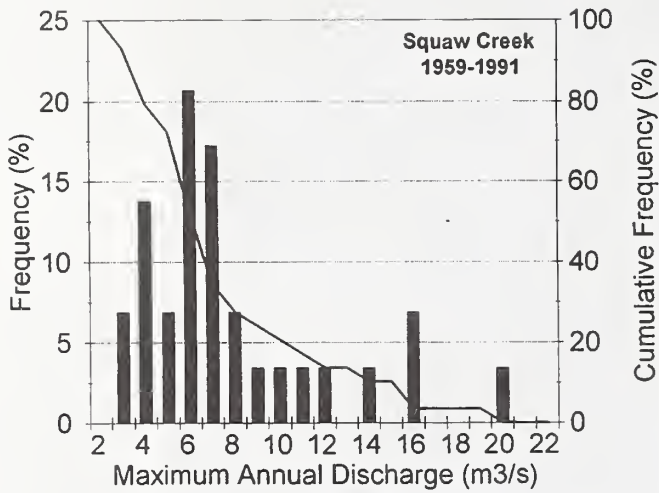
Figure 3.4 – High flow frequencies at Squaw Creek 1959-1991. No data for the years 1976-1978, and 1989.
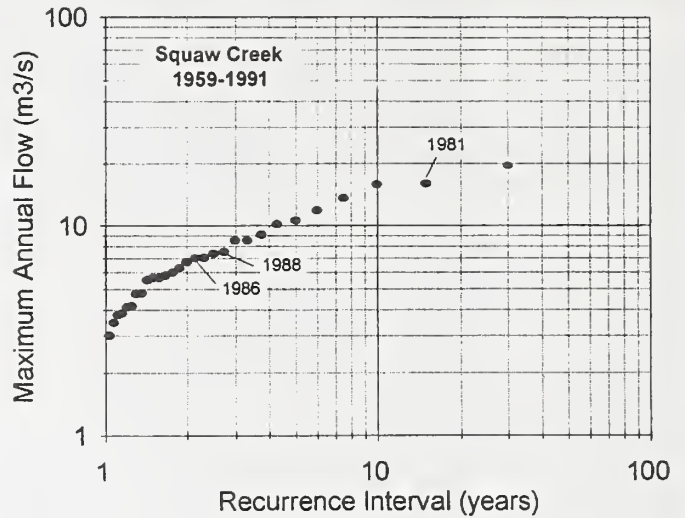
Figure 3.6 – Recurrence intervals of annual peak flows 1959-1991. No data for the years 1976-1978, and 1989.
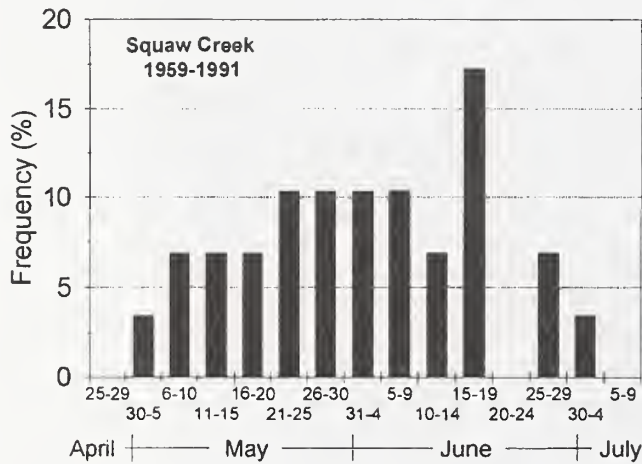
Figure 3.5 – Temporal distribution of annual peak flows 1959-1991. No data for the years 1976-1978, and 1989.

roundings, was surveyed in 1986 and in 1988 after the high flow period over a reach of about 70 m upstream from the detector block at the vehicle bridge. The results of these surveys are shown in two topographic maps (fig. 3.7 and 3.8).

An extreme high flow event in 1981 and a log jam burst in spring of 1983 (Section 5.2.1.3) played a major role in the shaping of the present[5] stream morphology in the measuring reach. During later years the stream only modified its channel by making the riffle-pool morphology more prominent[6].

In the reach above the confluence with the Gallatin River, Squaw Creek follows a meandering course in which the stream and its lateral bars cover a width of about 20 m and lie incised 1 to 2 m deep into an older gravel floodplain (fig. 3.9a – b). The general stream gradient in this reach is around 2%, but due to the riffle-pool morphology local gradients can vary. Those gravel bars that are part of the riffle-pool morphology are only exposed during low flows. The presence of lateral gravel bars is usually limited to one side of the stream and they are inundated by a decimeter or two when flow peaks during ordinary snowmelt with bankfull flows.

The asymmetrical stream cross-sections have a maximum depth of 0.6 to 0.7 m at bankfull flows during ordinary snowmelt high flow. Stream width increases from about 5–6 m during low flows to about 10 m during bankfull flows. A further increase in width would require much higher flows, because the left bank is confined by a terrace, and the right bank by a gravel berm. This berm levels out with the gravel bar a little farther upstream, but here the gravel bar is in a point bar position. It is just inundated during ordinary snowmelt high

---

[5] as of 1989

[6] Following the aggradation associated with the installation of the upstream detector log in 1990, the riffle-pool sequence shifted a few meters upstream.

Legend:

- ✕—✕—✕ Cross-section measured with "Tausendfüßler" profile meter
- → Flow direction
- Edge of the flood plain
- Riffle
- —— Low flow bed
- – – – High flow bed
- ✕ Logs
- Large boulders
- ★ Location of tube levels

**Squaw Creek
July 1988**

0   5   10 m

Detector log

Bridge
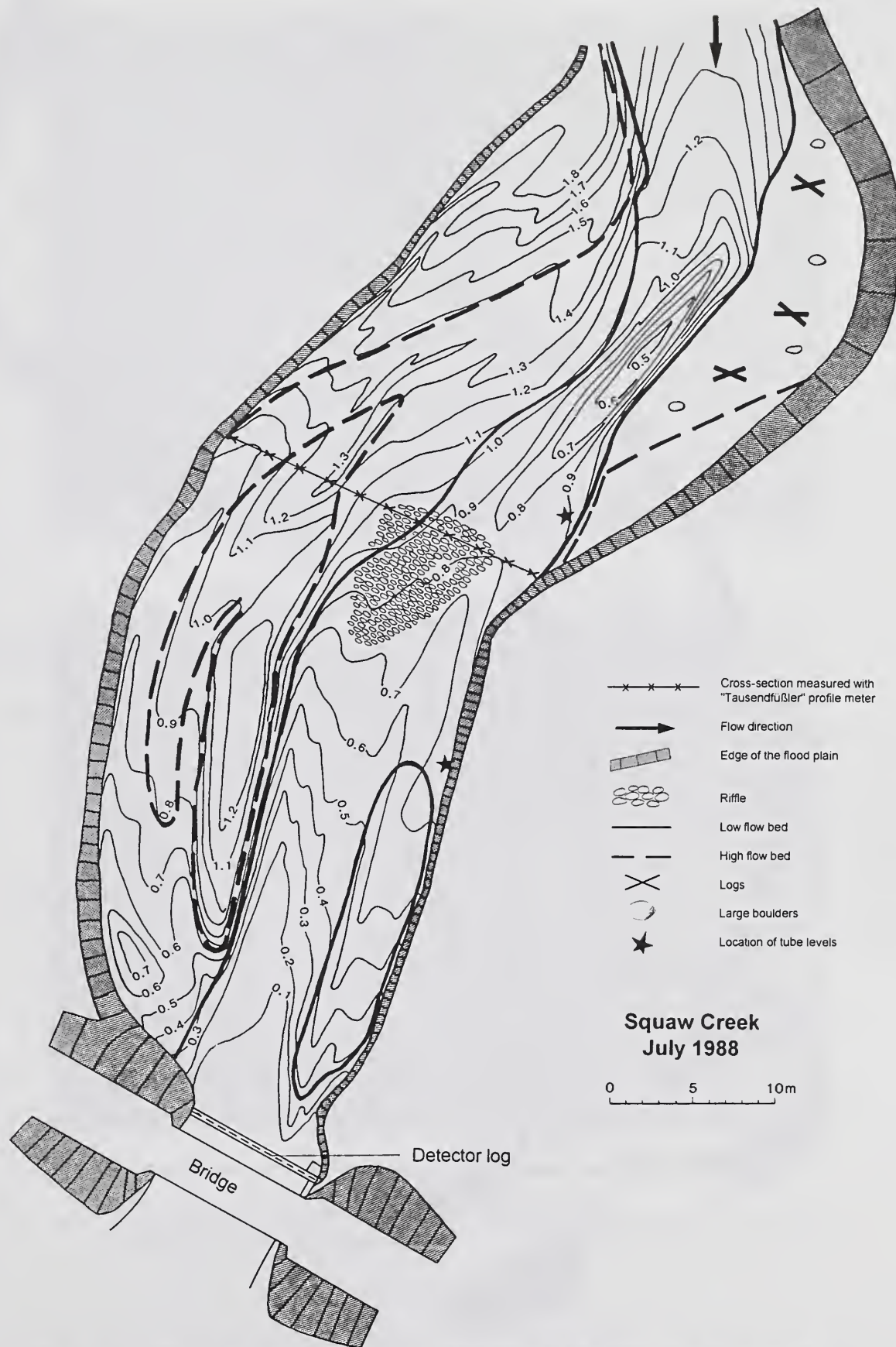
Figure 3.7 – Topographic map of the stream reach at the measuring site at Squaw Creek, survey 1988.

Legend:

Symbol	Description
–x– x– x–	Cross-section measured with "Tausendfüßler" profile meter
→	Flow direction
(hatched band)	Edge of the flood plain
(cluster)	Riffle
——	Low flow bed
– – –	High flow bed
✕	Logs
◯	Large boulders
★	Location of tube levels

**Squaw Creek
July 1986**

0 ——— 5 ——— 10 m

Detector log

Bridge
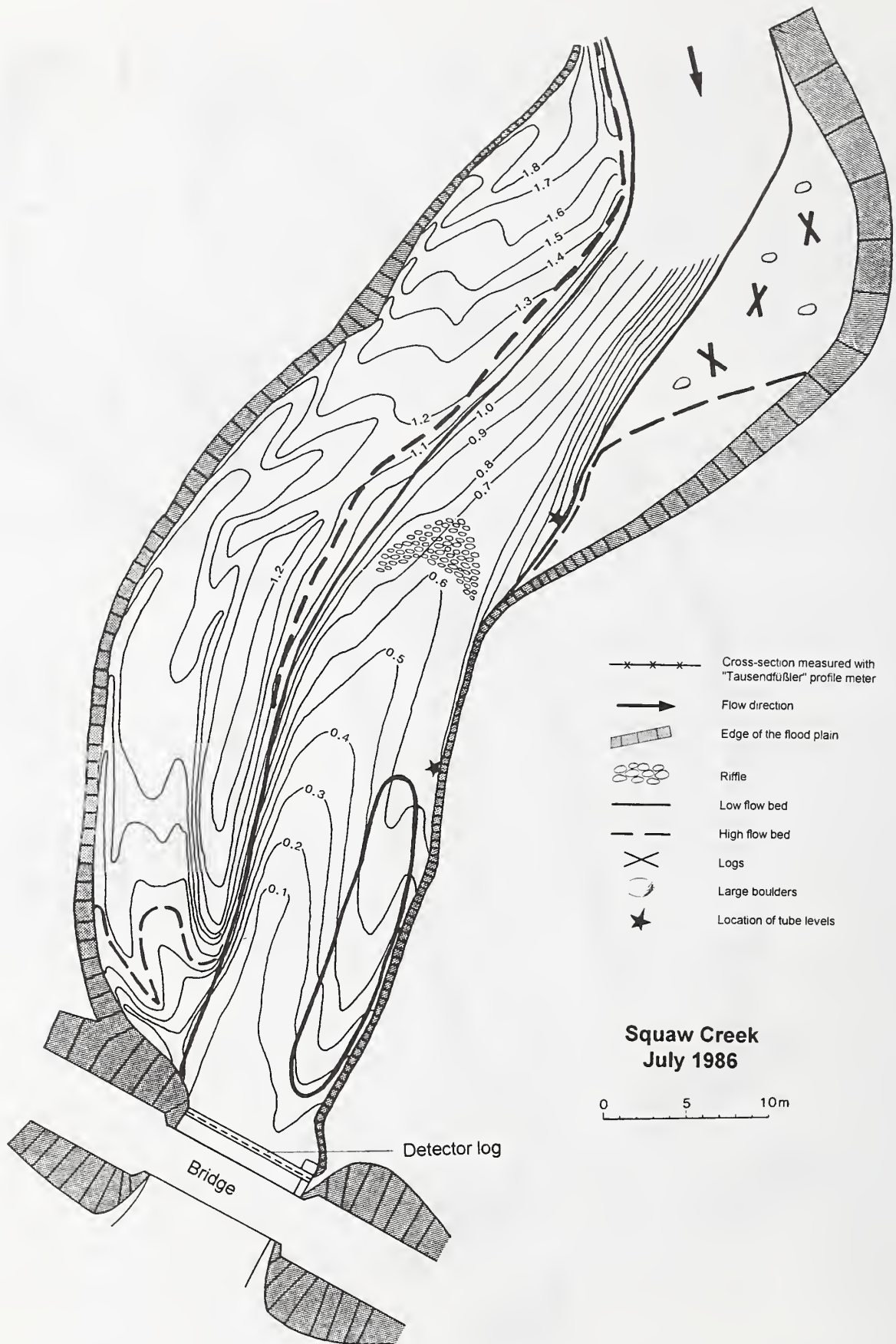
Figure 3.8 – Topographic map of the stream reach at the measuring site at Squaw Creek, survey 1986.

Figure 3.9 – Squaw Creek at the measuring reach in the beginning of snowmelt high flow (note high turbidity).
  a)   view upstream: right bank gravel bar that is just getting flooded
  b)   view downstream towards the vehicle bridge: culverts on the left bank indicate the locations of the water surface slope measurements

flows[7] and sediment transport on this bar is usually marginal, although pebble transport can already occur in shallow inundation.

3.4 Sedimentological and Petrological Conditions at Squaw Creek

3.4.1 Grain-size distributions in the measuring reach

Figure 3.10 gives a general idea about the grain-size distributions within the measuring reach. The grain-size spectra range from sand to cobbles with a diameter of 20 cm. Two samples from the gravel bar at the right bank were analyzed. Subsequently, a sample larger than 100 kg was taken from this bar in the measuring reach in 1988. Sampling reached from the gravel bar surface to a depth of about 0.5 m. The median grain size, including the sand fraction, was 22 mm (fig. 3.10: curve 2). A smaller sample taken in 1983 (Bugosh 1988) has a smaller grain-size range but a similar median grain size (curve 1). The grain-size distribution of the channel bottom is strongly dependent on the local stream morphology and varies within the reach scale. Custer et al. (1987) and Bugosh (1988) recorded the median grain size of the river bottom to be 125 mm (curve 3). The largest boulders are up to 30 cm.

3.4.2 Percentage of magnetic rocks

Later parts of this study will compare bedload signal rates registered with the magnetic tracer technique with the number of pebbles and cobbles that were caught with a large net-sampler as they passed over the detector log. Since only magnetic rocks can induce a signal, this comparison requires that for each bedload grain-size class the percentage of magnetic rocks is known.

A first sedimentological and petrological study of this kind was done by Monahan and O'Rourke (1982). They took 411 pebbles and cobbles from Squaw Creek and analyzed the effects of particle size, weight, volume, shape, and petrology on the magnetic field strength. The sample was collected from the gravel bars and the river bottom and comprised particles within the two size classes 32–64 mm and >64 mm. The results of this study show that

- 76% of all particles are volcanic rocks; the rest are sedimentary (limestones, siltstone, sandstones), metamorphic (basically gneiss), and intrusive rocks (basically granite);

- 97% of the volcanic rocks are magnetic;

- the percentage of volcanic rocks within the grain-size class of 32–64 mm is 66.7 and 77.2% for the grain-size class >64 mm; and
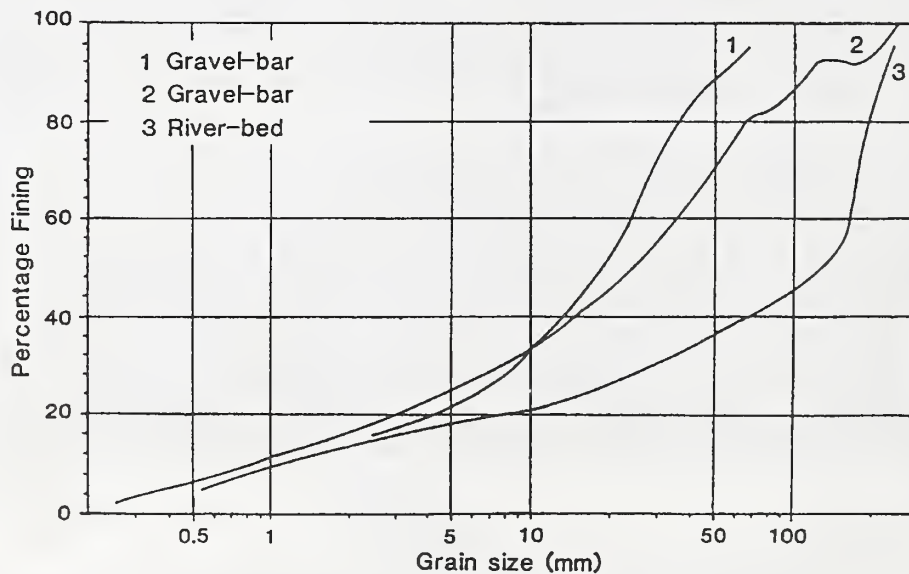
Figure 3.10 – Grain-size distribution of a gravel bar and the channel bottom.

[7] A more frequent flooding of this gravel is to be expected after the installation of second, upstream detector log in the stream in 1990. The burial of the log was not absolutely flush with the stream bottom, so sediment accumulated on the upstream side and raised the local water level. The lateral gravel bar should now be inundated at lower discharges already.
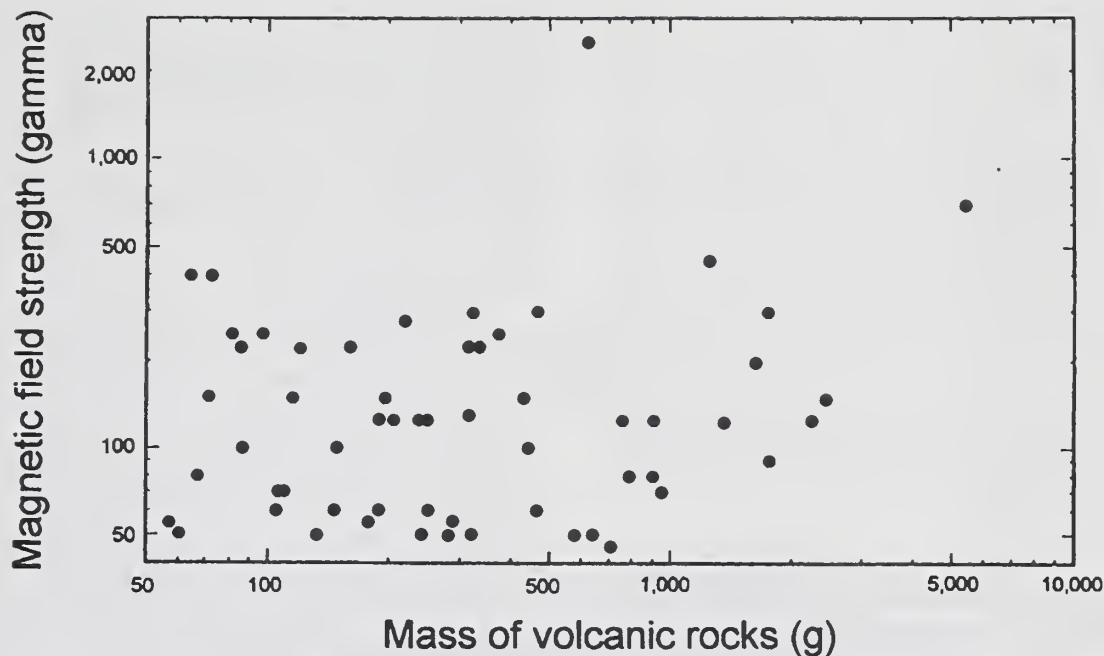
Figure 3.11 – Variability between magnetic field strength and particle size of volcanic rocks at Squaw Creek (data from Monahan and O'Rourke 1982).

- the magnetic content is not related to particle weight (fig. 3.11; $r^2 = 0.1$).

It was recognized during experiments with the newly installed detector log in 1986 that test pebbles of different volcanic petrology produced signals of different amplitude as they passed the detector log. Therefore, the variability of the magnetic properties and the percentage of highly and slightly magnetic rocks among the volcanic rocks was more closely examined. Using a bedload sample from the large net frame sampler (Section 4.4.4.2), the volcanic rocks were visually sorted according to their color, structure, and texture into three groups with the following characteristics:

- black, dense, fine-grained,
- gray, dense, porphyritic, and
- black or red and vesicular.

Because a magnetometer was not available at that time, the magnetic field strength of each volcanic rock group was tested by recording the angle up to which a small pebble (16–22 mm) could lift a small stud-finder magnet that can pivot around a center. While both the black and gray volcanics produced the same degree of pivoting in the stud-finder magnet, the vesicular extrusive rocks evoked hardly any motion on the magnet. Therefore, the vesicular rocks were eliminated from the group of "magnetic rocks."

The percentage of magnetic rocks was determined for each of the six size classes between 11.2 and 125 mm in 0.5 phi steps using pebbles and cobbles from several bedload samples collected with the net-sampler. Results of this analysis are shown in Figure 3.12. Cobbles have the highest percentage of magnetic rocks. The percentage of magnetic rocks decreases with decreasing grain sizes and reaches a minimum for pebbles around
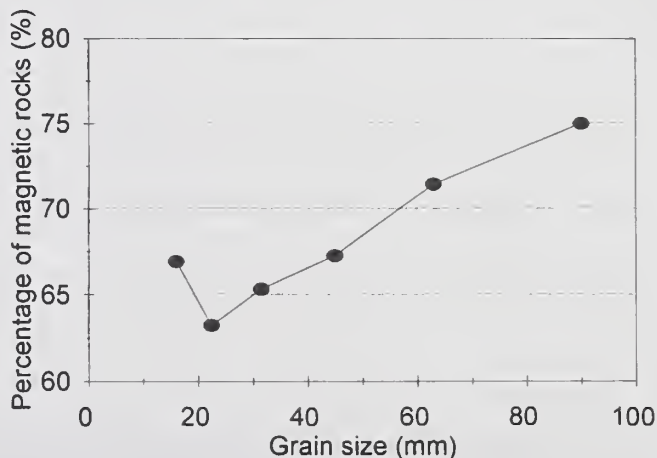
Figure 3.12 – Percentage of magnetic rocks determined for various bedload size classes.

19

20 mm, while smaller gravels have a higher percentage of magnetic rocks. This non-monotonic relation is attributable to the structural and textural stability of the volcanic rocks. The black and gray dense volcanic rocks withstand external impacts even in small grain sizes, while the vesicular rocks have their optimum existence around 20 mm and easily break or disintegrate when they are smaller or larger. Particles larger than 30 mm (more than 50 g) have on average magnetic field strengths larger than 40 gamma (Spieker 1988; see also fig. 3.11), which was the threshold for measurability with the magnetic tracer technique[8]. The percentage of magnetic rocks increases exponentially from 65% to 75% for pebbles and cobbles between 30 and 90 mm.

3.5 Description of the Measuring Site and Its Permanent Pieces of Instrumentation

The measuring site at Squaw Creek is about 50 m upstream of the confluence with the Gallatin River where a vehicle bridge crosses Squaw Creek. The foundations of this bridge narrows the stream width from a bankfull average of 10 m to 8.5m. The U.S. Forest Service installed two logs across the stream in front of the upstream side of this bridge to protect the bridge foundations from severe erosion. The logs are flush with the stream bottom on the upstream side, while scour on the downstream side has created an overflow. The accelerating flow at this position ensures that no particles are deposited on the logs. This was a good position to install the (first) detector log, since a rapid transport of the particles over the detector log was important for the quality of the bedload signals (4.4.2.2).

Three catwalks were installed at the bridge to facilitate access and measurements over, in front of, and behind the detector log. A small shelter at the stream bank housed measuring and registration equipment. The position of the measuring site within the reach is shown on the maps in Figure 3.7 and 3.8. The location of permanent and temporary equipment and measuring positions around the bridge in 1986 and 1988 are depicted in Figure 3.13.

The U.S. Forest Service maintained a gaging station at the downstream side of the bridge until 1986. This includes two staff gages on both sides of the bridge foundation and a stilling well on the left bank. A pipe extends diagonally downstream into the flow, adjusting the water level in the culvert to the water level in the stream. Water levels are measured with a float and registered on a Leopold and Stevens strip chart recorder.

Detailed descriptions of the individual measurements are given in various sections of Chapter 4[9].

Figure 3.13 – Set-up of the measuring site: schematic diagram showing the location of the detector log, the numbering of detector units, and the locations of bedload sampling (Helley-Smith: sampling points 1-8; net-sampler: spans detector unit 7/8). Flow width under the bridge is 8.5 m.

4. Selection and Performance of the Analyses of Coarse Material Bedload Transport

Based on forces and conditions that affect initial motion and transport of coarse bedload, parameters that should be measured are described and the methodological approach of the respective measurements at Squaw Creek is presented.

4.1 Forces Active During Initial Motion of Coarse Bedload

The following hydraulic and sedimentological forces are exerted on a coarse particle exposed to flow; the magnitude and effectiveness of each of the forces are dependent on stream gradient (fig. 4.1).

- Forces of flow F_D,
- Lift forces F_L,
- Gravity F_W ($\rho_s - \rho_w$);
- Friction between particles F_F (particle stability),
- Resulting force F.

Motion is initiated after the resulting shear stress F exceeds gravity F_W and friction F_F resulting from particle stability.
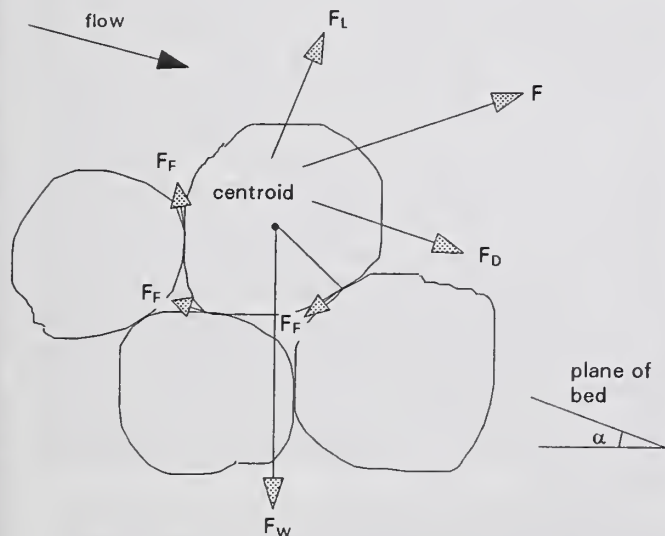
Figure 4.1 – Forces exerted on a particle on a rough stream bottom (after James 1990: 29).

4.1.1 Force of flow

Friction is exerted at the water-sediment contact between the channel bottom and the flow above it. This friction results from the velocity difference between the flowing water and the non-moving channel bottom with its specific roughness (Newton's shear stress approach). Friction between flow and channel bottom increases with increasing flow intensity, increasing roughness and irregularities in the channel bottom shape in its long- and cross-sectional profile.

The basic literature (e.g., Dingman 1984: 173-174, or Graf 1971: 84) describes the intensity of bedload transport as a function of one of the following parameters that characterize flow intensity minus a **critical** threshold value (indicated by the suffix "crit") that needs to be exceeded for incipient motion:

$$Q_b = f(Q - Q_{crit}) \quad \text{(Schoklitsch 1934 and 1943)}$$
$$Q_b = f(v - v_{crit}) \quad \text{(Hjulström 1935, and others, see Stelzer 1981)}$$
$$Q_b = f(\tau_o - \tau_{ocrit}) \quad \text{(Du Boys 1879; Shields 1936)}$$
$$Q_b = f(\Omega - \Omega_{crit}) \quad \text{(Bagnold 1977)}$$

where:

Q_b = bedload transport rate,
Q = flow discharge = $d \cdot w \cdot v$,
v = mean flow velocity = $Q/d \cdot w$,
τ_o = boundary shear stress = $\rho_w \cdot g \cdot d \cdot S_w$, or $\delta v/\delta d \cdot \eta + \varepsilon$, and
Ω = stream power = $Q \cdot S \cdot \rho_w$.

(For further explanations see list of symbols)

Many authors modified the stream flow parameters mentioned above. Bagnold (1977) and Reid and Frostick (1986) set up relationships between bedload transport rates and **unit stream power**, defined as:

$$\varpi = Q \cdot S_w \cdot \rho_w/w, \tag{1}$$

because this parameter has the same dimensions (kg/m · s) as bedload transport rates. Bathurst (1987) establishes relations between bedload transport rates and **unit discharge**

$$q = Q/w. \tag{2}$$

23

The force of flow is often quantified by the boundary shear stress

$$\tau_0 = \rho_w \cdot g \cdot d \cdot S_w. \qquad (3)$$

Einstein (Shen 1975) was the first to separate **total shear stress** τ_0 into the **grain shear stress** τ_0' resulting from grain roughness and **form shear stress** τ_0'' resulting from form roughness, i.e., the friction exerted on flow by the shape of the river bed. Bedload entrainment is mostly attributable to **grain shear stress,** which can either be determined from a measured velocity profile (Wiberg and Smith 1987) or be calculated according to the Prandtl law of the vertical velocity distribution in turbulent flow (Petit 1989 and 1990). Ackers and White (1973) found that bedload transport rates correlate best with **grain shear stress** τ_0' which they quantify by means of average flow velocity. This multitude of flow parameters indicates already that none of them seems to be generally superior in predicting bedload transport rates.

Shields quantified the forces needed for incipient motion by a dimensionless coefficient, the **mobility number** θ which he defined as:

$$\theta = \tau_0 / (\rho_s - \rho_w) \cdot g \cdot D, \text{ or, in another notation:} \qquad (4a)$$

$$\theta = (\rho_w / \rho_s - \rho_w) \cdot (d/D) \cdot S, \qquad (4b)$$

where g, d and D are acceleration due to gravity, water depth, and grain size, respectively. A third notation, known as the grain Froude number Fr^* denotes θ as:

$$\theta = Fr^* = v^* / g \cdot D, \qquad (4c)$$

where v^* is the **shear velocity** which is defined as $(\tau_0/\rho_w)^{0.5}$.

The Shields diagram sets this mobility number into relation with the dimensionless grain Reynolds number Re^* which is defined as:

$$Re^* = D \cdot v^* / v. \qquad (5)$$

The diagram indicates the relations between θ and Re^* at which entrainment occurs. As the mobility number includes the relative roughness denoted by the quotient of water depth to particle size (d/D), the mobility number θ acknowledges the friction exerted by flow on the river bottom to a certain extent. The mobility number has since been used by many authors to quantify the conditions of flow and channel roughness that produce

initial motion (e.g., Bagnold 1966; Ackers and White 1973; Allen and Leeder 1980, and many others).

4.1.2 Fluid density and lift forces

As the density of the transporting medium increases, the shear stress exerted by the fluid onto the particles increases as well. A decrease of the difference between the density of the fluid and the density of the coarse particles increases the hydrostatic lift, which helps to entrain particles. Apart from water temperature and dissolved matter, water density is mainly affected by the concentration of suspended sediment.

Some of the processes that initiate or enhance incipient motion besides hydrostatic lift are not fully explainable yet (James 1990). Upward directed components of stream flow, e.g., secondary flows (Richards 1982: 285), support lift forces. The effects of pressure differences in the interstitial water on lift forces is still controversially discussed (Williams et al. 1990). The narrowing of the stream lines as flow passes around exposed particles also exerts an upward force onto the particle according to the Bernoulli principle (Richards 1982: 84).

4.1.3 Turbulence

The fast temporal variation of the flow direction and velocity at one location is called turbulence. Turbulent flow can produce large pressure fluctuations, which are described as an impulse. The high temporal variability of the pressure fluctuations and the fact that impulses can attack a particle from all directions makes it possible to attack a particle at that point where its stability is least. Heathershaw and Thorne (1985), Thorne et al. (1989), and Williams et al. (1989a) analyzed the effects of the direction of the flow components and the strengths of the turbulences on the amount and grain-size distribution of bedload. Apperley and Raudkivi (1989) quantified the impulse that is exerted on particles of different exposure due to the temporal and spatial variation of stream components. They then determined which turbulence conditions produce entrainment.

It is very difficult to measure turbulence at a stream bottom in high energy mountain streams. Not only is the water depth relatively low and the flow fast, but the movable stream bed would require frequent adjustments of the positioning of the measurement instruments, and large moving

particles could damage the instruments. Likewise, it was not possible during the field seasons at Squaw Creek to determine the temporal and spatial variation of the flow components and their effect on bedload transport[1].

4.1.4 Spatial differentiation of flow forces

Flow in a mountain stream is three-dimensional and has certain patterns in longitudinal and cross-sectional direction. These flow patterns are associated with stream morphology (Petit 1987). For example, boundary shear stress, or the Froude-number, as a measure for the energy of flow, is highest at those parts in the cross-section where the water depth changes most pronouncedly over stream width. The locations of high and low Froude-numbers within an irregularly shaped cross-section change with increasing discharge (Blalock and Sturm 1981).

Locations of high and low energy of flow are also variable in the longitudinal direction. In irregular long-profiles, such as in step-pool or riffle-pool sections, reaches of highest shear stress move from step or riffle reaches during low flows to pools during high flows (Emmett et al. 1983; Petit 1987). If, therefore, a relationship between forces of flow and bedload transport is to be established, the forces of flow need to be measured in their spatial variability. However, such measurements necessitate an array of measuring devices and a large measuring crew, none of which was available during the field seasons at Squaw Creek between 1986 and 1988. Therefore, only relationships between bedload transport and water discharge within the entire cross-section were analyzed.

Based on the analysis by Grass (1970), Raudkivi (1976) and Zanke (1990) developed a probability approach that predicts the range and distribution of spatially arbitrary distributed flow conditions within a reach. This approach was not pursued at Squaw Creek, since the spatial variability of flow conditions is not arbitrarily distributed but follows certain spatial and temporal patterns that are dependent on stream morphology and discharge.

4.2 Measurements of Hydraulic Parameters at Squaw Creek

In order to determine flow discharge, and in order to be able to calculate other flow parameters used in the literature to quantify the forces of flow, the following hydraulic parameters were measured for the investigations of bedload transport during the field seasons of 1986 and 1988:

- several staff gages and stage recorders,
- cross-sectional flow velocities,
- cross-sectional water depth,
- stream width,
- stream gradient over a 17.3 m reach,
- suspended sediment concentration, and
- water temperature.

4.2.1 Gage heights, flow velocities, and water discharge

Water level was recorded by a Stevens and Leopold float stage recorder at the left side of the stream at the downstream side of the vehicle bridge (Section 3.5.)[2]. The float moves inside a culvert from which a 2 m pipe extends diagonally downstream into the flow. In order to compensate for laterally shifting flow, additional readings were taken in 2-hour intervals at two staff gages on both downstream sides of the bridge.

Flow velocities in 1986 were measured at two locations in the stream and with two different devices. One device was a suspended Ott current meter, which was lowered into flow from the downstream side of the vehicle bridge using a small crane (fig. 3.13). The propeller is attached to a 35 kg hydrodynamically-shaped body of lead with a foot that is set onto the stream bottom. All measurements were performed as one-point measurements at 40% of the water depth. The crane-suspended Ott current meter has the advantage that no device has to be held by man power into the flow which can reach velocities of 2 m/s. The disadvantage of this method is the high position of the lowest possible measurement (17 cm above ground).

---

[1] Measurements of turbulence near the stream bottom have been performed at Squaw Creek by J.J. Williams and P.A. Carling during the field season in 1991 and 1992 (Carling et al. 1993) using an electromagnetic current meter.

[2] This stage recorder had been installed by the U.S. Forest Service who collected stream flow data from 1959 to 1986. In later years this stage recorder was run by the Squaw Creek measuring crews.

The Ott current meter mounted on a wading rod was used either directly in a stream cross-section or down from one of the various catwalks attached to the bridge. Usually, the one-point method was used for all vertical measurements, except for a few measurements of velocity profiles carried out in 10 cm depth increments directly in the stream cross-section.

All of these catwalk locations were unsatisfactory for flow velocity measurements because local flow conditions were either characterized by high velocities and low flow depths, or by high turbulence and upwelling water at the downstream side of the bridge.

In 1988, Paul Carling and Mark Glaister used a rod with six vertically mounted propellers to measure detailed velocity profiles. Sequential stream flow measurements were done in the same cross-section in which P. Ergenzinger and T. Berry measured the cross-sectional variation of roughness and channel change (Section 4.3.3; Figures 4.6a–b).

All of these flow velocity measurements fail when flow velocities are high. The physical limit of operation at Squaw Creek is reached at bankfull flows. The current meter on a wading rod can no longer be held in the flow, neither by standing in the stream nor down from a flimsy catwalk. The suspended current meter becomes likewise unusable because it starts to randomly swing in the flow[3].

Flow velocity and depth measurements during less than bankfull flows were generally performed in 0.5 m intervals across the stream width. Measurements were repeated once or twice daily (or nightly, respectively), depending on the variation of stage height. Water discharge was determined from the velocity measurements. Using the continuous stage records and a separate stage-discharge relationship each year allowed us to establish the hydrographs for 1986 and 1988.

4.2.2 Water surface gradient

The water surface gradient was measured using two tube levels. The measuring principle of tube levels is explained in Figure 4.2. The upstream ends of two garden hoses were placed 17.3 m apart on the left bank upstream from the measuring reach. The hose ends were staked to the stream bottom perpendicular to flow. The hoses were then run along the stream bank down to the measuring site, where both hoses were bent vertically upwards and fastened on a board next to a meter stick. The water level in the hoses indicates the height of the water surface in the stream above the hose ends. The difference between the two water level readings in the hoses divided by the distance between the two hose ends gives the water surface slope over the reach between the two hoses. The position of the tube levels is pictured in Figure 3.9 (see culverts on the banks) and indicated on the maps in Figures 3.7 and 3.8.

4.2.3 Fluid density and viscosity

Water temperature, electric conductivity, and turbidity were either registered continuously or readings were taken in 1-to 2-hour intervals to determine density and viscosity of the water. In order to ensure that the water for turbidity monitoring represents the average cross-sectional suspended sediment concentration, a water pump was attached to a raft and positioned into the turbulent flow under the measuring bridge (fig. 3.13). Water was pumped from here continuously into a Hach turbidity meter, installed in an instrument shelter, and from there back to the stream. When turbidity changed, width- and depth-integrated suspended sediment samples were taken using a DH-84 sampler. Several rating curves between turbidity and suspended sediment concentration had to be established to account for the variable composition of suspended matter during the course of the high flows. A continuous record of suspended sediment concentration was thus obtained.

During the course of snowmelt high flow water temperature varied between 4° and 13°C. The effect of changes in water temperature on the water density is so minimal (Gertsen et al. 1974: 213) that water temperature is not accounted for in any fluid density consideration. The same is true for the concentration of dissolved matter, which at Squaw Creek is mainly calcium bicarbonate in concentrations of roughly 100 mg/l (Ergenzinger 1984). The highest suspended sediment concentration measured in 1986 and 1988 reached 1.6 g/l. This value is likewise too small to affect the water density relevantly.

---

[3] The substantial measuring bridge, newly installed in 1990, makes it possible to carry out flow velocity measurements in higher flows, since the rod can be wedged into notches and the bridge with its railing provides a firm stand for the operators.

The kinematic viscosity (v) of water increases with water temperature and is 0.0125 cm²/s for 4°C and 0.0155 cm²/s for 13°C. This effect is also considered to be negligible.

4.3 Sedimentological Analyses

4.3.1 Particle weight

The hydraulic forces propagating entrainment are counteracted by particle weight. Particle weight is a function of particle density and particle volume. The lengths of the three particle axes have to be known if volume is determined from particle dimensions. If particle shape is not too different from a sphere, particle dimensions can be approximated by the length of the *b*-axis (particle diameter).

4.3.2 Particle stability

Besides particle weight, entrainment is largely determined by particle stability. Einstein (1937: 67) remarked that "...the behavior of a single particle in flow is not only dependent on the hydraulic conditions, but is also highly influenced by the sedimentary conditions of the surrounding channel bottom."[4]

Particle stability does not only result from the particle rank within the grain-size spectrum (fig. 4.1). Even particles of the same grain-size can exhibit different stabilities. The absolute and the relative size, as well as the position to neighboring particles causes favorable or unfavorable conditions for stability, or entrainment, respectively.

Several approaches have been tried to quantify the stability of a particle among neighboring particles. Einstein (1950) applied the hiding fac-

$$S_w = (d1 - d2) / (x1 - x2)$$

d 1   water surface level indicated by upper slope tube
d 2   water surface level indicated by lower slope tube
x 1   length of upper slope tube
x 2   length of lower slope tube
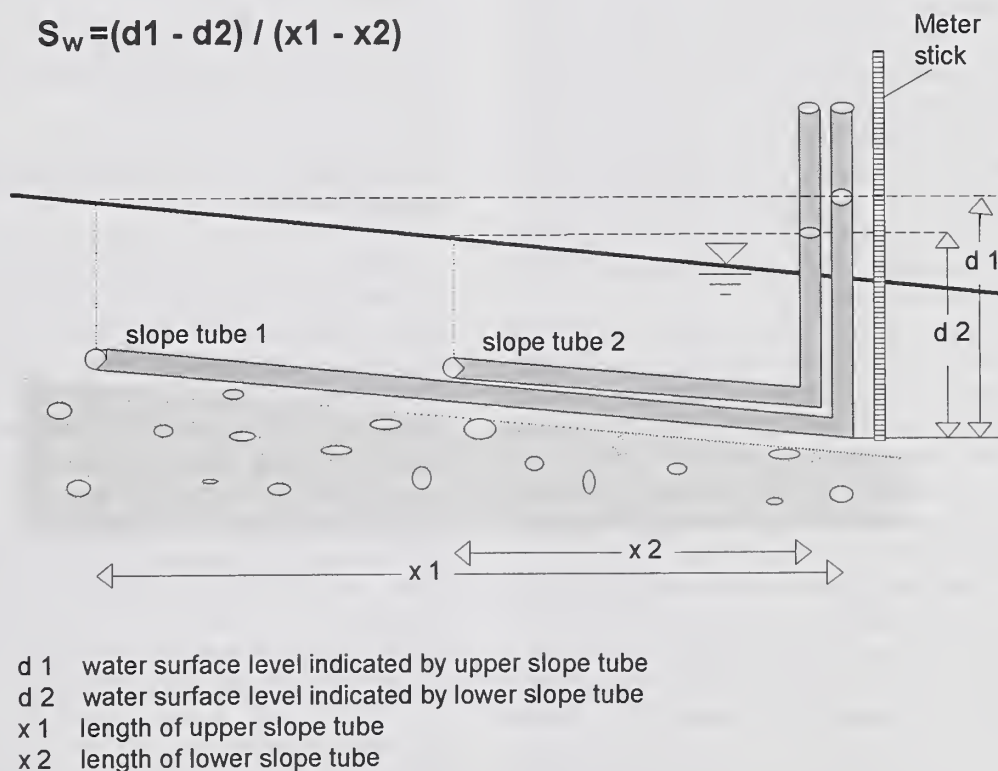
Figure 4.2 – The measuring principle of tube levels to measure water surface slopes (Bunte 1984: 73).

---

[4] Translation of citation "...daß das Verhalten des einzelnen Steins im bewegten Wasser nicht nur von den hydraulischen Bedingungen, sondern auch wesentlich von der Art der umgebenden Sohle beeinflußt wird."

tor, while Fenton and Abbott (1977) expressed stability by **relative protrusion**. Andrews (1983), Hammond et al. (1984), Bathurst (1987), and Wiberg and Smith (1987) describe in the so-called **Andrews' plot** how the critical shear stress needed for the entrainment of a certain particle size (D_i) from a grain-size mixture decreases as the grain size of the entrained particle increases. The grain size of the entrained particle (D_i) is normalized by putting it into relation with the median grain size (D_{50}) of the channel bottom material to obtain the relation D_i/D_{50}.

Komar and Li (1986), Komar (1987, 1988), and James (1990) use the **pivot angle** to quantify particle stability. The pivot angle is the angle a particle has to overcome as it rolls over the next particle, which is partly under and partly in front of it. The authors confirm the relatively high mobility of large particles and show for different sediment mixtures that higher shear stresses than indicated in the Shields diagram are needed to entrain small particles $(< D_{50})$, while particles $> D_{50}$ require lower shear stresses than indicated in the Shields diagram, which is based on unit sediment size. Ferguson et al. (1989) made similar observations for sandy sediment mixtures in a braided stream where particles coarser than sand were usually more favorably transported. This transport advantage of coarse particles can, of course, only extend to that grain size for which the flow has the competence. All larger particles remain in place and lead to a surface armoring.

Another aspect of particle stability refers to **particle clusters**. Brayshaw et al. (1983), Reid et al. (1984), Reid and Frostick (1984), Brayshaw (1985), and Billi (1988) found generally less favorable conditions of entrainment and transport for particles that were part of particle clusters[5]. Particle shape and sphericity also affect entrainment and transport rates (Komar and Li 1986; Gintz 1990; Schmidt and Ergenzinger 1992; Schmidt et al. 1992; James 1990; Carling et al. 1992). None of these aspects will be acknowledged in this study.

All of these studies on particle stability indicate that bedload transport with its specific grain-size distribution and its temporal variability is affected by the particle-size distribution of the river bottom. This size distribution causes the variability of particle stability and entrainment, and thus different transport intensities of particles of different grain sizes. The coarser and the wider the grain-size spectrum of the river bed, (i.e., the rougher a mountain stream bed), the larger the inhomogeneity of the stream bottom with respect to entrainment conditions and transport intensity[6].

The roughness of the stream bed is usually described by either **grain roughness**, which is characterized by a statistically relevant grain-size diameter (usually D_{50} or D_{84}), or by **relative roughness**, which is the ratio of grain roughness and water depth (e.g., D_{50}/d). Carling (1983), Bathurst (1985), and Wiberg and Smith (1987), for example, point out that the flow forces needed for entrainment (e.g., the mobility number) become lower the larger the relative roughness is, and the relative roughness decreases with increasing flow. However, all of these studies can only indirectly infer the variability of relative roughness from a change in water depth. The temporal and spatial variability of the channel bottom grain roughness itself which is attributable to the variability of the channel grain-size distribution can usually not be observed during high flows.

4.3.3 Spatial and temporal variability of roughness

The spatial variation of the grain-size distribution at the stream bottom could be analyzed if a rather large measuring effort was made. Detailed grain-size analyses could be carried out by sampling the stream bed during low flows (e.g., Mosley and Tindale 1985; Klingeman and Emmett 1982). Another method is the photo sieving procedure (perfected by Ibbeken and Schleyer 1986) where photos of the pebble and cobble cover of the stream bottom are digitized and areal percentages covered by a certain grain-size class are computed. A computer program then converts these fractional cover percentages into a channel bottom grain-size distribution.

The stream channel grain-size distributions to which this study refers were determined by Custer et al. (1987) and Bugosh (1988) during low flows. The need existed to develop new measur-

---

[5] The construction and destruction of particle clusters under various flow conditions was examined at Squaw Creek by De Jong and Ergenzinger in 1991 and 1992 (De Jong 1993).

---

[6] The above considerations do not include the aspect of sediment supply. A high supply of fine-grained sediment to a rough stream bed would probably result in high transport rates of fine material once the interstices are filled.

ing techniques that would register the spatial and temporal variation of grain and form roughness or relative roughness, respectively, which affect the energy balance of the stream and are likewise affected by the energy balance. These techniques need to be fast, work for both grain and form roughness, and be applicable during high flow conditions with bedload transport.

First experiences with such a cross-sectional profiling device were gathered at Squaw Creek by Ergenzinger and Berry in 1988 (Berry 1988). The methodology (explained in Section 4.5.2) made it possible to determine the spatial and temporal variation of the channel bottom shape and roughness along a cross-section during a high flow event (fig. 4.6). The methodology was further developed by Ergenzinger and Stüve (1989), and Ergenzinger (1992) who expressed channel bottom roughness by **k3-value**s[7]. The spatially and temporally variable, dynamic k3-value can then be integrated into various roughness analyses instead of a relevant grain-size diameter[8].

4.4 Sedimentological Measurements

Only a few measurements of coarse bedload transport exist in natural streams. Even more rare are temporally high resolution or continuous measurements, which make it possible to analyze the temporal variability and the grain-size spectrum of the transported material. In order to obtain data sets that would facilitate such analyses, several sedimentological parameters were measured at Squaw Creek during the field seasons of 1986 and 1988:

- temporal variation of coarse bedload transport,
- grain-size distribution of transported material and gravel bar deposits,
- particle transport rates,
- spatial and temporal variation of bedload grain sizes within a cross-section,

- and partially: temporal and spatial variation of cross-section geometry and roughness.

Before sampling methods and sedimentological analyses used at Squaw Creek are described, field techniques that facilitate a continuous or high temporal resolution record of coarse bedload transport will be reviewed.

4.4.1 Techniques for determination of coarse bedload transport under natural conditions

Manual bedload samples can be taken repeatedly and over extended time periods using bedload samplers (Emmett 1980*[9]; Emmett et al. 1982*; Jackson and Beschta 1982; Gomez 1983; Pitlick and Thorne 1987; Kuhnle et al. 1989), but this procedure is very time- and labor-consumptive while the temporal resolution is limited.

Indirect automated methods measure signals that produced by bedload transport. Schlatte (1984), Heathershaw and Thorne (1985*), Thorne et al. (1989), and Williams et al., (1989b*) used a hydrophone to register acoustic signals during bedload transport. Shock waves created by bedload bumping over a steel plate can be registered by piezoelectric sensors (Bänzinger and Burch 1990). Lenzi et al. (1990) and D'Agostino (1994*) used ultra sound waves to continuously scan the volume of bedload that accumulated in a large debris trap. The magnetic tracer technique makes use of artificially magnetic (Ergenzinger and Conrady 1982; Arkell et al. 1983; Reid et al. 1984) or naturally magnetic tracers (Section 4.4.2) which, induce signals as they pass a detector in the stream bottom. None of these procedures, however, makes it possible to continuously register the grain sizes of bedload transport.

Automated and direct measurements of the transported bedload can be achieved by a weighable bedload trap that monitors continuously the summed weight of the collected sediment (Reid and Frostick 1984, 1986; Reid et al. 1985; Lewis 1991*). However, the size of the trap often determines the duration of the monitoring,

---

[7] A k3-value is the larger of the two differences of three neighboring depths readings. Since one of the readings is replaced by a new reading as the measurements proceed across the stream width, each width increment is attributed a k3-value.

---

[8] Encouraging results regarding the measurability of the temporal variability of the cross-sectional micro-topography during high flows led to the development of a more stable device for Squaw Creek in 1991. The new device is firmly attached to a bridge and provides a better reproducibility of measurements. Detailed measurements of the cross-sectional stream topography, its temporal change and association with bedload transport were performed at Squaw Creek by De Jong and Ergenzinger in 1991 and 1992 (De Jong 1993; Ergenzinger et al. 1994).

---

[9] Citations with an asterisk (*) were added during translation.

because the traps can be filled to capacity before the end of a high flow event.

This problem does not occur in well equipped vortex or conveyor belt samplers. These samplers collect the entire bedload in a trap, usually a semi-circular tube, which is fitted flush into a concrete-lined stream bottom and which runs diagonally across the channel width. A spiraling flow develops in this "vortex tube" and carries sediment to the side of the stream where the water and sediment mixture gushes from an outlet in a retention wall into a sediment collection pit. A conveyor belt in the trap can support the lateral transport of bedload towards the collection pit. After the sediment has been weighed or sampled for further analyses, the surplus sediment is automatically carried back to the stream. These expensive and sophisticated devices have only been installed in a few streams: Oak Creek in Oregon (Milhous 1973*); Torlesse Stream in New Zealand (Hayward and Sutherland 1974*; Hayward 1980*); East Fork River in Wyoming (Leopold and Emmett 1976, 1977; Emmett 1980*; Emmett et al. 1980*; Klingeman and Emmett 1982); and in Virginio Creek in Italy (Tacconi and Billi 1987)[10]. A large part of the present analyses of the grain-size distribution of coarse material bedload transport is still based upon a data set that was collected by Milhous (1973) in the beginning of the 1970's and that since then has been reanalyzed in several publications. It is, however, not recommendable to base a large portion of the analyses of bedload transport grain-size distributions on a data set collected at a single stream. Data sets suitable for detailed analyses need to be collected in several different streams to account for different bedload processes in different stream types. Understandings about bedload transport gathered in one stream are not necessarily transferable to a different stream type.

During the Squaw Creek study, bedload transport was measured using two different systems:

- continuously with the **magnetic tracer technique** in order to analyze the temporal variability of bedload transport, and

- episodic and consecutively using a **Helley-Smith** and a **net-bedload sampler** in order to compare signal rates and actual particle transport rates and in order to analyze the

variability of grain-size distributions of coarse bedload transport.

4.4.2 Magnetic tracer technique

Among the various tracer techniques that can be used for coarse bedload (Bunte and Ergenzinger 1989), the magnetic tracer technique was appropriate for the conditions at Squaw Creek, because about 70% of the pebbles and cobbles are naturally magnetic and can serve as natural tracers.

4.4.2.1 Development of the magnetic tracer technique used at Squaw Creek

The development of the magnetic tracer technique to detect coarse material bedload transport goes back to Ergenzinger and Conrady (1982). The technique is based on the Faraday Induction Principle: a magnet passing a coil induces a voltage peak. The voltage change over time takes a sine-wave like form. Ergenzinger and Conrady (1982) used artificially magnetic tracers in their early experiment in a braided river in Calabria (southern Italy). They drilled holes into cobbles and inserted magnets. Since this was a tedious and non-practical enterprise, Squaw Creek was discovered as a site where naturally magnetic rocks could be used as natural tracers. First experiences of these studies were made by Ergenzinger and Custer (1982, 1983) who amplified and registered voltage signals induced by magnetic tracers as they passed a detector log installed in the bottom of the stream. First results regarding the temporal variation of bedload signals were demonstrated by Custer et al. (1986, 1987).

This early detection system (Ergenzinger and Custer 1982, 1983; Custer et al. 1986, 1987) needed to be improved in several aspects to meet the following requirements:

- bedload transport should be measurable in its spatial variability across the stream width,

- the signal–noise difference should be increased,

- electronic noise should be reduced, and

- a computer-based processing of the recorded signals should be achieved.

---

[10] Experiments have been carried out with a suspended vortex sampler at Squaw Creek in 1992. A flume of about 1.5 m width attaches at the overflow directly beyond the detector log. This flume leads the water and sediment mixture into a vortex tube at the end of the flume. The vortex tube reaches to a shallow bank where the bedload sediment can be caught in baskets.

Spieker (1988) developed a new magnetic tracer detection system for Squaw Creek in which both the detector log as well as the electronics were completely renewed. The new system was used during the snowmelt high flow in 1986.

4.4.2.2 Construction of the new measuring system[11]

The improvement of the measuring system started with the development and construction of a new detector unit in the stream bottom. Whereas the old detectors comprised physically individual units, which were prone to destruction and erosion, the new detector unit houses its electronics in a single, large wooden log that spans the entire stream width (fig. 3.13) and is held in place by the logs at the foundations of a vehicle bridge (fig. 4.3). The detector log is mantled with an aluminum cover to provide some protection against abrasion. The flush position of the detector log with the upstream channel bottom, and a small overflow on the downstream side of the log causes accelerated flow, which ensures that all particles are quickly transported over the detector log. A fast particle transport over the detector log is not only essential for a large signal amplitude, but it also makes sure that no pebbles are trapped in interstices close to the detector log where they could vibrate and cause noise signals.

Two parallel notches are cut into the upper side of the detector log about 15 cm apart. Each notch is about 1 inch wide and deep and houses 10 coils that are each 0.7 m long. Two coils are always wired together and form a unit 1.55 m long, including all spaces for wires, etc. The 5 coil units together span the entire stream width of 8.5 m at the bridge. The construction plan for the detector log is given in Figure 4.4. In order to ensure an even sensitivity over the length of a coil unit, each coil unit comprises 310 vertically mounted chokes[12], which were glued into plastic u-profile slots and connected in series. Each unit is placed into a second, slightly larger plastic u-profile slot where some space is allowed for the wiring. Finally, the entire second u-profile slot is filled with epoxy, covering coils and wires. These coil units are placed end to end into the notches in the de-

Figure 4.3 – Detector log is installed flush with the river bed and spans the entire stream width.

tector log. After all the wiring is in place, superfluous space in the notches is likewise filled to the rim with epoxy.

The requirements of a high signal-noise difference implies a strong amplification of the small bedload signals but, nevertheless, electronic noise should be suppressed. One way to solve part of this problem is the exclusion of at least externally derived noise. Therefore, coils were placed in two parallel rows. Signals that occur simultaneously on both the upstream and the downstream coil, and which are identical in their course over time, are identified as noise (e.g., due to alternating cur-

---

[11] The first two paragraphs of this chapter have been slightly extended during translation to provide a little more detail of the measuring system. For more detail regarding the construction of the detector log see the thesis by Spieker (1988). The second detector log installed at Squaw Creek in 1990 was also constructed according to Spieker (1988).

[12] A choke is an electronic part, less than half the size of a sugar cube; coils containing thin copper wire windings on a ferric core.
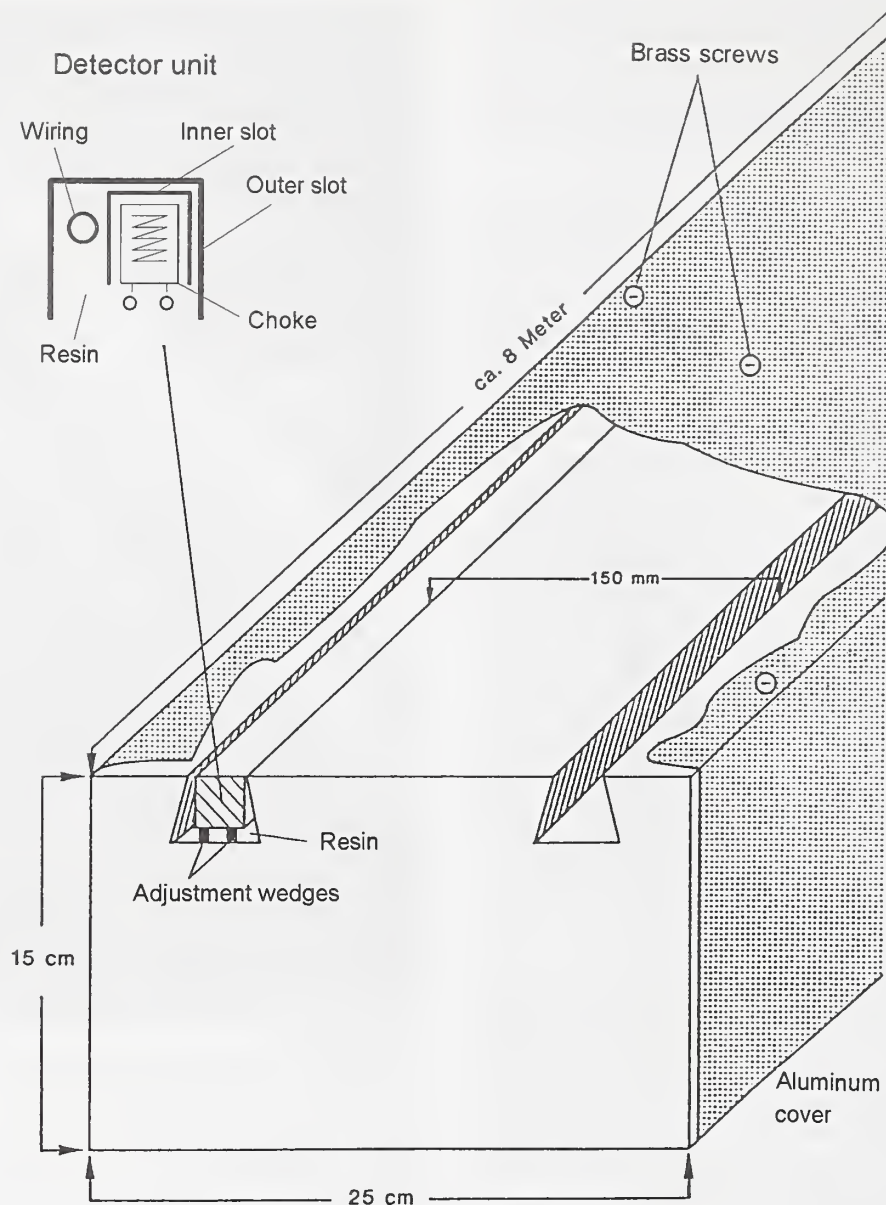
Figure 4.4 – Cross-sectional view of the detector log (Spieker 1988: 33, Spieker and Ergenzinger 1990).

rent in the power supply line, radio reception, lightning strikes, or impacts and vibrations of the detector log) and eliminated.

The time difference between two signals, recorded at the upstream and the downstream coils, can be used to calculate the velocity of the particle that crossed the detector log. The temporal variation of the voltage peak that is induced by a magnetic particle as it passes the detector log is shown in Figure 4.5. The duration of a bedload signal (time during which the voltage is changed) is 0.2–0.3 s for grain sizes between 30 and 70 mm

and decreases as the particle transport velocity increased over the detector log during higher flows.

4.4.2.3 Capacity of the magnetic tracer device

The measuring system as used in 1986 was set up to dependably produce signals if the magnetic field strength of the passing particle exceeded 40 gamma (which is statistically associated with grain sizes > 30 mm). Given the percentage of magnetic rocks > 30 mm, a total of 40% of the coarse bedload material can be registered at
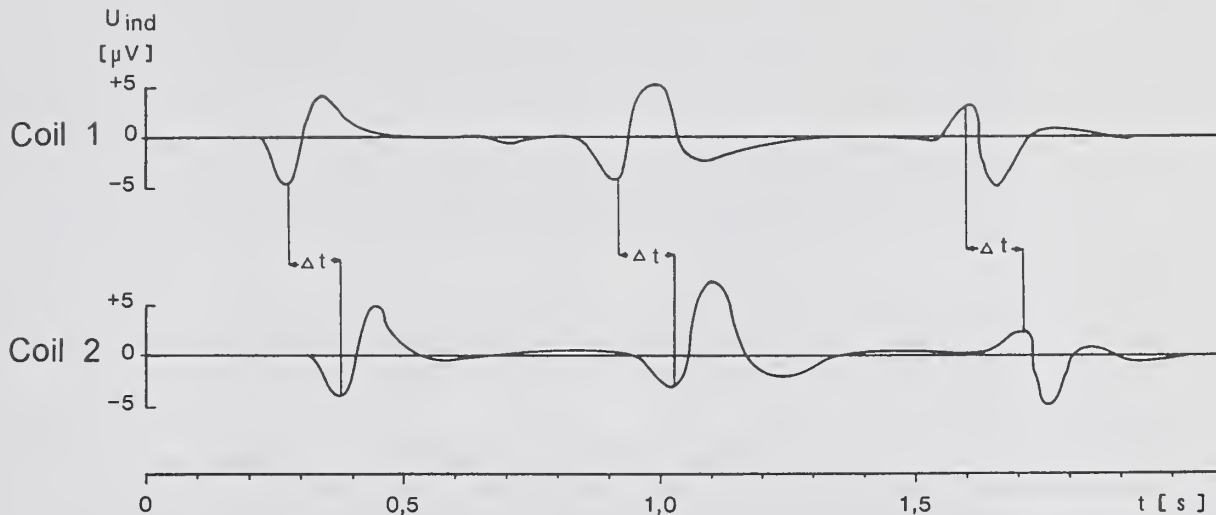
Figure 4.5 – Typical signals induced by natural magnetic tracers from Squaw Creek (Spieker 1988: 68).

Squaw Creek when using the magnetic tracer technique.

Analysis was needed regarding whether the capacity of the magnetic tracer technique would suffice to register particle transport rates expected at Squaw Creek during the usual snowmelt high flows. The duration of a signal is 0.2–0.3 s or less. Let us assume for the following considerations that, for reasons of simplicity, all particles >32 mm have the same constant velocity as they pass the detector log because flow at that location is accelerating. If all particles >32 mm take 0.25 s to register their signals, a maximum of 4 particles can be registered per second over a 1.55 m detector unit. This equals a particle transport rate of 160 pebbles and cobbles per minute per meter width. The largest bedload transport rate measured with the large frame sampler during the spring high flow of 1988 yields a transport rate of 43 pebbles and cobbles per minute per meter width (Table 1). A comparison between these two values shows that the

capacity of the magnetic tracer measuring device is generally sufficient for conditions during usual snowmelt high flows. The limits of the capacity will only be reached at a fourfold increase of particle transport rates, a value that is not to be expected during ordinary snowmelt high flows.

The measuring device, including concepts for further development, is described in more detail by Spieker (1988), Bunte et al. (1987), and Spieker and Ergenzinger (1990)[13].

Table 1. Number of particles transported in various grain size classes during the highest measured transport rate in 1988 ("usual" spring high flow).

Grain-size (mm)	Number of particles (particles/m·min)
32 - 45	28
45 - 64	12
64 - 90	2
90 - 125	0.7
125 - 180	0.06
total of particles > 32 mm:	43

---

[13] *R. Spieker's concept of signal registration included a frequency modulation in which the course of the signals (sine-wave-like temporal variation of the voltage peak induced by the magnetic particles) was transformed into the temporal variation of a sound that was then stored on a tape recorder. This procedure should ensure that not only the count of a signal but the entire course of a signal would be registered and could be used for a further analysis regarding the size or the velocity of the particle that caused the signal. This concept did not work for the continuous registration of bedload signals during the entire high flow in 1986. A new registration system for bedload signals induced by the magnetic tracer technique was designed in 1990 and 1991 at the Technische Fachhochschule, Berlin, by U. Achter and J. Brüggmann who completed a Master's degree under the supervision of Prof. G. Christaller (Achter and Brüggmann 1991). The electronics of the new registration system are linked to a computer that counts bedload signals for preset time intervals and provides numerical print-outs. Signal rates were recorded for a few days during the high flow in 1991 (De Jong 1993; Ergenzinger et al. 1994).*

4.4.3 Analyses of the bedload signals

Signals from several detector units were recorded simultaneously on a multi-channel strip chart recorder, which had to be able to graphically present the fast signals in a readable way. Figure 4.6a-b shows sections of the original strip chart records. A continuous registration of bedload signals over a period of several weeks shows fluctuating signal rates and amplitudes. This makes it difficult to chose an optimum speed for the paper advance and the degree of amplification, especially when one cannot be present at the stream to estimate the sediment transport intensity. A continuous fast paper speed can lead to problems in the paper advance mechanism and to financial constraints. A slow paper advance makes it difficult to distinguish between individual signals. When the measuring system was designed, the strip chart records were only meant to serve as a visual control of the registration. The paper advance was therefore usually set to a rather low speed of 1 mm/min. Practically, however, the entire analyses of bedload signals had to be based on the visual analyses of the strip charts (counting signals under a magnifying glass). Each signal is only depicted as an impulse that denotes the amplitude of the signal. The size of the particle cannot be inferred from the signal amplitude, because signal amplitudes are a function of several parameters:

- magnetic field strengths of the particles,
- distance between the particles and the detector log,
- velocity of the particles as they pass the detector log, and
- orientation of the magnetic axes of the passing particles in relation to the detector axis.

Although Spieker (1988) and Spieker and Ergenzinger (1990) suggest a methodology by which to deduce particle size from the duration of the signal, this methodology has yet to prove practical.

4.4.3.1 Determination of bedload signal rates

Coarse material bedload transport of magnetic particles was continuously registered on the central three detector units with the magnetic tracer device. The record extends over a period of almost 3 weeks (May 27–June 14) during snowmelt high flow in the spring of 1986.

Bedload signal rates were determined from long strip charts by counting signals from the detector unit 7/8 in the thalweg of the stream. Signals were summed for 1-hour intervals. Only signals with an amplitude larger than 1 mm were counted, and no further differentiation was made for larger signal amplitudes. This 1-mm threshold value was introduced because, during times with high signal rates, large signals could be counted more easily and more representatively than small signals. Time intervals with very high signal rates (>200 signals per hour) are generally difficult to quantify by counting signals from the strip charts.

Noise signals stemming from lightning strikes and vehicles can be easily identified and eliminated. Bigger problems are caused by noise attributable to differences in the electric potential of the various grounds. The ground from the power supply is different from the local ground in the shelter, which is again different from the local ground in the stream. Electronic noise is also created by people or bedload samplers moving close to the detector log or by other nonidentifiable sources. Usually, noise signals can be visually identified, but they cannot always be electronically prevented, and they interfere with the signal recording and the visual counting process.

In order to find out how well counted signal rates correspond to actual bedload transport, counted signal rates were compared with various bedload samples. Problems in the transformation of signal rates to bedload transport arise from several sources:

- the determination of signal rates by visual counting can be problematic,
- the statistical minimum particle size that can be recorded under high flow conditions is not known (does the minimal recordable particle diameter increase or decrease?),
- signal amplitudes do not translate into particle size (Section 4.4.3), and
- the relation between signal rates and bedload transport rates is not known because small particles are not recorded and because the percentage of small particles in bedload transport is variable.

Signal rates were therefore compared with several data sets of bedload samples.
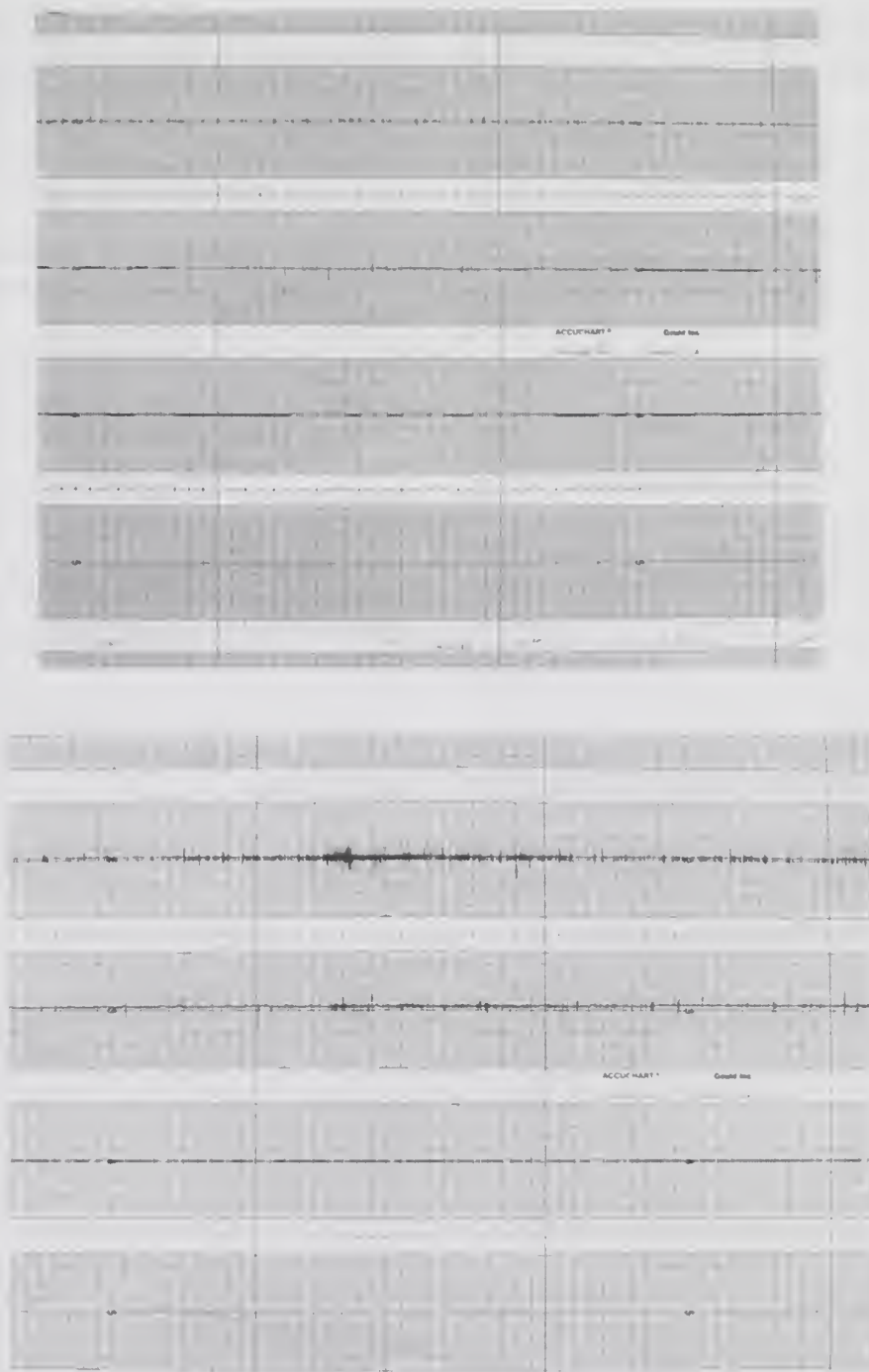
Figure 4.6 – Parts of strip chart records with signals from magnetic bedload particles.
Similar bedload transport intensities recorded with:
   a) fast paper advance of 5 mm/min,
   b) slow paper advance of 1 mm/min.

4.4.3.2 Comparison between bedload signal rates and temporally close bedload transport rates

The necessarily high detector sensitivity made it impossible to sample bedload with a Helley-Smith sampler close to the detector log while signals were being recorded. The electronic noise produced by this sampling disturbed the registration badly. A comparison between signal rates and simultaneous bedload transport rates is therefore not possible.

Alternatively, an attempt was made to compare signal rates with bedload transport rates that were sampled with a 3-inch Helley-Smith sampler half an hour before or after the registration of signal rates. This attempt failed for two reasons: a) the small Helley-Smith sampler is inappropriate for sampling pebble and cobble transport, and b) the signal rates fluctuate so much within half-hour time spans (fig. 4.7) that it is not possible to compare signal rates with temporally slightly lagged bedload transport. It had been planned for the next year's spring high flow to sample bedload transport with the large net-sampler, simultaneously with the registration of bedload signals. However, flows were not large enough during the spring high flow in 1987 to transport pebbles and cobbles. A calibration attempt could also not be repeated in the spring of 1988 because the magnetic tracer device malfunctioned and could not be repaired. A different approach had to be found to investigate the relation between signal rates and bedload transport.

4.4.3.3 Comparison between signal rates (1986) and bedload transport rates (samples taken in 1988)

Snowmelt high flows in 1986 and 1988 were similar, both in their temporal variation as well as in their daily peak flows. Both high flows had been preceded by years in which flow was not large enough to move pebbles and cobbles. This probably provided similar sedimentary conditions on the river bed for both years. It could then be assumed that bedload transport rates during the high flows in 1986 and 1988 are similar with respect to their amounts and grain-size composition. Therefore, an attempt was made to compare bedload signal rates registered in 1986 with bedload transport rates sampled in 1988 during similar flows.

The first step of this analysis was to determine the hourly transport rates of magnetic rocks in the size classes > 32 mm and > 45 mm for bedload
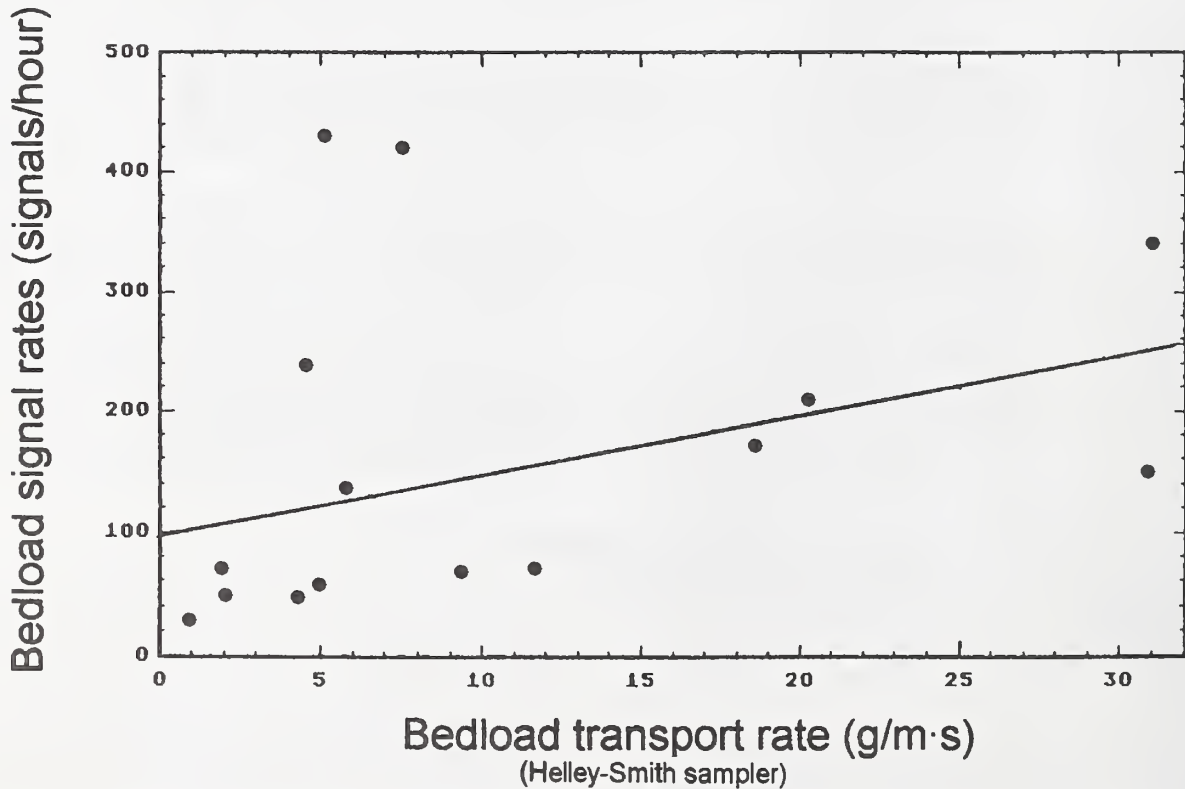
Figure 4.7 – Relation between signal count rates and bedload transport rates determined from samples taken with a 3-inch Helley-Smith sampler: $Qb_{sign} = 4.89 \, Q + 97$; $r^2 = 0.12$.
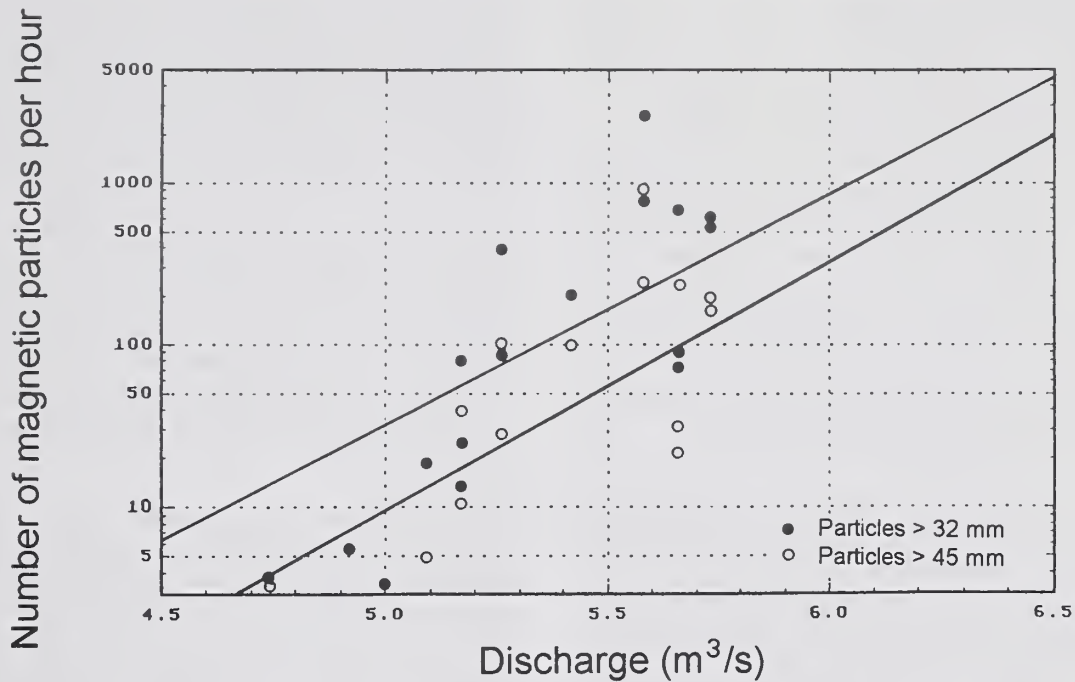
Figure 4.8. – Relation between hourly count rates of magnetic bedload particles in the net-sampler and flow discharge (1988) for two grain-size classes: a) >32 mm, and b) >45 mm.
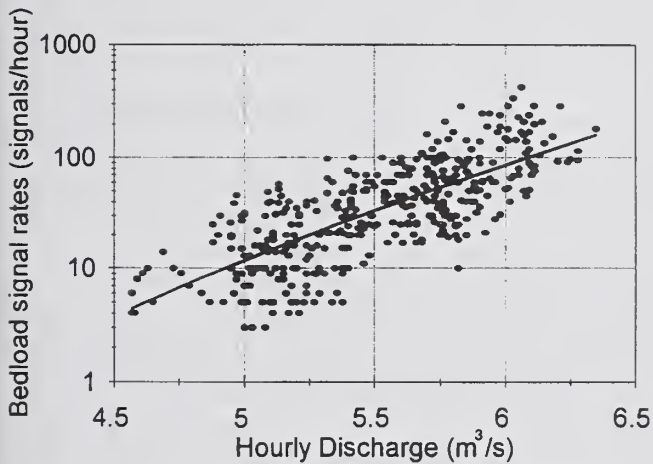
Figure 4.9 – Relation between hourly bedload signals rates and water discharge (1986): $Qb_{sign} = 2.68E-7 \cdot Q^{10.93}$, $r^2 = 0.56$.
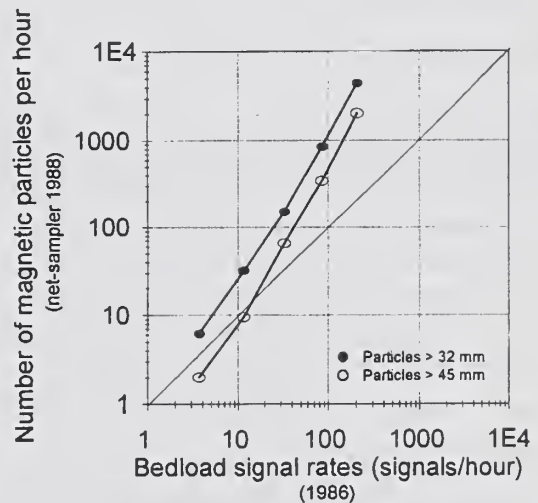
Figure 4.10 – Relation between hourly count rates of magnetic particles in samples from the net sampler (1988) and signal count rates (1986).

samples collected with the large net-frame sampler in 1988. These numbers were plotted versus the discharge values at the time when the samples were taken (fig. 4.8). Hourly bedload signal rates registered in 1986 were likewise plotted versus discharge (fig. 4.9). Regressions were fitted for both the relations. The data scatter is necessarily large for both sediment transport–discharge relations, because bedload transport is highly variable in its amount and grain-size composition. Using

these regressions, the number of particles >32 and >45 mm transported per hour was plotted versus the number of signals per hour for five discharge values between 4.5 and 6 m³/s (fig. 4.10). Perfect agreement between signal count rates and particle transport rates would yield a plot with data points along the diagonal. However, most of the data plot above the diagonal. This means that for large discharges the number of magnetic particles collected in the sampler exceeds the signal count

rate by a factor of 2 for particles >45 mm and even by a factor of 5 if the size range of the magnetic particles includes particles down to the size of 32 mm. This discrepancy can have three origins:

- the minimum grain size that can be registered dependably by the magnetic tracer technique during high flows is 45 mm or more instead of 32 mm as suggested by Spieker (1988),
- particle transport rates are different in both years, or
- a systematic mistake was made when counting signal rates on the strip charts.

The latter is the most plausible explanation. It was mentioned earlier (Section 4.4.3.1) that the counting procedure had been limited to large, better discernible signals with more than 1 mm amplitude, but this limitation was apparently not strict enought. So when bedload signal rates were tightly spaced on the strip charts, many of the small "tick marks" must have been overlooked. Thus, counted signal rates are too low for times of high bedload transport.

4.4.4 Representative bedload samples

Representative sampling of coarse bedload in mountain streams needs to meet several, usually incompatible, demands. Bedload samples need to be

- large enough to representatively include the large sizes,
- taken frequently enough to account for temporal variability of bedload transport,
- small enough to be maneuverable,
- taken at representative locations,
- taken with "doable" sampling effort.

Therefore, coarse material bedload sampling in mountain streams presents usually a compromise between the fulfillment of different demands.

There are no clear rules regarding the sample volumes and the sampling durations of bedload samples for representative grain-size analyses. Anastasi (1984) recommends a sample volume of 0.25 m³ if the maximum grain size is 100 mm. Ib-

beken (1974) suggests for the same D_{max} a minimum weight of 180 kg or a collection of at least 5 individual particles per grain-size class. The German DVWK[14] Bulletin "Solid Matter Transport in Streams" (1988) does not include grain sizes as large as 100 mm in its recommendations regarding necessary bedload sample volumes. Church et al. (1987) indicate necessary sample weights for various maximum grain sizes and degrees of accuracy in their Figure 3.9. If a D_{max} of 100 mm is to be represented by 0.1% of the sample mass, the total mass of the samples needs to be 1,400 kg. If the accuracy is reduced to 1%, the sample mass can be reduced to 140 kg. Bedload samples that large could not be collected during high flows at Squaw Creek.

In order to investigate the temporal variation of bedload transport and its grain-size distribution, samples have to be taken frequently and for short intervals (minutes) only. The sampling interval, however, needs to be long enough to sample enough material for a grain-size analysis of the coarse fraction of bedload. Besides, the practical aspect of sampling demands that samples are kept small to stay maneuverable in a fast flowing stream.

Given that bedload sampling is generally only part of the field program, it is nevertheless disproportionally labor-intensive and time consuming. At Squaw Creek it took the combined efforts of three persons for almost an hour to take one sample of coarse bedload with the large frame net-sampler. A small measuring crew is another problematic factor for bedload sampling.

4.4.4.1 Helley-Smith sampler

The standard sampler for bedload is the Helley-Smith sampler with a 3 by 3 inch or a 6 by 6 inch opening and a bag that holds about 10 kg of sediment and has a 0.25 mm mesh width. This sampler and its sampling properties are described in detail by Emmett (1980, 1981, 1982 and 1984). The advantages of a simple, low-cost, and, if flows are shallow and low, easy-to-handle device are counteracted by some pronounced disadvantages: if the channel bottom is rough, the contact between sampler and channel bottom is poor and fine-grained bedload moves in the gap between the sampler and the channel bottom. A constraint arising from the special conditions at Squaw Creek was that the metal parts used in the sam-

---

[14] *Deutscher Verband für Wasserbau und Kulturbau [German Association for Hydraulic and Civil Engineering]*

pler interfered with the magnetic tracer technique. In addition, the opening of 7.6 cm by 7.6 cm is too small to representatively sample pebble- and cobble-sized bedload. This limitation can only be partially overcome by using a larger Helley-Smith sampler. But as the orifice size becomes larger, it becomes increasingly problematic to hold the sampler in the stream.

During both high flows in 1986 and 1988 bedload samples were taken using a 3-inch, and sometimes a 6-inch, Helley-Smith sampler mounted to a wading rod in order to determine bedload transport rates and its fine material components. Samples were taken from a catwalk at the upstream side of the vehicle bridge about 1 m above the water surface (fig. 3.13).

Owing to the sampling conditions mentioned above, compromises were made regarding sampling intervals and frequencies and regarding the sample volumes. Disregarding the recommendations by Emmett (1988, 1981, and 1984: taking either one sample each 0.5 m or at least 20 samples per cross-section), sampling was limited to 8 cross-sectional locations spaced 1 m apart. Time constraints demanded this reduction. Sampling for 2 minutes at each cross-sectional location amounted to a total sampling time of more than 30 minutes per cross-section.

4.4.4.2 Net-bedload sampler

For bedload sampling and grain-size analysis at Squaw Creek, a sampler had to be developed that did not have the deficiencies mentioned above for the metal Helley-Smith sampler. Following preliminary experiments by Ergenzinger (1984) with a basket sampler (Mühlhofer 1933) a large net-sampler was constructed in which no metal parts were used. The wooden frame of the sampler fits with its orifice of 0.3 m by 1.55 m exactly over the width of one of the detector units on the stream bottom (Section 4.4.2.2 and fig. 3.13). The size of the orifice is large enough to sample even the coarsest material at Squaw Creek, and large volumes of sediment can be stored in the huge, 3-m-long net with 1-cm mesh width. Thus, all particles exceeding the grain-size class 11.2 mm can be sampled representatively (fig. 4.11a).

Although the net lets pass all particles <1 cm, the mesh width was purposefully chosen to be so large. The wide mesh-width lets the flow pass easily through the net. This keeps the pressure against the sampler at a minimum and ensures almost identical flow conditions inside and outside the sampler. Unfortunately, the net-sampler requires three people to operate it, but under con-

ditions of high flow, this net-sampler is more manageable than a Helley-Smith sampler, and it allows one to collect rather large sample volumes.

In order to provide a secure position for the net-sampler during the sampling interval, two strong wooden posts were fastened vertically between the catwalk and the stream bottom where they were wedged between some logs that span the stream at the upstream side of the vehicle bridge. The flow presses the frame of the net-sampler firmly against the wooden posts and places it securely just downstream of the detector unit 7/8 in the thalweg of the stream (fig. 4.11b). The snug fit of the sampler with the wooden logs ensures that no sediment can escape below the frame. The net floats in the stream at the downstream side of the log overflow. After the sampling time is over, the frame is pulled vertically out of the water, using a come-along that is fastened at the railing of the vehicle bridge. When the frame is just out of the water, the pressure of flow against the sampler is so far released that one of the vertical posts can be pulled out. The frame, held by a thick rope, floats downstream, pulling the net behind. Another rope pulls the frame, including the net and the bedload sample, onto the next shallow bank where the contents of the net is emptied into buckets.

One measuring cycle, excluding the actual sampling time, takes about an hour and requires the full strength of three persons. Sampling intervals were variable and lasted between 5 minutes and 1.5 hours, depending on the expected amount of bedload transport. Apart from episodic samples, consecutive samples were taken each 2 hours during two long-term sampling series.

4.4.5 Grain-size analyses

The Helley-Smith sampler provided sample sizes between 20 g and 6.3 kg. The grain-size spectra reached from sand to small cobbles. Samples from the net-sampler weighed between 100 g and 90 kg. The b-axis of the largest sampled cobble was 170 mm.

The sandy samples from the Helley-Smith sampler were first oven-dried (one day at 105°C) and weighed, then the organic particles (mostly conifer needles and larval cases of caddisflies) were eliminated by repeated washing. Afterwards the sample was dried again and weighed to determine the organic contents. The coarse samples from the net-sampler could be air-dried and organic material (mostly twigs and pine cones) could be picked out.

Figure 4.11 – Net-sampler with large wooden frame for coarse bedload at Squaw Creek:
a) sampler with 0.30 m by 1.55 m opening and 10 mm mesh width,
b) net-sampler in the stream causes only minor flow disturbance.

All samples were hand-sieved using wire mesh sieves in 0.5 ϕ intervals and the individual grain-size fractions were weighed. Weight and dimensions (the three axes) of cobbles > 64 mm was recorded individually for each particle. The number of particles was determined for each size fraction > 11.2 mm.

The small orifice of the 3-inch Helley-Smith sampler did not sample the coarse fraction of the bedload representatively. Grain-sizes were therefore only grouped into three fractions: sand (0.25 - 2 mm), fine gravels (2 - 22.4 mm) and coarse gravels (22.4 - 63 mm). The results of this analysis are presented in Table 2 in the appendix.

4.4.5.1 Percentiles and grain-size parameter

The cumulative weight percentages of individual grain-size fractions (sieve curves) do not plot as perfectly straight lines on probability paper (fig. 4.12 a-d). The question arises whether the samples are normally (Gaussian) distributed or not. The procedure developed by Schleyer (1987)[15] was used to determine the percentage agreement of the sample distribution with a Gaussian distribution. The percentage agreement ranged between 86 and 98% with a mean of 94%. Grain-size distribution can be said to resemble, but not to fit exactly a Gaussian distribution. The percentage fit does not improve for Rosin-type[16] distributions.

Although grain sizes of coarse material bedload samples are not exactly Gaussian distributed, an attempt was made to characterize the grain-size distributions using a standard grain-size analysis. The grain-sizes of the percentiles D_5, D_{16}, D_{25}, D_{50}, D_{75}, D_{84}, and D_{95} were graphically determined from the plot of cumulative weight percentages. Not all of the sieve curves reached 84 or 95% in the probability plot because the weight of the largest grain-size class often accounted for more than 5% of the total weight. These truncated grain-size distributions required that the respective percentiles were determined by extrapolation.

Fluvial grain size distributions are generally described by the Folk and Ward (1957) parameters. Another option is provided by the moment method where the moments 1-4 describe similar characeristics as the parameters "mean," "sorting," "skewness," and "kurtosis." "Mean," the coefficients for "sorting," "skewness," and D_{max} were determined for all samples collected with the net-sampler. Results are presented in Table 3a in the appendix. The same analyses were carried out for the coarse part (>11.2 mm) of the samples from the gravel bar and the stream bottom.

Results and discussion of these grain-size analyses are presented in Section 5.5.3. Compared to the **Folk and Ward (1957) parameters**, the **moments 1 to 4 (Schleyer 1987)** have the advantage that no high percentiles have to be extrapolated in truncated grain-size distributions. The moments were calculated using a computer program made by R. Schleyer[17]. The results of the grain-size analyses employing the **moment method** are described in Bunte (1990) and are not repeated in this text. The results are similar to those obtained by the Folk and Ward (1957) methodology, which are presented in this text.

4.4.5.2 Particle transport rates - an alternative method for grain-size analyses

Besides an improvement in the sampling technique to ensure a representative sampling of all (coarse) bedload grain sizes, grain-size analyses can only lead to comparable and detailed results (Section 5.5.4), if the methods used for a grain-size analysis are not affected by the fact that grain-size distributions can be truncated. A good method should further try to include and interpret irregularities in a grain-size spectrum, instead of trying to average it out. This can be achieved if the total sample volume is not referred to as 100%, because it is questionable whether the sample has collected the grain-size spectrum in its entirety. A grain-size analysis can only comprise that part of a grain-size spectrum which has actually been collected. The sampled bedload mass per grain-size class should therefore be the basis for further calculations, not a statistical average.

Individual particles interact at the channel bottom during bedload transport. The first step in

---

[15] R. Schleyer (formerly Dept. of Geology, Freie Universität Berlin) wrote a computer program, which A. Bartoloma (Dept. of Geology, Freie Universität Berlin) ran for me.

[16] A Rosin distribution is characteristic of crushed rock.

[17] R. Schleyer (formerly Dept. of Geology, Freie Universität Berlin)
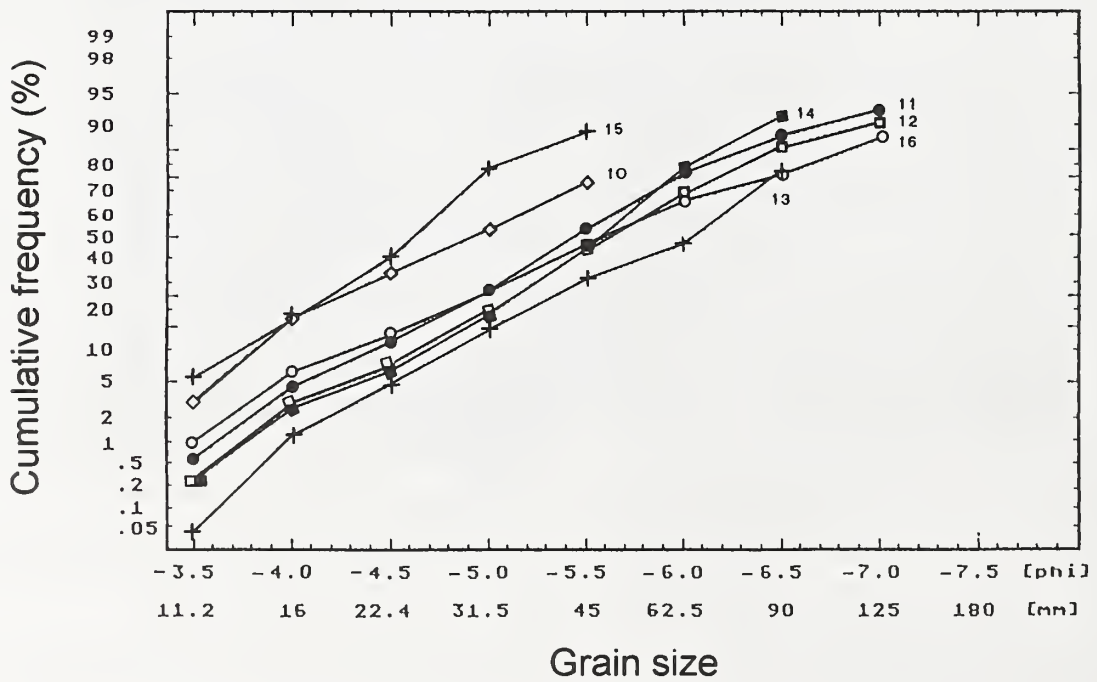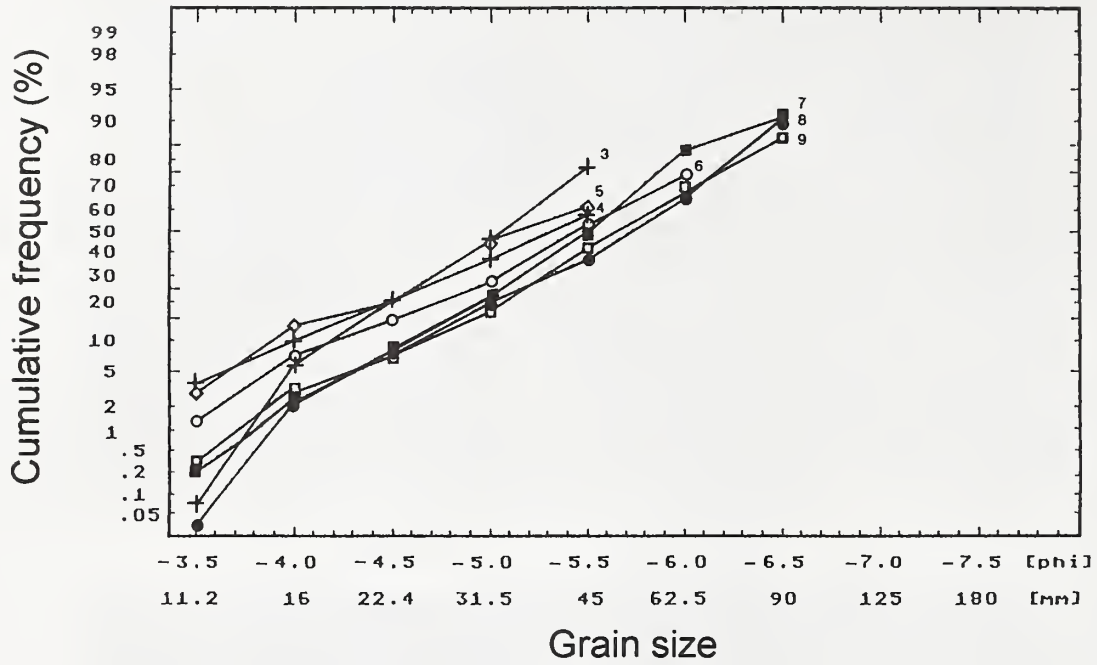
Figure 4.12 - Bedload samples from the net-sampler (1988): cumulative frequency distribution of grain-size classes plotted on probability paper.
a) sample numbers 3 - 9: sampled during rising and peak flows between May 20 and 24
b) sample numbers 10 - 16: sampled during rising and falling limb on May 24 - 25
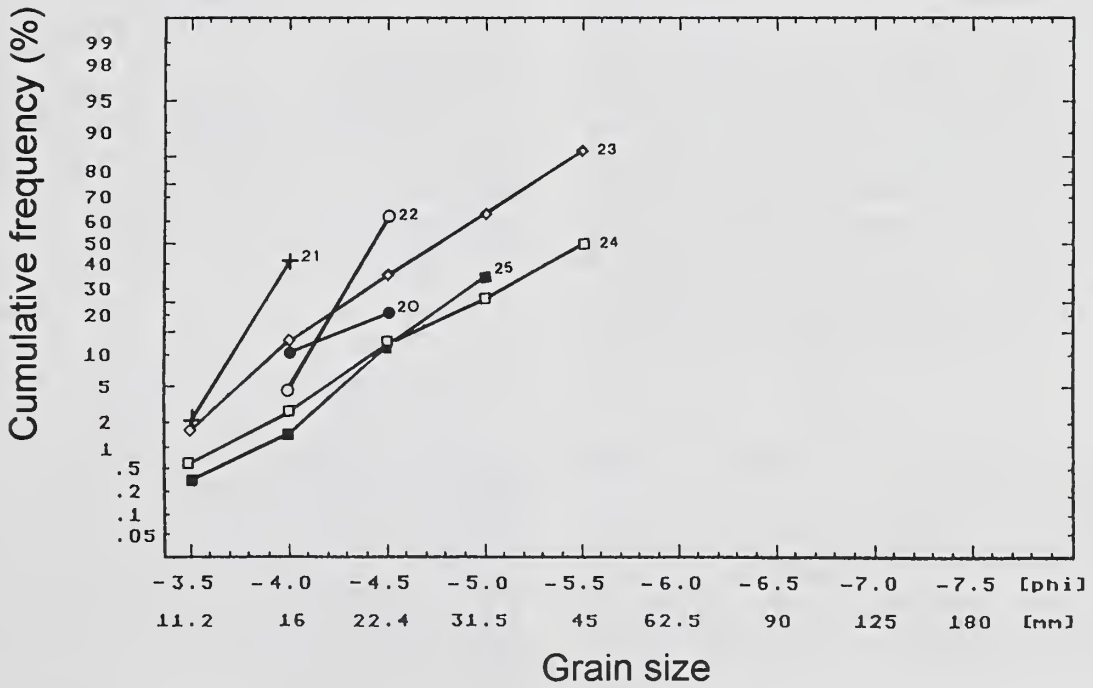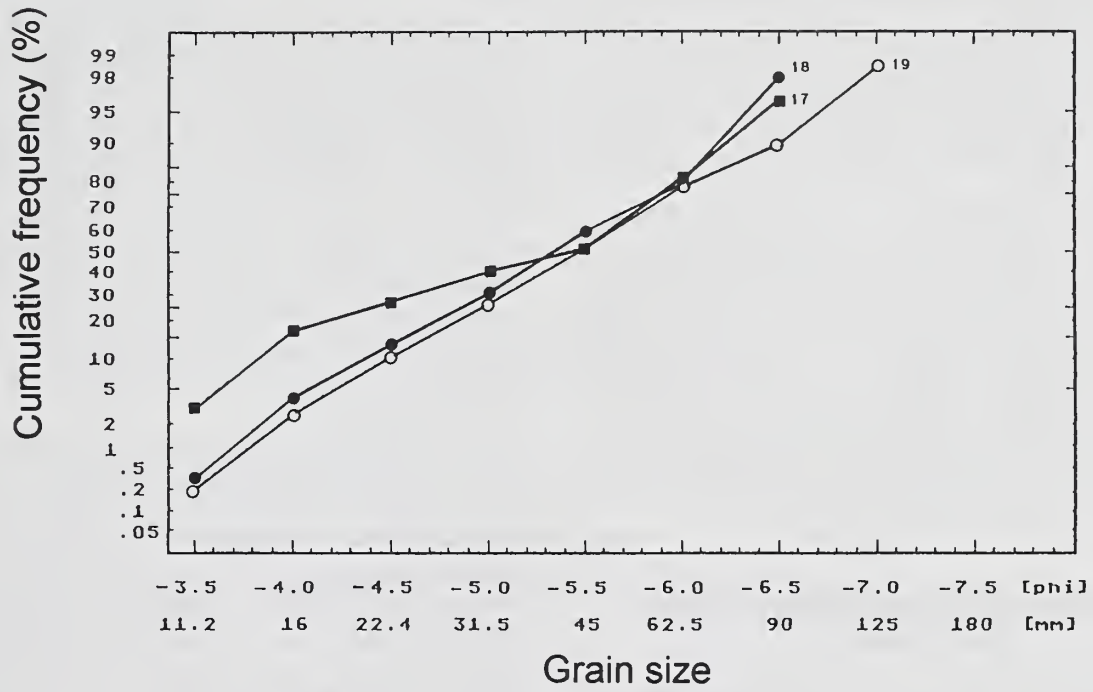
Figure 4.12 - Bedload samples from the net-sampler (1988): cumulative frequency distribution of grain-size classes plotted on probability paper.
　　　c) sample numbers 17 -19: sampled at various times during later days of the high flow between May 20 and 30,
　　　d) sample numbers 20 - 25: sampled at various daily times during falling limb of snow melt high flow May 31 - June 8.

the attempt to understand these processes is to quantify the number and grain sizes of particles involved in the process. Within the sand fraction it is difficult to identify individual grains, but within the pebble and cobble range counting the number of transported or sampled particles poses a promising opportunity for statistical analysis (Bunte 1992a).

Particle transport rates for pebbles and cobbles were determined by counting the number of particles for each grain-size class and calculating their transport rates in terms of numbers per meter and minute. Particle transport rates of all bedload samples are listed in Table 3b in the appendix. The unit of meters and minutes was chosen because it happened to have the least number of decimals. Results and discussions of this investigation are presented in Section 5.5.4.

4.5 Channel Geometry and Stream Morphology

Channel geometry and bedload transport are closely related. The cross-sectional channel shape influences bedload transport, but it is, in turn, affected by bedload which passes the cross-section, deposits in it or scours.

The spatial and temporal variation of the channel form can indicate various processes of bedload transport. Channel topography should therefore be registered continuously using a spatial scale that is appropriate for the stream type. As this posed an unmanageable enterprise, different procedures were tried that might provide an insight into the processes on the channel bottom. The following procedures were used at Squaw Creek in order to attempt an analysis of the channel form in different spatial and temporal scales:

- frequent and consecutive readings of the water surface slope,
- repeated and consecutive surveys of a cross-section during high flows, and
- survey of the stream morphology before and after a high flow.

4.5.1 Water surface slope

Given the premise that the water surface is roughly a positive copy of the stream channel topography[18], changes in the water surface topography should identify locations of channel change and, therefore, locations of bedload transport activity. The inclination of the water surface at a given time and location is however also dependent on the temporal variation of flow, as when a flood wave passes by. If the effects of the hydrograph can be subtracted from the temporal variation of the water surface slope, the remaining water surface behavior should indicate processes on the river bed.[19]

In an unerodible rectangular channel, the temporal variation of the water surface slope during the passage of a flood wave is equivalent to the course of the first derivative function (slope) of the hydrograph (fig. 4.13). The peak of the first derivative function corresponds with the most pronounced temporal change of discharge on the rising limb of flow. The first derivative function becomes zero during peak flow and the minimum of the water surface slope occurs at the time when flow rate recedes most strongly. The funciton of the theoretical water surface slope (first derivative function of the hydrograph) rises again and crosses the zero-line before the hydrograph starts its second rise.

The temporal variation of the water surface slope, which was measured at Squaw Creek consecutively for 2 days (May 23-25, 1988), differs from the course of the theoretical water surface slope in several aspects (fig. 4.13):

- the rise occurs in several steps,
- the maximum occurs with a delay of about 10 hours, and
- the shape of the function is wider (larger half-value width of the function).

The response of a measured water surface slope to changing flow is varied in a natural stream bed. An exponential increase of flow affects the function water surface slope in a positive way. This is partially counteracted by an increase in flow width, which has a negative effect on water surface slopes. However, the relatively

---

[18] Cross-sectional water levels change not only in correspondence to discharge variation but are also influenced by local channel geometry. Local water levels can mirror the channel geometry or run exactly opposite to it, depending on complex hydraulic processes like upwelling, downwelling, laterally pointing secondary flows, or the Bermoulli law regarding energy heads.

---

[19] Paragraph was added during translation for clarity.
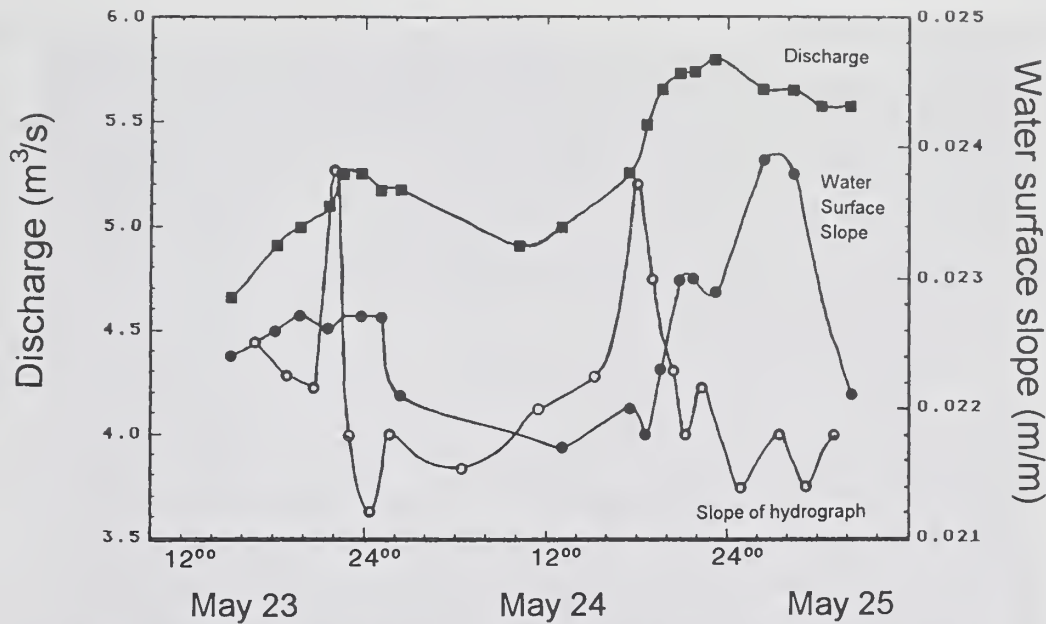
Figure 4.13 – Hydrograph, measured water surface slope, and the first derivative function (slope) of the hydrograph plotted over a 2-day period from May 23-25, 1988.

small change in flow width that occurs at Squaw Creek within the diurnal fluctuation of flow cannot account for the relatively large discrepancy between the temporal functions of the theoretical and measured water surface slope.

The cross-sectional water surface is far from being horizontal during high flows in high-energy streams. Gradients across the stream can reach several percent (Leopold 1982). The transformation of channel morphology causes bedload transport, and bedload transport, in turn, modifies the stream morphology. This variation of channel form is reflected in the topography of the water surface.

A rectangular channel shows a maximum in water surface slope during the fastest increase of flow on the rising limb of the flood wave. This peak in water surface slope not only leads to a precedence of the force of flow compared to discharge[20], but it also leads to a sudden increase in the state of the stream energy. Part of this energy is transmitted to the channel bottom where it causes erosion which changes the cross-sectional geometry. This channel change probably dampens the variability of the water surface slope during the passage of a flood wave. The measured water surface slope increases at a substantially slower

and delayed pace as would be expected for a stream in which the channel bottom could not react to flow conditions (fig. 4.13).

The fluctuating nature of the measured water surface slope strongly indicates that changes in water surface slope are affected by changes on the stream bottom. Adjustments of the channel bottom to the changing conditions of flow are typical for phases with high and unsteady flows.

If it is true that a water surface slope measured over two fixed points in the long profile of a bedload carrying mountain stream is affected in its temporal variation by the combined effects of hydrograph and channel change, then this fact can be used to identify periods of channel change between the two fixed points. If the measured water surface slope deviates from the theoretical temporal function of the water surface slope, then this deviation can indicate river channel change. The analysis of the temporal variation of the measured water surface slope can therefore serve as a means to identify river-bed adjustments between two points in an indirect way. The temporal variation of bedload transport can then be set into relation with local channel changes. That makes it possible to gain insights into the dynamics of bedload transport.

---

[20] This phenom is acknowledged in Bagnold's unit stream power, which includes the water surface slope S_w (= $Q \cdot S_w \cdot \rho_w$ /w). See list of symbols for notations.

4.5.2 Cross-section measurements

During the spring high flow of 1988, T. Berry (University of St. Andrews, GB) and P. Ergenzinger examined the temporal variability of the cross-sectional microtopography. The position of the cross-section is marked on the maps in Figure 3.7. Berry (1988) used the *"Tausendfüßler"* device for detailed profiling of the cross-sectional channel shape (Section 4.3.3). Since the profiling device was operated directly in the stream, it had to be a light-weight structure that was easy to set up and take down to account for the passage of driftwood. It was therefore constructed of a wooden board (2" by 4") positioned horizontally across the stream and mounted to thin metal posts hammered into the stream. The wooden board had borings in regular 10 cm intervals. A probing rod is lowered through the borings to the channel bottom. The length of the rod that extends above the wooden board is measured (fig. 4.14a-b). This x-y-directional measuring device makes it possible to repeatedly survey the same points in the stream cross-section [21].

Cross-sectional profile measurements were taken in 2- to 3-hour intervals during the passages of almost two daily snowmelt high flow waves on May 23-24, 1988, in the same cross-section in which P. Carling and M. Glaister measured velocity profiles. Combining Berry's (1988) results of changes in channel roughness and channel shape with the behavior of other parameters during this time (velocity profiles, water surface slope and bedload transport rates and grain-size distribution), makes it possible to gain some insights into the interactive processes involved in bedload transport.

4.5.3 River-bed morphology and bedload transport behavior

Similar to the interrelations between cross-sectional geometry and bedload transport, channel morphology and bedload transport are related as well. The morphology of a bedload carrying stream is pronouncedly affected by the nature of the energy expenditure. This is in turn dependent on the amount and locality of moveable bedload material.

A stream expends as little energy into its flow as possible. During high flows in streams with no limit of transportable material and erodible channel bottoms and banks (e.g., **braided streams**), this can be achieved by continuous bedload transport. This allows the stream morphology to adjust constantly to the changing conditions of flow (Chang 1980; Ergenzinger 1987). The low channel bottom stability in braided streams provides already a mobility of the entire channel bottom for relatively small high flows. The more bedload material is present for transport, the more continuous the energy transfer between the flow and the sediment and the smoother the development of the long-profile.

The stream morphology indicates if and how much the supply of transportable bedload is limited. A generally large sediment supply leads to the formation of in-stream gravel bars and other readily available sediment storage that can be easily emptied when the flow rises or the sediment supply drops. The dearth of transportable material in supply-limited mountain streams such as in boulder-strewn, step-pool, or pool-riffle streams (e.g., present streams of the Central Mountains in Germany[22]) leads to an energy surplus in the water flow, because flow can hardly expend its high kinetic energy by a sustained mobilization of bedload. The energy excess of the stream flow probably leads to discontinuous adjustment activities between flow and stream bottom and to the formation of irregular long-profiles. These stream systems are characterized by an alternation of rough, steep, and shallow high-friction reaches with deep pools in between. Step-pool or pool-riffle streams maintain their type of channel morphology during average high flows which only modify the present channel morphology. It takes rather large high flows to initiate a new adjustment of channel morphology to the new sedimentary and hydraulic conditions of flow. Squaw Creek measuring reach with its riffle-pool morphology falls into the category of supply-limited streams.

As the amount and composition of transportable bedload material influences the stream

---

[21] *The methodology was further developed by Ergenzinger and Stüve (1989), Ergenzinger (1992), Ergenzinger et al. (1994), and De Jong (1993) who calculated k3-values as a dynamic measure of channel bottom roughness and demonstrated a relationship between flow hydraulics, channel change and bedload transport.*

[22] *These stream conditions are probably comparable to those of mountains streams in the U.S. Appalachian Mountains.*

Figure 4.14 – Multiple cross-sectional measurements at Squaw Creek:
   a) channel bottom profiling with the first generation of the "Tausendfüßler" device
      (P. Ergenzinger and T. Berry),
   b) flow velocity profiles with a multi-propellor current meter (P. Carling and M. Glaister).

morphology, it is possible in turn to deduce the transport behavior of the stream from the stream morphology. The different phenomena of coarse bedload transport, i.e., the nature of the relation between bedload and flow, as well as the temporal variation and the grain-size distribution of the transported bedload are better understandable if the stream morphology is taken into consideration.

Regarding the still controversially discussed question of whether erosion and transport of coarse bedload occurs in dependence of grain sizes and flow strengths as selective transport or whether the entire grain-size spectrum is moved in equal mobility (Section 5.5.3), a hypothesis is formulated at this point that will be examined in later parts of this study together with the analyses of transported grain-sizes (particle transport rates, Section 5.5.8).

In supply-limited streams that carry coarse bedload, flows during bankfull stages (Leopold et al. 1964) will erode and transport only particles of the "right" size from the broad grain-size spectrum on the channel bottom. Transport rates during this selective transport are generally small.

Large particles that are not transportable accumulate on the channel bed and lead to the formation of an armor or a pavement. Only a few exposed large particles take part in transport. Very large forces of flow are necessary (at least locally) to tear up the armor and incorporate particles from the subsurface layer into bedload transport processes.

In coarse bedload carrying streams with mobile channel bottoms and banks (e.g. streams with readily available sediment supply), bedload transport occurs in equal mobility of all grain sizes owing to the large amount of transportable material within the high flow bed during bankfull flows. Transport rates for common stream flows are larger in these streams than in the supply-limited streams.

The preceding sections explained the hydraulic and sedimentary conditions that affect bedload transport and included a review of the present[23] literature. The measurements and analyses carried out in this study at Squaw Creek were described and the methodology of the procedures was explained. The results of the analyses are presented in the following chapters.

---

[23] *as of 1990*

5. Presentation and Discussion of Results

5.1 Statistical Analyses of the Relation Between Bedload Transport and Hydraulic Parameters

Bedload transport formulas are employed under the premise that bedload transport rates are describable as a function of hydraulic and sedimentary parameters (e.g., flow velocity, discharge rate, shear stress, stream power, and grain size). Many formulas include a threshold value that has to be exceeded to initiate coarse material bedload motion (Section 4.1). At this point it will be analyzed under which circumstances hydraulic parameters can be used to explain and predict transport rates of coarse material bedload transport.

5.1.1 Bedload signal rates and discharge

The analyses of the relations between bedload transport and flow started with the investigation of the relation between hourly signal rates and discharge. Signal rates recorded in 1986 are plotted versus discharge for rising and falling limbs of flow (fig 5.1). Data range over 1.5 orders of magnitude. The variability of signal rates for a given discharge extends over about one order of magnitude. The correlation between signal rates and discharge yields a much better correlation of $r^2 = 0.63$ for the rising limbs than for the falling limbs where r^2 is only 0.35. The general correlation for both rising and falling flows is $r^2 = 0.56$.

5.1.2 Bedload transport rates (Helley-Smith sampler) and discharge

In order to test whether this poor correlation between bedload transport and discharge is only confined to coarse particles or also valid for finer sediment, bedload transport rates calculated from samples collected with the 7.6 by 7.6 cm Helley-Smith in 1986 were compared to flow (fig. 5.2). The range of the data extends over slightly less than 1.5 orders of magnitude, while the variability of bedload transport rates is just below one order of magnitude. This similarity between the range and the variability of data lead to a low correlation of $r^2 = 0.32$. The relatively small range of the bedload data (and thus the poor correlation) are probably sampling artifacts. Helley-Smith samples were preferentially taken on daily rising and peak flows during the first part of the snowmelt high flow when sand transport rates are relatively
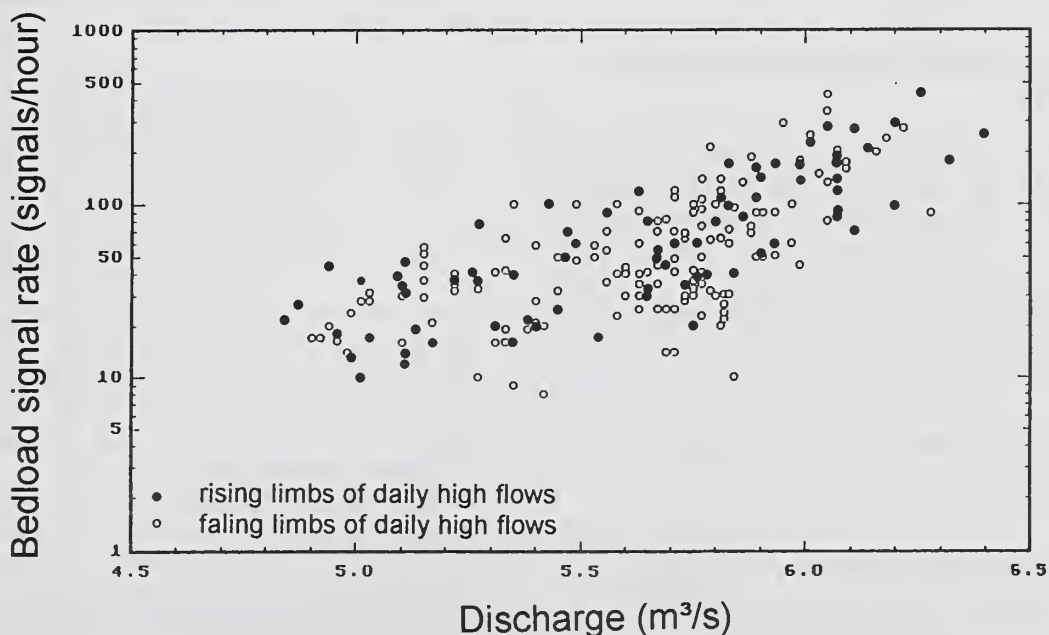
Figure 5.1 – Relation between hourly bedload signal rates (Qb_{sign}) and water discharge (Q) (1986):
a) for rising flow: $Qb_{sign} = 1.30\ E\text{-}6 \cdot Q^{10.23}$, $r^2 = 0.63$,   b) falling limbs of flow: $Qb_{sign} = 4.43\ E\text{-}5 \cdot Q^{8.06}$, $r^2 = 0.35$.
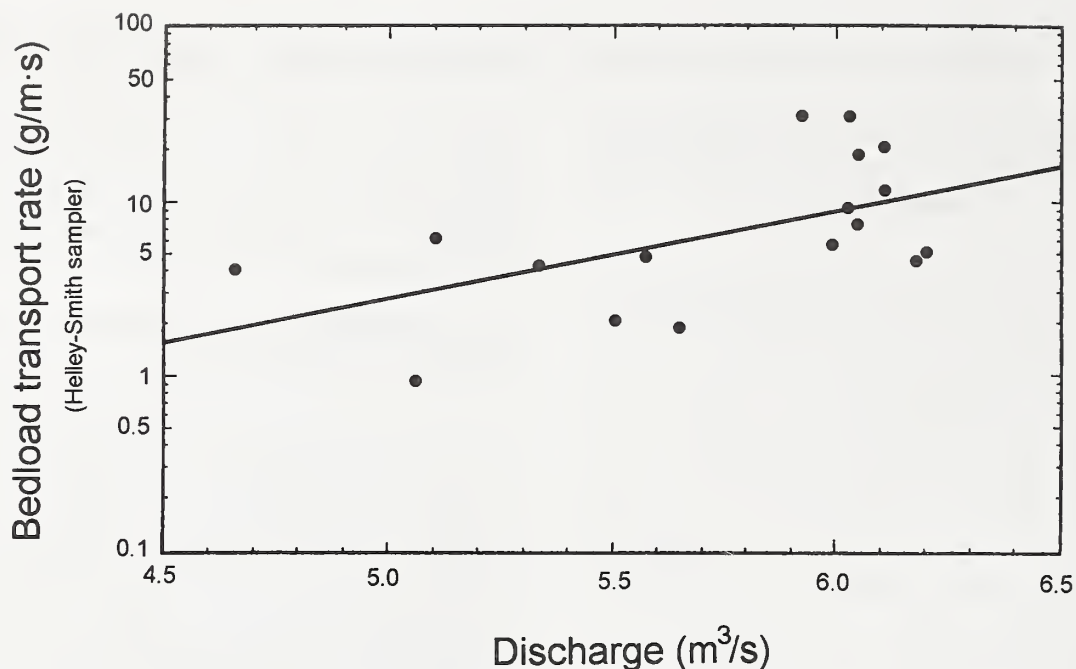
Figure 5.2 – Relation between bedload transport rates (*Qb*), sampled in 1986 with the 7.5 cm by 7.5 cm Helley-Smith sampler, 0.25 mm mesh width, and discharge (*Q*): $Qb = 0.0001 \cdot Q^{6.46}$, $r^2 = 0.32$.

high. Daily falling limbs and the later part of the high flow are not well presented in the data. The cobble part of bedload transport was, when it occurred, poorly presented in the samples because the opening of the Helley-Smith sampler was too small.

5.1.3 Bedload transport rates (net-sampler) and discharge

The relation between bedload transport and discharge was also analyzed for the spring high flow in 1988. Transport rates of the coarse bedload fraction were calculated from the samples collected with the net-sampler throughout the high flow period and plotted versus discharge (fig. 5.3). The range of the data extends over almost three orders of magnitude, while the variability extends over almost two orders of magnitude. This wide range of data provides, despite the scatter, a rather good correlation of $r^2 = 0.71$ for the power function regression.

5.1.4 Bedload transport rates (net-sampler) and stream power

A replacement of the hydraulic parameter "discharge" by "stream power" (Bagnold 1977: $\Omega = Q \cdot S_w \cdot \rho$ (Section 4.1.1) does not improve the statistical relation between bedload transport and flow ($r^2 = 0.63$) (fig. 5.4). The parameter **stream**

power was simplified in this calculation to the product of $Q \cdot S_w$, because the variability of the water density ρ is considered negligible).

5.1.5 Daily means of bedload signal rates and discharge

The next analytic step reduced the temporal scale of the flow - sediment relation. Daily discharge means were calculated for all days of the high flow using summed hourly discharges from one day's low flow to the next day's low flow. These values for mean daily flow were plotted versus mean hourly signal rates over the same time periods (fig. 5.5). This increase of time intervals produces an r^2 of 0.88 in the relation between flow and signal rates, a much better statistical relation than in the previous examples. The regression function attributes similar signal rates to discharge as Figure 4.9.

The statistical relation ($r^2 = 0.93$) is even better between daily maximum signal rates and daily mean signal rates (fig. 5.6). The maxima exceed daily means by a factor of three (Section 5.2.1.1). The close correlation both between daily mean signal rates and discharge, as well as between daily maxima and daily mean signal rates, indicate that the long-term relation between bedload and flow was generally steady during snowmelt high flow.
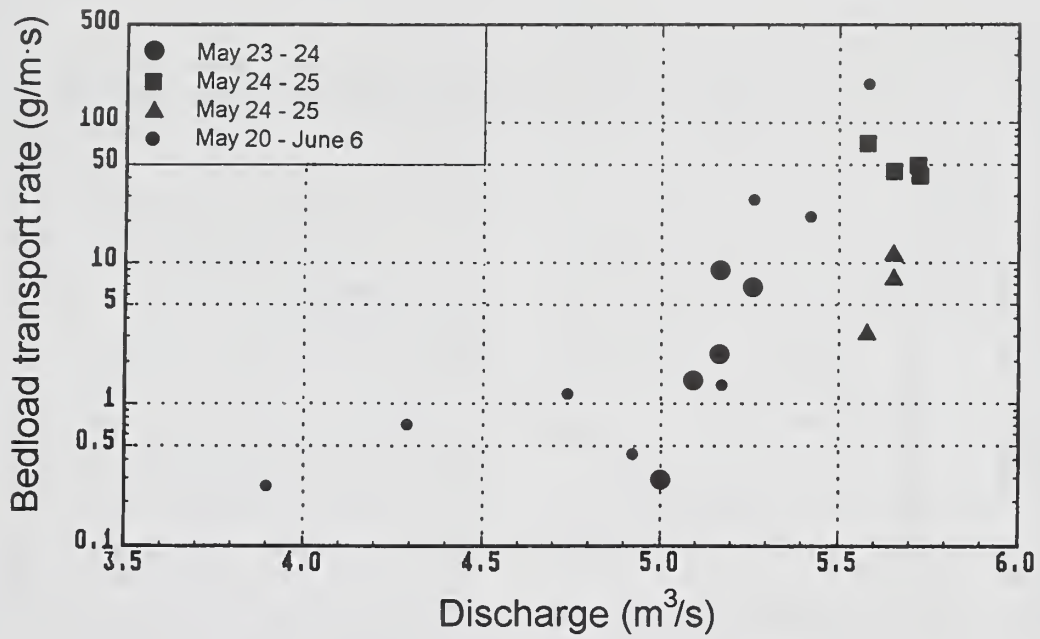
Figure 5.3 – Relation between bedload transport rates (*Qb*) sampled in 1988 with the 0.30 m by 1.55 m net-sampler, mesh width 10 mm, and discharge (*Q*):*Qb* = 4.428·*Q* 18.21, r² = 0.71.

Dynamics of Gravel-Bed Rivers. P. Billi, R.D. Hey, C.R. Thorne, P. Tacconi (editors), 1992, John Wiley & Sons Ltd., Chichester, England, Reproduced by permission of John Wiley and Sons Limited.
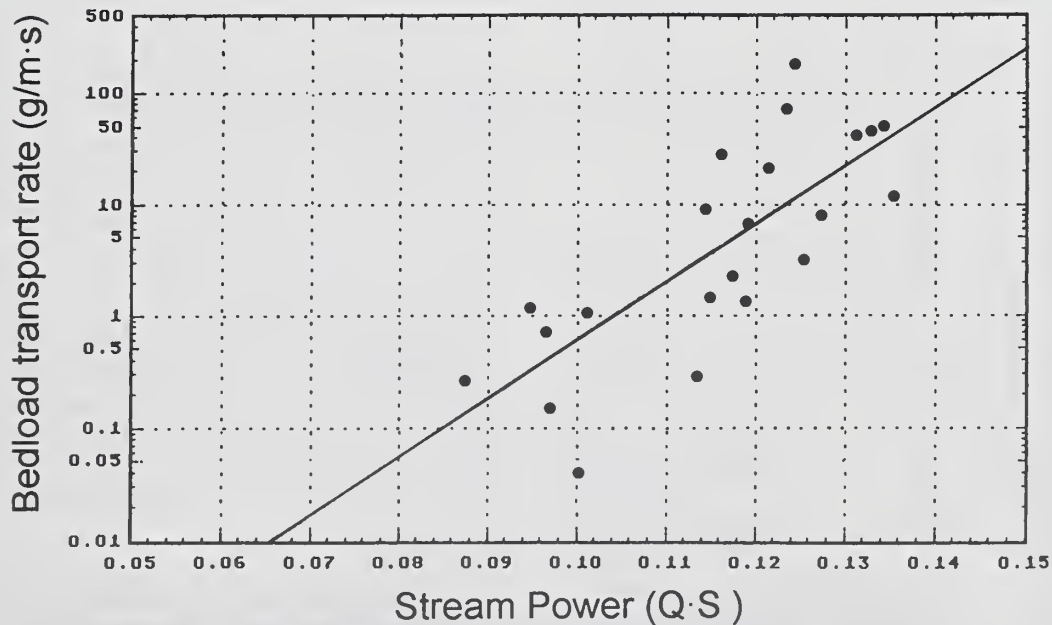
Figure 5.4 – Relation between bedload transport rates (*Qb*) sampled in 1988 with the net-sampler, (0.30 m by 1.55 m opening; mesh width 10 mm) and stream power (Ω), simplified to the product of discharge and water surface slope ($\Omega \approx Q \cdot S$): $Qb = \Omega$ 5.38E-6 e $^{117.61\ Qb}$, r² = 0.63.

51
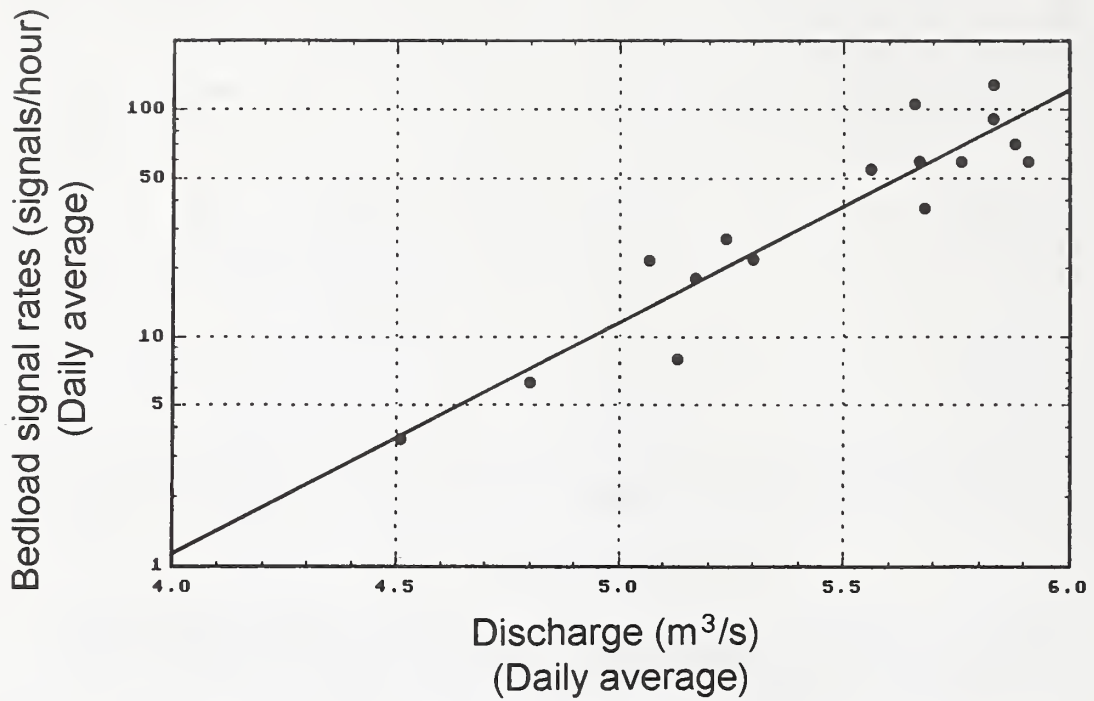
Figure 5.5 - Relation between day-averaged bedload signal rates (Qb_{sign}) and day-averaged discharge (from daily low flow to next day's low flow) (Q_{mean}): $Qb_{sign}= 2.67$ E-8 $\cdot Q_{mean}^{12.39}$, $r^2 = 0.87$.
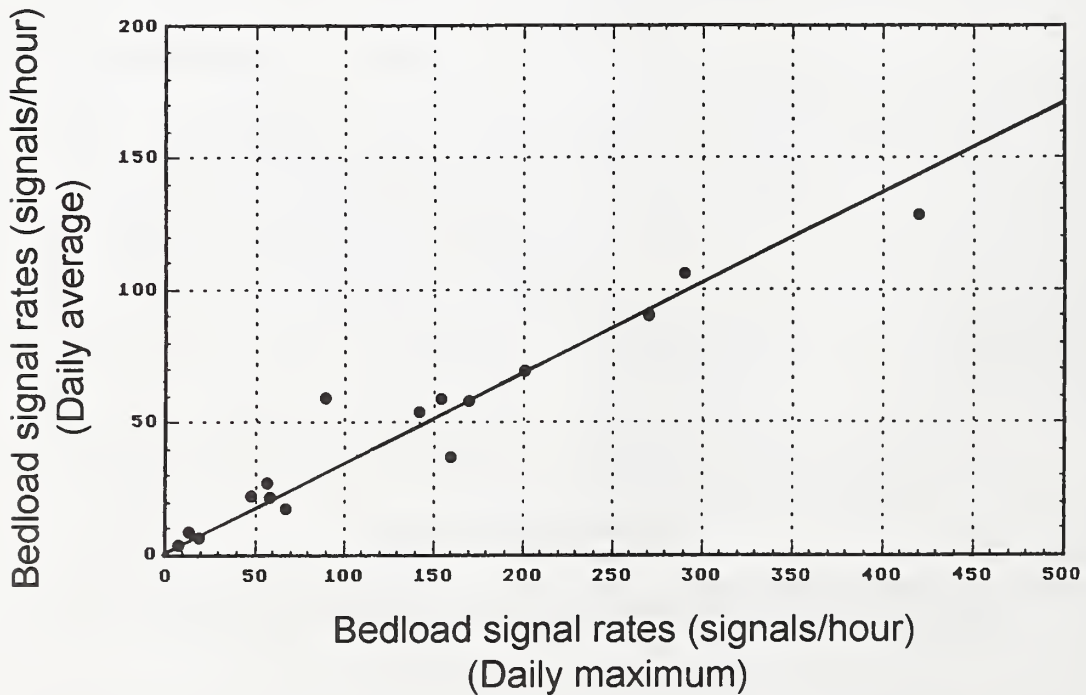
Figure 5.6 – Relation between mean and maximum bedload signal rates per discharge day (from daily low flow to next day's low flow).

5.1.6 Results

At Squaw Creek, hydraulic parameters like discharge or stream power are hardly appropriate to predict bedload transport rates within a temporal scale of hours. The accuracy of the prediction can be greatly improved, if the temporal scale is extended to daily mean values, which are the sum of many individual measurements. Bedload transport rates at Squaw Creek fluctuate so much that individual measurements will only give a rough estimate about the order of magnitude expected for bedload transport.

The poor correlation between bedload signal rates and discharge at Squaw Creek is partly due to fluctuating transport rates, especially after peak flow and on the falling limbs. It is also due to hysteresis effects with usually higher transport rates on the rising limbs than on the falling limbs of flow. Besides, hysteresis curves vary over the course of the hydrograph: they become lower and cross more frequently as the high flow proceeds. The question arises which changes occur in the relationship between the main parameters (hydraulic conditions, bedload transport, and channel shape) during the rising and falling limbs of flow and between the beginning and the end of the high flow period. The interactions between water and sediment have to be better known in order to analyze this question. This requires examination of the temporal variability of the hydraulic, sedimentary, and morphologic conditions on the stream bed. Such measurements require an immense measuring effort, which can only be achieved by the combined endeavors of a team.

The temporal structure of bedload transport will be analyzed in the next sections and compared with the temporal structure of the hydraulic parameters. The interactions between channel geometry and bedload transport will be explored by using a combination of measurements and analyses that permit at least a partial insight into the procedures that take place at the channel bottom.

5.2 Temporal Variation of Coarse Bedload Transport: General Considerations

Transport rates of coarse bedload transport are rarely steady, but temporally variable under both steady as well as unsteady flows. In most cases, the temporal variation of bedload follows a different pattern than the temporal variation of unsteady flows. The relation between bedload transport and flow is therefore unsteady, too, and varies over a wide range. The temporal variability of bedload transport rates is usually larger than the temporal variability of the flow. Therefore bedload transport is referred to as "fluctuating," which can even occur in a rhythmic way. Inconsistent relations between discharge and bedload transport or fluctuating and pulsating bedload transport rates have been documented in many field and laboratory experiments, under various hydraulic and sedimentary conditions, and in various temporal scales.

5.2.1 Former investigations

Although temporal variation of bedload transport has already been observed in natural streams in the 1930's by Ehrenberger (1931) at the Danube, and by Mühlhofer (1933) in the Inn, and in flume experiments by Einstein (1937) and Shields (1936), there are presently only a few systematic studies that get away from a single study and try to obtain a more general picture. Church (1985) and Gomez et al. (1989) tried to summarize and sort the present, often contradictory, results regarding the "unsteady nature" of bedload transport. The vague term "unsteady" already indicates the generally poor understanding and lacking systematicness of the current analyses.

The fluctuation of bedload transport rates leads to two main questions:

- What is the cause of the fluctuations?
- How can bedload be sampled in a representative way, despite of the fluctuations?

While the second problem is principally solvable using a probability analysis, the first question continues to pose a problem. A multitude of phenomena, patterns, and processes were observed for different time-scales, grain-sizes, and flows (following Sections). This variability makes the topic conceptually and methodologically difficult to manage and requires a systematic study.

5.2.1.1 Probability analyses of bedload fluctuations

Based on the analyses of the step length of individual particles during sediment transport (Einstein 1937) and on the analyses of the height, length, and travel velocity of migrating bedforms (Hamamori 1962: sand dunes with superimposed ripples), both researchers arrived at the conclusion that, given steady flow, bedload transport rates range between zero and about four times the mean bedload transport rate. High bedload trans-

53

port rates occur less frequently than low transport rates (Section 5.1.5). Einstein (1937) and Hamamori (1962) both set up probability distribution functions of bedload transport rates that describe, for different sampling intervals, the percentage frequency with which a certain relative bedload transport rate occurs. A relative transport rate is the ratio of a measured transport rate to the mean transport rate for that time period.

Such statistical analyses of the temporal variability of bedload transport rates have been pursued and modified by several authors (Carey and Hubbell 1986; Hubbell and Stevens 1986; Hubbell 1987; Hubbell et al. 1987; McLean and Tassone 1987; Gölz and Dröge 1989; Gomez et al. 1989). These authors provide probability density functions of rhythmic fluctuations of bedload transport rates during steady flows. These functions indicate the frequency with which a certain relative transport rate can be expected. Knowing this, sampling intervals, durations, and frequency can be estimated, in order to obtain representative samples of bedload transport rates for rating curves, in spite of fluctuating transport rates. However, the questions regarding the processes that cause the temporally unsteady or rhythmic phenomena have not been answered by these statistical procedures.

5.2.1.2 Comparability of published results regarding the temporal variability of coarse bedload transport

The interpretation and comparability of various phenomena and analyses regarding the temporal variation of bedload transport is problematic for two reasons:

- Fluctuations of bedload transport have been investigated separately for steady and unsteady flows; and

- The analyses extend over different temporal scales and are carried out in different temporal resolutions.

Separate investigation of fluctuations in bedload transport for steady and unsteady flows:

Coarse bedload in natural streams is only eroded and transported during high flow events. For this reason, temporal variations of coarse bedload transport in streams is almost exclusively investigated during unsteady flows. Laboratory experiments, on the contrary, keep discharges constant, for practical reasons and for parameter limitation. These different hydraulic and sedimentologic conditions of stream and flume experiments could mistakenly lead to the conclusion that fluctuations of bedload transport are necessarily caused by different factors during steady and unsteady flow.

The various methods employed to investigate the matter, the wide variability in hydraulic and sedimentary conditions, and the multitude of observed phenomena as well as the different arguments make it problematic to combine information from different studies. It is, however, important that this differentiation of bedload transport analyses into field and flume studies, which is basically due to practical reasons, does not lead to a separation of research results. Instead, more work should be put into the investigation of the hydraulic, sedimentologic, and channel geometric conditions that cause bedload fluctuations. It is possible that bedload fluctuations during the passage of a high flow wave are not only caused by processes linked to the special conditions of unsteady flow but are combined with those mechanisms of bedload fluctuations, which are observable under steady flows. Such combined analyses have so far not yet been described in the literature.

Studies of the temporal variation of coarse bedload transport that are carried out in laboratory experiments usually analyze bedload transport with high temporal resolution. These studies are therefore discussed together with the analyses of bedload signals from Squaw Creek in 5-minutes intervals (Sections 5.4.2.1 and 5.4.2.3).

Time scale of the analyses and their temporal resolutions:

Several time series of bedload transport recorded in different stream settings and in different temporal resolution are available in the literature. Gomez et al. (1989) put together an impressive list of the respective studies. Sampling time and sampling intervals are usually closely related.

A high temporal resolution of sediment transport (the order of minutes) limits the length of the record usually to a few hours (Hayward and Sutherland 1974[*1]; Klingeman and Emmett 1982; Jackson and Beschta 1982; Gomez 1983, Gomez et al. 1991[*]; Schlatte 1984; Pitlick 1987; Whiting et al.

---

[1] *Citations with an asterisk (*) were added during translation.*

1988; Kuhnle et al. 1989; Bänzinger and Burch 1990; Dinehart 1992, Dinehart, pers. com. 1993*; Rickenmann 1994*). Most of the time series listed comprise far less than 100 data points. The most detailed measurements in this category with over a hundred data points were performed by Carey 1985*; Lisle 1989* and Lisle, pers. com. 1993*; and Kuhnle, pers. com 1993*).

Studies with a medium temporal scale address bedload fluctuations in about hourly measurements during high flows that last for about a day (Campbell and Sidle 1985*; Reid et al. 1985; Reid and Frostick 1986b*; Tacconi and Billi 1987; Bunte 1991b; Kuhnle, pers. com. 1993*; D'Agostino 1994*).

Studies with a low temporal resolution (the order of days) analyze bedload waves over high flows that last for several days and a few months (Milhous 1973*; Nansen 1974*; Leopold and Emmett 1976*, 1977*; Emmett 1980*; Pitlick and Thorne 1987; Lisle 1989*; Lenzi et al. 1990). None of these studies analyze the temporal variation of bedload transport at several temporal scales.

The selection of a certain particular scale of the analyses carries with it the restriction to a certain set of parameters included in the investigations. Processes and parameters whose effects are not immediately visible at the particular time scale of interest are excluded from the analyses. The basic problem with this approach is the fact that short-term processes are naturally incorporated in long-term processes. Conversely, the short-term analyses need to pay attention to long-term processes, which are not considered if the temporal resolution is large (i.e., the analyzed time period is small).

Studies at all temporal scales describe bedload transport as unsteady or fluctuating. However, in spite of their relatively similar phenomena, time series are not comparable, because the processes interpreted to control bedload fluctuations are quite diverse. It is therefore rather problematic to transfer results from one time scale to the other by up-scaling or down-scaling.

5.2.1.3 Various forms of bedload-discharge relations in streams

An alluvial stream has reached equilibrium conditions when the energy expenditure of flow is at a minimum. If nonequilibrium conditions occur (change in water or sediment supply), flow and channel bottom need again to adjust to each other in order to minimize energy expenditure and retain equilibrium (Yang 1971; Yang et al. 1981). Repeated adjustments between the hydraulic conditions of flow and channel bottom characteristics are called **dynamic equilibrium**.

Dynamic equilibrium: steady and unsteady relations between discharge and bedload transport:

A river reach is in dynamic equilibrium if the input of bedload into a reach per unit of time equals the amount of bedload that is transported out of the reach according to the capacity of flow. A steady relation (good-fitting rating curve) between discharge and bedload transport rate would be the result. This condition is rarely observable over short time intervals during unsteady high flow conditions in bedload carrying streams. Natural streams are typically characterized by a dynamic equilibrium. Short-term aggradation and degradation equal out without any net gain or loss over time. These adjustments naturally imply local channel change, because bedload does not move constantly but is transported over some distance, covers this distance in several distinct steps, and finally comes to rest for some time (Ergenzinger et al. 1989; Schmidt et al. 1989, 1992*[2]; Schmidt and Ergenzinger 1990, 1992*).

If an increase in discharge produces a change in the local hydraulic conditions of a stream that is in dynamic equilibrium or if some local sediment movement occurs, the stream responds to this disturbance with another local sediment dislocation. That is how, step by step, one sediment dislocation leads to a another one. The adjustments of the river bed to hydraulic conditions can take place more easily and continuously, the more transportable the available material. A dynamic equilibrium between flow and bedload transport is optimally developed in braided streams where all channels are perfectly mobile (Section 4.5.3).

Supply-limited, bedload carrying streams develop a dynamic equilibrium only over rather long time intervals, which means that a good rating curve is only obtained by averaging a number of bedload transport rates. Given the relatively small amount of mobile bedload material, the channel bottom cannot adjust continuously to the changing local conditions of unsteady flow during the passage of high flow waves. The forces of

---

[2] *Citations with an asterisk (*) were added during translation to supplement the listing.*

flow need to exceed a relatively high threshold value before they can cause a sediment dislocation. This produces an unsteady adjustment process between flow and channel bottom. Unsteady relations between discharge and bedload transport and fluctuating transport rates are the consequences (Section 5.1).

A simple form of an unsteady relation between discharge and sediment transport is indicated by the hysteretic effects of rating curves: transport rates are different for the same discharges on the rising and the falling limb of flow. A rating curve can become absolutely chaotic if a combination of the above criteria leads to some abrupt changes in bedload transport.

Larger transport rates on the rising limbs of flow:

Larger transport rates on the rising limbs of flow than for the same flows on the falling limbs lead to clockwise hysteresis. This precedence of bedload transport in comparison to flow can be attributed to several reasons, some of which are sampling artifacts.

The distance between sediment sources and a measuring site immensely affects the course of the temporal variation of bedload transport and the shape of the rating curve. If bedload is sampled in a short distance below the sediment source, bedload transport rates will show a pronounced increase already on the rising limb of flow. If the sediment source has already been emptied when flow decreases, this will produce strong hysteretic effects (Klingeman and Emmett 1982).

The sequence of the high flow events and the length of the time spans between events modify the rating curve shape as well, because prior flow conditions have an effect on the sedimentological conditions of the river bed at the start of a new high flow. If high flows follow each other closely, sediment sources can become depleted during rising flow. Then after initially high transport rates, no sediment is left for the falling limbs of flow (Reid et al. 1985; Bänzinger and Burch 1990).

Sequential high flow events can also alleviate hysteretic effects. If a rather small high flow event is preceded by a time period with flows around the threshold of motion, flows can easily erode even large particles from an unconsolidated channel bottom during the rising limb of flow (Reid et al. 1985). The same phenomenon has been observed by Klingeman and Emmett (1982) for two consecutive high flow events. Bedload transport set in during the second high flow event at exactly

the same discharge at which it had ceased during the previous event. The unconsolidated channel bottom obviously provided the same sedimentological conditions for both events.

If the channel bottom comprises the only sediment source and discharge does not reach the competence to transport all grain sizes, the coarse, nontransportable material deposits on the channel bottom while transport rates decrease and come to a halt (**static armor**: Gomez 1983). This conclusion contrasts with studies by Parker and Klingeman (1982), Andrews and Parker (1987), and Parker et al. (1982) who consider an enrichment of coarse particles at the channel bottom (armoring) and the associated increase in channel bottom roughness as necessary agents to maintain coarse bedload transport rates and its coarse grain-size distribution (**mobile armor**; Section 5.3.1).

Larger transport rates on the falling limbs of flow:

If the channel bottom is still armored at the beginning of high flow, bedload transport will reach its maximum only on the falling limb. Bedload transport rates can be several factors higher than they were on the rising limb (Klingeman and Emmett 1982). The degree of channel stabilization or the time span needed to erode a bottom particle, respectively, depends on the duration of the low flow period between the high flow events (Reid et al. 1985), and thus on the sedimentary conditions of the river bed (Bänzinger and Burch 1990).

In accordance with the example given above, a large distance between sediment source and measuring site will likewise lead to a delayed arrival of the sediment with respect to the hydrograph, so that peak transport rates will only occur during the falling limbs of flow (Klingeman and Emmett 1982). A counterclockwise hysteresis is the result.

Disequilibrium: long-term change in the rating curve:

A change in the water and sediment budget involves a disruption in the stream's equilibrium state. The discharge–transport relation not only changes over mid–term and long-term time periods but is also characterized by extreme unpredictability. The loss of the equilibrium conditions and the disruption of the sediment-discharge relationship can be produced by a change of sediment supply following both natural or human impacts (Section 1.2).

A prominent change in the sediment-discharge relationship has been observed at Squaw Creek on two occasions during the last decade. The first time this happened was when an extreme high flow event with a 20-year recurrence interval mobilized the entire stream bed and noticeably altered the channel morphology during a rain-on-snow event in the spring of 1981. When the river bed adjusted to the new conditions, the unconsolidated channel bed continued to provide transportable sediments for weeks as the high flow receded (Ergenzinger and Custer 1983).

The second event occurred at Squaw Creek during the snow melt of 1983 after a sudden log jam burst just upstream the measuring site. The contents of this sediment storage became available, and transport rates, as well as grain sizes, exceeded the usual values by multitudes. This event also altered the channel morphology. The high sediment supply and aggradation increased the water level so that erosion could attack those parts of the channel that had not been subject to erosion under comparable flows before. Several small gravel bars and a bank line that had been considered as stabile were eroded. The right channel, formerly separated by an in-stream gravel bar, aggraded and became exposed during the falling limb of flow. Squaw Creek shifted its bed entirely into what had formerly been the left channel and degraded it by several tens of centimeters. This, in turn, increased transport rates gain (Bugosh 1988; Bugosh and Custer 1989; Section 3.3).

A similar disturbance in the rating curve was demonstrated by Pitlick and Thorne (1987) at the Roaring River and Fall River in Rocky Mountain National Park (CO). Following a dam break, large amounts of sediment were mobilized. A misfit of the temporal variation of bedload transport with the hydrograph was observable for all measuring stations downstream from the break, and transport rates were disproportionately large or small.

The above gave a brief literature review regarding the analyses of temporal variations of bedload transport in the medium- and long-term time scale. Examples from the literature showed how preceding discharge events and sedimentological conditions on the stream bed affected the temporal relation between discharge and bedload transport in stream systems of both equilibrium and disequilibrium conditions. The next step in this study will analyze the temporal variation of bedload transport at Squaw Creek in an hourly resolution and compare it with the course of the hydrograph.

5.3 Temporal Variation of Bedload Signal Rates at Squaw Creek Based on 1-hour Intervals

The statistical analyses of the relations between hydraulic parameter and bedload transport show only fair correlations when the temporal scale is reduced (daily mean values) (Section 5.1; fig. 5.5). The poor correlations between hydraulic parameters and bedload transport in 1-hour resolution (fig. 4.9 and fig. 5.1), as well as for single, individual samples (fig. 5.2 and fig. 5.3), indicate that, within the short-term time scale, bedload transport is influenced by other parameters than flow. These parameters need to be identified and analyzed.

5.3.1 Data measured at Squaw Creek in 1986 and 1988

The following data were measured and analyzed at Squaw Creek during the high flows of 1986 and 1988. The combined information of these data sets could be used to examine the temporal variability of bedload transport:

- bedload signal rates for 1-hour intervals over a 17-day period (1986) (Sections 4.4.2, 4.4.3, 5.3.2),
- bedload signal rates in 5-minutes intervals over a 3-day period (1986) (Sections 4.4.3 and 5.4),
- individual and consecutive bedload samples (1988) (Sections 4.4.4 and 5.5.8),
- hydrographs 1986 and 1988 (Section 5.3.2),
- 8- to 12-hour time series of water surface slope (1986 and 1988) (Sections 4.2.2 and 5.3.3),
- Cross-section topography measurements (1988) (Sections 4.3.3 and 5.3.4), and
- velocity profiles (1988), (Sections 4.2.1 and 5.3.4).

The magnetic tracer technique was used to measure bedload signals continuously during snowmelt high flow in spring of 1986. Signals were computed in high temporal resolution (Section 4.4.2). Signal rates show a strong temporal variation, they fluctuate, and sometimes they even pulsate rhythmically (fig. 5.7a and b). The temporal variability was studied on the basis of analyses in 1-hour and 5-minute resolutions. Time series obtained at Squaw Creek and their subsequent analyses differ from other published time series in two ways:
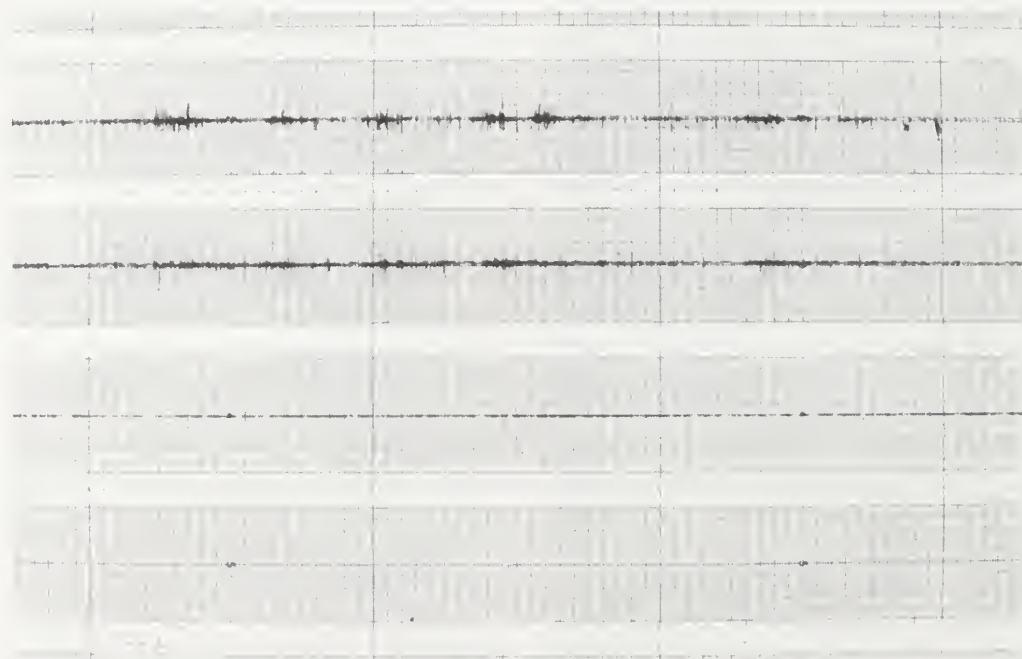
Figure 5.7a - b Temporal variation of bedload signals:
    a) fluctuating transport,
    b) pulsating transport.

Upper lines: detector unit 5/6 in the center of the stream;
Center lines: detector unit 7/8 at the thalweg position;
Lower lines: detector unit 9/10 at the right bank.

- **Both time series are very long.** The time series at 1-hour resolution contain 425 data values points and covers almost the entire 17-day snowmelt high flow period. The time series at 5-minute resolution comprises 890 data values and covers a 3-day interval in the middle of high flow.
- Fluctuations of bedload transport are analyzed in **two different time scales** for the same time interval.

This extremely long continuous record of bedload transport from Squaw Creek provides an opportunity to analyze the temporal variation of bedload transport with respect to both persistence and periodicity of transport waves. A further analyses of bedload transport in different time scales could investigate whether bedload transport fluctuations are the product of superimpositions of various transport processes, which then cause the further temporal pattern of bedload transport.

5.3.2 Bedload patterns [3]

The upper part of Figure 5.8 shows a 17-day hydrograph of the 1986 snowmelt at Squaw Creek, Montana between May 27 and June 14, 1986. Until the night of May 4 to 5, flow is snowmelt dominated. The hydrograph shows the diurnal fluctuations of flow typical for a snowmelt regime. Daily discharge waves increase steeply and decrease at a lesser rate (Section 3.2.1). Two thunderstorms in the afternoon of June 5 and in the early morning of June 9 produce storm flows that are effective enough to override the diurnal fluctuations of flow.

The lower part of Figure 5.8 shows the temporal variation of signals rates produced by naturally magnetic pebbles (andesites) passing over a detector log[4]. The continuous record of signals was counted for hourly intervals. The time series of signal rates show that bedload transport disintegrates into a series of distinct bedload waves. Signal rates increase on the daily rising

Figure 5.8 – Temporal variation of bedload signal rates in 1-hour resolution over a 17-day period during a typical snow melt high flow in 1986.

---

limbs of flow. After peak flow around midnight, signal rates drop drastically. Much lower signal rates are registered at the beginning of the falling limbs than during the same discharge rates on the rising limb. A few hours later, on the falling limb during early morning hours, bedload activity sets in again and shows fluctuating signal rates (Bunte et al. 1987). Regarding these observations, a bedload transport pattern is discernible for the daily flood waves. Bedload waves can be differentiated into three parts. The three colors denote recurring patterns of signal rates for individual high flow days:

- **Large bedload waves:** Each daily rising limb of flow is associated with a wave of bedload transport that peaks around peak flow. The bedload wave can be twin-peaked (May 30 and 31). Signal rates strongly decrease to very low rates after peak flow.

- **Secondary bedload waves:** During snowmelt days secondary bedload waves occur on the falling limbs of flow about 4-6 hours after the peak of the large bedload waves. During the wider hydrographs of storm runoff secondary waves occur about 7 hours after peak of bedload transport.

- **Tertiary bedload waves:** This bedload wave also takes place during the fall limbs of flow about 5 hours after the peaks of the secondary bedload waves. This bedload waves is also frequently twin-peaked with both maxima about 4-5 hours apart.

Bedload transport repeats this pattern on all days when daily mean discharge is larger than 5.5 m³/s (almost bankfull flow). Days with lower flows show this pattern only in a fragmentary way, but the 5-hour frequency of bedload waves is usually maintained (June 3/4 and 4/5). Two storm flows occur on June 5 to 7, and on June 9 to 12. The hydrographs are characterized by steep rising limbs and 2 to 4-day flow recessions. Bedload waves maintain their pattern during this storm runoff, but take a longer time and are more symmetrical than during snowmelt days. These two storm flows offer a good opportunity to compare the temporal variation of bedload transport and the size of individual bedload transport waves and to explain their dynamics.

Large bedload waves:

Both storm flows have similar rising limbs regarding their steepness and amplitude. The second storm flow peaks only 0.2 m³/s higher than the first one. Initially, bedload transport increases for both storm flows, but around peak flows the size and the duration of the bedload waves take a slightly different course for each storm event. During the second storm flow signal rates decrease shortly after peak flow and reach their minimum 6 hours after the maximum of the bedload wave. During the first s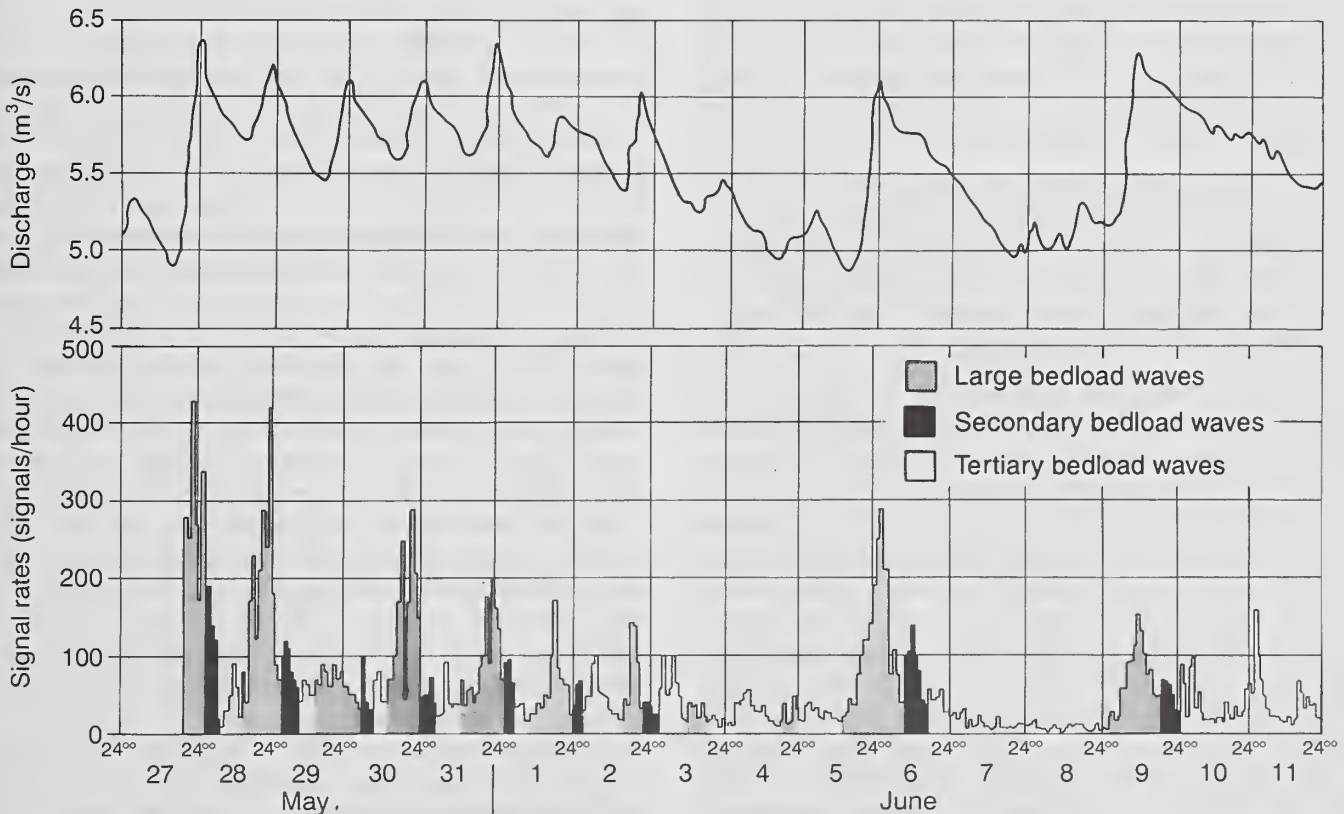torm flow signal rates increase until two hours after peak flow, and reach a maximum twice as high as during the second event. The reason for this different behavior in bedload transport must be due to previous conditions of flow and sedimentary conditions on the river bottom. Prior to the first storm flow, bedload transport was low but never ceased. Transportable sediments must have been stored on the river bottom close to the measuring station and then transported across the detector log as soon as the flow increased again. Therefore, in spite of lower discharges, bedload transport is higher during the rising limb of the first storm flow.

Secondary and tertiary bedload waves:

The rate of flow decrease is similar for both storm events during the first day of the recession. Secondary and tertiary bedload waves are similar in their patterns, but vary in their amplitudes. Although discharge is about 0.3 m³/s less for the first event compared to the second one during the beginning of the recession, the first event still has the larger secondary bedload wave. It is assumed that this bedload wave is generated from bedload material stored in nearby riffle-pool sections. This material reaches the detector during the secondary wave. The tertiary bedload wave is smaller during the first storm event than its twin-peaked counterpart during the second storm. The capacity of flow would have been sufficient to transport a larger amount of sediments during the first storm (compared with the transport rates during the early morning of June 3), but the supply of transportable sediments is now exhausted. Contrarily, a new mass of sediments must have reached the site during the relatively large tertiary wave of the second storm event.

The later parts of both storm flow recessions behave differently, both with respect to flow as well as to sediment transport [5]. The falling limb of the first storm flow has reached low discharges and minimal transport rates during its second day on June 7. However, compared to the discharge on June 4, transport capacity should have been sufficient to transport a threefold amount of sediment. The second day of the falling limb of the second event shows a completely different behav-

ior. Flows being as high as on an average snow-melt day, another large bedload wave occurs - around midnight - without any peak or even an increase in discharge. This bedload peak reaches the same amplitude as its predecessor 40 hours ago, although the discharge has meanwhile decreased by 0.5 m³/s.

The reason might be that bedload material was made available on the river bottom during the relatively high flows of the second runoff event. As the sediment supply around the measuring site seemed to have been depleted for some time during the largest flows of the second runoff event, these sediments now reach the measuring site with a 40-hour delay and form this unexpected bedload wave. Since this bedload wave is not associated with an increase of flow, the supply of bedload is too limited to form a subsequent secondary wave. However, a tertiary wave forms in due time.

Similar processes of sediment supply exhaustion and replenishment must be held responsible for the wavy patterns of bedload transport during the snowmelt days [6]. Despite of the wavy nature of bedload transport, the total amount of signals per discharge day (from low flow to next day's low flow) correlates strongly with the total amount of discharge during that period ($r^2 = 0.87$) (Section 5.1.5). This indicates that the long-term (day-to-day) relationship between discharge and bedload transport is balanced.

However, the proportions of these three waves to each other change over the duration of the snowmelt flow. Both the peak rate and the duration and thus the total amount of signals within the primary bedload wave decrease strongly with time. This pronounced diminishment of the primary waves is partially counteracted by the secondary and tertiary waves, although both of these waves are much less variable during the snowmelt high flow period. In the time between May 28 and June 4, the secondary (brown) waves tend to just slightly decrease with time, while the amplitude and duration of the signals within the tertiary (orange) waves increases over the same time period. This gradual shift with losing primary waves and gaining tertiary waves means that during the first days of snowmelt high flow

bedload transport is strongest on the rising limbs of flow, suggesting the transport of nearby available bedload material. During the later days of high flow, the nearby or easily available storage seem to be depleted. A strong tertiary wave at the end of the falling limbs of daily flow suggests that the material from relative distant sources has reached the site and the amount of daily bedload transport is strongly supplemented by the arrival of this new material.

Bedload waves of similar patterns have been reported to occur in flood waves by Schlatte (1984), Reid et al. (1985), Bänzinger and Burch (1990), and Jackson and Beschta (1982). All cases were marked by the abrupt decrease of large transport rates soon after the peak flow, as well as by one or more small bedload waves on the falling limbs of flow. Reid et al. (1985) explain bedload waves at Turkey Brook (Great Britain) as the result of traction carpets where the entire upper layer of the channel bottom moves downstream in lobes of different width and velocity. Jackson and Beschta (1982) suggest that channel change is the reason for these bedload waves. No explanation is given by the other authors for the abrupt decrease of transport rates and the isolated bedload waves on the falling limbs.

Naden (1987a, 1987b, and 1988) modeled the movement of single, coarse particles within a two-grain-size mixture and computed the temporal variation of calculated bedload transport rates in high temporal resolution. Naden determined particle erosion and transport from the parameters channel geometry, flow conditions, absolute, and relative particle size. Transport rates were determined by the distance over which particles were transported. This modeled temporal variation of transport rates during the passage of a flood wave shows, similar to the temporal variation of bedload transport at Squaw Creek, the abrupt decrease of transport rates after the peak flow has occurred. Although Naden quantified her parameters with only a few size classes, her results are highly encouraging to continue the analyses of the interactions between flow, single particle movement, channel geometry, and bedload transport rates.

---

[5]
This paragraph was added during translation for reasons of clarity.

[6]
This paragraph was added during translation for reasons of clarity.

5.3.3 Comparison of the temporal variation of bedload transport with the temporal variation of the water surface slope

The preceding section attempted to relate the size of the bedload waves to the "history" of flow and inferred stream bed conditions. The following sections will focus on the interactions between flow conditions and channel geometry at a sediment source and analyze the effects of these interactions on the temporal variation of bedload transport.

It was explained in Section 4.5.1 how the temporal variation of the water surface slope can be used to indirectly indicate local channel change and a dislocation of bedload.

In 1986 and 1988, the locations for water surface slope measurements (the ends of the tube levels) were on the left bank 17.3 m apart. The upper location is at the downstream end of a pool, and the lower site is situated at the upstream end of the next pool downstream, with a riffle section in between. The riffle is located in the center of the stream, about 5 m from the left bank and 35 m upstream from the detector log (fig. 3.7). Hydrographs, the temporal variation of water surface slope, and signal rates, or sequential measurements of bedload transport, respectively are depicted for several time intervals during the high flows of 1986 and 1988 (fig. 5.9 a-c).

The course of the water surface slope shows several peaks in all three cases. Maxima in signal rates or bedload transport rates apparently coincide with the second or third increase or peak of the water surface slope. To take a closer look at the causes of the sudden water surface slope increases that occur after peak flows, the behavior of the water levels themselves at the upstream and downstream locations was examined. Figures 5.10 and 5.12 show the examples from May 30 to June 1 in 1986 and May 23-25 in 1988. The sequence of the individual water level readings is numbered. Figures 5.11 and 5.13 graphically present the sequence of the water surface gradient between the two measuring points for both high flows.

The numbered water levels in Figure 5.9b and 5.10, and the corresponding water surface slopes in Figure 5.11 makes it possible to follow the water surface activities step by step. The comparison between water levels and bedload transport rates lead to the following observations: during the first half of rising flow in the night from May 31 to June 1, 1986, water surface slope reacts as expected: both the upstream and downstream water levels, and the slope in between them, increase from measuring time 1 to measuring time 3. Discharge and water surface slope reach their peaks simultaneously at measuring time 4. Both water levels, upstream and downstream, are higher than expected according to stage height. Additional bedmaterial must have accumulated both on the upstream and the downstream side of the riffle to cause this increase in the local water level. Signal rates at the detector log indicate strong bedload transport activity. At measuring time 5 signal rates strongly decrease (fig. 5.9b). Both water levels are slightly reduced, but they maintained their slope (fig. 5.11). At measuring time 6 the upper water level decreases while the lower water level is somewhat increased. Bedload must have dislocated from the riffle towards the pool. A further transport of bedload towards the pool is now also indicated by an increase in the lower water level (time 7). High signal rates indicate vivid bedload transport activity. The lower water level has decreased at time 8 while the upper water level remains unchanged. The bed material that was just transported towards the pool has now left the measuring reach. New material has not accumulated on the riffle yet.

By analogy, it is also possible during the night from May 30 to 31 in 1986 to identify a correspondence between the sequence of the water level changes at the upper and lower end of the riffle and the temporal variation of bedload signals. Bedload material accumulates at the riffle and is then scoured and transported towards the pool. The pool is emptied and new material accumulates at the riffle. After the pool has been cleared, bedload signals immediately reach their maximum (fig. 5.9b).

The sequence of water level changes at the upper and lower tube levels and discharge is also shown in comparison with bedload transport rates sampled in the night of May 24 to 25 in 1988 with the net-sampler (fig. 5.12). Figure 5.13 graphically presents water levels and surface slopes. Increasing water levels and slopes (measuring time 1 to 5) indicate again sediment accumulation on the riffle during rising flows. Although some material is transported towards the pool, the pool is only beginning to be emptied at time 6. A high bedload transport rate follows. Both water levels continue their rise during waxing flow (time 7). Times 8 and 9 indicate again large bedload dislocations with accumulations at the riffle and scour at the pool (time 8), and scour at both the riffle and the pool at time 9. A large bedload transport rate passes the measuring site
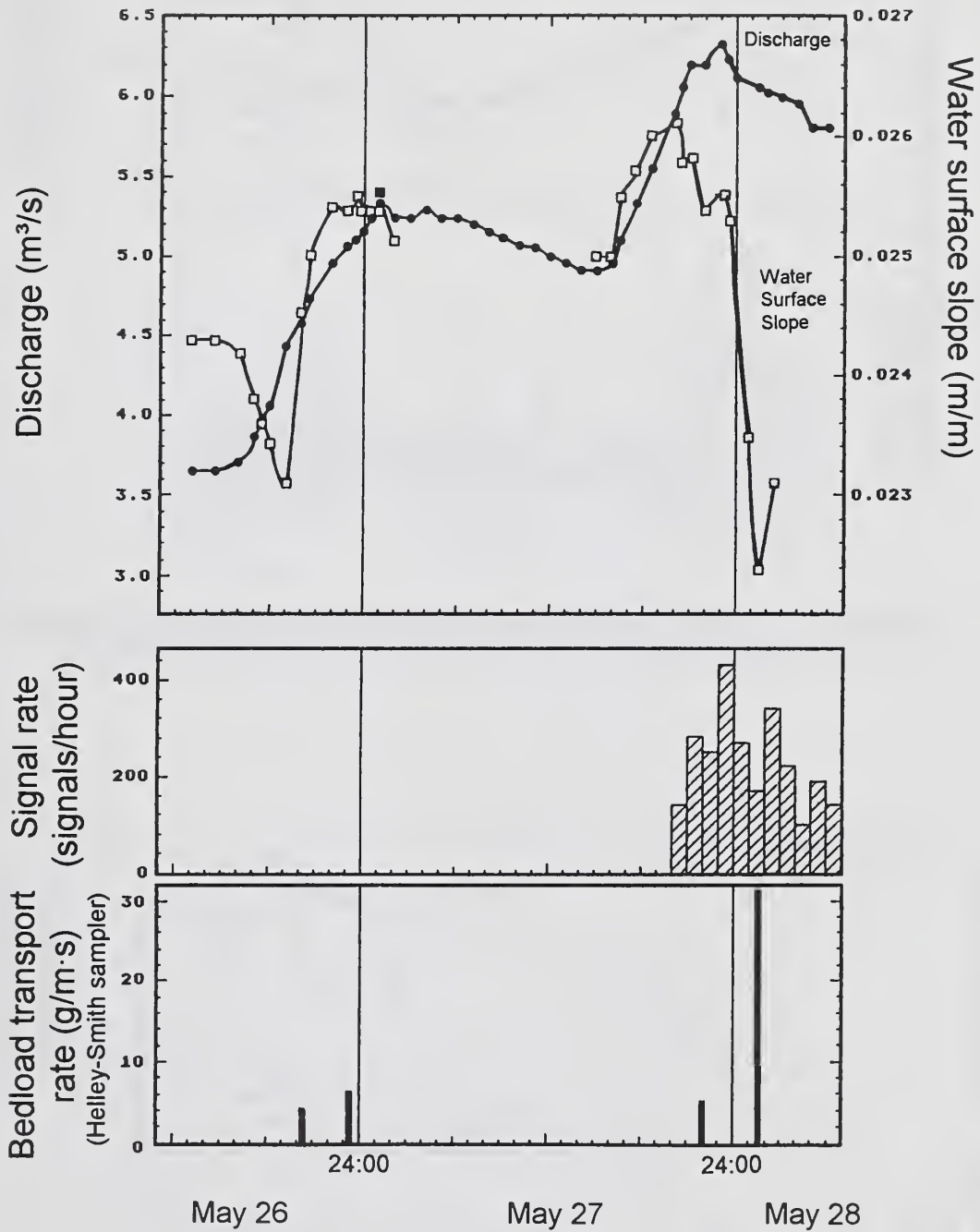
Figure 5.9a – Hydrograph, measured water surface slope, and bedload signal rates over a 2-day period from May 26-28, 1986. (The recording of signal was only started on May 27, 20:00. System tuning during the first two days of high flow (May 27-28) altered the sensitivity of the registration. Signal count rates may have been lower during this period).
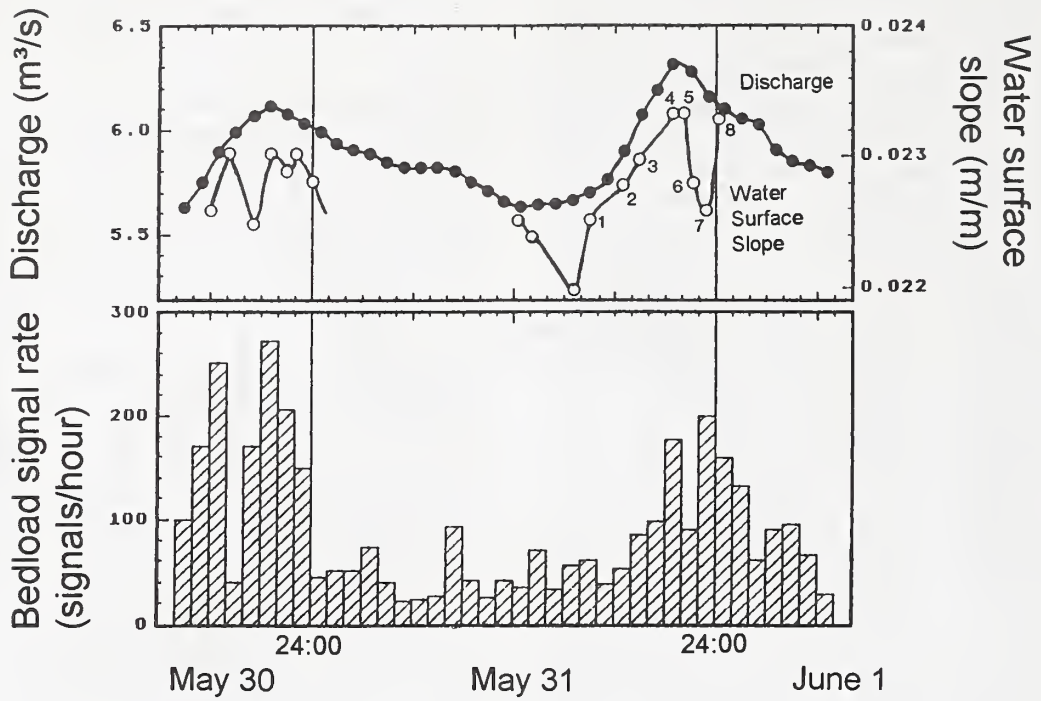
Figure 5.9b – Hydrograph, measured water surface slope, and bedload signal rates plotted over a 2-day period from May 30 to June 1, 1986. Sequence of measuring times is numbered.
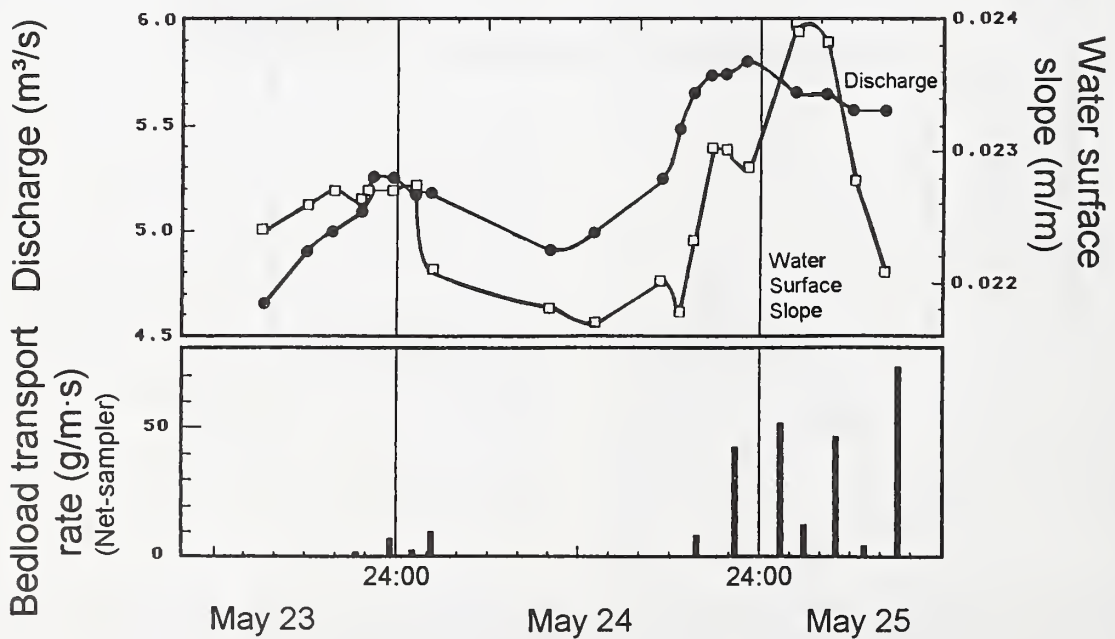
Figure 5.9c – Hydrograph, measured water surface slope, and bedload transport rates determined with the net sampler plotted over a 2-day period from May 23-25, 1988.

64
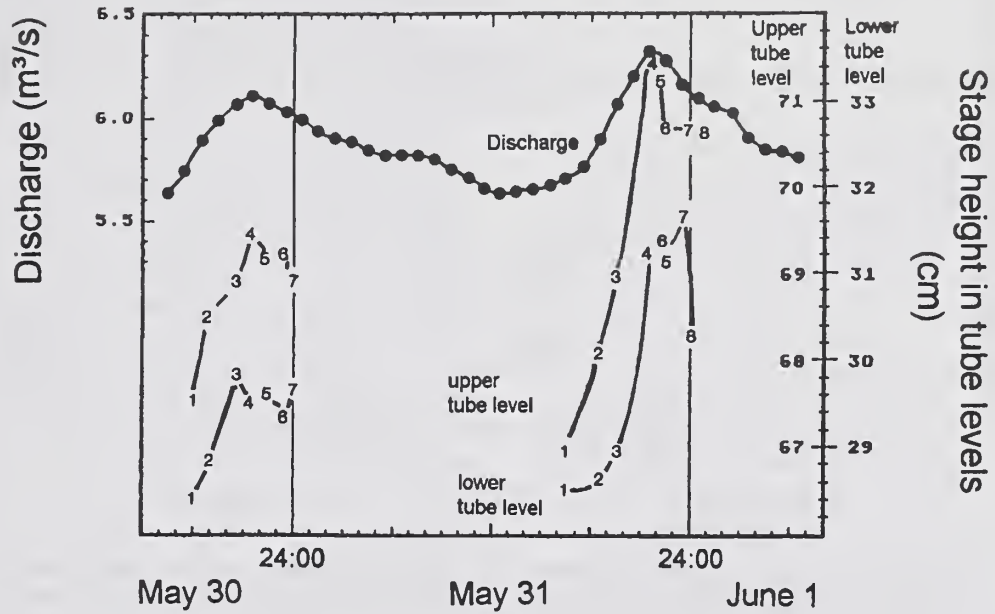
Figure 5.10 – Hydrograph, bedload signal rates, and measured water levels at the upper and lower water level tubes plotted over a 2-day period from May 30 to June 1, 1986. The sequence of measuring times is numbered. Water level heights are above an arbitrary datum.
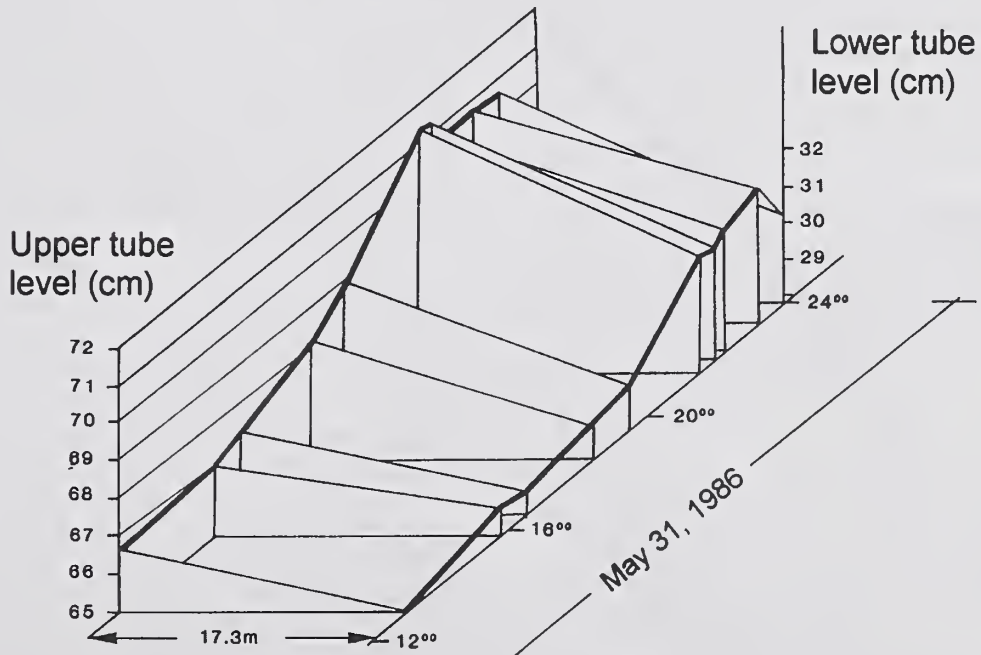
Figure 5.11 – Temporal variation of water surface levels at the upper and lower water level tubes during the high flow wave of May 31 to June 1, 1986.
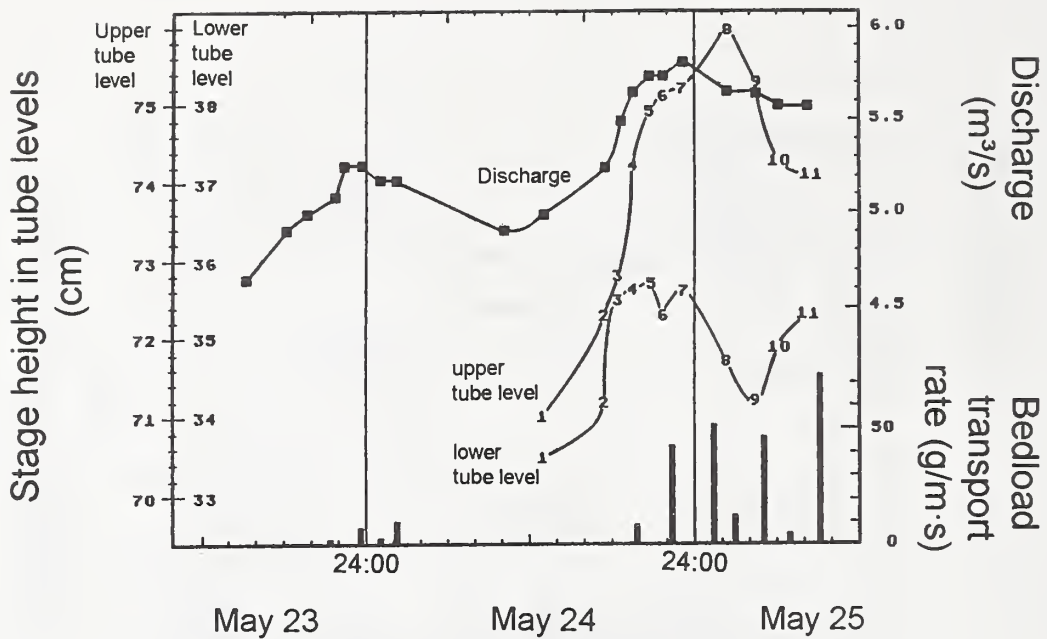
Figure 5.12 – Hydrograph, bedload signal rates, and measured water levels at the upper and lower water level tubes plotted over a 2-day period from May 23-25, 1988. The sequence of measuring times is numbered. Water level heights are above an arbitrary datum.
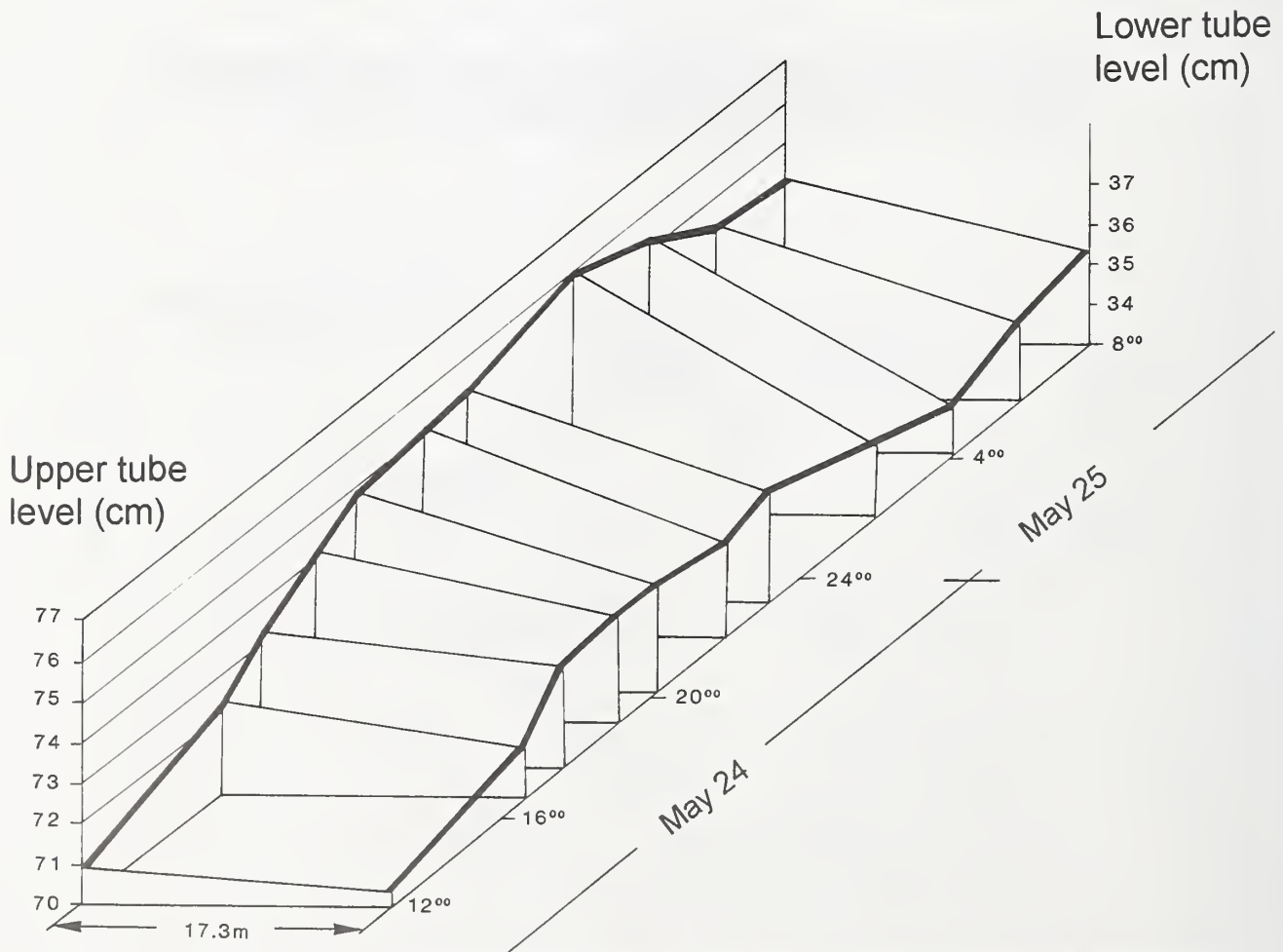
Figure 5.13 – Temporal variation of water surface levels at the upper and lower water level tubes during the high flow wave of May 24-25, 1988.

at the detector log soon afterwards. Water levels at time 10 and 11 indicate again sediment dislocation from riffle to pool. Large bedload transport rates are sampled downstream a little later.

The aggradation and degradation of sediment stored at a riffle and bedload waves following this process can be seen at Squaw Creek by observing the water surface dynamics recordable by sequential water level reading. Sediment accumulates on a riffle, is transported from riffle to pool, and finally leaves the pool. Bedload waves are recorded 35 m downstream at the detector log on the falling limbs of flows about an hour after these sediment dislocations have occurred. Jackson and Beschta (1982) documented similar observations at Flynn Creek in Oregon. A pronounced change in bedload transport rates occurs synchronously with changes in channel geometry. Sediment is deposited on a riffle during rising flows. This sediment is eroded as discharges continues to rise. This leads to a strong increase of bedload transport rates. Scour at the temporary sediment storage on the riffle ceases after peak flow has passed. Bedload transport rates stay high for awhile, but decrease as sediment is deposited on the riffle during waning flow. Another bedload wave follows after the riffle sediment storage is depleted again.

Sequential changes of water surface slope on the rising limbs of flow can, unfortunately, not be used to indicate that bedload transport waves result from a step-wise dislocation of sediment from riffles to pools. The temporal change of water surface slope is the response to a combination of effects, such as the volume of flow, its unsteadiness, and changes in flow width. On the steep rising limbs it is difficult to distinguish the proportions of water surface slope that are attributable to an increase of flow from responses to other factors.

A combined team effort featuring the simultaneous detailed surveys of the channel bottom geometry and continuous registrations of water surface slope and bedload transport need to be accomplished in order to gain a better understanding of the dynamics of the temporal variability of bedload transport. The inexpensive tube levels could be used in several locations in the stream long profile. The analyses of the temporal and spatial variations of the water surface slope could make it possible to follow bedload waves on their way downstream and determine their travel velocity. Present results indicate that bedload waves cover the 35 m distance between the riffle and the detector log in less than 1 hour.

This means that bedload waves at Squaw Creek move with a speed in the order of centimeters to decimeters per second.

5.3.4 Cross-sectional changes across the riffle

Berry (1988) analyzed the temporal and spatial variation of channel geometry across a riffle during the spring high flow in 1988 at Squaw Creek. The cross-sectional profile was measured in 10 cm increments using the "Tausendfüßler" profiling device each 3 hours over a time period of 29 hours (Sections 4.3.3 and 4.5.2).

Berry's analyses during the passage of a high flow wave of May 23 to 24, 1988, showed that changes in the cross-sectional stream geometry are limited to individual sections of 1-2 m width, which add up to a total active width of 4-6 m. The variability of the channel bottom geometry ranged between 5 and 20 cm.

The measuring period of cross-sectional profile measurements, unfortunately, does only partially overlap with the period of simultaneous water surface slope, flow velocity, and bedload transport measurements. Therefore, the only statement that can be made for the night of May 24, 1988, is that the extent of cross-sectional changes increases with flow. Some aspects of the cross-sectional development are also visible in the sequential measurements of the water surface slope: A phase of sediment accumulation in the cross-section between 18:00 and 21:00 hours corresponds with an increase of water surface slope, while the water surface slope decreases again during an erosional phase between 21:00 and 23:20 hours, May 24, 1988.

Fast surveys of the channel geometry are necessary in order to establish the relation between bedload waves and channel change. A measuring time of less than 5 minutes would be desirable because bedload waves are often not longer than 20 minutes (Section 5.4).

Based on the present observations, two questions arise:

- Why is bedload material cyclically accumulated and scoured from a riffle?

- What is the function of a riffle-pool morphology with respect to channel change and bedload transport?

Starting with the second question, the next paragraphs try to shed some light onto these questions.

Riffle-pool morphology: [7]

Riffles and pool are spatially sequential phenomena along the stream long profile. The distance between riffles and pools depends on discharge conditions and the amount of transportable sediment. Leopold et al. (1964) give a pool-to-pool distance (l) as:

$$l = (5 \text{ to } 7)\, w \qquad (6a)$$

where l is the pool-to-pool distance and w is the stream width. Morisawa (1985) gives the pool-spacing as:

$$l = 5.42\, w^{1.01} \qquad (6b)$$

This formula can be simplified to:

$$l = 5.5\, w \qquad (6c)$$

which gives a pool-to-pool distance between 45 and 55 for Squaw Creek with a bankfull stream width of 8-10 m. The measured pool-to-pool distance at Squaw Creek is about 50 m. This corresponds well to the distance given by both authors.

A riffle-pool morphology makes it possible for a supply-limited stream to minimize its energy expenditure (Yang 1971). Other than in a transport-limited braided stream, supply-limited streams have only small amounts of transportable sediment available to minimize energy expenditure. The adjustment between flow and channel geometry is therefore limited to a few locations within the stream morphology. Coming from a narrow and deep pool, the stream "fans" widely in the reach of a riffle. The downstream energy of flow is decreased by the distribution of flow into a new cross-sectional form with shallow depth and large width, as well as by the larger absolute and relative roughness and a more turbulent flow. While a high shear stress in the pools during high flows ensures the transit of bedmaterial and keeps pools clear of sediment accumulations, riffles become the "staple locations" of sediment transport. Sediment arrives, is sorted according to the interactions between local hydraulics and stream roughness, and sent off again in a new distribution.[8]

Cyclic accumulation and scour at a riffle:

P. Carling and M. Glaister had performed their detailed velocity-profile measurements in 0.5 m spacings in the same cross-section in which Berry (1988) conducted her cross-sectional surveys (fig. 4.14a–b). For some time intervals these two measurements overlapped. Owing to the Prandtl law of vertical velocity distribution, the gradients of the isovels can be used to calculate the boundary shear stress (τ_0). P. Carling and M. Glaister could then plot the temporal variation of the boundary shear stress (τ_0) over a cross-section at Squaw Creek.

Comparing these cross-sectional and temporal variations of boundary shear stress with the cross-sectional and temporal variation of the channel microtopography, Berry (1988) found that often large roughness is smoothed by large shear stresses which erode the coarsest particles. When shear stresses are small, large roughness tends to be reduced by an in-fill of the interstices with fines.

This result was further extended in this study into a conceptual model describing the relation between the temporal and spatial sequences of roughness and channel change and the temporal variation and spatial variation of the shear stress exerted onto the stream bottom.

5.3.5 Conceptual model regarding the adjustment of the stream bottom to flow hydraulics across a riffle

The model introduced below should help to explain processes and effects that occur as the bed particles are dislocated during the adjustment of the channel bottom to the hydraulics of flow (fig. 5.14).

The primary condition is a rough channel bottom at a riffle where coarse particles have settled. The four columns in the diagram of Figure 5.14 show different flow depths in rows 1 and 3. The flow depths in these four columns can either depict a temporal or a spatial sequence. Flow depths

---

[7] *The study on stream morphology by Montgomery and Buffington (1993) had not appeared yet.*

[8] *Emmett et al. (1983) show how the zones of highest stream power shift from riffles during low flows to pools during high flows. That way riffles become short-term sediment storage during high flows, while pools become long-term storage for sediment between high flows (see Meade 1985). Thompson (1994) indicates in his thesis that the high stream power in pools during high flows is due to the fact that the downstream oriented part of flow comprises only the central part of the pool cross-section, while lateral parts of the pool are dominated by recirculating eddies with no net downstream movement of flow.*
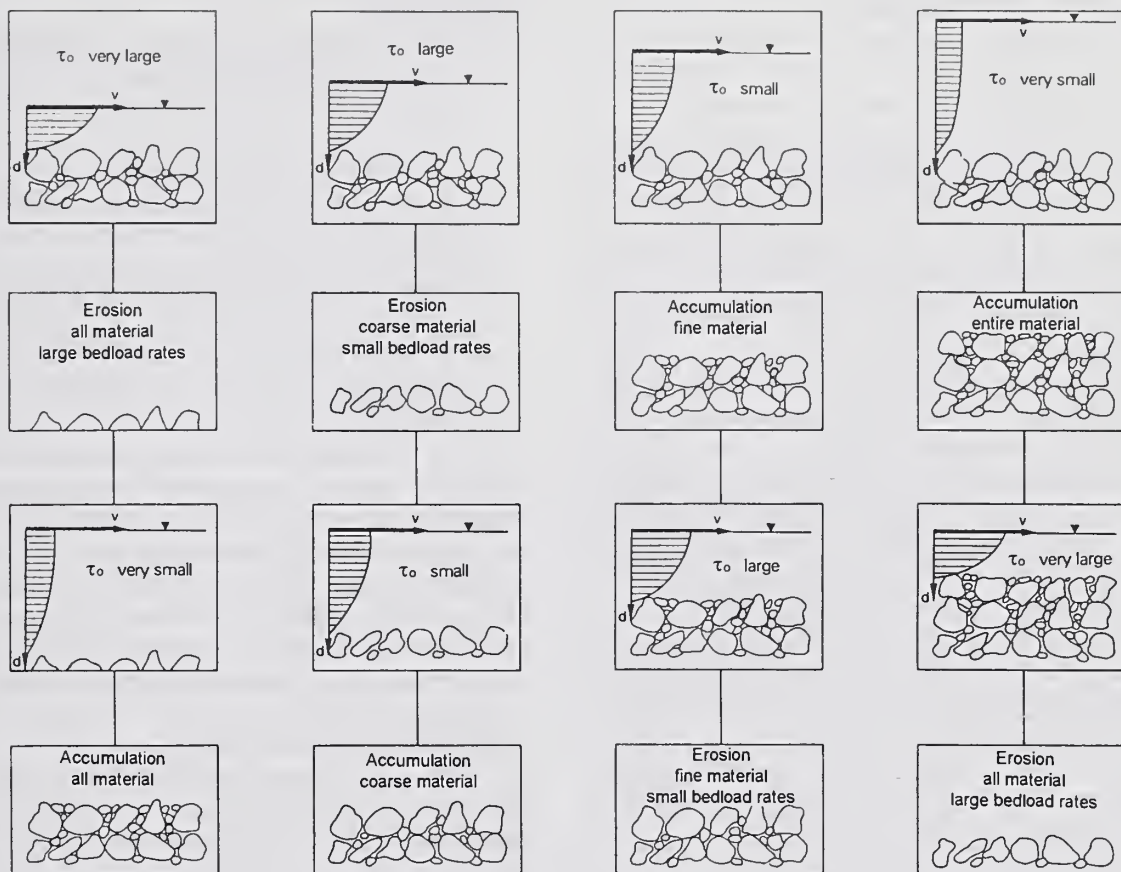
Fluctuating bedload transport with varying grain-size distribution
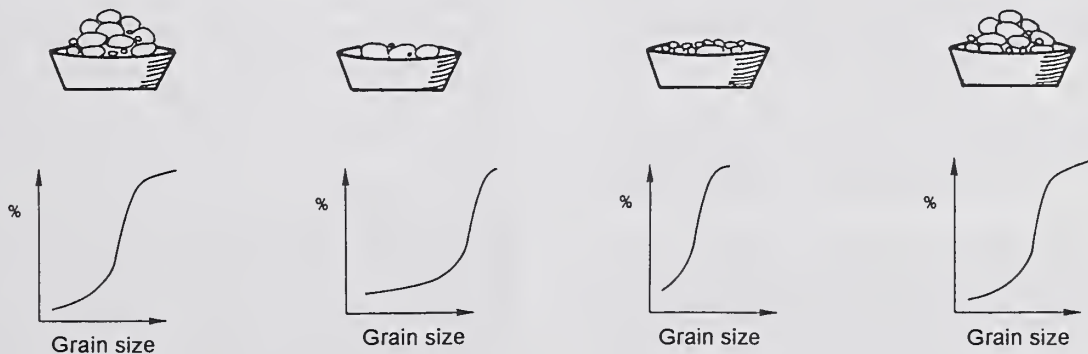
Figure 5.14 – Conceptual model demonstrating different degrees of river bed adjustment processes in response to the sedimentological conditions at the stream bottom and flow hydraulics at a riffle reach.

affect the shape of the velocity profiles. The larger the vertical velocity gradients, the larger the shear stress τ_0 exerted onto the stream bottom. This proportionality is expressed by the shear stress equation for Newtonian fluids:

$$\delta v /_{\delta d} = {}^1/_{(\eta+\varepsilon)} \tau o \qquad (7)$$

where $\delta v /_{\delta d}$ denotes the velocity gradient, and η and ε are the dynamic viscosity and the eddy viscosity.

The differentiation of shear velocities into very large, large, small, and very small in the upper row of the diagram in Figure 5.14 is only to denote relative differences.

The adjustment of the channel bottom to the hydraulics of flow takes different behaviors, depending on the relative size of the shear stress and the grain-size composition of the stream bed. In step 2 of the model, large shear stresses erode the coarsest particles from the top of the stream bed, while small shear stresses fill interstices with fines (Berry 1988). When shear stresses are extremely large or extremely small, the channel bottom cannot adjust to flow by a few single particle dislocations within the upper surface layer only. Extremely large shear stresses erode an entire surface layer 1-2 grain-size diameters thick. (Berry (1988) measured a depth variability of 5-20 cm within the course of a high flow day.) If local shear stresses are very small, a likewise thick layer of particles is deposited.

The channel bottom conditions produced by step 2 of the model are again exerted to various shear stresses in step 3. The extent of the newly acting shear stress depends on the previous degree of channel change. If the water level in each scene is fixed on the same absolute level in which it was at the start of the cycle, then water levels increase with the depth of prior erosion and decrease with the thickness of prior deposition.

In step 4, the channel bottom adjusts again in response to the strength of flow given from the vertical velocity gradients and to the roughness conditions. Small shear stresses on a rough channel bottom lead to a deposition of coarse particles. Large shear stresses on a smooth channel lead to a winnowing of the fines that had filled the interstices before. Extreme changes of local shear stresses again cause large channel changes. The high erosion or accumulation rates do not only alter the roughness, but also the shape of the channel.

The following patterns of bedload transport dynamics emerge from this model conception with respect to the amounts and grain-size distribution of the sediment involved in the adjustment dislocations:

- If the channel adjustment is limited to individual particles of different grain sizes from the upper surface layer, this causes the movement of small amounts of bedload that is either predominantly coarse or predominantly fine, depending on roughness and flow conditions (fig. 5.14 column 2 and 3).
- If the entire bottom layer is reformed during large-scale river bed adjustments, this involves high bedload transport rates that comprise the entire grain-size spectrum (column 1 and 4).

The processes, schematically depicted in columns 1 to 4, can either represent a spatial variation or a temporal sequence. The extent of the channel change and its temporal variance determine the fluctuations of bedload transport. The fluctuations alternate between large transport rates with wide and even grain-size spectra and small transport rates with narrow and uneven grain-size spectra, which have been truncated on either their coarse or their fine end.

Before this conceptual model is tested against the grain-size distributions of serial bedload samples later in Section 5.5, Section 5.4 will examine the phenomena of bedload waves observable under high temporal resolution and try to identify the respective transport mechanisms.

5.3.6 Results

The various forms of river bed adjustments in coarse bedload carrying stream can be combined as follows: If a stream is in dynamic equilibrium bedload transport during "ordinary" high flows is more continuous, when more transportable sediment is available. A fluctuation of bedload transport rates in mountain streams indicates discontinuous adjustments between the conditions of flow and the conditions on the stream bed. If the equilibrium of a stream is disturbed by impacts on both the water and sediment budget from a natural or human source, this can lead to unpredictable bedload transport rates and a drastic change of the channel morphology.

Most time series of coarse bedload transport in streams shown in the literature are either of short duration and comprise only the passage of a one-day high flow wave or the temporal resolution of

the records is not sufficient for an analysis of the temporal variability. A 17-day continuous record of coarse material bedload transport (pebbles and larger) was obtained using the magnetic tracer technique at Squaw Creek. This long record makes it possible to analyze the temporal variation of bedload transport with respect to periodicity, persistence, and correspondence to discharge.

The visual analysis of fluctuating transport rates at Squaw Creek during a snowmelt high flow indicates a pattern of three bedload waves that occur during each discharge wave: The primary bedload wave corresponds to rising and peak flow, and another secondary and tertiary bedload wave pass on the falling limbs of flow. The size of the bedload waves is attributable to the preceding history of flow and the conditions on the river bed (degree of consolidation).

The temporal variation of coarse bedload transport can usually not be compared with other parameters in their temporal variations because, in most of the cases, flow is the only other parameter that is recorded as a time series. This restriction reduces the analyses of the bedload fluctuations, or unsteady bedload transport - discharge relations, to a mono-causal interpretation. However, recognizing that bedload transport is part of a complex system of interactions, a mono-causal interpretation is not adequate, especially since various studies have attributed the temporal variations of bedload transport to a number of different causes in different streams. Bedload transport results in its temporal variation from a combination, or an interaction, of various processes. Therefore, it should be attempted to measure these parameters (e.g., channel geometry, grain-size distribution of the river bed and of bedload, and flow conditions) in their temporal and spatial variation, so that time and spatial series can be related to the temporal and spatial phenomena of bedload transport.

Measurements at Squaw Creek made it possible to compare time series of bedload transport and discharge with fragmentary time series of water surface slope, channel geometry and bedload transport rates and their grain-size distributions. Even if the temporal and spatial resolution of these measurements leaves much to be desired, they can nevertheless demonstrate that bedload transport is part of a complex interactive system. Based on the analyses of water surface slope, primary bedload waves near peak flow can be inter-

preted as discontinuous adjustment processes of the channel bed to flow conditions at a riffle area. For the time period around peak flow, and on the early recession, the unsteady behavior of the water surface slope can be used as an indicator for accumulation and erosion of bedload material at a riffle and its subsequent dislocation into and out of a downstream pool. Unfortunately, it is not possible to extend this analysis to the rising limbs. The effects of the fast changing water level during the approach of a flood wave override the effects of channel change on the temporal course of the water surface slope. The analyses could well be extended during the entire falling limbs of flow, if a larger measuring crew or an automated recording was available. Continuous and temporal high resolution measurements of hydraulic conditions, changes of channel geometry, and roughness are necessary to analyze bedload transport processes in their causal relations with hydraulic conditions, and the sedimentologic, geometric and morphologic conditions of the stream bottom.

The combined results of the cross-sectional micro-profile measurements at a riffle carried out by P. Ergenzinger and T. Berry and simultaneous measurements of the spatial and temporal variations of the velocity profiles by P. Carling and M. Glaister (fig. 4.14a - b) could be extended to a conceptual model that explains the processes of bedload transport in a riffle reach. The model describes a temporal or spatial variation of bedload transport and its grain-size distribution from the interactions between flow hydraulics and channel roughness.

5.4 Analyses of the Temporal Variation of Bedload Transport in High Temporal Resolution

Processes that lead to fast fluctuations of bedload transport (in the order of minutes) can be analyzed in two different ways:

1) other parameters are measured in a comparably high resolution and time series are compared for similar patterns, or

2) the temporal structure of the fluctuations is investigated assuming that the temporal variation of bedload transport is a function of several temporally varying parameters and their effects are superimposed.

Comparison between high temporal resolution time series of bedload transport and other stream parameters:

It is very difficult to perform quantitative temporal high resolution field measurements of sedimentological processes at the channel bottom (e.g., variability of channel geometry, roughness, passage of bedforms, bedload transport rates and their grain-size distributions). Such measurements are usually restricted to the manageable environment of laboratory investigations, unless new measurement techniques are developed and applicable for field conditions e.g., a shallow water sonar for a fast registration of channel bottom roughness and geometry or the magnetic tracer technique for fast registration of bedload signals and their grain-sizes (Spieker 1988). Some high-tech measurements of flow forces, such as the fast registration of extent and direction of flow velocities (turbulence) and the amount and grain sizes of sediment transported as a response to turbulence activity can be done at the bottom of relatively deep and manageable tidal waters with small grain sizes (Heathershaw and Thorne 1985). But such measurements are problematic in shallow, turbulent flows in rough, high energy mountain streams.[9] Laboratory analyses are a much easier environment for such experiments (Brayshaw 1985; Williams et al. 1990; Apperley and Raudkivi 1989).

Analyses of the temporal structure of bedload waves

It can be hypothesized that the temporal variation of bedload transport comprises the sum (or the product) of various processes that lead to temporally varied bedload transport rates. The sedimentary effects of several temporally varied processes are hidden within the temporal structure of long time series from measurements in streams. A time series analysis can statistically separate different bedload transport frequencies and check bedload waves for superimposition of various bedload frequencies that might be attributable to the respective processes. Laboratory experiments, on the contrary, eliminate many of the parameters that affect bedload transport. Transport patterns thus derived might only provide reduced insights into the processes that occur

in natural streams. The question arises in how far laboratory experiments are suitable to analyze the combination of processes that lead to a temporal variability of bedload transport in **gravel-bed streams**.

5.4.1 Analyses of bedload waves at Squaw Creek based on 5-minute intervals

A more detailed analysis of fluctuating transport rates requires a larger time scale than the 1-hour resolution used in Section 5.3. A time period of 74 hours, from May 30, 22:00 to June 2, 24:00, was selected from the 17-day time series of 1986 to perform an analysis in higher temporal resolution. Signal rates were calculated for 5-minute intervals and plotted in Figure 5.15. The time series yielded 890 data. The course of bedload transport, that was already considered to be fluctuating in a 1-hour resolution, was found to disintegrate into many small bedload waves as the temporal scale is enlarged by a factor of 12. These bedload waves are analyzed with respect to periodicity, amplitude, duration, and symmetry employing different methods:

- Visual analysis,
- Statistical time series analysis, and
- Statistical analysis.

5.4.1.1 Visual analysis
A visual analysis of the time series leads to the following results (fig. 5.16):

1) The relation between bedload transport and discharge becomes more apparent if the peaks of **largest waves are connected by a drawn line**. This new "course" of bedload transport is quite comparable to the course of flow, but shows a lag time to flow of about 1.5 hours.

2) A **line connecting all bedload peaks** makes especially those bedload waves visible which occur each 5-6 hours during the falling limbs of flow.

3) This line also points out the smallest bedload waves that follow each other in a 1-hour frequency. These waves are best detectable on the falling limbs of flow on June 1 and 2.

4) A **line connecting all minima** or "troughs" of the bedload waves (provided that the wave between the minima has a duration of more than 5

---

[9] As part of the research project granted to P. Carling by the US Army Corps of Engineers (final report by Carling et al. 1993), J. Williams and P. Carling succeeded to perform measurements of turbulence at Squaw Creek in 1991 and 1992, using an electromagnetic current meter (EMCM). Acoustic signals from bedload motion close to the EMCM were intended to be recorded with a hydrophone. Unfortunately, flows were not high enough during the presence of the researchers to cause substantial bedload transport.

minutes) shows a periodicity of 1.5 hours for the large bedload waves that pass during highest flows.

A interrelation exists between the time of occurrence of bedload waves and the amplitude of these bedload waves. The amplitude is defined as the highest signal rate within a bedload wave. The following links are visible from Figure 5.17:

- Bedload waves occurring around **daily peak flows** have amplitudes between 18 and 42 signals per 5 minutes with a mean

signal rate of 25. These waves will be called **major** bedload waves.

- Bedload waves occurring about **each 5 hours** have amplitudes between 11 to 15 signals per 5 minutes with a mean signal rate of 12. These waves will be called **minor** bedload waves.

- **Small** bedload waves with signal rates of 5-10 signals per 5 minutes are observed to pass in **hourly frequencies**.
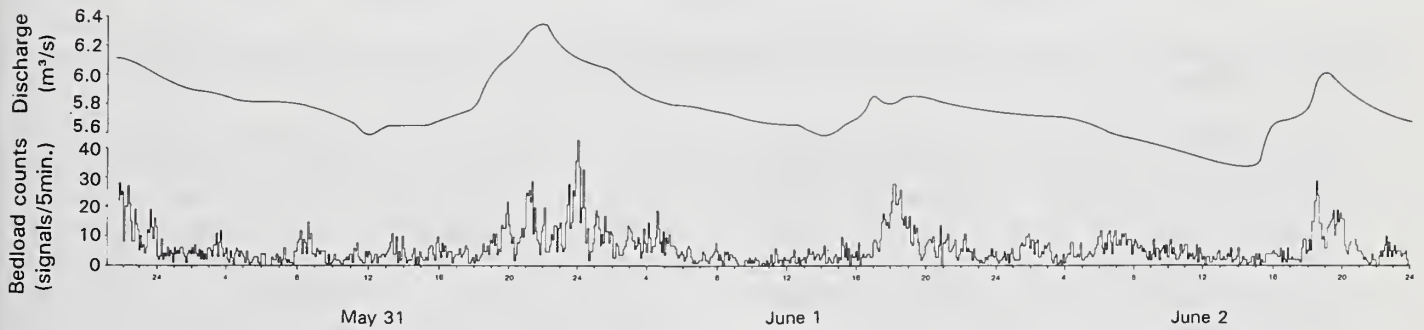
Figure 5.15 – Temporal variation of bedload signal rates in 5 - minute resolution over a 3-day period from May 31 to June 2, 1986.

Dynamics of Gravel-Bed Rivers. P. Billi, R.D. Hey, C.R. Thorne, P. Tacconi (editors), 1992, John Wiley & Sons Ltd., Chichester, England, Reproduced by permission of John Wiley and Sons Limited.
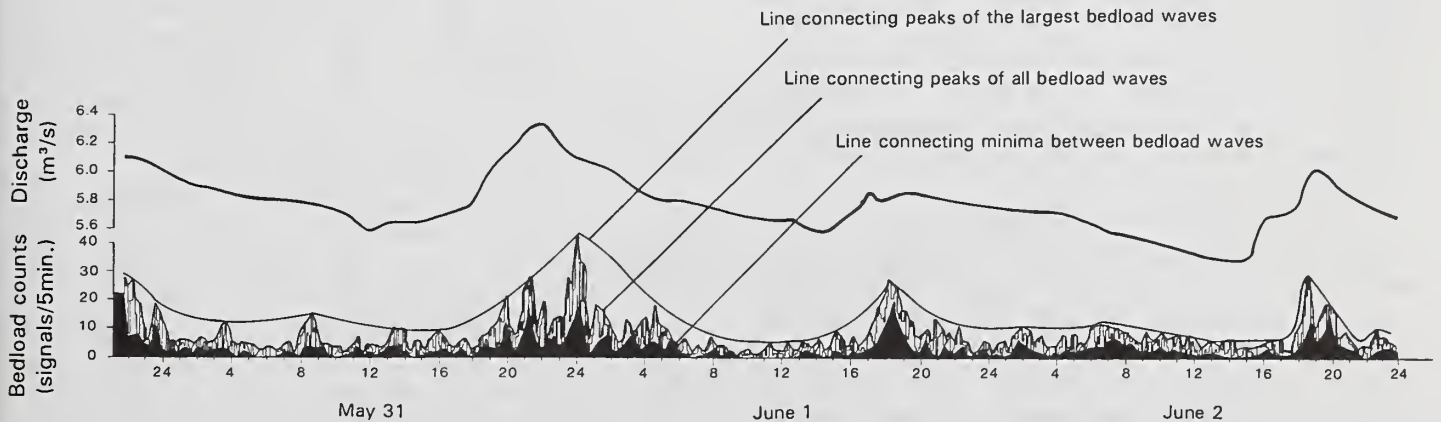
Figure 5.16 – Drawn lines connecting: a) the maxima of the largest bedload waves, b) the relative maxima of bedload waves (smaller peaks), and c) the minima between bedload waves.
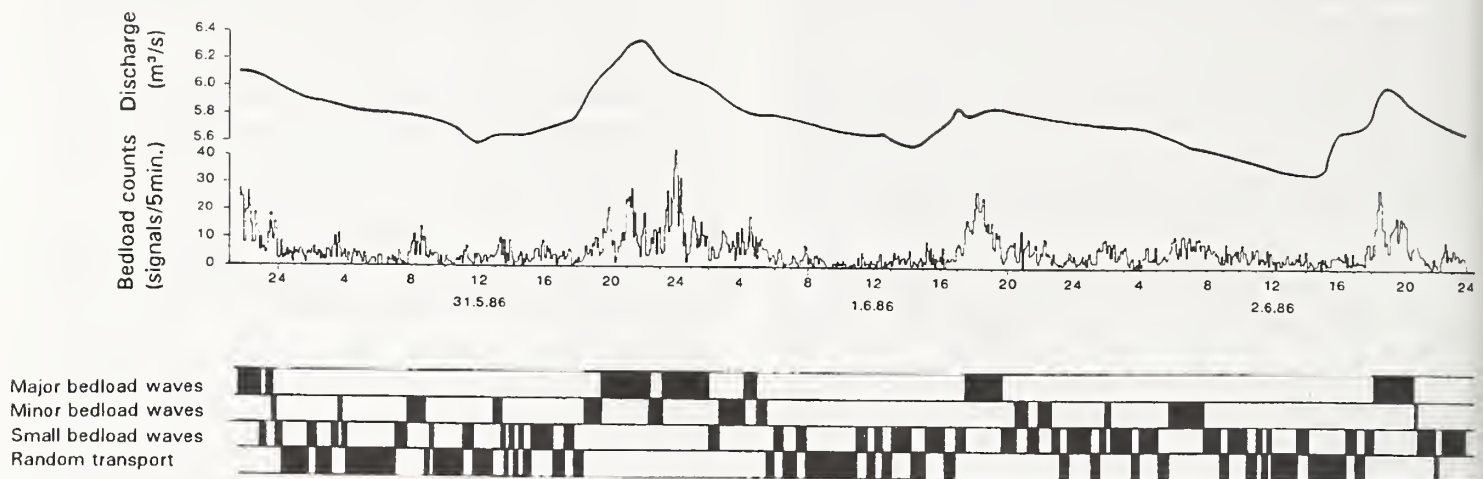
Figure 5.17 – Temporal occurrence of various bedload waves during the passage of several high flow waves over a 3-day snow melt high flow period.

• A wave structure is no longer apparent when signal rates drop below 4 signals per 5 minutes. This transport is therefore called **random**. Although there is probably a random aspect in bedload transport at all times, random transport is only visible when transport rates are too low to exhibit waves.

5.4.1.2 Statistical time series analysis

The visual analysis of the time series was supplemented by a statistical analysis in the form of a Fourier Transformation and a spectral analysis (König and Wolters 1972; Belke 1974; Chatfield 1980; Yevjevich 1972).

A FORTRAN program written by G. Reusing (Math. Geology, FU Berlin) was used to perform a Fourier Transformation (harmonic analysis). The periodogram obtained from the Fourier analysis of the entire time series with 876 data shows peaks at a frequency of 24 and 4.3 hours (fig. 5.18a). A graphical smoothing of the jagged graph indicates additional frequencies of 5, 2.5, 1.5, and 1 hours (fig. 5.18b).

This analysis was supplemented by a spectral analysis of the time series, because a periodogram only determines the periods that make the largest contribution to total variance, but a periodogram does not define the amplitudes of the respective bedload waves. The spectral analysis characterizes the short-term temporal variations of bedload transport by its frequency distribution. A spectral density function was calculated using also the entire time series. Results were plotted as a smoothed periodogram (fig. 5.19a) where the or-

dinate denotes the amplitude of the bedload waves in number of signals per 5 minutes. The frequency of occurrence per 5-minute interval is plotted on the abscissa. The frequency is transformed into periods by taking the reciprocal value and multiplying by 5. The peaks in the smoothed periodogram indicate the periodicity of the time series. The spectral density function of Figure 5.19a shows only one peak at a frequency that corresponds to a periodicity of 1.5 hours. Smaller frequencies (or larger periods) are not visible in the smoothed periodogram.

An additional trend analysis showed that the time series was superimposed by a tenth order trend. After this trend had been eliminated, the spectral analysis was repeated. Results were again plotted in a smoothed periodogram (fig. 5.19b). Two peaks emerge above the level of significance of 3.5 signals per minutes. They appear at frequencies of 0.013 and 0.06 per 5-minute interval. This means bedload waves with a 6.4- and 1.4-hour periodicity are indicated. Several smaller peaks are visible within this periodicity.

In order to focus on the analysis of shorter frequencies and exclude the effects of long frequencies (24 hours), the entire time series was divided into 3 partial time series, each of which comprises an entire high flow day. Two spectral analyses were performed with each of these data sets, one with the original data, and one using data from which a fourth order trend had been eliminated prior to the spectral analyses. The frequencies of bedload waves above the level of significance (3.5 signals per 5-minute interval) were transformed into periodicities. Several peri-
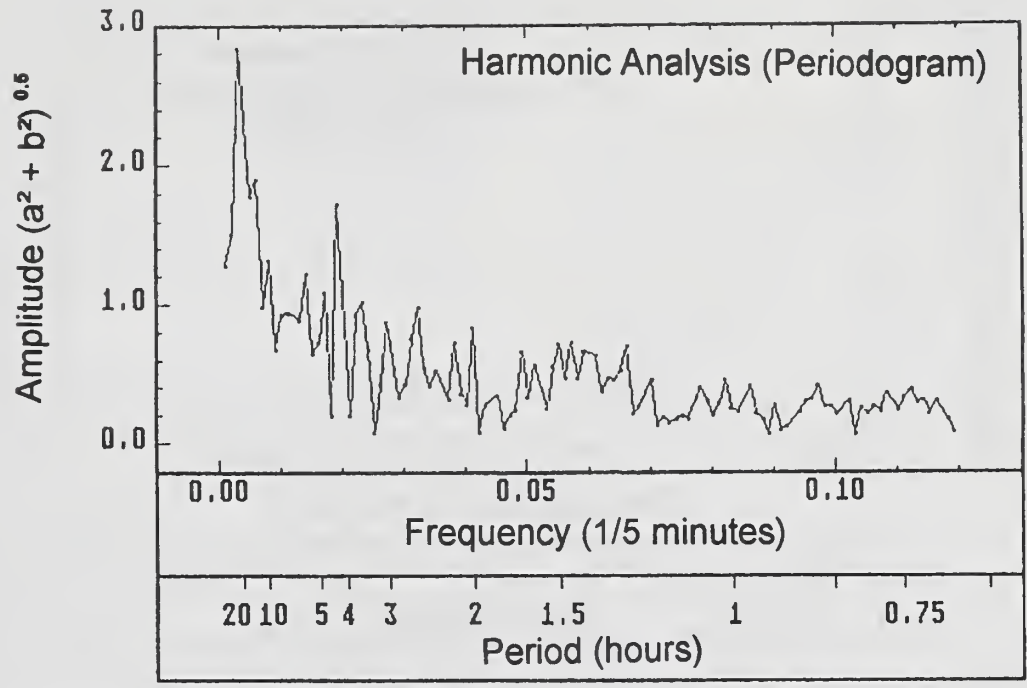
Figure 5.18a – Harmonic analysis (periodogram) of the entire time series at 5-minute resolution (plot of original data).
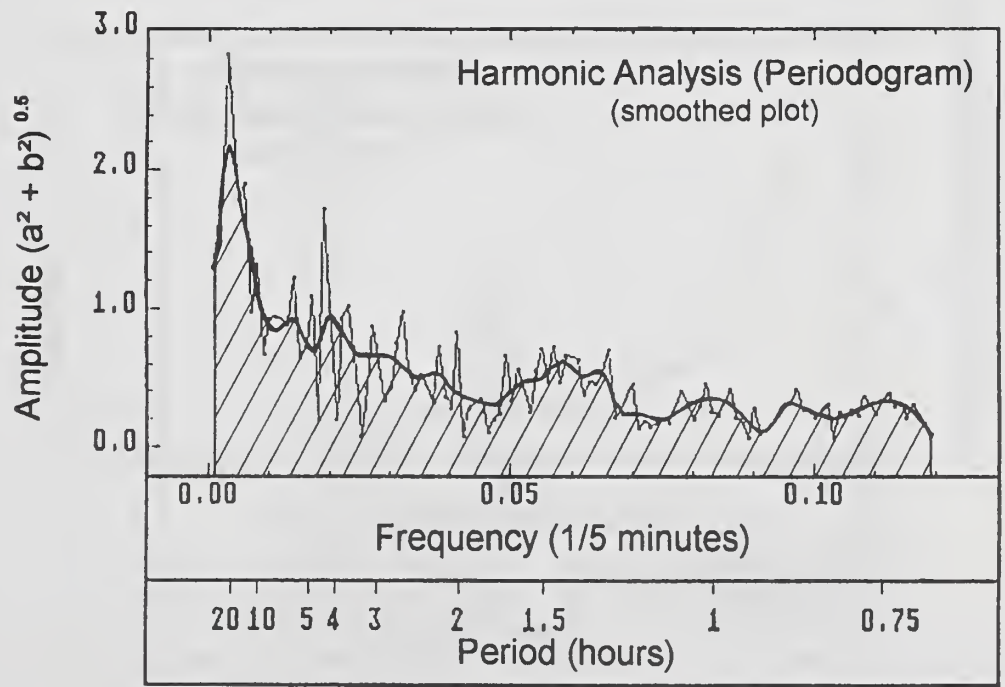
Figure 5.18b – Harmonic analysis (periodogram) of the entire time series at 5-minute resolution (plot of original and graphically smoothed data output).
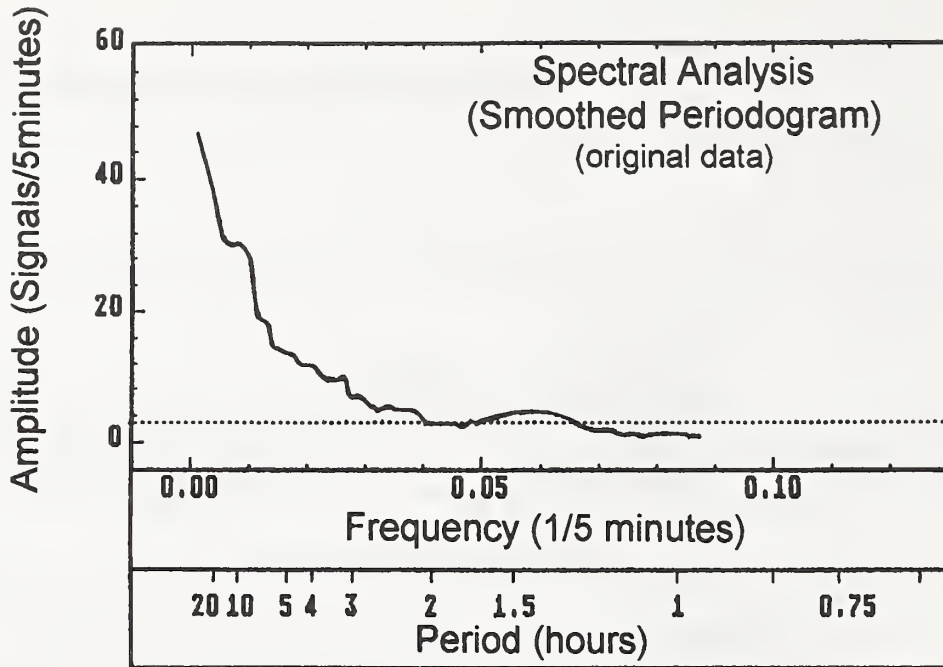
Figure 5.19a – Spectral analysis (smoothed periodogram) of the entire time series at 5-minute resolution (original data used).
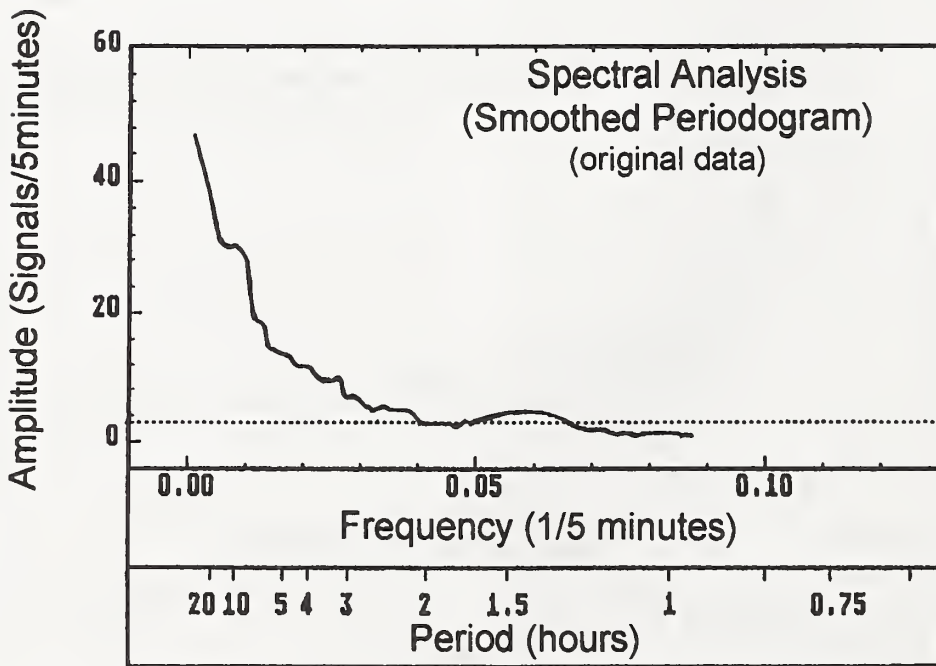
Figure 5.19b – Spectral analysis (smoothed periodogram) of the entire time series at 5-minute resolution (after elimination of a 10th-order trend from original data).

odicities in the range between 1 and 6 hours were indicated.

All values of periodicities obtained in any of the spectral and harmonic analyses performed were combined in one data set and divided into 12 classes of periods in 0.5-hour intervals. A frequency distribution of all recognized periodicities is plotted in Figure 5.20. Periodicities of 1.5, 2, 3, and in the range between 4.5 - 6.5 hours were found to occur most often. This rather indistinctive result is not very satisfying and requires further analysis.

The visual inspection and the statistical time series analysis indicated different periodicities. While the visual analysis identified bedload waves that occur in 1-hour, 5-hour, and 24-hour intervals, the statistical time series analysis indicated periodicities of 1.5, 2, 3, and 4.5 to 6 or 6.5 hours. This list of periods found by the spectral analysis can probably be reduced to three values since a period that is an integer-multiple of a lower period, is probably an artifact of the analytical procedure. The reduction leaves the periods of 1.5 hours, 2 hours, and 6.5 hours to be identified by the statistical time series analysis. **Small** waves with a 1-hour period and **random** transport which are both identifiable visually are not detected by the statistical time series analysis, although at least the amplitudes of the smallest wave (5-10

signals per 5-minute interval) are still above the level of 3.5 signals per 5-minute intervals considered significant in the statistical time series analysis.

Accepting the 1-hour periodicity as real, the 2-hour periodicity indicated in the statistical time series analyses is regarded as a multiple of the 1-hour periodicity and therefore eliminated. Thus, combining all periodicities that have been identified both statistically and visually and neglecting all periodicities that are interpreted to be an integer-multiple of a lower period, the **periodicities** 1-1.5, 5-6, and 24 hours are attributed to represent bedload waves at Squaw Creek.

The next step of the analysis is comparing the relation between **amplitudes** and periodicities of the bedload waves, which were indicated by the spectral analysis of the entire time series after the elimination of a tenth order trend (fig. 5.19b). Note that the spectral analysis did not indicate the 24-hour periodicity. A linear relationship was found between amplitudes and periodicities of bedload waves (fig. 5.21), yielding the regression

$$y = 3.34 \, x + 0.132, \, r^2 = 0.92, \qquad (8)$$

where y denotes the amplitudes, and x the periodicities of the bedload waves and r^2 is the correlation coefficient. This highly correlated linear relation is odd, because it incorrectly predicts
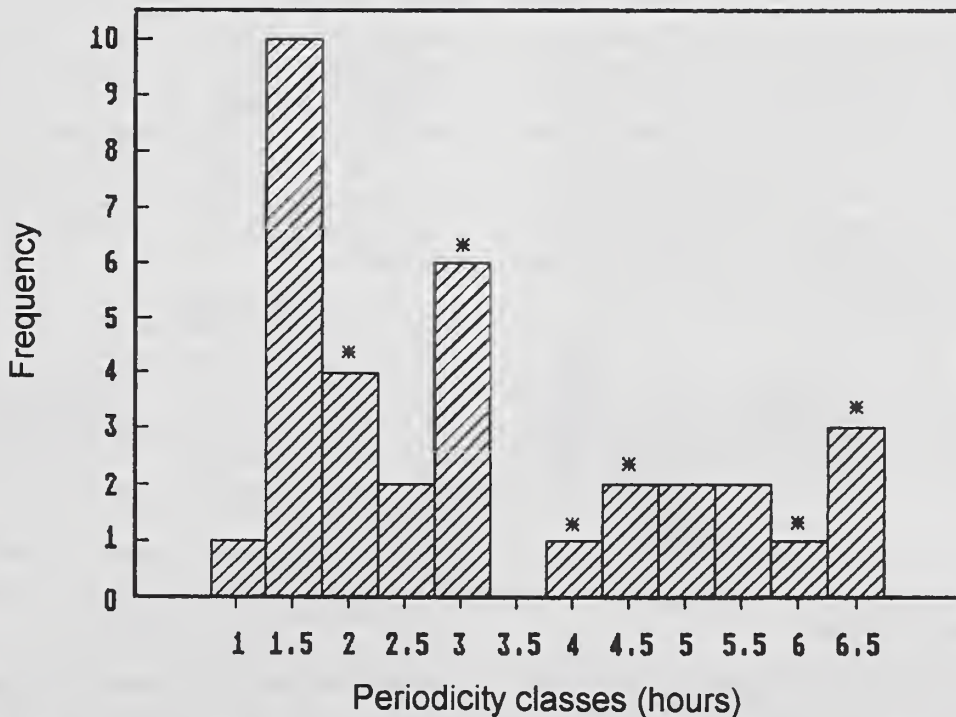
Figure 5.20 – Frequencies of periodicity classes observed in the analysis of the entire time series and the analyses of partial time series.
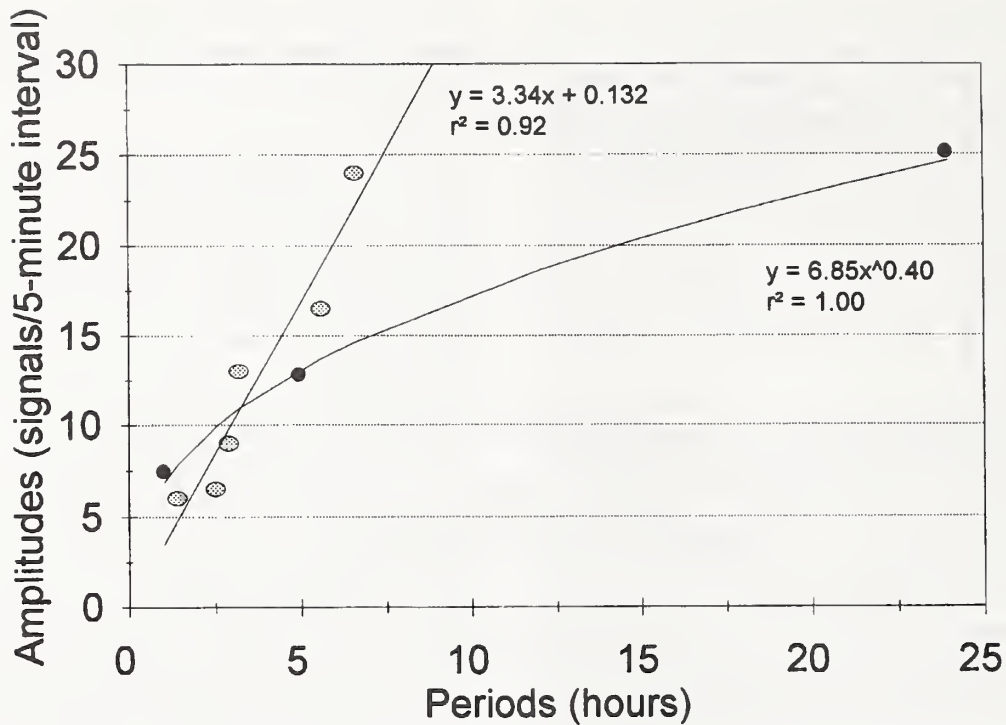
Figure 5.21 – Relation of bedload wave amplitudes with their periods: a) linear function: data from spectral analysis of the entire time series, b) power function: data from visual interpretation.

the relation between amplitudes and periodicities for large bedload waves. The visual analysis indicated that the large bedload waves during peak flows have amplitudes in the range of 18 to 42 signals per 5-minute interval with a mean peak signal rate of 25. The extrapolation of equation (8) however, gives an amplitude of about 80 signals per 5-minute interval, i.e., the extrapolation over predicts the value from the visual analysis by a more than a factor of three. Using the values for periodicities and the respective amplitudes from the visual analysis (Section 5.4.1.1), their regression best fits a power function relation with

$$y = 6.85 \, x^{0.4} \qquad (9)$$

While according to the spectral analysis amplitudes increase with the same rate as periodicities, the visual analysis indicates that amplitudes double only with a six-fold increase of the periodicities.

5.4.1.3 Statistical analysis

Because the statistical time series analysis proved inconsistent results, a further attempt to analyze short-term bedload fluctuations was conducted by investigating the symmetry of the bedload waves. The symmetry is the relation between the amplitude and the duration of a bedload wave.

There is no rule regarding the duration of a bedload wave. In this study the duration was determined to extend from one absolute minimum value in the course of the time series to the next absolute minimum. An absolute minimum value was defined as a minimum that is smaller than the previous minimum and smaller than the following minimum. A "zero" signal rate per 5-minute interval was always considered to be an absolute minimum.

The duration was determined for each bedload wave and plotted in a frequency diagram (fig. 5.22). The wave durations were also marked according to the size class of the waves (Section 5.4.1.1). This procedure indicated that the fluctuations during **random** transport lasted for 5-50 minutes, the **major** and **minor** bedload waves extended for 55-105 and 50-95 minutes, respectively. The duration of the **small** waves was most variable and extended over the entire range of durations from 5-105 minutes.

When frequency distributions are plotted for each wave class individually, the results could indicate that the frequency of the durations decreases with the lengths of the duration of bedload waves which may behave according to a Poisson process (fig. 5.23a). In order to test this
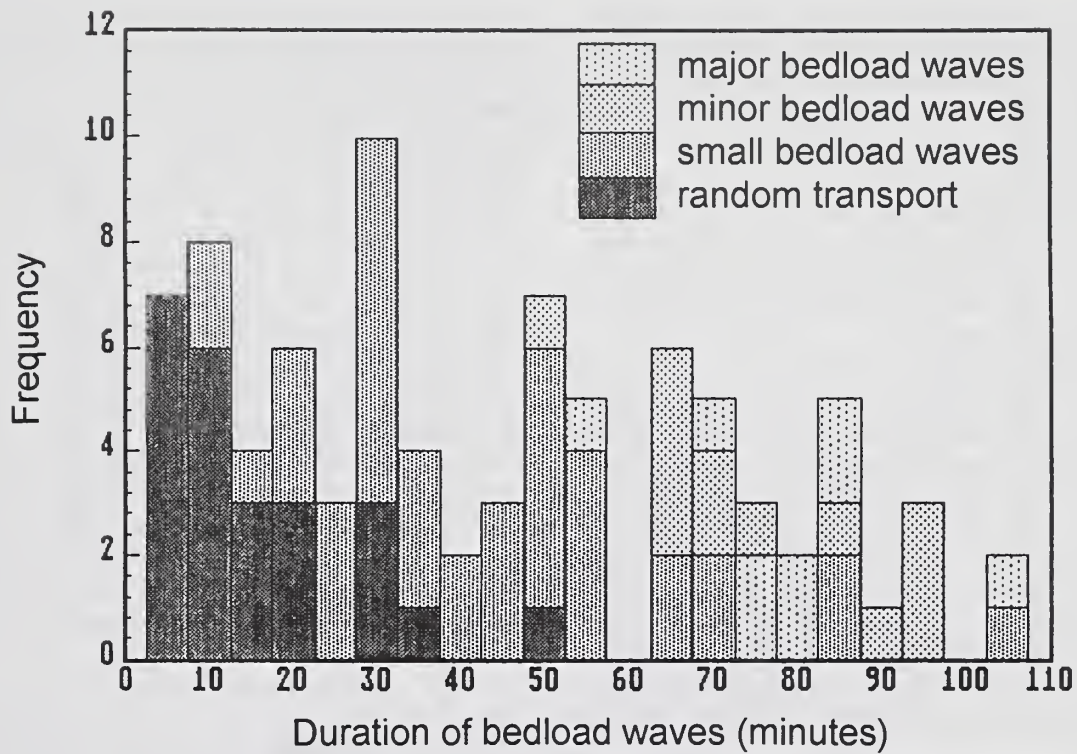
Figure 5.22 – Frequencies of duration of bedload waves for the four size classes.
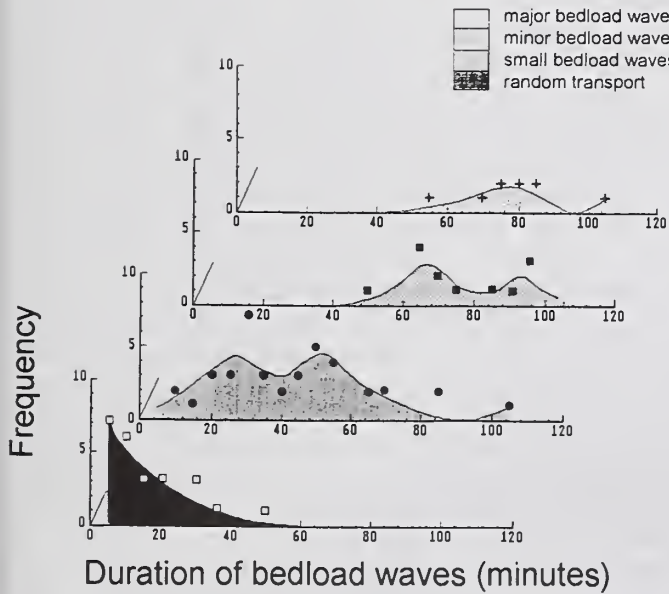
Figure 5.23a – Frequencies of duration of bedload waves for each individual size class.
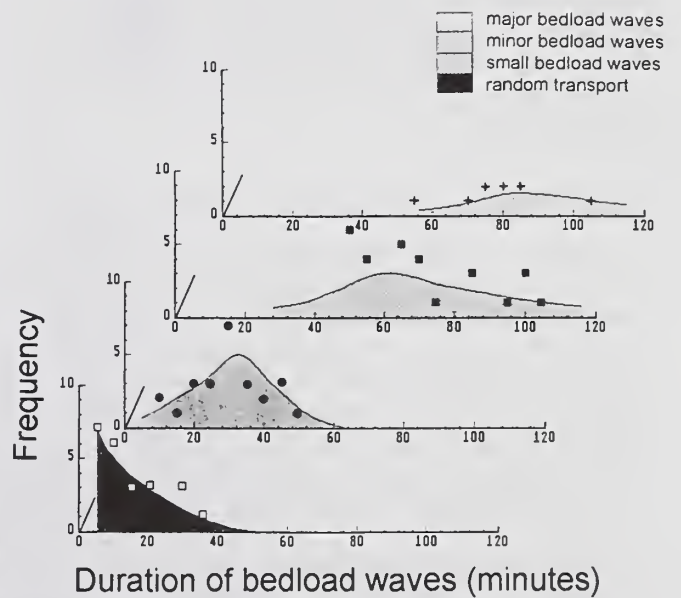
Figure 5.23b – Frequencies of duration of bedload waves for each individual size class (Poisson-distribution?).

speculation, the bimodal frequency distributions of the small and the minor waves were broken up and, violating class-boundaries, the second mode in these distributions was allocated to the next larger bedload wave class (fig. 5.23b). The consequence of this assumption would be a general increase in the duration of bedload waves. Mean duration for random, smallest, minor, and major waves would be increased to 5, 30, 60, and 90 minutes, respectively, and thus increase by about 30 minutes per wave class.

The statistical relation between amplitudes and duration of bedload waves was investigated next. Amplitudes were plotted versus the duration of bedload waves. There is no difference in the rate with which amplitude and duration increase for the 3 smallest groups of bedload waves. Even calculated mean amplitudes increase regularly with the mean durations per bedload wave class from random transport to minor bedload waves (fig. 5.24, Table 4). Matters are different for major bedload waves, which are characterized by relative short durations given the height of their amplitudes.

The relation between amplitudes and durations of bedload waves can be used as a means to roughly indicate the "shapes" of the bedload waves (fig. 5.25): From random transport fluctuations to minor bedload waves, wave sizes increase symmetrically by an even growth in both the maximum transport rate as well as the duration of transport. Major bedload waves, on the contrary, gain most of their mass through an increase in transport rates, not by an extension of their duration (fig. 5.25).

5.4.1.4 Results of the time series analyses

Table 4 combines the results of the time series analyses of short-term fluctuations of bedload transport at Squaw Creek from the previous sections. Four types of bedload waves that occur during ordinary snowmelt high flows can be distinguished with respect to their periodicity, duration, amplitude, symmetry, and discharge.

Periodicity and the associated amplitudes are the most distinctive attributes of bedload waves.

With respect to duration of a bedload wave, major and minor bedload waves are distinctly different from random transport, but small waves take an intermediate position as they can exhibit both long and short durations. A relatively sharp dissimilarity exists between major bedload waves and random transport with respect to discharge. While random transport, as well as small and minor bedload waves can all occur during discharges in the range of 5.38 - 5.88 m³/s, major waves and random transport exclude each other unless random transport is always present, but is only recognized when not overwhelmed by larger fluctuations. When it comes to the "shape" of the bedload waves, i.e., the relation of amplitude and duration, only major waves form a category of their own. Amplitudes and duration increase linearly for the other three wave classes (minor, smallest, and random). However, these classifications do not identify the processes that lead to the formation of these waves.

The previous section interpreted major bedload waves which occur at about peak flow with a 1.5 hour periodicity as unsteady adjustment processes of the channel bottom. The question is whether the same interpretation can be applied to minor and small waves.

Minor and small bedload waves differ from major waves not only in their size, but also in their relation between amplitude and duration. There is no apparent reason why river bed adjustments should occur in regular 5-hour and 1-hour periodicities during the falling limbs of flow in the form of minor and small bedload waves. Time series analysis of parameters other than discharge and bedload signals are not available to assist with an interpretation. The possibility that these waves are unsteady adjustments of the stream bed can however not be dismissed. The generally smaller force of flow on the falling limbs, and the relatively small temporal change of flow, could lead to less intensive adjustment processes which involve less material, and thus cause shorter and less intensive bedload waves. By the same token, the generally smaller forces of flow may require a longer time span to build up local flow conditions so that a threshold is exceeded and coarse bedload

Table 4. Results of time series analyses of short-term bedload fluctuations (5-minute resolution) at Squaw Creek, 1986.

Wave Type	Periodicity (hrs)	Amplitude (sign./5min)	Duration (min)	Sign./Wave (ampl.×dur./2)	Discharge (m³/s)	mass increase (ampl. & dur.)
Major	24 (18-26)	25 (19-42)	78 (55-105)	195	5.85-6.28	asymmetric
Minor	5 (4- 6)	12 (11-18)	76 (50-95)	93	5.58-6.02	symmetric
Small	1-1.5 (1- 3)	7 (5 -10)	45 (5-105)	33	5.38-5.97	symmetric
Random	-	3 (1 - 4)	16 (5- 50)	5	5.38-5.88	symmetric

The range of data is given in brackets.
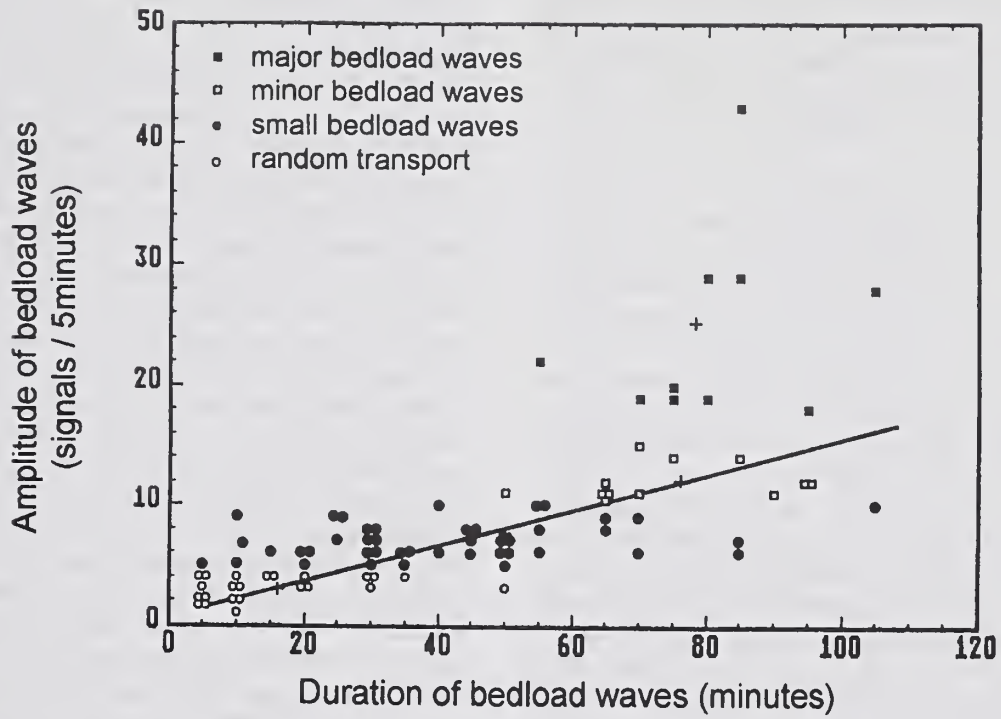
Figure 5.24 – Relation between amplitudes and durations of bedload waves.
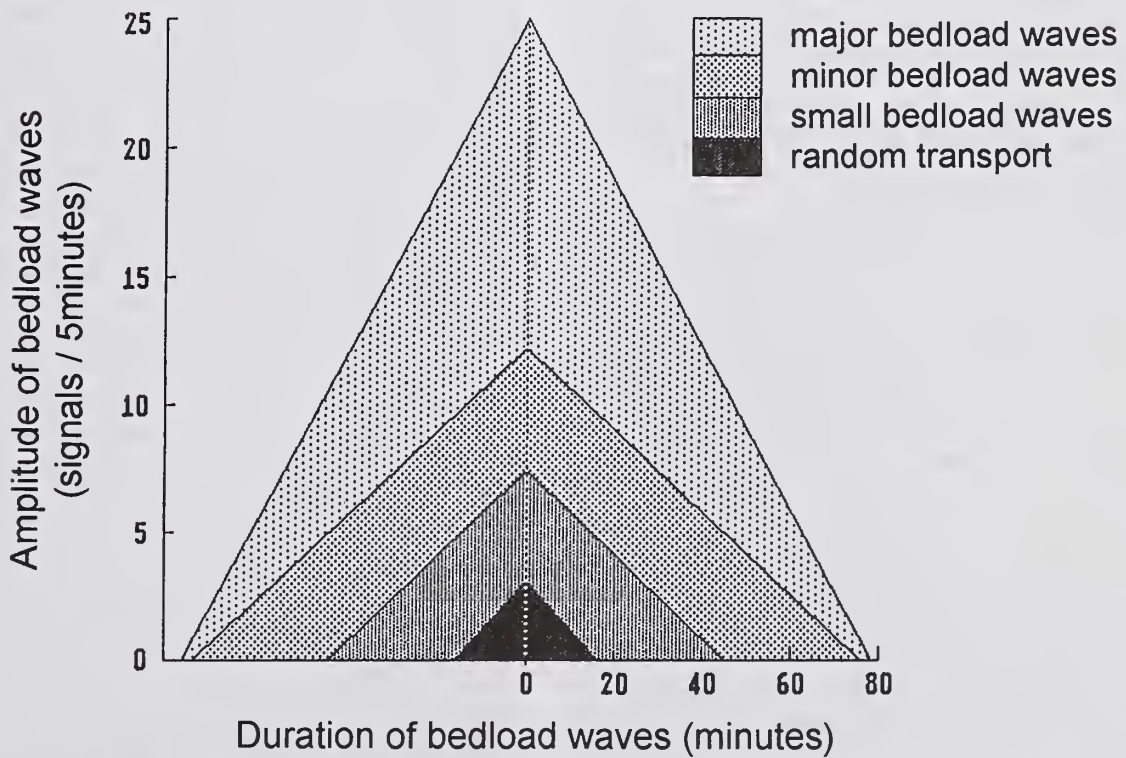
Figure 5.25 – "Shape" of bedload waves in the four size classes, calculated from the increase of amplitudes and durations.

can be transported. This process could explain the 5-hour interval between individual bedload waves. Smallest waves that recur in 1-1.5-hour frequency could then be interpreted as lesser adjustment processes that are limited to the exchange of single particles.

The wave structure vanished during the low transport rates in random transport. Particles seem to follow each other in arbitrary time spans, and only a few, single particles are still in motion. Random transport is not restricted to small discharges. In fact, random transport can be observed shortly after peak flows when discharges are still high (about 6 m³/s) and during falling limbs, to discharges near the threshold of coarse bedload motion (about 3.5-4 m³/s). Especially after very large flows, such as the high flow in 1981 that produced very high transport rates (Section 5.2.1.3,II), the unconsolidated and rough bottom can sustain the transport of single particles for a long time. Transport only stops after the last particles have found a place from which they can not be eroded by current forces of flow. More field measurements with detailed analyses of the hydraulic and channel geometric conditions are necessary to investigate the processes that lead to the **minor** and **small** waves.

The following section reviews the process-oriented literature regarding short-term fluctuations of bedload transport. It will then be assessed if processes identified in other studies are transferable to the stream conditions at Squaw Creek.

5.4.2 Laboratory experiments

Rhythmically pulsating sediment transport has frequently been observed in laboratory experiments. The pulsating nature of bedload transport was in all cases associated with the migration of bed forms (ripples, dunes, or bedload sheets). The studies by Carey and Hubbell (1986), Hubbell and Stevens (1986), Hubbell et al. (1987), Hubbell (1987), McLean and Tassone (1987), and Gomez et al. (1989) are mostly concerned with sampling strategies during fluctuating transport rates. Other laboratory studies, for example by Ikeda and Iseya (1986), Iseya and Ikeda (1987), and Kuhnle and Southard (1988) examine the sedimentary processes that govern the migration of bed forms. The studies experiment with different grain-size compositions, different kinds and rates of sediment supply (constant rates or recirculating systems), and different forces of flow during steady and unsteady flow conditions and analyze the effects on bedload fluctuations.

Based on experiments with different sediment size mixtures (Ikeda and Iseya 1986), Iseya and Ikeda (1987) found that depending on the ratio of sand to gravel a fluctuating transport pattern develops at a sand content of 30%. The fluctuations result from the process of longitudinal sorting in which the sediment of various grain sizes is segregated into cross-sectional strips with smooth and rough channel bottoms and a transitional reach in between. The longitudinal sequence of various stream channel roughnesses regulates the transport mechanism and leads to the formation of bedload sheets. The rough front of the bedload sheet is composed of gravel without a matrix fill. This is followed by a smooth and plane section upstream where a sandy matrix fills the gravel framework. A transitional section follows upstream and makes the connection to the next rough front. Sand is winnowed out from the gravels in the smooth, plane section and the reach is lowered by this action. This exposes the gravel particles which, subsequently, are transported with large speed and are then deposited at the rough front. This mechanism causes an apparent downstream migration of a bedform. As the coarse front passes a measuring point, gravel transport rates reach their maximum. Shortly afterwards the sand transport reaches peak rates when the gravelly-sandy section passes by. The migration of bedforms thus causes fluctuating, fractional transport rates that are characterized by a temporal lag of the fines in comparison to the coarser particles. The migration of bedforms that results from the process of longitudinal sorting will be referred to as bedload sheets.

Dietrich et al. (1989) show the dependence of the mode of transport on the supply rate of bedload material. The sediment availability controls the sedimentological conditions on the stream bottom. If the amount and grain-size distribution of the supplied material meets the competence and capacity of flow, longitudinal sorting takes place and bedload sheets form as defined by Iseya and Ikeda (1987). When sediment supply is reduced and falls below the competence and capacity of flow, an increasingly larger part of the stream bottom becomes armored. This begins at the sides of the stream and proceeds towards the center, until transport is confined to a narrow strip around the thalweg where coarse bedload transport continues in the presence of fine bedload material. As supply declines, the fluctuations become increasingly slow. Ferguson et al. (1989) observed this confinement of bedload transport to

a sandy-gravelly stream center under natural conditions.

Kuhnle and Southard (1988) use a relatively coarse grain mixture comprising sand to pebbles with 32 mm diameter for their laboratory experiments on bedload sheets. In a temporal resolution of minutes, they analyze not only the sedimentary composition and dynamics of the downstream migrating bedload sheets, but also the dependency of the relative of size of the bedload waves (Qb_{max}/Qb_{min}), and their periodicity on the rate of flow and sediment supply. The frequency of bedload fluctuations increases with increasing flow and sediment supply, while the amplitudes of the oscillations decrease. This result is remarkable in two ways. At Squaw Creek, amplitudes of the fluctuations increase non-linearly with periodicity. But while at Squaw Creek large amplitude bedload waves are generally associated with large discharges (and large bedload transport rates), Kuhnle and Southard (1988) find that the fluctuations of bedload transport become faster and smaller in amplitude with increasing sediment supply (Dietrich et al. 1989).

5.4.2.2 Field experiments

Several field experiments used measuring equipment that could register bedload transport with a temporal resolution of minutes, using hydrophones, vortex samplers, or piezoelectric elements (e.g., Schlatte 1984; Tacconi and Billi 1987; Bänzinger and Burch, 1990; Rickenmann 1994). But none of these studies measured or analyzed the time series of any other parameters but discharge. They can therefore only show the phenomenon of fluctuating bedload transport, but cannot identify the processes that cause it.

Other field experiments found explanations for a fluctuating bedload transport. Kuhnle et al. (1989) sampled bedload with a temporal resolution of minutes using a Helley-Smith type sampler during a large and almost steady high flow. Bedload transport was found to fluctuate. The grain-size spectrum ranged from sand to large pebbles (64 mm). Based on the temporal variation of the grain-size distribution of consecutive samples (fractional transport rates), Kuhnle et al. (1989) concluded that the fluctuations represented the migration of bedload sheets. However, the sampling was performed in a concrete-lined venturi-like measuring reach. The hydraulic conditions were not specified for either the upstream reach, or the measuring reach. Measured bedload transport rates reached 0.8 kg/m·s which is more than 10 times the bedload transport rates sampled at

Squaw Creek with the large net sampler during the (typical) spring high flow of 1988 (Section 5.3).

Whiting et al. (1988) also observed the migration of bedload sheets at Duck Creek during an unspectacular high flow in which flow velocities ranged from 0.62-0.91 m/s and Froude numbers from 0.34-0.39. The grain-size spectrum at Duck Creek is considerably smaller than at Squaw Creek. The maximum grain size is 10 mm. Whiting et al. (1988) concluded that bedload sheets form due to the particle instability characteristic of bedload movement in moderately and poorly sorted gravels. The interaction between coarse and fine particles leads to a stop-and-go motion. Coarse particles slow or stop each other, trap finer sediment in their interstices, and thus provide a smooth bed for other coarse particles to pass over.

The hydraulic and sedimentological conditions encountered in these studies, as well as the phenomena of bedload waves as described by Ikeda and Iseya (1987), are so different from the conditions that are ordinarily encountered at Squaw Creek that it is difficult to draw analogies from those experiments to fluctuating bedload transport at Squaw Creek, as it occurred during years of ordinary sediment transport in 1986 and 1988. This makes a closer comparison of the results from other studies with the results from Squaw Creek necessary.

5.4.2.3 Comparison of the results from other studies with the results from Squaw Creek

Fluctuating bedload transport, caused by the migration of bedload sheets, has been observed in field and laboratory experiments under various hydraulic and sedimentologic conditions. Two question arise:

1) How comparable were the hydraulic and sedimentological conditions of these studies to the conditions at Squaw Creek?

2) Can bedload waves that occur during ordinary spring high flow conditions at Squaw Creek result from the migration of bedload sheets?

Comparability of hydraulic and sedimentologic conditions at Squaw Creek with other studies:

Laboratory experiments on fluctuating transport rates usually use only small grain sizes ranging from sand to small gravels (Ikeda and Iseya 1986; Iseya and Ikeda 1987; Dietrich et al. 1989). Laboratory experiments are also usually run with relatively low flow depths, high flow velocities and supercritical flow conditions (Ikeda and Iseya 1986; Iseya and Ikeda 1987; Kuhnle and Southard 1988). Kuhnle and Southard (1988) are an exception in as much as they use sand-gravel

mixtures with a maximum grain size of 32 mm. But even these sediment mixtures do not cover the grain-size spectrum in coarse bedload carrying mountain streams, where the largest (almost annually) transported clasts nearly always reach a diameter of several decimeters.

How is it possible to deduce the transport behavior of medium and coarse gravels in natural streams from the transport behavior of sand and fine gravels produced under the extreme hydraulic conditions in laboratory experiments? A transfer of laboratory results to natural streams has to make use of the similarity laws[10]. Vollmers (1989a) questions whether it is possible to transfer the hydraulic conditions during sediment transport in natural streams to model laboratory conditions and vice versa, because of the unsolvable conflict that the model has to satisfy both the Froude- and the Reynolds-similarity. Vollmers (1989a and b) indicates though, that a Froude-model can be used for hydraulically rough

conditions when the density of the sediment remains unchanged. Froude- (or Reynolds-) similarity means that Froude- (or Reynolds-) numbers have to be the same, both in nature and the flume model. The demand for Froude-similarity requires that the dimensional laws given in Table 5 (Bollrich et al. 1989) are used for scaling. Table 5 gives an example for the dimensional transfer from nature to model and vice versa in the scale of 1:10.

These similarity laws were used to scale up the dimensions of the flow and sediment parameters used in the laboratory experiments H1, H3, and H5 by Kuhnle and Southard (1988) by a factor of 10. The scaled up grain-size spectrum of the lab experiments ranges from 1.25 mm to 32 cm, a range frequently encountered in mountain streams. The results of the scale transfer are summed in Table 6.

A linear increase of the length dimensions leads to a power function increase of the flow

Table 5. Similarity laws for scaling (1:10) under Froude-similarity.

Parameters	Similarity Relations		Example for Scaling (1:10)			
			Model $\rightarrow$ Nature		Nature $\rightarrow$ Model	
Length	l_r	$= l_N/l_M$	l_M	$= 0.1\ l_N$	l_N	$=\ 10\ l_M$
Area	A_r	$= l_r^2$	A_M	$= 0.01\ A_N$	A_N	$= 100\ A_M$
Velocity	v_r	$= l_r^{0.5}$	v_M	$= 0.316\ v_N$	v_N	$=\ 3.16\ v_M$
Time	t_r	$= l_r/v_r = l_r^{0.5}$	t_M	$= 0.316\ t_N$	t_N	$=\ 3.16\ t_M$
Flow Rates	Q_r	$= v_r/A_r = l_r^{5/2}$	Q_M	$= 0.00316\ Q_N$	Q_N	$= 316\ Q_M$

r = relation; N = natural size; M = model size

Table 6: Transfer of the hydraulic and sedimentologic dimensions used in laboratory experiments by Kuhnle and Southard (1988) to natural conditions in a scale of 1:10.

	w (m)	d (m)	Q (m³/m·s)	$Q_{b\,input}$ (kg/m·s)	S (-)	v (m/s)	Fr (-)	Period. (minutes)	$Q_{b\,max}/Q_{b\,min}$ (-)
Run H1	0.53	0.046	0.035	0.034	0.019	0.76	1.12	9.8; 14.2; 26.1	57.3
$\rightarrow$Nature	5.3	0.46	1.09	0.99	0.019	2.38	1.12	31.0; 45.0; 82.6	
Run H3	0.15	0.074	0.067	0.098	0.015	0.90	1.06	6.0; 6.7	8.7
$\rightarrow$Nature	1.5	0.74	2.11	2.91	0.015	2.85	1.06	19.0; 21.2	
Run H5	0.15	0.069	0.089	1.073	0.021	1.29	1.57	3 ?	2.2
$\rightarrow$Nature	1.5	0.68	2.81	33.87	0.021	4.08	1.57	9.5	

w = flow width; d = flow depth; Q = discharge; $Q_{b\,input}$ = rate of sediment supply; S = gradient; v = flow velocity; Fr = Froude number; Period. = Periodicities; $Q_{b\,max}/Q_{b\,min}$ = ratio between largest and smallest bedload transport rates.

---

[10] Mathematical transformation algorithm (similarity criteria) that allows the dimensional transfer of parameters such as length, area, flow velocity, time, and discharge between laboratory models of streams and their natural counterparts. See also Vollmers (1989b) and Bechteler et al. (1994).

rates. How do the scaled-up discharges from Kuhnle and Southard's flume experiments correspond to the high flow discharge conditions at Squaw Creek? The first step in trying to answer this question was to find out which discharge at Squaw Creek would become supercritical and reach a Froude-number of 1.12 as in Kuhnle and Southard's laboratory run H1 (Table 6).

A logarithmic regression was fitted through the relation between Froude-number and discharge for a typical cross-section at Squaw Creek. An extrapolation indicated that a Froude-number of 1.12 would be reached at high flow discharges of about 15 m³/s. This is a conservative estimate because gravel bars would be flooded after a bankfull flow of about 6 m³/s is exceeded. The flooding would change the hydraulic radius to such a degree that the extrapolation would not be valid in many cross-sections, and flows would probably have to be larger than 15 m³/s to be fully supercritical.

If the flows in run H1 were scaled up, so that grain-sizes in run H1 meet the grain-size spectrum at Squaw Creek, the scaled-up hydraulic conditions suggest flows larger than 15 m³/s at Squaw Creek. This is an enormous flow for Squaw Creek and has a recurrence interval of about 20 years. (The effects of such a high flow have been described in Section 5.2.1.3.II).

Froude-numbers of 1.57 which were reached in Kuhnle and Southard's laboratory run H5, can perhaps occur locally at Squaw Creek, but flows with a Froude-number of 1.57 as a cross-sectional average would probably only be reached during catastrophic floods. Kuhnle and Southard (1988) have modeled the hydraulic conditions of very large floods in their flume experiments. The same is true for the laboratory experiments by Ikeda and Iseya (1986) and Iseya and Ikeda (1987), who barely exceed the coarse sand fraction in their experiments and work with supercritical flows that have Froude-numbers between 0.97 and 1.49.

If the similarity law used for transforming unit flow rates (m³/m·s) is also used to scale up unit sediment flux rates (kg/m·s), the sediment input rates used in the laboratory runs H1, H3, and H5 by Kuhnle and Southard (1988) yield stream sediment supply rates of 0.99, 2.91, and 33.87 kg/m·s, respectively (Table 6). Such transport rates would likewise be enormous for Squaw Creek, where short-term peak transport rates of coarse bedload

reach only 0.2-0.3 kg/m·s during typical snowmelt high flows [11].

The results of the comparisons above is that data obtained and processes modeled in flume experiments with small grain-sizes in the sand and fine gravel range **cannot be transferred to coarse bedload carrying streams without paying attention to the similarity laws.** If the sedimentologic and hydraulic parameters used in laboratory experiments are scaled up by a factor necessary to make flume grain-size distributions comparable to mountain streams, then the subsequently scaled up hydraulic conditions and sediment supply rates mimic enormous floods. Such extreme flood conditions would probably cause extensive channel change and provide much bedload material for transport.

Another factor that makes the transferability of laboratory bedload transport results to stream conditions problematic is the occurrence of bedload transport phenomena that result from the hydrological and sedimentological "prehistory" of the stream that can hardly be incorporated into the flume experiments.

Can bedload waves that occur during ordinary spring high flows at Squaw Creek result from the migration of bedload sheets?:

The studies mentioned above observed that bedload sheets develop from the process of longitudinal sorting of grain-sizes, i.e., the sequence of strips on the river bottom with different roughness. The development of this process requires several sedimentological and hydraulic conditions:

- high proportion of sand in bedload,
- large supply of sediments that are transportable under the respective hydraulic conditions,
- the proper mixture between sand and coarse bedload, and
- almost steady flows with the respective capacity.

These sedimentologic and hydraulic characteristics do not represent the typical conditions encountered at Squaw Creek on an annual or biannual basis. Furthermore, the nature of bedload waves at Squaw Creek is not comparable to the description of bedload of bedload sheets. The respective relationships between amplitude and

---

[11] *Bedload transport rates of several kg/m·s have been observed by Dinehart (1992) in the North Fork of the Toutle River after the coarse bedload sediment provided by the eruption of Mount St. Helens reached the measuring site and passed in gravel dunes.*

85

duration of the bedload fluctuations and the discharge at which bedload waves occur are different for bedload waves and bedload sheets.

A rhythmically pulsating bedload transport where bedload waves not only have even durations but also even amplitudes is characteristic for the migration of bedload sheets. Increased flows and increased sediment supply typically increase the frequency of the pulsations. Observations at Squaw Creek, however, show that increasing flows are associated with decreasing frequencies of bedload waves, i.e., the duration of the waves becomes longer. Besides, the temporal variation of bedload transport at Squaw Creek with the occurrence of bedload waves of different sizes could rather be characterized as fluctuating. A rhythmic pulsation of bedload transport is only observed very infrequently.

Another difference between the sedimentological conditions at Squaw Creek and those that lead to the formation of bedload sheets is the availability of bedload material and the magnitude of transport rates. Although during the night of May 31 to June 1, 1986, bedload waves showed an even frequency of 1.5 hours, the amplitudes of those bedload fluctuations varied from wave to wave (fig. 5.17). Fluctuating transport rates were also observed at Squaw Creek during a similar high flow in 1988. However, particle transport rates of bedload samples taken with the large net sampler in 1-2 hour intervals during the night from May 23 to 24, 1988, are low (fig. 5.35, Section 5.5.8, Table 3a–b in the Appendix). Even the largest bedload transport rates move only about one coarse particle (11.2 mm) per meter width and second (fig. 5.32, Section 5.5.5). These low transport rates indicate limited sediment supply. A low sediment availability does not permit the development of longitudinal sorting of different grain sizes, which is a prerequisite for the formation of bedload sheets.

Under normal snow-melt high flow conditions, Squaw Creek does not exhibit the conditions necessary for the formation of bedload sheets. Nor are the characteristics of the bedload fluctuations observed at Squaw Creek in agreement with those observed for bedload sheets elsewhere. Bedload waves that occur at Squaw Creek during ordinary high flow conditions do therefore not result from bedload sheets and the process of longitudinal sorting.

The sedimentologic and hydraulic conditions that may lead to the development of bedload sheets will only occur at Squaw Creek under extreme conditions, when the armor layer breaks up during long-lasting very high flows or when the destruction of a sediment storage provides the sediment supply necessary for the development of bedload sheets. Such conditions occurred during a huge snowmelt high flow with a 20-year reoccurrence interval in 1981 and 2 years later when a log jam burst provided a large enough sediment supply to cause the formation of bedload sheets during snowmelt high flows of ordinary magnitude.

5.4.3 Temporal variation of signal rates in very high temporal resolution

During the rising limb of flow on June 2, 1986, from 15:10 in the afternoon to 20:30 at night signal rates were registered in high temporal resolution at the detector unit 5/6 which spans a width of 1.55 m in the center of the stream. The paper advance on the strip chart recorder was increased to a rate of 5 mm/minute.

Transport dynamics vary during this time period (fig. 5.26 a, b, c). In the beginning of the rising limb (15:10 -17:40) signal rates are low and range between 0 and 3 signals/minute, indicating mostly random transport for this time period. Further on the rising limb (17:40 - 18:30) bedload transport activity increases over the 1.55 m detector unit to rates of 15 signals per minute and bedload particles start to move in groups or "**families.**" This period falls into the categories of small bedload waves and the beginning of major waves. Signal rates reach their maximum between 18:30 and 18:40. This is the peak of a major bedload wave. The transport of single particle "families" lasts for about 10-30 seconds and "families" appear in about 1-minute intervals. Short-term peak rates might reach about 1 or 2 signals per second. The reasons for this "family" transport are unclear. The number of particles that pass per unit width and time is too small to enable particle interaction within the group.

This observation of very fast fluctuations of signal rates with the occurrence of pebble "families" is not in agreement with the concept of bedload sheets which slowly migrate downstream. Although about 10 pebble or cobble particles, and perhaps some finer material, might gather to continue their travel as a "family", it is not conceivable that these "families" form a migrating bedform or a bedload sheet. The passage of bedload sheets should show initially high transport rates of large particles as the coarse front of the bedload sheet moves through. Rela-
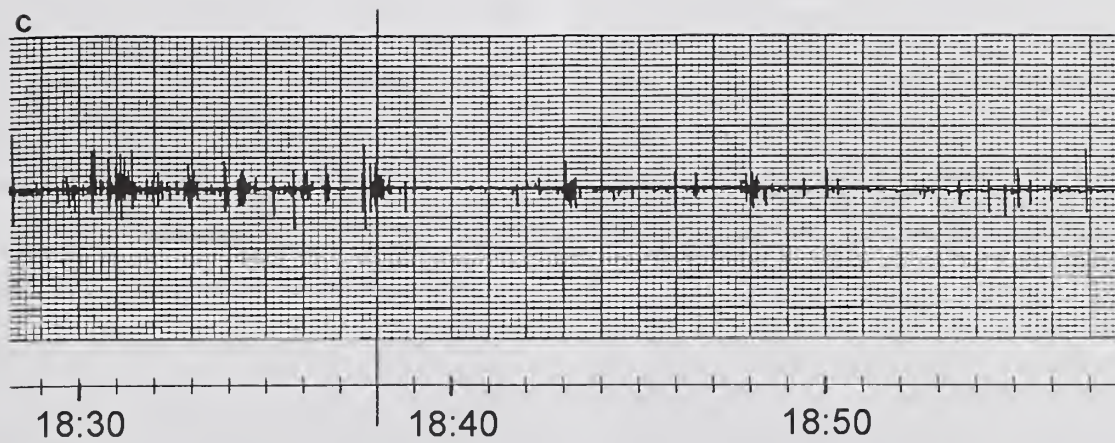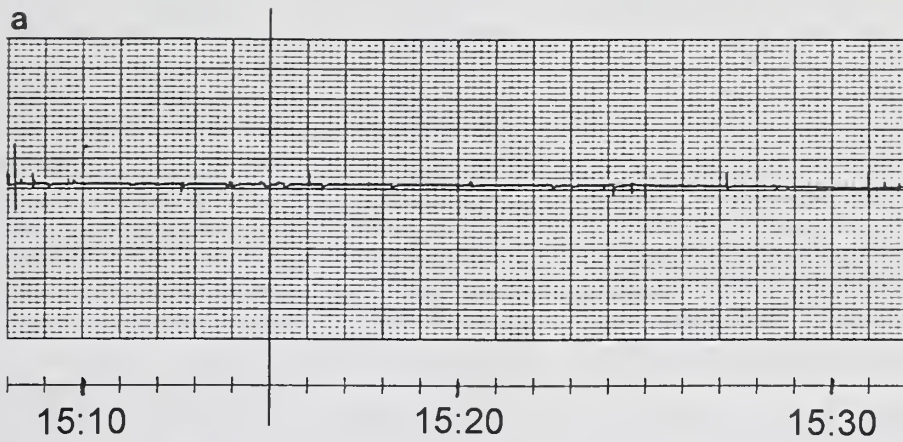
Figure 5.26a-c – Temporally high resolution registration of bedload signals: a) random transport, b) and c) "family"-transport of various intensities.

tively low and steady signal rates should follow as the more sandy part of the bedload sheet passes by. This is not the pattern of bedload transport at Squaw Creek.

5.4.4 Results

The visual analyses of the time series of bedload transport in high temporal resolution (5-minute intervals) shows that bedload fluctuations during the 3-day time period can be distinguished according to their periodicity, amplitude, and symmetry and grouped into four categories:

- **major** bedload waves,
- **minor** bedload waves,
- **small** bedload waves, and
- **random** transport.

Fourier transformations and spectral analyses performed to supplement the visual analyses turned out to be of little help in the discrimination and interpretation of the cause of bedload waves due to methodological differences.

Major bedload waves which occur around peak flow were attributed to the temporal variation of river bed adjustments. **Minor** and **small** bedload waves which occur predominantly on the falling limbs of flow with a periodicity of 5-hours and 1-hour, respectively, could perhaps also result from river bed adjustments. But due to lower and less variable flows these adjustments take place in lower frequencies and involve less bedload material. Temporal high resolution analyses of the flow and channel bottom conditions are needed to better investigate the origin of bedload waves in mountain streams.

Several process-oriented laboratory experiments indicate a transport mechanism in which the fluctuation of bedload transport is due to the migration of bedload sheets. This transport mechanism is based on a particular longitudinal sequence of channel bottom roughnesses (longitudinal sorting). Coarse particles build the front of the bedform, and a mixture of sand and gravels follows upstream. Bedload transport rates are of pulsating nature. The frequency of the pulsations increases with discharge and sediment supply.

If the hydraulic and sedimentologic conditions of flume experiments are scaled up using the similarity laws to meet the sedimentological dimensions of mountain streams (e.g., enlarged by a factor of 10), it becomes evident that mountain streams would have to experience enormous floods and/or a high sediment supply rates in order to produce bedload sheets.

Streams with a large width/depth ratio and a sediment mixture with plenty of sand and fine gravels could have enough sediment supply to develop bedload sheets. None of these conditions was true for Squaw Creek during ordinary snowmelt high flows with a 2-year recurrence interval. Besides, the temporal structure of bedload fluctuations at Squaw Creek which features waves of different periodicities, amplitudes and symmetry does not coincide with the temporal structure of bedload waves that result from bedload sheets. Bedload waves at Squaw Creek can therefore not result from the migration of bedload sheets.

The analyses of bedload transport in supply-limited mountain streams should focus on two issues. One issue is the investigation of the temporal and spatial variation of river-bed adjustments. The other issue is the investigation of bedload particle interactions as well as the interactions between bedload and the particles which are part of the river bed. High temporal resolution observations of bedload transport at Squaw Creek has shown that during peak transport rates bedload transport disintegrates into a series of short-term (10-30 s) bedload fluctuations in which a group of maybe 10 particles travel together as a "family." An interaction between moving bedload particles is hard to imagine since the concentration of moving particles per width and time is very low.

The analyses of both issues require not only information about the temporal and spatial variation of hydraulic conditions, and the river bottom form and roughness, but also continuous measurements of bedload transport and its grain-size distribution. Such measurements, however, require techniques that are only in the process of being developed. Results of grain-size distribution analyses of sequential samples taken with the large net sampler are given in the next section.

5.5 Bedload Grain-size Distribution

Together with the analysis of the temporal variation of bedload transport, the grain-size distribution analysis of bedload transport is one of the most important issues in coarse material bedload transport investigations. The processes of bedload transport are determined by the interactions between the different grain-sizes. A study of the grain-sizes and their temporal variation are a fundamental part in the investigation of coarse bedload transport processes.

5.5.1 Comparability problem of present investigations

Other than the studies concerned with the migration of bedload sheets, grain-size distributions of coarse bedload material from natural streams has not been studied very intensively from a process-oriented point of view. Suitable data are scarce (Komar 1989), anyway.

Only recently have grain-size analyses of bedload from mountain streams been intensified. These studies investigate criteria of incipient motion of individual grain-size fractions from sediment mixtures. The backgrounds for these analyses were discrepancies between incipient motion conditions described in the Shields diagram and those observed for particles from sediment mixtures. The divergence is larger, the coarser and wider the grain-size distributions are. The investigations of incipient motion lead to further questions of whether transported grain-size spectra vary with flow intensity (**selective transport**) or whether all grain sizes are equally mobile irrespective of discharge (**equal mobility**) (Section 5.5.3).

However, differences in the methodologies of studies make it problematic to compare the results of grain-size analyses from different studies. The comparability among field measurements suffers especially from the wide range of sedimentological conditions encountered in different stream types and from the different sampling techniques and strategies employed for coarse bedload transport (Komar and Shih 1992; Ashworth and Ferguson 1989a). Flume studies differ from conditions encountered in mountain streams by their usually finer grain-size distributions and their relatively large sediment supply rates (e.g., Wilcock and Southard 1989).

Besides the differences in channel bed conditions and sampling, another problem with comparability is posed by the different methods of data analyses. Wilcock (1988) shows how the incipient motion analysis leads to completely different results depending on whether the estimate of critical shear stress ($\tau_{o\ crit}$) is based on the largest grain displaced or on the smallest shear stress needed to move some small quantity of bedload. While the first methodology demonstrates a strong grain-size dependency of $\tau_{o\ crit}$ with grain size, the latter confirms their independence.

Most of the studies regarding the discharge (in-)dependency of incipient motion and transport describe their grain-size distributions by a single percentile only (usually D_{50}). Some studies plot various index numbers versus each other to indicated initial motion criteria, a practice which sometimes demands quite a high degree of abstraction from the reader. Newer studies try to address more characteristics of grain-size distributions than their central tendency and bring back to usage grain-size parameters like **sorting** and **skewness** or **particle transport rates** (Komar and Shih 1990 and Komar and Shih 1992, Bunte 1992a and 1992b).

Studies of coarse bedload transport grain-size distributions are generally in need of better field techniques to increase the availability, the representativeness and comparability of data sets from different streams. The inter-study comparability of bedload data is further in need of meaningful and generally accepted methods of data analyses.

5.5.2 Temporal and spatial variation of bedload transport rates and their grain-size distributions at Squaw Creek

Bedload samples taken at Squaw Creek with a 3" by 3" Helley-Smith sampler during the high flow of 1986 were used to study the

- cross-sectional variability of bedload transport (Section 5.5.2.1) and
- temporal variation of its grain-size distribution in the course of a high flow (Section 5.5.2.2).

The first topic should indicate the paths of sediment transport. The latter should provide some insight into the sources of sediment and the temporal variability of the sedimentological conditions of the river bed. The temporal variability of bedload grain-size distributions was also studied in higher temporal resolution using sequential samples taken in 2-hour intervals with the net-sampler in during the high flow in 1988 (Section 5.5.8).

5.5.2.1 Cross-sectional variation of bedload transport and its grain-size distribution

Bedload samples taken with the Helley-Smith sampler at eight locations across the stream (fig. 3.13). Bedload grain-sizes vary over the cross-section and are associated with a spatial variation of bedload transport rates. The four sampling points closest to the banks of the stream produce predominantly sandy samples and small transport rates. Bedload transport in the center of the stream has larger transport rates, larger amounts of gravel and stronger variations of transport rates of samples from the same location. A similar observation has been made by Pitlick (1987). Ordi-
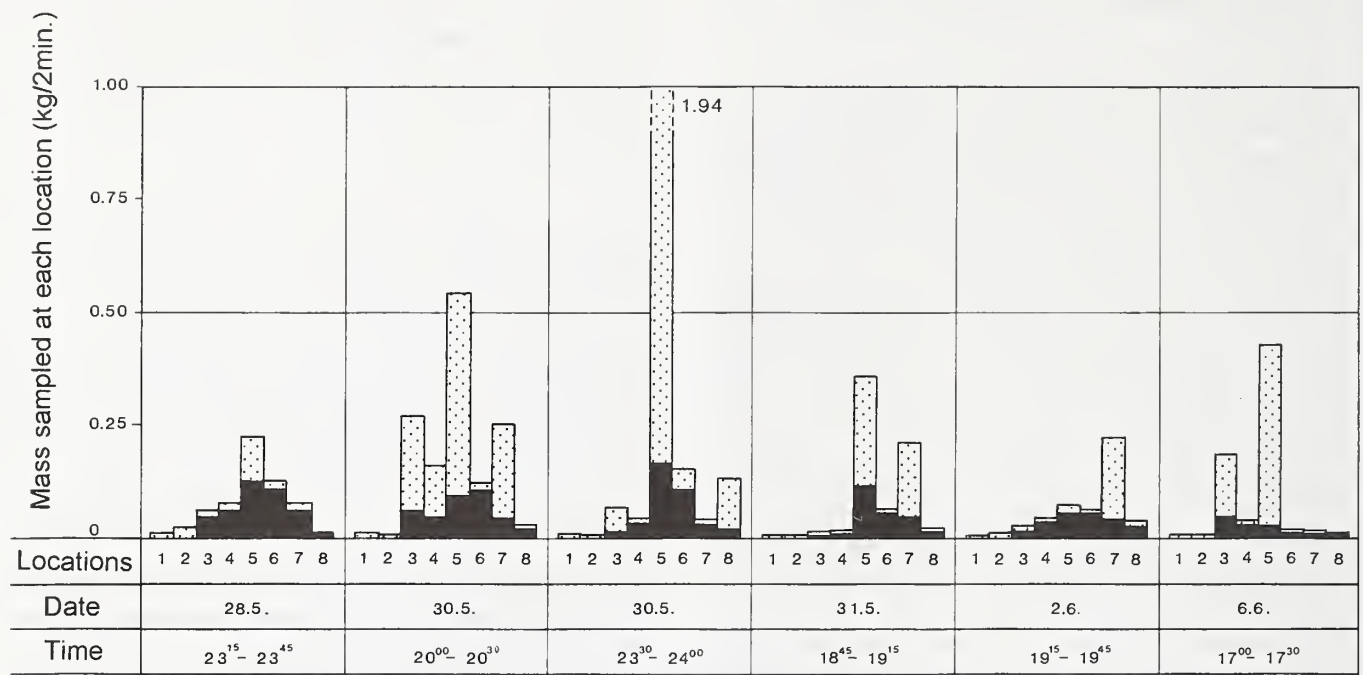
Figure 5.27 – Spatial variation of bedload transport, sampled with Helley-Smith sampler along a cross-section (measuring locations 1-8) over several days. *Stippled bar*: gravel portion; *black bar*: sand portion.

nary snowmelt high flows confine the transport of coarse bedload to a Section a few meters in the center of the stream (fig. 5.27). The analyses of the signal rates confirm this centralization. Both photographs in Figure 5.7a-b, Section 5.3.1, show from top to bottom bedload signals registered on the detector units 5/6 in the center of the stream (upper lines), on the detector unit 7/8 right from the stream center, but at thalweg position (center lines), and on the unit 9/10 at the right bank (bottom lines). The position of the detector units in the stream is also shown in Figure 3.13. The detector unit 9/10 at the right bank exhibits much smaller signal rates than the central detector units. The central detector unit 5/6 has a slightly higher daily signal count than the unit 7/8 on its right side. Signal rates on both units can vary by 100% for individual hours, but the general trend of the bedload fluctuations is always maintained on both units. Similar observations regarding the spatial variability of bedload transport were made by Reid et al. (1985).

5.5.2.2 Change of grain-size distribution during the course of the high flow

During the snowmelt high flow of 1986, bedload samples were taken with the 3" Helley-Smith sampler on several days of the high flow, especially during the rising limbs, at about the same

discharge each day. Bedload transport rates and grain-size distributions varied. The numerical results of the sieve analyses are given in Table 2 (appendix).

In the beginning of the high flow (second high flow day) bedload transport is dominated by sand (fig. 5.28a and b) when transport rates are rather low. Higher transport rates are mainly composed of fine gravel (2 - 22.4 mm). Later days of the high flow produce samples with a constantly low content of the sand and fine gravels. An increase of bedload transport rates is mostly attributable to an increase in the coarse gravel fraction (22.4 - 63 mm).

Although the competence of the flows is similar in both cases, different grain-size distributions are transported in the beginning and the end of the high flow. Similar observations have been made by Klingeman and Emmett (1982), Gomez (1983), Reid et al. (1985), and Reid and Frostick (1986). These differences can only be explained by a change in the grain-size composition of the transportable material. In the beginning of the high flow, bedload is comprised mainly of fines which are "winnowed out" from deposits produced on the falling limb of the last major high flow. After the interstices have been cleared during the first few days of the new high flow, larger particles become exposed and can also be eroded

90
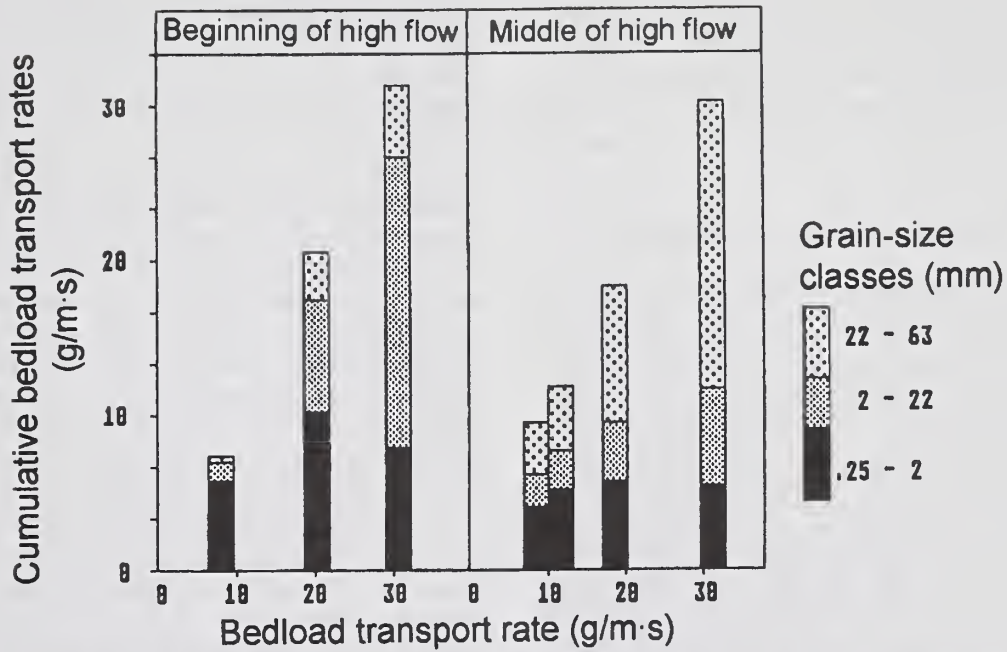
Figure 5.28a – Grain-size distributions (in absolute terms) for different bedload transport rates during the beginning and the middle part of the high flow period (Helley-Smith sampler, 1986).
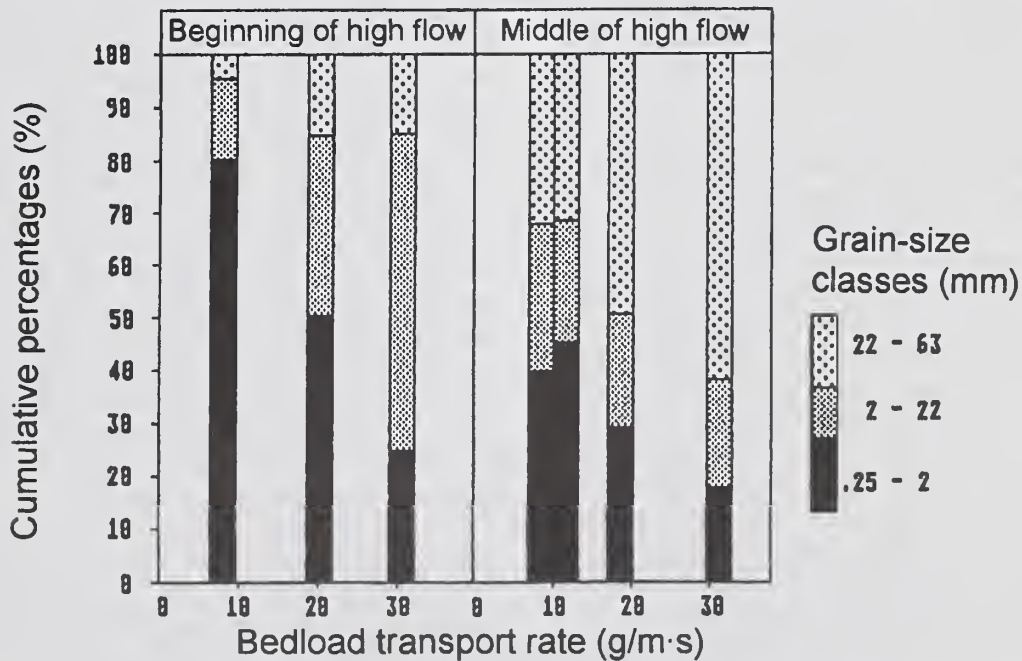
Figure 5.28b – Grain-size distributions (as percentages) for different bedload transport rates during the beginning and the middle part of the high flow period (Helley-Smith sampler, 1986).

and transported during later high flow days. The grain-size spectrum of bedload transport is thus not only dependent on the current force of flow, but is also strongly affected by the previous hydrological and sedimentological history which determines the sedimentary conditions on the stream bed.

5.5.3 Selective transport or equal mobility?

Incipient particle motion from widely sorted gravel beds is dependent on the absolute particle size as well as the grain-size distribution of the sediment mixture surrounding the particle (Section 4.3.2). The effects of "hiding and exposure" (Fenton and Abbot 1977) can have a large influence on initial motion. Erosion of a large particle surrounded by finer grains does not necessarily require larger forces of flow than does erosion of a small particle from the aggregation of larger clasts. Owing to these results it was concluded by several researchers that as soon as a threshold discharge was exceeded and just a few particles would start to move, the entire material on the channel bottom would be set into motion immediately hereafter. This mechanism, under which all grain sizes are equally mobile at initial motion and during transport, was called **equal mobility** (Parker and Klingeman 1982; Parker et al. 1982; Andrews 1983; Andrews and Parker 1987). An enrichment of coarse particles on the stream bottom and the accordingly increased roughness were seen as necessary agents to sustain bedload transport in its amount and grain-size distribution since it formed a **mobile armor**. This means that some of the coarse particles are always so far exposed and so unstable that they can be eroded and transported during relatively small forces of flow. This interpretation contrasts with studies by Gomez (1983) who describes a **progressive coarsening** of the channel bottom. As the sediment supply becomes reduced while flow is either constant or declining, flow loses its competence to transport all particle sizes on the stream bed. While transport rates are slowly declining, particles too coarse to be transported are deposited on the stream bed until bedload transport rates are reduced to almost zero. This process forms a **static armor**.

Controversy still exists with respect to both the definition of the technical terms, as well as the sedimentological and hydraulic requirements necessary for bedload transport to take place in equal mobility or as selective transport (Kuhnle 1992; Komar and Shih 1992; Shih and Komar 1990b;

Ashworth et al. 1992; Wilcock and Southard 1989; Wilcock 1992; Bunte 1990 and Bunte 1992a). It is also still controversially discussed whether the definition of equal mobility implies the non-dependency of the bedload grain-size distribution on discharge conditions, or whether equal mobility means the similarity of the bedload grain-size distribution with the grain-size distribution of the stream bed. The concept of selective transport implies that the effects of the relative grain-size of a particle are less important on initial motion and transport than the absolute grain size ("hiding and exposure"). This would mean that depending on the competence of flow only the particles of the right size will be selectively eroded and transported. Grain-size spectra of bedload would change with changes in discharge.

In order to study, if, or under which circumstances, bedload transport at Squaw Creek operates according to the principles of selective transport or equal mobility, the grain-size distributions of bedload and stream bed material need to be registered continuously. The latter presents a problem which can presently not be solved. The detailed cross-sectional measuring device introduced as "Tausendfüßler" in previous Sections (4.3.3; 4.5.2; 5.3.4) is a step towards the solution of this measuring task. Several studies have tried to infer different processes of the river bed development during bedload transport using the bedload grain-size distribution. Gomez (1983) and Wilcock (1992) could interpret a progressive coarsening of the stream bed, while Kuhnle (1992) observed a progressive smoothing. Whether a stream bed develops as mobile armor that supports bedload transport, or as static armor that prevents bedload transport seems to depend on the rate of sediment supply and needs to be further investigated (Sutherland 1987). Nouh (1990) suggests that the grain-size distribution of the bed armor layer is not only affected by hydraulic parameters such as depth and velocity of flow, but also by the duration and unsteadiness of the flows.

A lot of work remains to be done in the research approach that tries to investigate the interactions between the river bed and bedload transport by the analyses of the grain-size distribution of the transported material.

The following sections analyze whether gravel bedload at Squaw Creek is transported selectively or in equal mobility. The first step is a detailed analysis of the grain-size distributions of the coarse samples taken episodically with the net sampler (11.2 mm > D > 180 mm) during the high flow in 1988. Sampling technique and procedure

have been described in Section 4.4.4.2, sieve analyses and the determination of percentiles are described in Section 4.4.5. The grain-sizes of 7 percentiles (D_5, D_{16}, D_{25}, D_{50}, D_{75}, D_{84}, and D_{95}) were calculated in ϕ-units and are listed in Table 3 in the appendix.

5.5.3.1 Variation of percentiles with discharge

To test the relation between bedload grain-size distribution and discharge, the grain sizes of each of the 7 percentiles (see above) were plotted versus the discharge at which the sample had been taken (fig. 5.29). The data scatter, but power function regressions were fitted through the relations between percentiles and discharge for each of the 7 percentiles. Although the curved course of the functions marks a log-log relationship, a linear scale was chosen for the abscissa because the discharge values range over half an order of magnitude only. If regression functions overlapped, the functions of the larger percentiles were deleted below the cross point because the percentile of a D_{95} cannot be smaller than the percentile of a D_{84}. This is a statistical artifact.

The regression functions form a function group that originates at a common point (the threshold of motion) and opens towards increasing flows. This group of curves indicated clearly that the grain-size distribution of bedload becomes coarser with increasing flow. Bedload at Squaw Creek is definitely transported **selectively** during ordinary events when snowmelt high flows reach bankfull levels and no sediment except bed material is supplied to the stream.

Larger than ordinary high flow discharges did not occur during the measuring period at Squaw Creek. Therefore no data support the extrapolation of these graphs. But as long as transport occurs selectively, flow competence increases with increasing discharge, producing coarser grain-size spectra for higher flows. This rule can, however, only be extended until the point at which the coarsest particles of the stream bottom are part of bedload transport, after the armor layer has broken up. If discharges continue to rise, the grain-size distribution cannot coarsen anymore, because it cannot become coarser than the grain-size composition of the river bed. If no additional
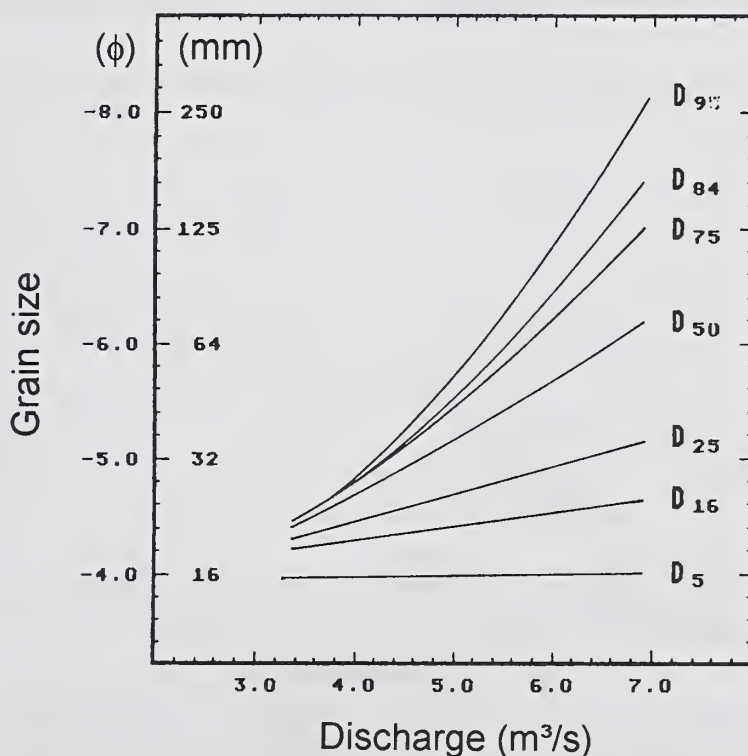
Figure 5.29. – Variation of grain-size distributions with discharge: the grain-sizes of the 7 percentiles increase as flow rises (samples from the net-sampler, 1988).

sediment sources are supplied to the stream, the transported grain-size distribution will reach a constant state after a certain discharge threshold has been exceeded and equals the grain-size distribution of the channel bed. An equal mobility of all grain sizes has been reached. The transport mode of equal mobility will at Squaw Creek only occur during extremely large events with high sediment supply which also lead to a drastic change in the channel morphology.

This concept of varying transport modes between initial motion and highest transport rates is schematically presented in Figure 5.30. This diagram demonstrates clearly how for supply-limited mountain streams the grain-size distribution initially coarsens with increasing flow and sediment availability during selective transport. The transport mode changes to equal mobility as flow, and especially sediment availability, increases during extreme events. Stream systems with a generally high sediment supply (e.g., braided streams, streams with alternate bars, etc.) or streams with a temporary high sediment supply (e.g., after log jam bursts) reach the state of equal mobility much faster during increasing flows. The transient phase of selective transport is then short and confined to the beginning of bedload motion.

5.5.3.2 Variation of grain-size parameter with discharge

Apart from the discharge dependency of the bedload grain-size distribution (fig. 5.29), it will also be studied whether standard grain-size parameters like skewness and sorting (Folk and Ward 1957) as well the parameter D_{max} show a systematic response to increasing flows at Squaw Creek. The respective parameters were calculated for all samples and their relation to flow discharge was plotted in Figure 5.31a, b, and c.

The D_{max} of the grain-size distributions at Squaw Creek increases as flow rises, similar to the studies by Wilcock (1988), Ashworth and Ferguson (1989a), and Komar and Shih (1992). Increasing flow further produces poorer sorting of the grain-size distribution and decreasing skewness. Grain-size spectra become wider and more symmetric as flows increase.

These results agree with the studies by Komar and Shih (1992) and Shih and Komar (1990b) regarding the general shift of the grain-size spectrum with flow, which means the studies generally agree on the selectivity of bedload transport. But results from Squaw Creek depart from the results by the above authors in as much as the response of the grain-size spectra to in-
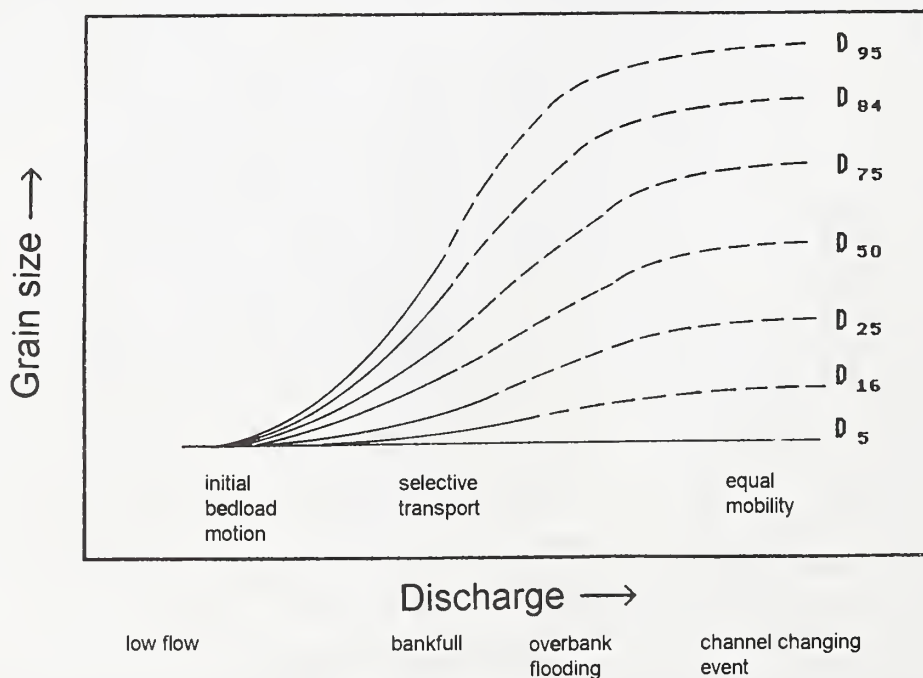
Figure 5.30 – Schematic diagram indicating the variation of the grain-size distribution with increasing flow for Squaw Creek: from selective transport during ordinary snow melt high flows to equal mobility during extreme events.
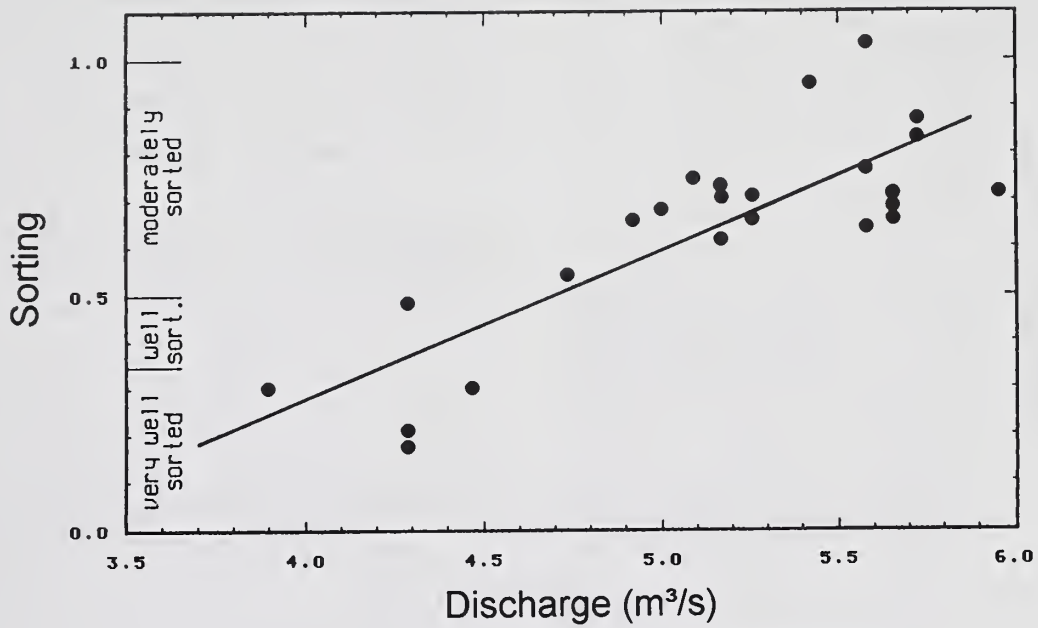
Figure 5.31a – Relation of grain-size distribution sorting and discharge.

Dynamics of Gravel-Bed Rivers. P. Billi, R.D. Hey, C.R. Thorne, P. Tacconi (editors), 1992, John Wiley & Sons Ltd., Chichester, England, Reproduced by permission of John Wiley and Sons Limited.
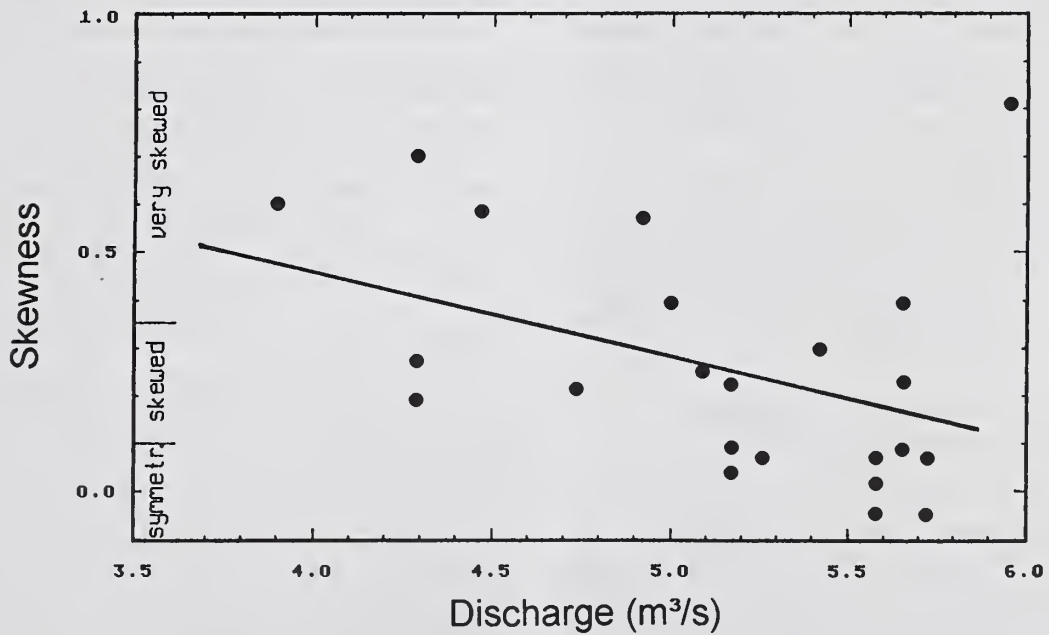
Figure 5.31b – Relation of grain-size distribution skewness and discharge.

Dynamics of Gravel-Bed Rivers. P. Billi, R.D. Hey, C.R. Thorne, P. Tacconi (editors), 1992, John Wiley & Sons Ltd., Chichester, England, Reproduced by permission of John Wiley and Sons Limited.
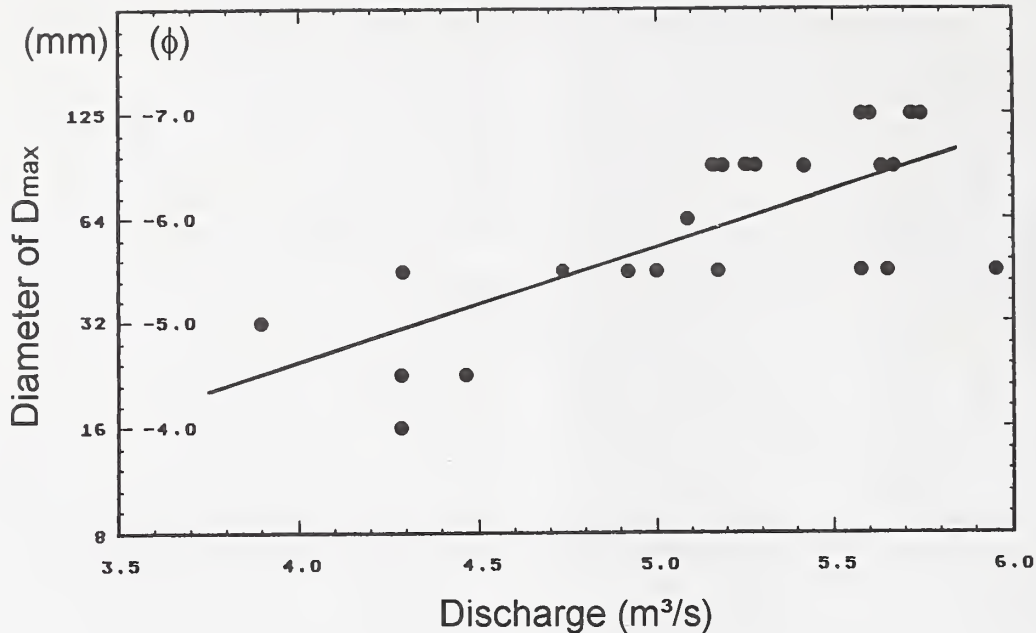
Figure 5.31c – Relation of maximum bedload grain size and discharge.

creasing flows is exactly contrary: increasing flow or increasing shear stress makes transported grain-size spectra become more skewed and more narrow in the data from Oak Creek analyzed by Komar and Shih (1992) and Shih and Komar (1990b). Besides, contrary to results in Figure 5.29, the D_{50} of the Oak Creek data increases at a faster rate with flow than D_{max}.

In order to find the reasons for this systematic disagreement between the behavior of the two data sets, the significance and applicability of these standard grain-size parameter for grain-size spectra encountered in coarse material bedload transport has to be examined.

5.5.4 Applicability of standard grain-size analyses for coarse material bedload

It was assumed that the disparity between the sedimentary response reported by Komar and Shih (1992) and Shih and Komar (1990b) for Oak Creek and the sedimentary behavior observed at Squaw Creek results from the incomparability of the respective grain-size distributions. Komar and Shih (1992) and Shih and Komar (1990b) analyze grain-size spectra that range from sand to cobbles, while the smallest grain-size class of the samples analyzed at Squaw Creek was much larger (11.2 mm). It is therefore investigated whether the

grain-size parameters of both data sets will follow the same trend for increasing flows, when the range of grain-sizes in both data sets is equalized. The Oak Creek data were therefore artificially truncated at 11.2 mm, and the coarser residue was normalized to represent 100%. **Skewness** and **sorting** were recalculated and plotted versus discharge. Skewness and sorting show now the same trend in their discharge dependency as data from Squaw Creek: sorting of the coarse grain-size spectra increases with flow, while skewness decreases. The transported grain-size spectra become wider and more symmetrical with increasing flow.

This analysis shows that standard grain-size parameters, such as sorting and skewness, respond sensibly to a change in the range of the sampled grain-size spectrum. Studies by Schleyer (1987) and Forest and Clark (1989) confirm this phenomenon. These studies also point out that completely different grain-size distributions can show the same values for certain grain-size parameters. The standard grain-size parameters like sorting and skewness, as well as the percentiles, will only provide a meaningful statement and comparability if they are exclusively applied to grain-size distributions that are similar. This similarity implies that both data sets resemble the same statistical distribution (e.g., Gaussian, log-

96

normal, Rosin) and are truncated to the same degree at both ends. Standard grain-size parameters are only suitable for a comparison of coarse bedload material, if the samples are part of the same "population" which means that the applicability is limited to samples taken under similar sedimentological and technical conditions at one stream (Bunte 1992a).

It is, however, technically and practically problematic to take representative bedload samples without truncating the grain-size spectrum on either the coarse or the fine end, especially in streams that carry coarse bedload with wide grain-size distributions ranging from sand to boulders. Therefore, depending on the bedload transport characteristics of the respective stream, the sampling technique employed, or the chosen method of grain-size analyses, grain-size distributions of bedload samples are usually truncated to various degrees on their fine and coarse ends (Schleyer 1987).

The incompleteness of sampled bedload grain-size spectra on the fine end can be due to several factors:

- a gap between the sampler opening and the stream bottom,
- large mesh widths of the sampling bag, and
- the often small proportion of fines within a bedload sample of coarse sediment.

The lack or the dearth of the coarse fraction within bedload samples can be attributed to

- small sampler openings,
- small sample sizes,
- short sampling times, and
- coarsest fractions are usually transported less frequently.

The chance is that the transport of the coarsest fractions will be underrepresented.

Bedload samples from coarse bedload carrying streams, and especially when sampled over a few minutes only, do not only have truncated ends, but also irregular grain-size distributions in general. This means that the mass, or number of particles, respectively per sieve class is over-or underrepresented in relation to neighboring size classes, leading to a deviation from a Gaussian (or lognormal) distribution by itself. This surplus or dearth of particles within a certain size fraction does not necessarily present an unsystematical statistical variation. These irregularities within the sampled grain-size spectra could give important hints regarding the processes of coarse material

bedload transport. Since it cannot be clarified off-hand which part of the grain-size variability is due to sampling artifacts and which parts represent a bedload process, the entire variability of sampled grain-size spectra should therefore be explicitly incorporated into a grain-size analysis and not be averaged out by fitting a Gaussian (or log-normal) distribution to the data set by all means.

The general incomparability of results from standard grain-size analyses of coarse bedload samples with their typically truncated and irregular grain-size distributions do not need to be a reason to drop comparative grain-size analyses of coarse bedload material altogether. But it is necessary to develop new procedures that make it possible to compare results of grain-size analyses of coarse bedload samples without restriction (Bunte 1992b). A new possibility for such analyses is suggested in the next section.

5.5.5 Particle numbers and particle transport rates

It has already been shown in Section 4.4.5.2 how the grain-size distributions of coarse bedload samples can be determined by counting the number of particles per sieve class, and relating this number to a unit of flow per width and time (Appendix Table 3b). The determination of **particle transport** rates for an increment of time and space is a simple and effective method to characterize both bedload transport rates and their grain-size distributions.

Fractional particle transport rates of samples taken during the snowmelt high flow in 1988 are plotted in histograms in Figure 5.32. In order to show the grain-sizes of bedload transported during an ordinary snowmelt high flow and the relation of bedload material to other sedimentological stream units, the number of particles per sieve classes larger than 11.2 mm was also determined for a sample from a gravel bar and the channel bottom.

The gravel bar that was sampled developed during a large rain-on-snow event in 1981. The berm along this gravel bar formerly divided Squaw Creek into two branches, until a log-jam burst in 1983 altered the channel morphology again and resulted in an aggradation and subsequent abandonment of the former right channel. The present position of the gravel bar is shown in Figure 4.14 (lower left part) and in the maps of Figures 3.7 and 3.8. The sample from the gravel bar was taken as a bulk sample at the streamward side of the gravel bar. The distribution of the

Figure 5.32 – Number of particles present per size class in samples from the gravel bar, and the channel bottom; particle transport rates per size class of bedload samples collected with the net-sampler in 1988.

Dynamics of Gravel-Bed Rivers. P. Billi, R.D. Hey, C.R. Thorne, P. Tacconi (editors), 1992, John Wiley & Sons Ltd., Chichester, England, Reproduced by permission of John Wiley and Sons Limited.
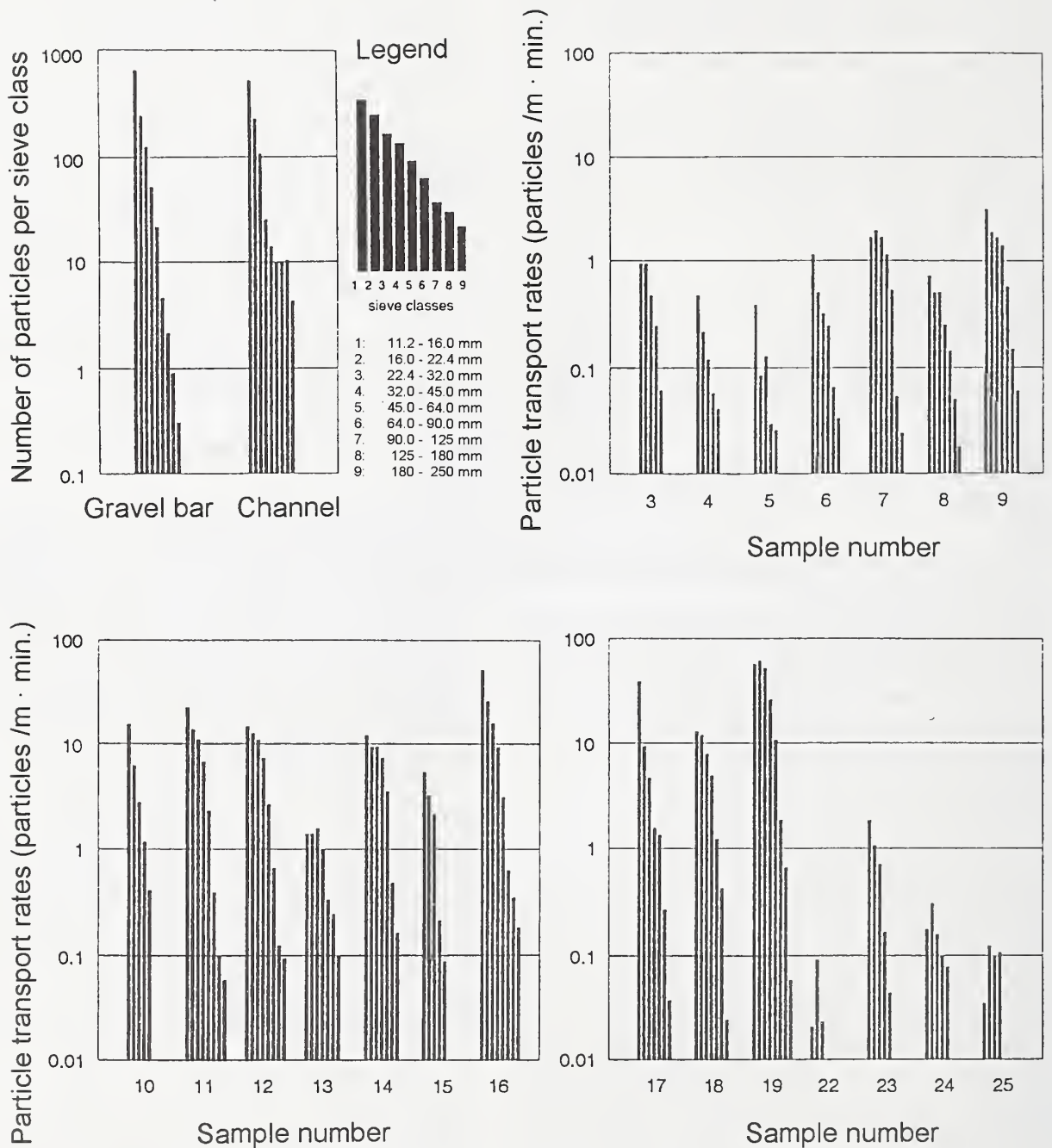
coarse fraction of this sample is very symmetrical. The number of particles per grain-size class >11.2 mm decreases exponentially with increasing size class (fig. 5.32).

The sample from the channel bottom was taken from a riffle area during low flows and comprises only the surface layer. The grain-size distribution shows a regular decrease of particle numbers per sieve class only for small gravels < 32 mm. Compared to the grain-size distribution of the gravel bar, pebbles between 32 and 64 mm are slightly underrepresented on the channel bottom, while an abundance exists for cobbles > 64 mm. These cobbles and small boulders stabilize the channel bottom as a pavement (Sutherland 1987). Some of the cobbles are blocky and originate from nearby talus. Being wedged into each other these large clasts enhance the surface armor.

Bedload samples taken during an ordinary high flow in 1988 are numbered from 3 to 25 according to Table 3 in the Appendix. The decrease of particle transport rates for increasing grain-size classes is more irregular in bedload samples than in the sample from the gravel bar. Compared to the regular grain-size distribution of the gravel bar, bedload samples tend to have a slight dearth of small pebbles < 32 mm, but a relative abundance of medium and large pebbles 32 - 64 mm. This indicates a favorable transport of the medium and large pebbles at Squaw Creek. The preferential transport of medium and large pebbles could indicate a progressive armoring of the channel bottom (Wilcock and Southard 1989). The coarsest particles that have found a stable position, accumulate on the stream bottom. Small pebbles find erosion resistant niches in gravel pockets[12] and in the interstitial spaces. Medium and large pebbles apparently have the greatest difficulty in finding protected places. Bedload samples from very small transport rates (sample numbers 5, 20, 21, 22, 24, and 25) show very pronounced irregularities in their grain-size distributions.

5.5.6 Variation of particle transport rates per grain-size class with flow discharge

The grain-size analysis used to distinguish between **selective transport** and **equal mobility** in Section 5.5.3 was based on the percentiles of the grain-size distribution which characterize the competence of the flow to transport bedload. If particle transport rates are used for such an analysis, this approach will pay consider both the competence as well as the capacity of flow. Particle transport rates analyze not only a variation of transported grain sizes, but also a variation in the amount of bedload transport per grain-size class.

In order to test whether particle transport rates occurred in dependency of flow volume, particle transport rates of all bedload samples (in particles per meter and minute) were plotted against flow, individually for each grain-size class (fig. 5.33). The data scatter is large, especially for discharges > 5 m³/s. Particle transport rates per grain-size class range over almost two orders of magnitude. Exponential functions were fitted through the data of each grain-size class to better visualize and compare the response of particle transport rates to flow. The regression functions for all grain-size classes are combined in the last partial plot in Figure 5.33. Two groups of regression functions can be distinguished :

- functions 1 to 4, representing the small grain-size classes between 11.2 - 45 mm, and
- functions 5 to 7, representing the large grain-size classes between 64 - 125 mm.

With the exception of the regression function 1, which presents particle transport rates of the smallest grain-size class 11.2 - 16 mm, regression functions run almost parallel to each other.

The thresholds of motion for pebbles between 11.2 and 45 mm are reached as discharges approach and pass 3.5 m³/s. A particle transport rate of 0.01 particles per meter per minute is defined as initial motion, because a log-partitioned ordinate cannot exhibit the value of "zero." This minimal transport rate represents the transport of 1 particle per meter width per 100 minutes. The transport of pebbles and cobbles > 45 mm only sets in when a threshold of 4.5 m³/s is exceeded. For grain sizes > 45 mm, discharge has to increase incrementally for the incipient motion of each larger grain-size class. Wilcock's (1988) finding that the critical shear stress needed for initial motion is independent of the particle size can not, at least for particles > 45 mm, be confirmed for Squaw Creek.

It is also assumed for Squaw Creek that a larger data set would parallel the graphs of the functions for smaller gravels. A log-partitioning of the abscissa and the use of power function relationships might also help to parallel the graphs.

---

[12] see Barta et al. 1993

99
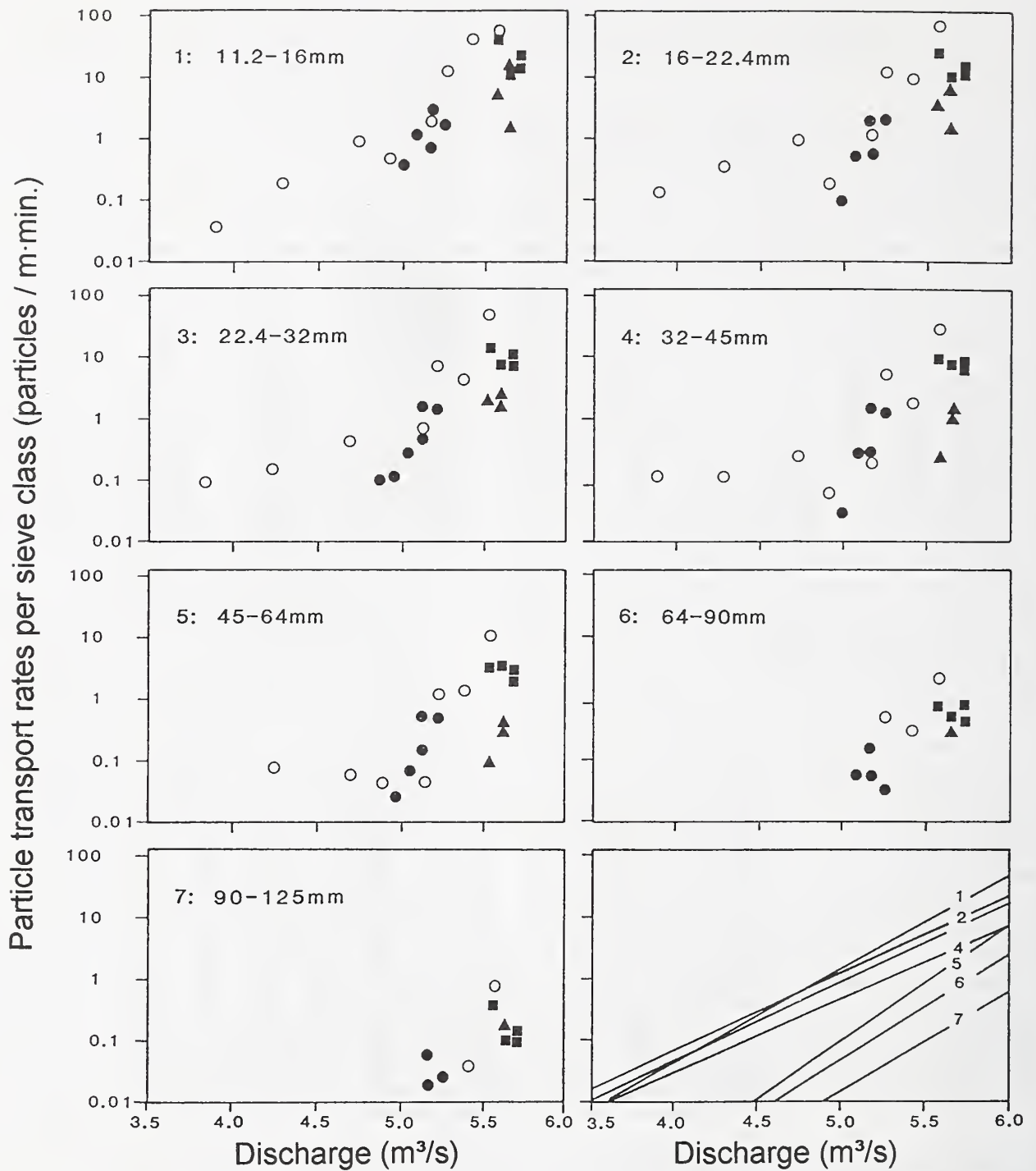
Figure 5.33 – Increase of particle transport rates of 7 size classes with flow. The plot on the lower right shows the regression functions calculated for all size classes. ● = small bedload samples on the beginning rising limb; ■ = large bedload transport rates during fluctuating transport; ▲ = small bedload transport rates during fluctuating transport; O = other samples. Symbols are further explained in Section 5.5.8.

Dynamics of Gravel-Bed Rivers. P. Billi, R.D. Hey, C.R. Thorne, P. Tacconi (editors), 1992, John Wiley & Sons Ltd., Chichester, England, Reproduced by permission of John Wiley and Sons Limited.

The abscissa was kept linear due to the small range of the discharge values. Non-intersecting functions would demonstrate more clearly that a next higher discharge threshold value has to be exceeded for the next larger grain-size class to be set into motion. However, more data are needed to prove this.

The results of this study show, comparable to the analyses of the percentiles in Section 5.5.3.1, the discharge dependency of transported grain-size spectra. **Selective transport** of coarse bedload sediments could therefore be confirmed for Squaw Creek by both methods.

In his discussion of Bunte (1992), Komar (1992) also carried out a particle transport analysis for his data set from Oak Creek which he had used in his previous studies. Komar's results regarding the discharge dependency of initial motion and the transported grain sizes agree with those from Squaw Creek. The discrepancy between the response of the grain-size distributions to increasing flow at Oak Creek (Komar and Shih 1992) and at Squaw Creek (Bunte 1992a) has been eliminated. The particle transport analysis makes it possible to compare grain-size spectra from any gravel populations, irrespective of grain-size truncations or internal distribution irregularities.

5.5.7 Grain-size composition of bedload during various transport rates

The scatter in the relations between fractional particle transport rates and discharge (fig. 5.33, Section 5.5.6) is large. The hypothesis is that the composition of bedload might be affected by the intensity of the transport, or that certain grain-size fractions are transported preferentially. The investigation started by plotting particle transport rates (particles/m·min), individually for each grain-size class, versus the total bedload transport rate (g/m·s) of the respective sample (fig. 5.34). Power functions were fitted through the data sets of each grain-size class and combined in the last plot of Figure 5.34. Compared to the relations between particle transport rates and discharge (fig. 5.33), data scatter much less in their relations between fractional particle transport rates and total bedload transport rates.

In the medium pebble range (22.4 - 45 mm), the number of particles transported per grain-size class per meter and minute increases very regularly with the total bedload transport rate. Scatter occurs in the relations between particle transport rates and total bedload transport rates for both the smaller and the larger gravel sizes. The number of

medium-sized pebbles (22.4 - 45 mm) within a certain total bedload transport rate is well predictable, while the number of the smaller and larger pebbles is more variable.

The parallelism of the regression functions in the last partial plot in Figure 5.34 shows that generally, the number of transported particles per grain-size class increases regularly with increasing bedload transport rates. The distance between the regression functions increases for higher grain-size classes. This means that the grain-size distributions, or the decrease of fractional particle transport rates with increasing grain-size (fig. 5.32), can be described by an exponential function. The number of transported particles per grain-size class decreases by a factor of about 0.3 per grain-size class within the three smallest gravel classes. For pebbles and cobbles > 32 mm, particle transport rates decrease by a factor of 2 - 4 from one grain-size class to the next larger grain-size class.

Grain-size classes > 125 mm could not be incorporated into the analyses because the number of sampled particles was not sufficient for a statistical analysis. It can however be assumed that the increase of particle transport rates with increasing flow and increasing total transport rates conforms to the regularities demonstrated in Figures 5.33 and 5.34.

5.5.8 Temporal variation of particle transport rates

Bedload samples taken with the net-sampler in 2-hour intervals during ordinary snowmelt high flows of 5 - 6 m³/s of the nights of May 23 - 24 and May 24 - 25, in 1988 were used to study the temporal variation of the relation between fractional particle transport rates and total bedload transport rates. The timing of the sampling, the magnitude of bedload transport rates, and rough indications of grain-size compositions are depicted in Figure 5.35. Similar to fluctuating signal rates in 1986 (fig. 5.8), highly variable bedload transport rates can also be observed for the high flow in 1988, especially during the falling limb of flow (fig. 5.35). Figure 5.3 (Section 5.1.5) shows the strong variation of bedload transport rates with discharge. The question arises, whether this variation of bedload transport rates during unsteady flows coincides with a variation of the transported grain-size spectra. The unsteadiness of flow is by no means extreme, as discharge ranges only between 5.00 and 5.26 m³/s during the first night, and between 5.58 and 5.73 m³/s during the second night.
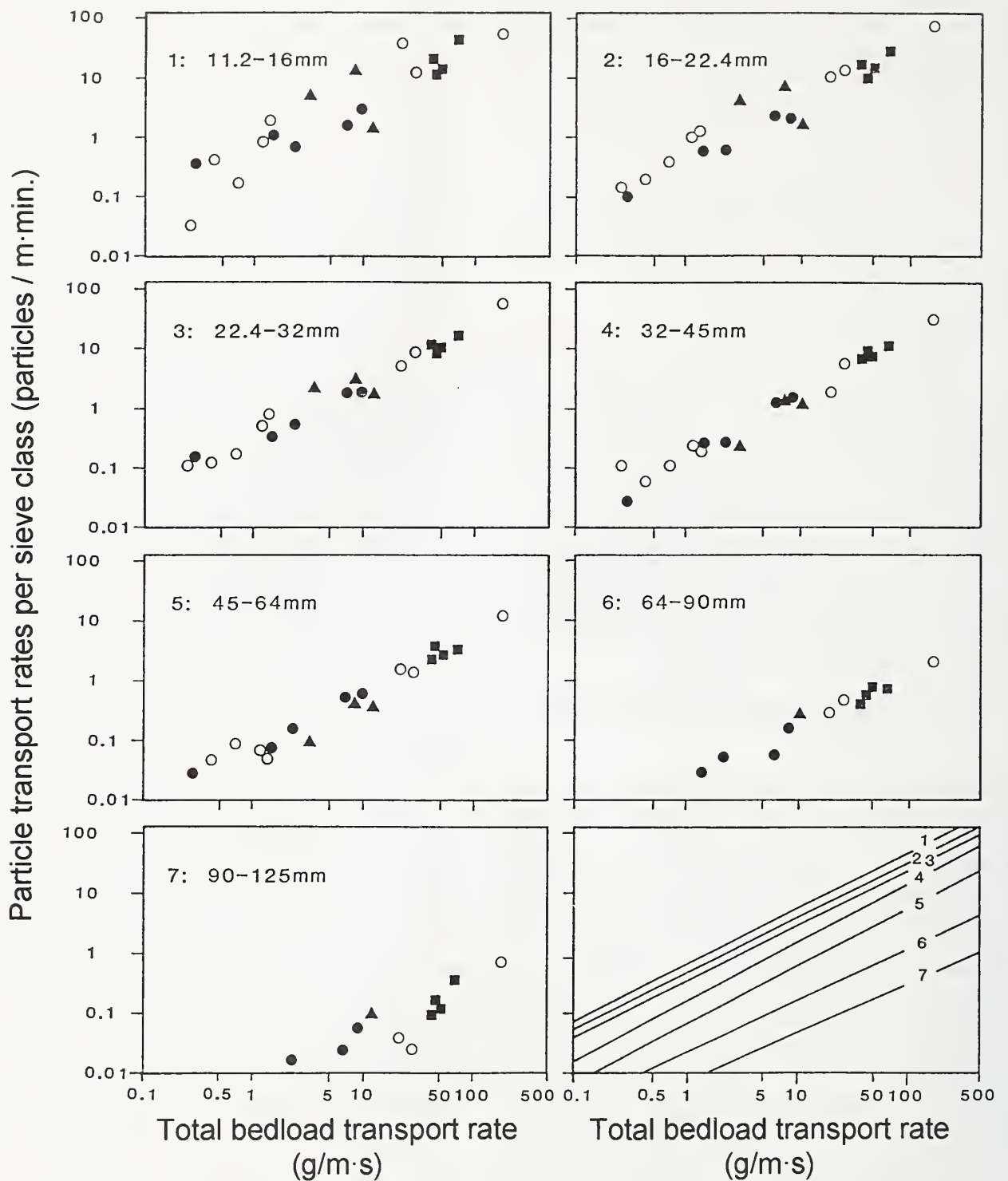
Figure 5.34 – Increase of particle transport rates of 7 size classes with total bedload transport rates. The plot on the lower right shows the regression functions calculated for all size classes. ● = small bedload samples on the beginning rising limbs; ■ = large bedload transport rates during fluctuating transport; ▲ = small bedload transport rates during fluctuating transport; O = other samples. Symbols are further explained in Section 5.5.8.

Dynamics of Gravel-Bed Rivers. P. Billi, R.D. Hey, C.R. Thorne, P. Tacconi (editors), 1992, John Wiley & Sons Ltd., Chichester, England, Reproduced by permission of John Wiley and Sons Limited.
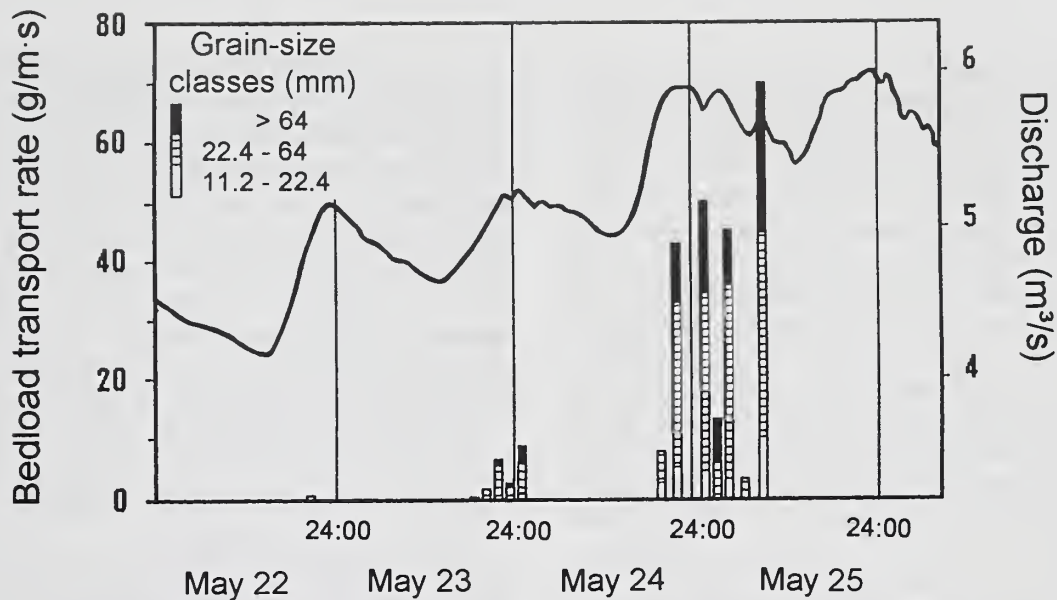
Figure 5.35 – Temporal variation of bedload transport rates and their grain-size distributions during snow melt high flow of 1988 (samples from net-sampler).

Data plotted in Figures 5.3 and 5.35 were grouped into three groups according to discharge volumes and bedload transport rates. Each group was assigned a signature. The numbering of the samplers refers to the numbering in Table 3a-b (Appendix) and Figure 5.32.

Group 1) Sequential samples taken during the night of May 23 - 24 during rising flow with

Q: 5.00 - 5.26 m³/s;

Qb: 0.29 - 9.25 g/m·s;

sample nos.:   5 - 10,

signature: ●

Group 2) Sequential samples with **large** bedload transport rates taken during the night of May 24 - 25 on rising and falling flow with

Q: 5.58 - 5.73 m³/s;

Qb: 41 - 72 g/m·s;

sample nos.:   11, 12, 14, 16,

signature: ■

Group 3) Sequential samples with **small** bedload transport rates taken during the night of May 24 - 25 on rising and falling flow with

Q: 5.58 - 5.73 m³/s;

Qb: 3 - 12 g/m ·s;

sample nos.:   10, 13, 15,

signature: ▲

All other bedload samples were plotted using the symbol O. The same set of signatures has been used in Figures 5.33 and 5.34, which is referred to again.

Bedload samples of the **group 1** (●), taken consecutively during rising flow, do not show much fluctuations in their bedload transport rates, nor in their grain-size composition. Among particle transport rates of small pebbles >32 mm, only those two of the five samples with the highest particle transport rates plot close to the regression functions which relate particle transport rates of a certain grain-size class to flow discharge. These regressions indicate the average capacity of flow to transport particles of different size classes at Squaw Creek. The other three samples of group 1 plot below the average trend, indicating that less bedload material than the average capacity of flow is transported at these times. This systematic dearth in the transport rates of small pebbles (11.2 - 32 mm) cannot be observed for larger pebbles and cobbles. Here, particle transport rates do not deviate systematically, but randomly from the average competence of flow.

Particle transport rates of large bedload transport rates taken in the next night's series of samples during higher flows (**group 2, ■**) correspond better with the average capacity of flow to transport a certain rate of particles at Squaw

103

Creek. Particle transport rates are close to or slightly above the regression function. This means that transport rates respond in general to the average capacity of flow. Bedload samples of **group 3** (▲) are distinguished from group 2 by their generally smaller transport rates. In all partial plots of Figure 5.33 with grain-size classes smaller than cobbles (< 64 mm), triangles (▲) plot below the regression functions indicating that less particles than given by the capacity of flow are transported. This lack of transported particles becomes the more prominent, the larger the pebble sizes (< 64 mm). Particle transport rates of cobbles > 64 mm respond only in one of the three samples to the predicted amount. The other two samples did not transport cobbles at all.

Figure 5.34 is used to study whether this dearth of particle transport rates in samples with generally small transport rates is restricted to certain grain sizes or whether the samples, although their transport rates are small, still carry an even grain-size distribution. In the series of bedload samples taken during rising flows with little fluctuations in bedload transport rates (**group 1, •**) particle transport rates of the smallest grain-size class (11.2 - 16 mm) scatter slightly in their relation to total bedload transport rates. In the next larger grain-size class (16 - 22.4 mm) particle transport rates are slightly underrepresented. Particle transport rates of all other grain-size classes increase regularly with increasing bedload transport rates.

The two groups of samples (■) and (▲) collected on the rising and falling limb during the next night's higher flows show their difference also with respect to particle transport rates and grain-size distributions. For the group with the large bedload transport rates (■) particle transport rates follow the general trend of the regressions for all grain-size classes. Large bedload transport rates always exhibit a broad and symmetrical grain-size spectrum. Small bedload transport rates, on the contrary, have generally truncated grain-size distributions in which particle transport rates for small grain-size classes (11.2 - 32 mm) deviate trendlessly from the general trend of the data. Particle transport rates for medium grain-size classes (32 -64 mm) of group 3 are also usually less than indicated by the general trend. The transport rates of cobbles are either as high as expected, or cobbles are not transported at all.

Competence and capacity of the flow increases as the discharge rises. Particle transport rates of individual grain-size classes increase systematically with discharge. Grain-sizes are, according to

the competence of flow, transported selectively. At the onset of coarse bedload motion, transport rates fluctuate only to a minor extent (•). As discharge increases, bedload transport rates and the number of transported particles per grain-size class continues to rise and, depending on the force of flow, larger and larger particles become part of bedload. Transport continues to be selective with respect to flow competence. The fluctuations in the amount and grain-size composition of bedload becomes more eminent for large flows. This enforces an increasing scatter in the statistical relations between bedload transport, or particle transport rates of various grain-size classes, respectively, and discharge.

The results of the analyses regarding the temporal variation of particle transport rates can be summed up as follows:

- In the beginning of a high flow wave with moderately high discharges particle transport rates are generally low during the night of May 23 - 24 (group 1, •).

- As a larger high flow wave passes the following night of May 24-25, strong fluctuations of bedload transport are especially prominent after peak flow on the beginning of the falling limb:

  ○ Small bedload transport rates have grain-size distributions with variable transport rates of small particles (11.2 - 32 mm). Cobbles (> 64 mm) are only temporarily part of bedload transport, and medium pebble sizes (32 - 64 mm) are usually underrepresented (group 2, ▲).

  ○ Large bedload transport rates on the crest of the bedload waves have regular particle transport rates in all grain-size classes (group 3, ■).

These patterns of temporal variation of bedload transport rates and their grain-size distribution correspond well with the conceptual model, introduced in Section 5.3.5 (fig. 5.14), which describes river bed adjustment processes in a riffle area which are described below.

In the beginning of a high flow wave when discharges are still small, bedload transport rates are low and relatively steady. Interactions between the river bed and the hydraulic forces are limited to the minor exchange of small gravels. Flow forces are not high enough yet to mobilize larger material.

Strongly **fluctuating bedload transport rates** with variable grain-size compositions indicate

vivid interactions between hydraulics and the river bed when daily (or better "nightly") discharges are high. Irregular grain-size spectra which are especially variable in their contribution of small pebbles or large cobbles are transported during low transport rates. On the contrary, high bedload transport waves have wide, regular, and untruncated grain-size spectra.

When transport rates are small, and either too fine or too coarse, bedload transport is extremely selective. The selectivity of the transported grain-sizes is in this case not dominated by the general, cross-sectional average, of the competence of flow, but by the very local hydraulic and sedimentologic conditions at a nearby sediment storage. Depending on the constellation of the local hydraulics and sedimentologic conditions on the river bed, small pebbles are not erodible when they are caught in the interstices of the larger rocks. Small pebbles are however transported in abundance when they are winnowed out from the voids at the stream bottom at a time or at a place where local forces of flow temporarily gain strength. This, in turn, exposes the large clasts which then can also be eroded and transported. The medium and large pebbles are only involved in these interactions of **hiding and exposure** to a minor degree, since they are too big to be trapped in the interstices, but small enough to be transported easily by the forces of flow exerted onto the river bed. Small pebbles and large pebbles or cobbles interact on the river bed and either hinder or enforce each other's mobility. The medium pebbles are only partially involved in these interactions and are therefore transported at a more even rate.

The large bedload transport rates with even grain-size distributions are not attributable to the relatively minor river bed adjustments which are induced by roughness changes within the surface layer. Large transport rates during the passage of bedload waves are probably associated with major river bed adjustments which incorporate more than a particle exchange just at the surface layer. Adjustment activities which reach to deeper layers and change the local channel form mobilize relatively large amounts of sediment which is derived from material from the coarser surface layer and the finer subsurface substrate.

5.5.9 Results and conclusions

Little is known about the processes that lead to a temporal and spatial variation of bedload transport rates and their grain-size distributions

in mountain streams. It is still methodologically difficult to measure the relevant processes and current techniques of coarse bedload transport analysis still need to be improved and standardized. Analyses of bedload transport material collected during ordinary snowmelt high flow conditions with a 3-inch Helley-Smith and a special net-sampler at Squaw Creek show the following results and lead to following conclusions:

Coarse material bedload transport at the measuring site on the downstream end of a pool-like section is confined to a width of a few meters in the central part of the stream around the thalweg. Sand can be transported over the entire width of the stream, although the largest transport rates also occur in the central part of the cross-section.

The shift in bedload grain-size distribution from predominantly sandy samples in the beginning of the annual high flow to predominantly gravelly samples later on in the high flow shows that the transported grain-size spectrum not only responds to the current forces of flow, but is also dependent on the "history" of flow which affects the current sedimentological conditions of the river bed. This has implications for flow competence analyses. Only bedload samples collected under similar conditions regarding channel bottom roughness and sediment supply can be used for such analyses.

The results of standard grain-size analyses show that bedload grain-size distributions collected during ordinary snowmelt high flows at Squaw Creek are strongly dependent on discharge volume. Bedload therefore occurs as **selective transport**. Unless a sediment storage is tapped (e.g., by a log-jam burst) and releases unusual amounts of transportable gravels, the state of **equal mobility** will be reached at Squaw Creek during very large flows only, after even the largest clasts of the channel bottom have become mobile. This will probably require extreme high flow events which will cause a drastic change in the channel morphology.

Standard methods of grain-size analyses (e.g., percentiles, Folk and Ward 1957), only provide comparable results for coarse bedload samples when samples are part of the same population. This means that samples need to have been taken under similar sedimentological and technical conditions in the same or a very similar stream. The analysis of particle transport rates is not restricted to such conditions.

The analysis of particle transport rates which refer to both the competence as well as the capac-

ity of flow (i.e. the amount and grain-size distribution) provides some indirect information of the processes on the river bed. Together with information derived from various prior analyses (the temporal variation of bedload transport, various kinds of bedload waves, rudimentary insights into changes in channel form and roughness and local flow hydraulics, and, last but not least the coincidence of changes in water surface slope and bedload waves), a lively picture can be developed that combines observed phenomena and inferred results and shows how bedload transport could work at streams like Squaw Creek.

Transport rates of samples taken during flows just above the critical discharge of coarse bedload transport are generally small. Transported grain-size distributions are very irregular (samples no. 21, 22, 24, and 25). This **random** transport of individual particles can be explained by the effects of **hiding and exposure** which allows particles to be transported easily when they are exposed to flow. As discharges increase, particle exchange and adjustment processes are initiated at the river bed. Bedload transport rates increase with flow and bedload waves are only **small**. Particles sizes are transported **selectively** in accordance with the competence of flow.

Larger flows during snowmelt bring with them strong fluctuations of bedload transport rates with variable grain-size distributions. The interpretation of this temporal variability of bedload transport rates and their grain-sizes corresponds well to the conceptual model (Section 5.3.5) that describes the adjustment processes on the river bed.

When bedload transport rates are small during fluctuating transport, their grain-size distributions are irregular. Cobbles (> 64 mm) can be completely missing, while fine gravels (11.2 - 32 mm) are either under- or over represented. Transport rates in the medium pebble range are generally small. This kind of transport phenomena indicate minor river bed adjustments which are attributable to changes in the roughness of the river bed.

Major bedload waves have high particle transport rates in all grain-size classes. A wide and complete grain-size spectrum is transported. This kind of bedload transport indicates major adjustment processes which are not limited to roughness changes at the surface layer, but extend to changes in the channel form which involves subsurface material as well.

The processes of coarse material bedload transport in mountain streams cannot be inferred from the analysis of grain-size distributions and bedload transport rates alone without incorporating other parameters that influence bedload transport. Bedload transport is a partial aspect of the fluvial interactive system that includes the channel morphology and roughness, the hydraulic conditions, and sediment transport which results from the adjustment activities between the solid and the fluid components. New conceptual models are required to explain the dynamics of the fluvial system within the reach scale. New measurement techniques are needed to register fluvial processes in high temporal and spatial resolution. These data sets can then be used to verify the conceptual models or to prove them wrong.

6. Summary

Temporal variations of coarse material bed-load transport rates and their grain-size distributions result from interactions and adjustments between the hydraulics of flow and the sedimentological and morphological conditions of the river bed. Since these interactions are quite complex and appropriate measurement techniques are usually not available, little is known about the dynamics of bedload transport in mountain streams.

New measurement techniques were developed at Squaw Creek, and these techniques facilitated detailed investigations of the temporal variability and grain-size distribution of coarse material bedload transport and of some of the parameters affecting it. Field measurements were carried out during snowmelt high flows in 1986 and 1988 at Squaw Creek, a gravel-bed mountain stream in Montana, USA. The analyses presented in this study are based on a rather large array of time series and individual measurements of various parameters measured by several techniques:

6.1 Measured Data Sets

6.1.1 Bedload transport

Continuous registration
- signal rates of coarse bedload transport (1986): A 17-day time series in 1-hour resolution and a 3-day time series in 5-minute resolution *(magnetic tracer technique)*

Sequential bedload samples in 2- 3-hour intervals
- bedload transport rates and grain-size distributions (1986 and 1988) *(large net-sampler)*

Individual bedload samples
- bedload transport rates and grain-size distributions (1986 and 1988) *(large net-sampler and Helley-Smith sampler)*

6.1.2 Hydraulic Parameters

Continuous registration
- hydrographs (1986 and 1988) *(stage recorder)*

Sequential measurements in 2- 3-hour intervals
- local water levels (1986 and 1988) *(stage readings)*

- water surface slopes (1986 and 1988) *(stage readings in water level tubes)*
- flow velocities (1986 and 1988) *(several current meters)*

Individual measurements
- local water levels (1986 and 1988) *(stage readings)*
- water surface slopes (1986 and 1988) *(stage readings in water level tubes)*
- flow velocities (1986 and 1988) *(several current meters)*

6.1.3 Channel Geometry

Sequential measurements in 2- 3-hour intervals
- temporal and spatial variation of cross-sectional topography (1988) *("Tausendfüßler" profile meter)*
- indirect: temporal variation of water surface slopes (1986 and 1988) *(stage readings in water level tubes)*

Individual Measurements
- Two topographic stream surveys (1986 and 1988) *(theodolite and transit surveyor's level)*

Many of these data sets could not have been obtained without the development or special adjustment of measuring techniques to match the conditions at Squaw Creek.

6.2 Measuring Techniques

6.2.1 Magnetic Tracer Technique

The magnetic tracer technique was especially designed for the investigations at Squaw Creek and constructed by Spieker (1988). The electronics detect the passage of naturally magnetic pebbles and cobbles over a detector log and register signals from particles with magnetic field strength > 40 gamma. Such particles are, statistically seen, > 32 mm. The transport of 44% of the magnetic bedload can thus be registered at the measuring site (Section 4.4.2). Signal rates counted from the record yield a time series of bedload transport unique in its combination of length and resolution (Section 4.4.3).

6.2.2 Representative Sampling of Coarse Material Bedload

Both a 3-inch and 6-inch Helley-Smith sampler were found to be inappropriate for sampling pebble and cobble bedload. The net-sampler consisting of a wooden frame and a fishing net was designed to fit the Squaw Creek site. The large orifice of 0.3 m by 1.55 m representatively samples even the largest cobbles. Samples are truncated at 11.2 mm due to the 10 mm mesh width. The large mesh, however, kept the flow forces exerted on the sampler at a maneuverable level (Section 4.4.4).

6.2.3 Water surface slope

The temporal variation of the theoretical water surface slope (equaling the first derivative function of the hydrograph) and the actual water surface, measured with water level tubes over a riffle reach between two points 17.3 m apart, show a discrepancy. Given the conditions at the measuring site, these deviations can be interpreted as variations in the cross-sectional channel geometry (Sections 4.5.1 and 5.3.3).

6.2.4 Measuring Channel microtopography with the Tausendfüßler Profiling Device

P. Ergenzinger and T. Berry developed and tested a profile meter designed to accurately and repetitively measure a cross-sectional profile of the river bed. Consecutive measurements make it possible to analyze the temporal and spatial variations of channel bottom roughness and shape (Section 4.5.2).

The combination of the results from the various measurements made it possible to indicate the interactions between the hydraulic, sedimentological, and morphological conditions of the stream and the dynamics of bedload transport.

6.3 Relation Between Discharge and Bedload Transport

All formulas used to describe bedload transport are based on the assumption that a strong relation exists between bedload transport rates and volume of flow. Analyses of data sets from Squaw Creek do not support this hypothesis. Hourly signal rates and sequentially sampled bedload transport rates only show low statistical correlations with flow discharge or stream power

of $r^2 \approx 0.6$ (Section 5.1). The sequence of discharges, i.e., the "history of flow" has a strong impact on actual bedload transport rates, too, as it modifies the sedimentary conditions of the river bed. Thus, hysteresis effects occur (Section 5.2.1.3). Not only the amount of bedload but also its grain-size distribution is subject to the hysteresis effects. Bedload is more fine-grained during the first days of an annual high flow than bedload of comparable rates sampled during the same discharge on later high flow days (Section 5.5.2.2).

A prediction of bedload transport rates from hydraulic parameters yields acceptable results only when using time-averaged data to predict daily loads (Section 5.1). A poor statistical relation between instantaneous flow and bedload transport indicates that sedimentological conditions, such as stream roughness, armoring, bedforms, geometry, morphology, and sediment supply play an important role in determining bedload transport rates and its grain-size distribution.

6.4 Bedload Waves: Interaction Between Flow Hydraulics, and River Bed Conditions

Combining time series and individual measurements recorded for various parameters reveals some insight into the dynamics and interactions of the fluvial system within the reach scale at Squaw Creek.

Hourly bedload signal rates fluctuate and show wave patterns, which are repeated in a modified way during many of the daily fluctuations of flow. A **primary bedload wave** (sometimes twin-peaked) tends to correspond to peak flow, while two additional bedload waves (**secondary and tertiary waves**) occur during the falling limbs of flow (Section 5.3.2). The size of the bedload waves can often be ascribed to antecedent conditions of flow and the propagation of sediment supplied from storage.

A higher temporal resolution (5-minute intervals) reveals that bedload waves disintegrate into a series of bedload transport pulses (Section 5.4.1). **Major waves**, **minor waves**, **small waves**, and **random transport** can be distinguished according to the wave periodicity, amplitudes, duration and discharge (Section 5.4.1.4). None of these waves can result from the migration of **bedload sheets** (Section 5.4.2.3).

A temporal coincidence between changes in channel geometry and the occurrence of bedload waves can be shown by comparing the dynamics of the water surface slope with bedload dynamics.

The temporal and spatial variations of the water surface elevation seems to indicate the passage of bedload over a riffle area, starting with aggradation on the riffle followed by degradation and transport to the pool. A bedload wave occurs soon after falling water levels indicate that the pool has been emptied (Section 5.3.3).

Temporal and spatial variation in the river bottom roughness and form could be related to temporally and spatially varying shear stress. Berry (1988) showed for a cross-section at Squaw Creek that a simultaneous occurrence of large roughness and large shear stress lead to the erosion of the biggest particles, while small shear stresses lead to a smoothing of the roughness by accumulation of fines in interparticle voids (Section 5.3.4).

In order to better describe the adjustment processes between hydraulic and sedimentary parameters and the connection of these adjustments with the temporal variation of bedload transport rates and their grain-size distributions, the results of the temporal and spatial variations of channel roughness, flow hydraulics, and bedload transport rates were combined in a conceptual model (Section 5.3.5). The temporal variation of bedload transport rates and their transported grain-size spectra can be well described by this model. Including the results of the analyses of the temporal variation of bedload transport, a vivid picture can be established indicating how transport rates, grain-size distributions, and periodicity of bedload waves can act together as shown below.

As discharges increase during the rising limbs of daily flows, **systematic particle exchange and adjustment processes** are initiated at the river bed. Transport rates increase with flow and wave activity is moderate. Particles sizes are transported selectively in accordance to the competence of flow. The higher discharges around daily snowmelt peak flows bring with them strong fluctuations of bedload transport rates with variable grain-size distributions. These fluctuations are the result of **discontinuous adjustment processes** between spatially and temporally variable conditions of flow, roughness, and channel geometry.

Major bedload waves occur around peak flows and on the beginning falling limbs. Particle transport rates are high in all grain-size classes. A wide and complete grain-size spectrum is transported. This kind of bedload transport indicates adjustment processes that are not limited to roughness changes at the surface layer but extend to changes in the channel form that involves subsurface material as well. When bedload **transport rate**s are **small** during this fluctuating transport (wave troughs), their grain-size distributions are irregular. Cobbles (> 64 mm) can be completely missing, while fine gravels (11.2–32 mm) are either under- or over-represented. Transport rates in the medium gravel range are generally small. This kind of transport phenomena indicate minor river bed adjustments that are attributable to changes in the roughness of the surface layer. Depending on local conditions of flow and roughness, the river bottom becomes alternatively smoother of rougher, which in the erosional phase is accomplished by a selective removal of either fine gravels from interstices or exposed large particles.

Bedload waves classified as **minor** (with a 5-6 hour recurrence) and as **small** (1-hour recurrence) are mostly observed during the falling limbs (Section 5.4.1) when flows gradually decline. These waves are interpreted as minor adjustment processes between flow and the river bed.

Flows that just exceed the critical discharge of gravel transport produce low transport rates with irregular grain-size distributions. The effects of **hiding and exposure** allows individual particles to be transported when exposed. This produces a **random** transport.

6.5 Particle Transport Rates: An Alternative Method to Analyze Bedload Transport and Its Grain-size Composition

Results of standard grain-size analyses can only be compared if samples cover a similar grain-size range and similar distributions. Sediment samples taken with different techniques at different streams differ in their grain-size range and distributions. Parameters like "sorting" and "skewness" as well as the grain sizes of the percentiles can show identical numbers for different grain-size distributions. The analysis of particle transport rates developed in this thesis and supported by Komar (1992) is free of such restrictions and facilitates unproblematic comparability of coarse grained sediment samples (Sections 4.4.5.2, 5.5.4, and 5.5.5). Particle transport analyses combine the analyses of both the capacity and the competence of flow.

6.6 Selective Transport or Equal Mobility?

The dependency of the grain-size distribution on discharge (selective transport) was proved for an ordinary snow-melt high flow with a 1-2 year recurrence interval at Squaw Creek: grain-size spectra transported become coarse with increasing flow. Static and discharge independent grain-size spectra approximating the grain-size distribution of the river bottom (equal mobility) will be transported at Squaw Creek only during extreme flow events that also drastically change the channel morphology (Sections 5.5.3 and 5.5.6). The larger the amount of transportable sediment available to flow, the smaller the range of flow between selective transport and equal mobility. A wide range of flow needs to be passed in steep mountain streams before selective transport can switch to equal mobility.

7. References

Achter, U. and J. Brüggmann, 1991. Rechner-gestütztes Meßdatenerfassungssystem für Kleinsignale. [Computer supported data recording system for small signals.] Thesis submitted to the Department of Information Sciences at the Technische Fachhochschule Berlin in partial fulfillment of the requirements of a M.S. degree.

Ackers, P. and W.R. White, 1973. Sediment transport: new approach and analysis. *Journal of the Hydraulics Division*, ASCE, 99(HY11): 2041-2060.

Allen, J.R.L. and M.R. Leeder, 1980. Criteria for the instability of upper-stage plane beds. *Sedimentology* 27: 209-217.

Anastasi, G., 1984. Geschiebeanalysen im Felde unter Berücksichtigung von Grobkomponenten. [Field analyses of gravels with special emphasis to coarse particles]. *Mitteilungen der Versuchsanstalt für Wasserbau, Hydrologie und Glaziologie der ETH Zürich*, No. 70.

Andrews, E.D., 1983. Entrainment of gravel from naturally sorted riverbed material. *Geological Society of America Bulletin* 94: 1225-1231.

Andrews, E.D. and G. Parker, 1987. Formation of a coarse surface layer as the response to gravel mobility. In: *Sediment Transport in Gravel-Bed Rivers*. C.R. Thorne, J.C. Bathurst and R.D. Hey (eds.). John Wiley and Sons, New York, p. 269-300.

Apperley, L.W., and A.J. Raudkivi, 1989. The entrainment of sediments by the turbulent flow of water. *Hydrobiologia* 176/177: 39-49.

Arkell, B., G. Leeks, M. Newson and F. Oldfield, 1983. Trapping and tracing: some recent observations of supply and transport of coarse sediment from upland Wales. *Special Publications of the International Association of Sedimentation* 6: 107-119.

Ashworth, P.J. and R.I. Ferguson, 1986. Interrelationships of channel processes, changes and sediments in a proglacial braided river. *Geografiska Annaler* 68A (4): 361-371.

Ashworth, P.J. and R.I. Ferguson, 1989. Size-selective entrainment of bed load in gravel bed streams. *Water Resources Research* 25(4): 627-634.

Ashworth, P.J., R.I. Ferguson and M. Powell, 1992. Bedload transport and sorting in braided channels. In: *Dynamics of Gravel Bed Rivers*. P. Billi, R.D. Hey, C.R. Thorne and P. Tacconi (eds.), John Wiley and Sons, Chichester, p. 497-515.

Bagnold, R.B., 1966. An approach to the sediment transport problem from general physics. *U.S. Geological Survey Professional Paper* 422-I, 37pp.

Bagnold, R.B., 1977. Bed load transport by natural rivers. *Water Resources Research* 13(2): 303-312.

Bänzinger, R., and H. Burch, 1990. Acoustic sensors (hydrophones) as indicator for bed load in a mountain torrent. In: *Hydrology in Mountainous Regions*. IAHS Publ. no. 193: 207-214.

Barta, A.F., P.R. Wilcock and C.C. Shea, 1993. Entrainment of gravel in steep streams. *EOS, Transactions, American Geophysical Union*, Supplement to Vol. 74(43), p. 311.

Bathurst, J.C., 1985. Flow resistance estimation in mountain rivers. *Journal of Hydraulic Engineering* 111(4): 625-643.

Bathurst, J.C., 1987. Critical conditions for bed material movement in steep, boulder-bed streams. In: *Erosion and Sedimentation in the Pacific Rim*. IAHS Publ. no. 165: 309-318.

Bathurst, J.C., 1988. Flow processes and data provision for channel flow models. In: *Modelling Geomorphological Systems*. M.G. Anderson (ed.), John Wiley and Sons, Chichester, p. 127-152.

Belke, D., 1974. Die statistische Analyse von Grundwasserständen mit dem Ziel der Extremwertprognose. [Statistical analysis of groundwater levels with the aim of extreme value prognosis.] *Technischer Bericht No. 13*, Institut für Hydraulik und Hydrologie der TH Darmstadt.

Berry, C.T., 1988. Cause of cross-sectional channel change in a gravel bed river at Squaw Creek, Montana. Thesis submitted as an integral part of a Master's degree in Geography with Social Anthropology at the University of St. Andrews, GB.

Billi, P., 1988. A note on cluster behavior in a gravel-bed river. *Catena* 15: 473-481.

Blalock, M.E. and T.W. Sturm, 1981. Minimum specific energy in compound open channels. *Journal of the Hydraulics Division*, ASCE, 107(HY6): 699-717.

Bollrich, G. and Autorenkollektiv, 1989. Technische Hydromechanik. Bd. 2, Spezielle Probleme. [Technical Hydromechanics. Vol. 2, Special Problems.] VEB Verlag für Bauwesen, Berlin.

Brayshaw, A.C.; L.E. Frostick and I. Reid, 1983. The hydrodynamics of particle clusters and sediment entrainment in coarse alluvial channels. *Sedimentology* 30: 137-143.

Brayshaw, A.C., 1985. Bed microtopography and entrainment thresholds in gravel-bed rivers. *Geological Society of America Bulletin* 96: 218-223.

Bugosh, N., 1988. Field verification of predictive bedload formulas in a coarse mountain stream. A thesis submitted in partial fulfillment of the requirements for the degree of Master of Science in Earth Sciences, Montana State University, Bozeman, USA.

Bugosh, N., and S.G. Custer, 1989. The effect of a log-jam burst on bedload transport and channel characteristics in a head-waters stream. In: *Proceedings of the Symposium on Headwaters Hydrology.* W.W. Woessner, and D.F. Potts (eds.), Missoula, MT, USA, p. 203-211.

Bunte, K. 1984. Wasser- und Feststoffhaushalt als Function der Morphologie des Vorfluters. [The Impact of stream morphology on water and sediment budget.] Unpublished thesis submitted for the degree of Master of Science to the Dept. of Physical Geography at the Freie Universität in Berlin, Germany, 190pp.

Bunte, K., 1990. Experiences and results from using a big-frame bed load sampler for coarse material bed load. In: *Hydrology in Mountainous Regions.* IAHS Publ. no. 193: 223-230.

Bunte, K., 1991. Bedload samples collected with the net-sampler at Squaw Creek in 1991: transport rates and grain-size distributions. Unpublished manuscript.

Bunte, K., 1992a. Particle number grain-size composition of bedload in a mountain stream. In: *Dynamics of Gravel Bed Rivers.* P. Billi, R.D. Hey, C.R. Thorne and P. Tacconi (eds.), John Wiley, Chichester, p. 55-72.

Bunte, K. 1992b. Discussion of Komar and Shih (1992): Equal grain mobility versus changing grain sizes in gravel-bed streams. In: *Dynamics of Gravel Bed Rivers.* P. Billi, R.D. Hey, C.R. Thorne and P. Tacconi (eds.), John Wiley, Chichester, p. 93-96.

Bunte, K. and P. Ergenzinger, 1989. New tracer techniques for particles in gravel bed rivers. *Bulletin de la Societé Geographique de Liège* 25: 85-90.

Bunte, K., S.G. Custer, P. Ergenzinger, and R. Spieker, 1987. Messung des Grobgeschiebetransportes mit der Magnettracertechnik. *Deutsche Gewässerkundliche Mitteilungen* 31 (2/3): 60-67.

Campbell, A.J. and R.C. Sidle, 1985. Bedload transport in a pool-riffle sequence of a coastal Alaska stream. *Water Resources Bulletin,* American Water Resources Association 21(4): 579-590.

Carey, W.P., 1985. Variability in measured bed-load-transport rates. *Water Resources Bulletin,* American Water Resources Association 21(1): 39-48.

Carey, W.P., and D.W. Hubbell, 1986. Probability distributions for bedload transport. In: *Proceedings of the Fourth Federal Interagency Sedimentation Conference,* Las Vegas, Nevada. Vol. I. Subcommittee on Sedimentation of the Interagency Advisory Committee on Water Data, p. 4.131-4.140.

Carling, P.A., 1983. Threshold of coarse sediment transport in broad and narrow natural streams. *Earth Surface Processes and Landforms* 8:1-18.

Carling. P.A., 1989. Hydrodynamic models of boulder berm deposition. *Geomorphology* 2: 319-340.

Carling, P.A. and M. Glaister, 1987. Rapid deposition of sand and gravel mixtures downstream of a negative step: the role of matrix infilling and particle overpassing in the process of bar-front accretion. *Journal of the Geological Society of London* 144: 543-551.

Carling, P.A. and M.A. Hurley, 1987. A time-varying stochastic model of the frequency and magnitude of bed load transport events in two small trout streams. In: *Sediment Transport in Gravel-Bed Rivers.* C.R. Thorne, J.C. Bathurst and R.D. Hey (eds.). John Wiley and Sons, New York, p. 897-919.

Carling, P.A., A. Kelsey and M.S. Glaister, 1992. Effect of bed roughness, particle shape and orientation on initial motion criteria. In: *Dynamics of Gravel Bed Rivers.* P. Billi, R.D. Hey, C.R. Thorne and P. Tacconi (eds.), John Wiley, Chichester, p. 23-36.

Carling, P.A., J.J. Williams, M.G. Glaister and H.G. Orr, 1993. Particle dynamics and gravel-bed adjustments. Final report of a project funded by the United States Army, European research office of the U.S. Army, London, Great Britain, contract no. DAJA45-90-C-0006, 47pp.

Chang, H.H., 1980. Geometry of gravel streams. *Journal of the Hydraulics Division,* ASCE, 106(HY9): 1443-1456.

Chang, H.H., 1987. Modelling fluvial processes in streams with gravel mining. In: *Sediment Transport in Gravel-Bed Rivers.* C.R. Thorne, J.C. Bathurst and R.D. Hey (eds.). John Wiley and Sons, New York, p. 977-987.

Chatfield, C., 1980. *The Analysis of Time Series.* Chapman and Hall, London.

Church, M., 1985. Bed load in gravel-bed rivers: observed phenomena and implications for

computation. In: *Proceedings of the Canadian Society for Civil Engineering Annual Conference, Saskatoon, Sk.*, p. 17-37.

Church, M., 1987. Discussion to Andrews and Parker (1987) "Formation of a coarse surface layer as the response to gravel mobility". In: *Sediment Transport in Gravel-Bed Rivers*. C.R. Thorne, J.C. Bathurst and R.D. Hey (eds.). John Wiley and Sons, New York, p. 314-322.

Church, M., D.G. McLean and J.F. Walcott, 1987. Bed load sampling and analysis. In: *Sediment Transport in Gravel-Bed Rivers*, C.R. Thorne, J.C. Bathurst and R.D. Hey (eds.), John Wiley and Sons, New York.

Clarke, R.T., 1990. Statistical characteristics of some estimators of sediment and nutrient loadings. *Water Resources Research* 26(9): 2229-2233.

Colosimo, C., V.A. Copertino and M. Veltri, 1988. Friction factor evaluation in gravel-bed rivers. *Journal of Hydraulic Engineering* 114(8): 861-876.

Custer, S.G., 1992. A review of natural-gravel-transport-detection experiments at Squaw Creek, Montana, 1981-1991. In: *Streams Above the Line. Channel Morphology and Flood Control*. Proceedings of the Corps of Engineers Workshop on Steep Streams. M.L. Pearson (ed.), U.S. Army Corps of Engineers Miscellaneous Paper Hl-94-4, p. 3.1-3.28.

Custer, S.G., K. Bunte, R. Spieker and P. Ergenzinger, 1986. Timing and location of coarse bedload transport: Squaw Creek, Montana. *EOS, Transactions, American Geophysical Union*, Vol. 67(44), p. 943.

Custer, S.G., P.E. Ergenzinger, N. Bugosh and B.C. Anderson, 1987. Electromagnetic detection of pebble transport in streams: a method for measurement of sediment transport waves. In: *Recent Developments in Fluvial Sedimentology*. F. Ethridge and R. Flores (eds.), Society of Paleontologists and Mineralogists Special Publication 39: 21-26.

D'Agostino, V., M.A. Lenzi and L. Marchi, 1994. Sediment transport and water discharge during high flows in an instrumented watershed. In: *Dynamics and Geomorphology of Mountain Rivers*. P. Ergenzinger and K.-H. Schmidt (eds.), Lecture Notes in Earth Sciences 52: 67-81, Springer Verlag, Berlin.

De Jong, C., 1993. Temporal and spatial interactions between river bed roughness, geometry, bedload transport and flow hydraulics in mountain streams - examples from Squaw Creek, Montana (USA) and Lainbach/Schmiedlaine, Upper Bavaria (Germany).

Ph.D. thesis submitted to the College of Earth Sciences at the Freie Universität Berlin, Germany, 180pp.

Dietrich, W.E., J.W. Kirchner, H. Ikeda, and F. Iseya, 1989. Sediment supply and the development of the coarse surface layer in gravel-bedload rivers. *Nature* 340: 215-217.

Dingman, S.L., 1984. *Fluvial Hydrology*. W.H. Freeman and Company, New York.

Dinehart, R.L., 1992. Evolution of coarse gravel bedforms: field measurements at flood stage. *Water Resources Research* 28(10): 2667-2689.

Dinehart, R.L., 1993. Data of sequential bedload measurements (Helley-Smith) from the North Fork of the Toutle River, 1989-1991. Pers. Communication 1993.

Du Boys, M.P., 1879. Études du regime et l'action excercée par les eaux sur le lit à font de gravieres indefinement affouilable. *Annals des Ponts et Chaussées*, Series 5(18): 141-195.

DVWK, 1988. Feststofftransport in Fließgewässern -Berechnungsverfahren für die Ingenieurspraxis. [Solid matter transport - Computation procedures for engineers.] *DVWK-Schriften* 87, Paul Parey, Hamburg.

Ehrenberger, R., 1931. Direkte Geschiebemessung an der Donau bei Wien und deren bisherige Ergebnisse. *Wasserwirtschaft* 34.

Einstein, H.A., 1937. Der Geschiebetrieb als Wahrscheinlichkeitsproblem. [Bedload transport as a probability problem]. *Mitteilungen der Versuchsanstallt für Wasserbau an der Eidgenössischen Technischen Hochschule in Zürich*.

Einstein, H.A., 1950. The bed-load function for sediment transportation in open channel flows. In: *U.S. Dept. of Agriculture, Soil Conservation Service*, Technical Bulletin 1026.

Emmett, W.W., 1980. A Field Calibration of the Sediment Trapping Characteristics of the Helley-Smith Bedload Sampler. *Geological Survey Professional Paper* 1139, Washington, DC.

Emmett, W.W., 1981. Measurement of bed load in rivers. In: *Erosion and Sediment Transport Measurements*, IAHS Publ. no. 133: 3-15.

Emmett, W.W., 1984. Measurement of bedload in rivers. In: *Erosion and Sediment Yield: Some Methods of Measurement and Modelling*. R.F. Hadley and D.E. Walling (eds.), Geo Books, Norwich, Great Britain, p. 91-109.

Emmett, W.W., L.B. Leopold, and R. M. Myrick, 1983. Some characteristics of fluvial processes in rivers. Proc. of the Advanced Seminar on Sedimentation, Aug. 15-19, 1983, Denver, CO. *U.S. Geological Survey Circular* 953.

EOS, 1989, July 25. Transactions of the American Geophysical Union, 70(30): 738.

Ergenzinger, P., 1965. Morphologische Untersuchungen im Einzugsgebiet der Ilz (Bayrischer Wald). [Morphological studies in the Ilz catchment, Bavarian Forest.] In: *Berliner Geographische Abhandlungen* no.2.

Ergenzinger, P., 1982. Über den Einsatz von Magnettracern zur Messung des Grobgeschiebetransportes. [Using magnetic tracers for measurements of coarse material bedload transport.] In: *Beiträge zur Geologie der Schweiz -Hydrologie* - 28(II): 483-491.

Ergenzinger, P., 1984. Bestimmung der Geschiebefracht mit Hilfe von ferromagnetischen Schottern. Endbericht zum DFG-Project Er 32/13-1 "Magnetschotter" [Determination of bedload using ferromagnetic gravels. Final report of the research project "Magnetic Pebbles" funded by the German Research Council, project no. Er 32/13-1.]

Ergenzinger, P., 1985. Messung der Geschiebebewegung und des Geschiebetransportes unter Naturbedingungen. [Measurement of bedload movement and bedload transport under natural conditions]. *Landschaftsökologisches Messen und Auswerten* 1(2/3): 141-157.

Ergenzinger, P., 1987. Chaos and order - the channel geometry of gravel bed braided streams. In: *Catena Suppl.* 10: 85-98.

Ergenzinger, P., 1992. River bed adjustments in a steep step-pool system: Lainbach, Upper Bavaria. In: *Dynamics of Gravel Bed Rivers*. P. Billi, R.D. Hey, C.R. Thorne and P. Tacconi (eds.), John Wiley, Chichester, p. 415-430.

Ergenzinger, P. and K. Bunte, 1989. Endbericht zum DFG Projekt ER 32/17-2 "Magnetgeschiebe". [Final report of the research project "Magnetic Tracer Technique" funded by the German Research Council, project number ER 32/17-2], 54pp.

Ergenzinger, P. and J. Conrady, 1982. A new tracer technique for measuring bedload in natural channels. *Catena* 9: 77-80.

Ergenzinger, P.J. and S.G. Custer, 1982. First experiences measuring coarse material bedload transport with a magnetic device. In: *Mechanics of Sediment Transport*. B.M. Sumer and A. Müller (eds.), Proceedings of Euromech 156, 223-227.

Ergenzinger, P.J. and S.G. Custer, 1983. Determination of bedload transport using naturally magnetic tracers: first experience at Squaw Creek, Gallatin County, Montana. *Water Resources Research* 19(1): 187-193.

Ergenzinger, P. and P. Stüve, 1989. Räumliche und zeitliche Variabilität der Fließwiderstände in einem Wildbach: Der Lainbach bei Benediktbeuren in Oberbayern. [Spatial and temporal variability of friction in a mountain torrent: the Lainbach near Benediktbeuren in Upper Bavaria.] In: *Göttinger Geographische Abhandlungen* 86: 61-79.

Ergenzinger, P., C. de Jong, and G. Christaller 1994. Interrelationships between bedload transfer and river bed adjustment in mountain rivers: an example from Squaw Creek, Montana. In: *Process Models and Theoretical Geomorphology*. M.J. Kirkby (ed.), John Wiley and Sons, New York, p. 141-158.

Ergenzinger, P., K. -H. Schmidt, and R. Busskamp, 1989. The pebble transmitter system (pets): first results of a technique for studying coarse material erosion, transport and deposition. *Zeitschrift für Geomorphologie N.F.* 33(4): 503-508.

Fenton, J.D and J.E. Abbott, 1977. Initial movement of grains on a stream bed: the effects of relative protrusion. *Proceedings of the Royal Society of London* A 352: 523-537.

Ferguson, R.I., K.L. Prestegaard and P.J. Ashworth, 1989. Influence of sand on hydraulics and gravel transport in a braided gravel-bed river. *Water Resources Research* 25(4): 635-643.

Folk, R.L. and W.C. Ward, 1957. Brazos River Bar: a study in the significance of grain size parameters. *Journal of Sedimentary Petrology* 27(1): 3-26.

Forrest, J. and N.R. Clarke, 1989. Characterizing grain-size distributions: evaluation of a new approach using a multivariate extension of entropy analysis. *Sedimentology* 36: 711-722.

Geiger, H., 1989. Die Wildbachverbauung - Vom Sperrenbau ehemals zur integralen Sanierung der Einzugsgebiete heute. [Mountain stream engineering: from former check dams to present integral watershed stabilization.] *Wasser und Boden* 41(8): 453-457.

Gellert, T.W, H. Kürstner, M. Hellwich and H. Kästner, 1970. *Mathematik*. [*Mathematics*.] VEB Bibliographisches Institut, Leipzig.

Gerthsen, C., H.O. Kneser and H. Vogel, 1974. *Physik*. [*Physics*.] Springer Verlag, Berlin.

Gintz, D., 1990. Die Messung der Grobgeschiebebewegung mit Hilfe von Eisen- und Magnettracern am Lainbach, Oberbayern. [Measurements of coarse bedload movements using iron- and magnetic tracers at the Lainbach, upper Bavaria.] M.S. thesis submitted to the Dept. of Physical Geography at the Freie Universität Berlin, Germany.

Gölz, E., 1990. Suspended sediment and bed load problems of the upper Rhine. *Catena* 17: 127-140.

Gölz, E., and B. Dröge, 1989. Zur morphologischen und sedimentologischen Charakeristik des Rheins. [Morphological and sedimentological characteristics of the Rhein]. *Deutsche Gewässerkundliche Mitteilungen* 33(3/4): 85-91.

Gomez, B., 1983. Temporal variations in bedload transport rates: the effect of progressive bed-armouring. *Earth Surface Processes and Landforms* 8: 41-54.

Gomez, B., W.W. Emmett, and D.W. Hubbell, 1991. Comments on sampling bedload in small rivers. In: *Proceedings of the Fifth Federal Interagency Sedimentation Conference, March 18-21, 1991, Las Vegas, NV.*, Subcommittee of the Interagency Advisory Committee on Water Data, p. 2.65-2.72.

Gomez, B., R.L. Naff, and D.W. Hubbell, 1989. Temporal variation in bedload transport rates associated with the migration of bedforms. *Earth Surface Processes and Landforms* 14: 135-156.

Graf, H.W., 1971. *Hydraulics of Sediment Transport*. McGraw-Hill, New York.

Gravel Bed Rivers, 1982. R.D. Hey, J.C. Bathurst, and C.R. Thorne (eds.), John Wiley, Chichester.

Griffith, G.A., 1981. Flow resistance in coarse gravel bed rivers. *Journal of the Hydraulics Division*, ASCE, 107(HY7): 899-918.

Hamamori, A., 1962. A theoretical investigation on the fluctuation of bed-load transport. *Hydraulics Laboratories Delft*, Report R4, Serie 2.

Hayward, J.A. and A.J. Sutherland, 1974. The Torlesse stream vertex-tube sediment trap. *Journal of Hydrology* (N.Z.) 13(1): 41-53.

Heathershaw, A.D., and P.D. Thorne, 1985. Seabed noises reveal role of turbulent bursting phenomenon in sediment transport by tidal currents. *Nature* 316: 339-342.

Herbich, J.B. and Schulits, 1964. Large-scale roughness in open-channel flow. *Journal of the Hydraulics Division*, ASCE, 90(HY6): 203-230.

Hey, R.D., 1979. Flow resistance in gravel-bed rivers. *Journal of the Hydraulics Division*, ASCE, 105(HY4): 365-379.

Hickin, E.J., 1983. River channel changes: retrospect and prospect. *Special Publications of the International Association of Sedimentology* 6:61-83.

Hjulström, F., 1935. Studies of the morphological activities of rivers as illustrated by the River Fyris. *Bulletin of the Geological Institute*, University of Uppsala 25: 221-527.

Hubbell, D.W., 1987. Bed load sampling and analysis. In: *Sediment Transport in Gravel-Bed Rivers*. C.R. Thorne, J.C. Bathurst and R.D. Hey (eds.), John Wiley, Chichester, p. 89-118.

Hubbell, D.W. and W.W. Sayre, 1964. Sand transport studies with radioactive tracers. *Journal of the Hydraulics Division*. Proceedings of the American Society of Civil Engineers, 90(HY3): 39-18.

Hubbell, D.W. and H.H. Stevens Jr., 1986. Factors affecting accuracy of bedload sampling. *Proceedings of the Fourth Federal Interagency Sedimentation Conference*, Las Vegas, Nevada. Vol. I. Subcommittee on Sedimentation of the Interagency Advisor Committee on Water Data, p. 4.20-4.29.

Hubbell, D.W., H.H. Stevens Jr., J.V. Skinner, and J.P. Beverage, 1987. Laboratory Data on Coarse-Sediment Transport for Bedload-Sampler Calibrations. *U.S. Geological Survey Water-Supply Paper* 2299: 1-31.

Ibbeken, H., 1974. A simple sieving and splitting device for field analysis of coarse grained sediments. *Journal of Sedimentary Petrology* 44(3): 939-946.

Ibbeken, H. and R. Schleyer, 1986. Photo sieving: a method for grainsize analysis of coarse-grained, unconsolidated bedding surfaces. *Earth Surface Processes and Landforms* 11: 59-77.

Ikeda, H. and F. Iseya, 1987. Thresholds in the mobility of sediment mixtures. In: *International Geomorphology*, Part I. V. Gardiner (ed.), John Wiley and Sons, Chichester, p. 561-570.

Iseya, F., and H. Ikeda, 1987. Pulsations in bedload transport rates induced by longitudinal sediment sorting: a flume study using sand and gravel mixtures. *Geografiska Annaler* 69A(1): 15-27.

Jackson, W.L. and R.L. Beschta, 1982. A model of two-phase bedload transport in an Oregon Coast Range stream. *Earth Surface Processes and Landforms* 7: 517-527.

James, C.S., 1990. Prediction of entrainment conditions of nonuniform, noncohesive sediments. *Journal of Hydraulic Research* 28(1): 25-41.

Karl, J., 1989. Erosionsschutz in den Alpen. [Erosion protection in the Alps.] *Wasser und Boden* 41(8): 463-466.

Karl, J., J. Mangelsdorf and K. Scheurmann, 1975. Der Geschiebehaushalt eines Wildbachsystems, dargestellt am Beispiel der oberen Ammer. [Bedload budget of a mountain stream: an example from the upper Ammer.] *Deutsche Gewässerkundliche Mitteilungen* 19(5): 121-132.

Klingeman, P.C. and W.W. Emmett, 1982. Gravel bedload transport processes. In: *Gravel Bed Rivers. Fluvial Processes, Engineering and Management*. R.D. Hey, J.C. Bathurst, and C.R. Thorne (eds.), John Wiley, Chichester, p. 141-179.

Knighton, A.D., 1983. Models of stream bed topography at the reach scale. *Journal of Hydrology* 60: 105-121.

Knighton, A.D., 1989. River adjustment to changes in sediment load: The effects of tin mining on the Ringarooma River, Tasmania, 1875-1984. *Earth Surface Processes and Landforms* 14: 333-359.

König, H. and Wolters, J., 1972. *Einführung in die Spektralanalyse ökonomischer Zeitreihen.* [Introduction to spectral analysis of economic time series.] Verlag Anton Hain, Meisenheim am Glan, Germany.

Komar, P.D., 1987. Selective entrainment by a current from a bed of mixed sizes: a reanalysis. *Journal of Sedimentary Petrology* 57(2): 203-211.

Komar, P.D., 1988. Sediment transport by floods. In: *Flood Geomorphology*. V.R. Baker, R.C. Kochel and P.C. Patton (eds.), p. 97-111.

Komar, P.D., 1989. Flow-competence evaluations of the hydraulic parameters of floods: an assessment of the technique. In: *Floods: Hydrological, Sedimentological and Geomorphological Implications*. K. Beven and P.A. Carling (eds.), John Wiley and Sons, Chichester, p. 107-134.

Komar, P.D., 1992. Discussion of Bunte (1992) " Particle number grain-size composition of bedload in a mountain stream". In: *Dynamics of Gravel Bed Rivers*. P. Billi, R.D. Hey, C.R. Thorne and P. Tacconi (eds.), John Wiley, Chichester, p. 69-71.

Komar, P.D. and Z. Li, 1986. Pivoting analysis of the selective entrainment of sediments by shape and size with application to gravel threshold. *Sedimentology* 33: 425-436.

Komar, P.D. and S.-M. Shih, 1992. Equal mobility versus changing bedload grain size in gravel-bed streams. In: *Dynamics of Gravel Bed Rivers*. R.D. Hey, J.C. Bathurst, and C.R. Thorne (eds.), John Wiley, Chichester, p.73-106..

Kuhnle, R.A., 1992. Fractional transport rates of bedload on Goodwin Creek. In: *Dynamics of Gravel Bed Rivers*. R.D. Hey, J.C. Bathurst, and C.R. Thorne (eds.), John Wiley, Chichester, p.141-155.

Kuhnle, R.A., 1993. Data of sequential measurements of bedload transport (Helley-Smith) at Goodwin Creek, 1984-1988. Pers. communication, 1993.

Kuhnle, R.A., and J.B. Southard, 1988. Bed load transport fluctuations in a gravel bed laboratory channel. *Water Resources Research* 25(2): 247-260.

Kuhnle, R.A., J.C. Willis, and A.J. Bowie, 1989. Variations in the transport of bed load sediment in a gravel-bed stream, Goodwin Creek, northern Mississippi, U.S.A. In: *Fourth International Symposium on River Sedimentation, Beijing, China*. p. 539-546.

Leeder, M.R., 1983. On the interaction between turbulent flow, sediment transport and bedform mechanics in channelized flow. In: *Special Publications of the International Association of Sedimentologists* 6: Modern and Ancient Fluvial Systems. J.D. Collinson and J. Lewin (eds.), Blackwell Scientific Publications, Oxford, GB.

Lenzi, M.A., L. Marchi and G.R. Scussel, 1990. Measurement of coarse sediment transport in a small Alpine stream. In: *Hydrology in Mountainous Regions,1*, IAHS Publ. no. 193: 223-230.

Leopold, L.B, M.G. Wolman and J. P. Miller, 1964. *Fluvial Processes in Geomorphology*. W.H. Freeman & Co., San Francisco, 522 pp.

Leopold, L.B. and W.W. Emmett, 1976. Bedload measurements, East Fork River, Wyoming. *Proceedings of the National Academy of Sciences, USA* 73(4): 1000-1004.

Leopold, L. B. and W.W. Emmett, 1977. 1976 bedload measurements, East Fork River, Wyoming. *Proceedings of the National Academy of Sciences, USA*, 74(7): 2644-2648.

Leopold, L.B., 1982. Water surface topography in river channels and implications for meander development. In: *Gravel Bed Rivers. Fluvial Processes, Engineering and Management*. R.D. Hey, J.C. Bathurst, and C.R. Thorne (eds.), John Wiley, Chichester, p. 359-387.

Lewin, J.L, 1979. Initiation of bed forms and meanders in coarse-grained sediment. *Geological Society of America Bulletin* 87: 281-285.

Lighthill, M.J. and Whitman, G.B., 1955. On kinematic waves. I: Flood movement in long rivers. *Proceedings of the Royal Society of London*, Series A, Mathematical and Physical Sciences 229(1178): 281-317.

Lisle, T.E., 1989. Sediment transport and resulting deposition in spawning gravels, north coastal California. *Water Resources Research* 25(6): 1303-1319.

Lisle, T.E., Data of sequential bedload measurements (Helley-Smith) from Prairie Creek, 1981. Pers. communication, 1993.

Macklin, M.G., 1989. Sediment transfer and transformation of an alluvial valley floor: the River

South Tyne, Northumbria, U.K. *Earth Surface Processes and Landforms* 14(3): 233-246.

McDowell, D.M., 1989. A general formula for estimation of the rate of transport of non-cohesive bed-load. *Journal of Hydraulic Research* 27(3): 355-361.

McLean, D.G. and B. Tassone, 1987. Discussion of Hubbell (1987) "Bed load sampling and analysis". In: *Sediment Transport in Gravel-Bed Rivers*. C.R. Thorne, J.C. Bathurst and R.D. Hey (eds.), John Wiley, Chichester, p. 109-113.

McMannis, W.J. and Chadwick, R.A., 1964. Geology of the Garnet Mountain quadrangle, Gallatin County, Montana. *Montana Bureau of Mines and Geology, Bulletin 43*, Butte, MT., 47pp.

Meyer-Peter, E. and R. Müller, 1948. Formulas for bed-load transport. In: *International Association of Hydraulic Research*, 2nd Meeting, Stockholm, p. 39-64.

Milhous, R., 1973. Sediment transport in a gravel-bottomed stream. Ph.D. thesis, Oregon State University, Corvallis, USA.

Milhous, R., 1982. Effect of sediment transport and flow regulation on the ecology of gravel-bed rivers. In: *Gravel Bed Rivers. Fluvial Processes, Engineering and Management*. R.D. Hey, J.C. Bathurst, and C.R. Thorne (eds.), John Wiley, Chichester, p. 819-841.

Monahan, S. and O'Rourke, E., 1982. An analysis of the variables influencing the measurements of coarse bedload movement at Squaw Creek. Independent Study submitted to Prof. Custer, Montana State University.

Montgomery, D.R. and J.M. Buffington, 1993. Channel classification, prediction of channel response, and assessment of channel condition. Report TFW-SH10-93-002 prepared for the SHAMW committee of the Washington State Timber/Fish/Wildlife Agreement, 107 pp.

Mühlhofer, L., 1933. Untersuchung über die Schwebstoff- und Geschiebeführung des Inn nächst Kirchbichl. [Investigation of suspended load and bedload in the river Inn near Kirchbichl]. *Die Wasserwirtschaft*: 1-6, 43pp.

Morisawa, M., 1968. *Streams. Their Dynamics and Morphology*. McGraw-Hill Book Company, New York, 175 pp.

Mosley, M.P. and D.S. Tindale, 1985. Sediment variability and bed material sampling in gravel bed rivers. *Earth Surface Processes and Landforms* 10: 465-482.

Naden, P., 1987a. An erosion criterion for gravel-bed rivers. In: *Earth Surface Processes and Landforms* 12: 83-93.

Naden, P., 1987b. Modeling gravel-bed topography from sediment transport. *Earth Surface Processes and Landforms* 12: 353-367.

Naden, P., 1988. Models of sediment transport in natural streams. In: *Modelling Geomorphological Systems*. M.G. Anderson (ed.), John Wiley, Chichester, p. 217-258.

Nanson, G.C., 1974. Bedload and suspended-load transport in a small, steep, mountain stream. *American Journal of Science* 274: 471-486.

Nouh, M., 1990. The self armoring process under unsteady flow conditions. *Earth Surface Processes and Landforms* 15: 357-364.

Ohde, R., B. Surholt and D. Glandt, 1990. Untersuchungen zum Einfluß wasserbaulicher Maßnahmen auf das Vorkommen substratgebundener Insektenlarven in einem Flachlandfluß des Sandmünsterlandes. [Studies on the effects of hydraulic engineering measures on the occurrence of interstitial insect larvae in a low-land river in the sandy part of the Münsterland (Germany).] *Wasser und Boden* 42(2): 86-100.

Parker, G. and P.C. Klingeman, 1982. On why gravel bed streams are paved. *Water Resources Research* 18(5): 1409-1423.

Parker, G., S. Dhamotharan and H. Stefan, 1982. Model experiments on mobile, paved gravel bed streams. *Water Resources Research* 18(5): 1395-1408.

Petit, F., 1987. The relationship between shear stress and the shaping of the bed of a pebble-loaded river, La Rulles - Ardennes. *Catena* 14: 453-468.

Petit, F., 1989. The evaluation of grain shear stress from experiments in a pebble bedded flume. *Earth Surface Processes and Landforms* 14: 499-508.

Petit, F., 1990. Evaluation of grain shear stress required to initiate movement of particles in natural rivers. *Earth Surface Processes and Landforms* 15: 135-148.

Pitlick, J.C., 1987. Discussion of "Bed load sampling and analysis" by D.W. Hubbell. In: *Sediment Transport in Gravel-bed Rivers*. C.R. Thorne, J.C. Bathurst, and R.D. Hey (eds.), John Wiley, Chichester, p. 106-108.

Pitlick, J.C. and C.R. Thorne, 1987. Sediment supply, movement and storage in an unstable gravel-bed river. In: *Sediment Transport in Gravel-Bed Rivers*. C.R. Thorne, J.C. Bathurst, and R.D. Hey (eds.), John Wiley, Chichester, p. 156-187.

Raudkivi, A.J., 1976. *Loose Boundary Hydraulics*. Pergamon Press, New York, 397 pp.

Rehfeld, G., 1990. Einsatz von Fangsteinen zur Erfassung und Bewertung der Makrozoobenthos Besiedlung in Fließgewässern. [Using gathering stones for registration and evaluation of the macro-zoobenthos population in streams.] *Wasser und Boden* 42(2): 100-102.

Reid, I. and L.E. Frostick, 1984. Particle interaction and its effects on the threshold of initial and final bedload motion in coarse alluvial channels. In: *Sedimentology of Gravels and Conglomerates*. E.H. Koster and L. Steel (eds.), Canadian Society of Petroleum Geology, Memoir 10: 61-88.

Reid, I. and L.E. Frostick, 1986. Dynamics of bedload transport in Turkey Brook, a coarse grained alluvial channel. *Earth Surface Processes and Landforms* 11: 143-155.

Reid, I., A.C. Brayshaw and L.E. Frostick, 1984. An electromagnetic device for automatic detection of bedload motion and its field application. *Sedimentology* 31: 269-276.

Reid, I., L.E. Frostick, J.T. Layman, 1985. The incidence and nature of bedload transport during flood flows in coarse-grained alluvial channels. *Earth Surface Processes and Landforms* 10: 33-44.

Richards, K., 1982. *Rivers. Form and Processes in Alluvial Channels.* Methuen, London, 358 pp.

Rickenmann, D., 1994. Bedload transport and discharge in the Erlenbach stream. In: *Dynamics and Geomorphology of Mountain Rivers*. P. Ergenzinger and K.-H. Schmidt (eds.). Lecture Notes in Earth Sciences 52: 53-66, Springer Verlag, Berlin.

Sayre, W.W. and D.W. Hubbell, 1965. Transport and dispersion of labeled bed material, North Loup River, Nebraska. *Geological Survey Professional Paper* 433-C, 48pp.

Scheurmann, K., 1989. Bekämpfung der Tiefenerosion geschiebeführender alpiner Fließgewässer durch Stauregelung. [Controlling depth erosion in bedload carrying alpine streams by check dams.] *Wasser und Boden* 41(8): 466-470.

Schlatte, H., 1984. Anwendung einer akustischen Geschiebemeßmethode an der Möll. [Application of an acoustic method to measure bedload transport at the river Möll]. In: *Beitrag zur XII. Konferenz der Donauländer über hydrologische Vorhersagen*, Bratislava, p. 4-5.1 - 4-5.9.

Schleyer, R., 1987. The goodness-of-fit to ideal Gauss and Rosin Distributions: a new grain-size parameter. *Journal of Sedimentary Petrology* 57(5): 871-880.

Schmidt, K. H., and P. Ergenzinger, 1990. Radiotracer und Magnettracer. Die Leistungen neuer Meßsysteme für die fluviale Dynamik. [Radio tracer and magnetic tracer: the accomplishments of new measuring systems in analyzing fluvial dynamics]. *Die Geowissenschaften* 8(4): 96-102.

Schmidt, K. H, and P. Ergenzinger, 1992. Bedload entrainment, travel lengths, step lengths, rest periods, studied with passive (iron, magnetic) and active (radio) tracer techniques. *Earth Surface Processes and Landforms* 17: 147-165.

Schmidt, K. H., D. Bley, R. Busskamp, and D. Gintz, 1989. Die Verwendung von Trübemessung, Eisentracern und Radiogeschieben bei der Erfassung des Feststofftransportes im Lainbach, Oberbayern. [Applying turbidity measurements, iron tracers and radio tracer to measure sediment transport at the Lainbach river in upper Bavaria]. *Göttinger Geographische Abhandlungen* 86: 123-135.

Schmidt, K. H., D. Bley, R. Busskamp, P. Ergenzinger and D. Gintz, 1992. Feststofftransport und Flußbettdynamik in Wildbachsystemen. Das Beispiel des Lainbachs in Oberbayern. [Sediment transport and channel dynamics in mountain torrents. The example of the Lainbach in upper Bavaria]. *Die Erde* 123: 17-28.

Schoklitsch, A., 1934. Geschiebetrieb und die Geschiebefracht. [Bedload and bedload transport rates.] *Wasserkraft und Wasserwirtschaft* 39(4): 1-7.

Schoklitsch, A., 1962. *Handbuch des Wasserbaus.* [Handbook of Hydraulic Engineering.]. Springer Verlag, Wien.

Sediment Transport in Gravel-bed Rivers, 1987. C.R. Thorne, J.C. Bathurst, and R.D. Hey (eds.), John Wiley, Chichester.

Shen, H.W. and R.M. Li, 1973. Analysis of resistance over staggered roughness. *Journal of the Hydraulics Division*, ASCE, 99(HY11): 2169-2174.

Shen, H.W., 1975. Hans A. Einstein's contribution in sedimentation. *Journal of the Hydraulics Division*, ASCE, 101(HY5): 469-488.

Shields, A., 1936. Anwendung der Ähnlichkeitsmechanik und der Turbulenzforschung auf die Geschiebebewegung. [Application of similarity principles and turbulence research to bedload movement]. *Mitteilungen der Preußischen Versuchsanstalt für Wasser- und Schiffbau, Berlin,* Vol. 26, 26 pp.

Shih, S.-M. and P.D. Komar, 1990a. Hydraulic controls of grain-size distributions of gravels in

Oak Creek, Oregon, USA. *Sedimentology* 37: 367-376.

Shih, S.-M. and P.D. Komar, 1990b. Differential bedload transport rates in a gravel-bed stream: a grain-size distribution approach. *Earth Surface Processes and Landforms* 15: 539-552.

Spieker, R., 1988. Entwicklung, Aufbau und Geländeerprobung einer Meßeinrichtung zur Registrierung von Reisegeschwindigkeit und Korngröße natürlicher Grobgeschiebe während der Transportphase. [Development, construction and field testing of a measuring device to register transport velocities and grain sizes of natural coarse bedload during transport]. Thesis submitted to the Dept. of Physical Geography of the Freie Universität Berlin, Germany, in partial fulfillment of the requirements of a M.S. degree.

Spieker, R. and P. Ergenzinger, 1990. New developments in measuring bedload by the magnetic tracer technique. In: *Erosion, Transport and Deposition Processes*, IAHS Publ. no. 189: 171-180.

Stelczer, K., 1981. *Bed-load Transport. Theory and Practice.* Water Resources Publication, Littleton, CO.

Sutherland, A.J., 1987. Static armor layers by selective erosion. In: *Sediment Transport in Gravel-Bed Rivers.* C.R. Thorne, J.C. Bathurst, and R.D. Hey (eds.), John Wiley, Chichester, p. 243-267.

Tacconi, P. and P. Billi, 1987. Bed load transport measurement by a vortex-tube trap on Virginio Creek, Italy. In: *Sediment Transport in Gravel-Bed Rivers.* C.R. Thorne, J.C. Bathurst, and R.D. Hey (eds.), John Wiley, Chichester, p. 583-616.

Vollmers, H.-J., 1989a. Die Möglichkeiten der wasserbaulichen Versuchstechnik. [Possibilities offered by the techniques of hydraulic physical modeling.] 4. Fortbildungslehrgang für technische Hydraulik: Berechnung des Feststofftransportes für die Ingenieurpraxis. München, Neubiberg, April 19-21, 1989.

Vollmers, H.-J., 1989b. The state of art of physical modelling. In: *Sediment Transport Modeling.* S.S.Y. Wang (ed.). American Society of Civil Engineers, New York, p. 7-12.

White, W.R. and T.J. Day, 1982. Transport of graded gravel bed material. In: *Gravel Bed Rivers. Fluvial Processes, Engineering and Manage-*ment. R.D. Hey, J.C. Bathurst, and C.R. Thorne (eds.), John Wiley, Chichester, p. 181-223.

Wiberg, P.L. and J.D. Smith, 1987. Initial motion of coarse sediment in streams of high gradient. In: *Erosion and Sedimentation in the Pacific Rim.* IAHS Publ. no. 165: 299-308.

Wilcock, P.R., 1988. Methods for estimating the critical shear stress of individual fractions in mixed-sized sediment. *Water Resources Research* 24(7): 1127-1135.

Wilcock, P.R. and J.B. Southard, 1989. Bed load transport of mixed size sediment: fractional transport rates, bed forms, and the development of a coarse bed surface layer. *Water Resources Research* 25: 1629-1641.

Wilcock, P.R., 1992. Experimental investigation of the effect of mixture properties on transport dynamics. In: *Dynamics of Gravel Bed Rivers.* R.D. Hey, J.C. Bathurst, and C.R. Thorne (eds.), John Wiley, Chichester, p.109-139.

Whiting, P.J., W.E. Dietrich, L.B. Leopold, T.G. Drake, and R.L. Shreve, 1988. Bedload sheets in heterogeneous sediment. *Nature* 16: 105-108.

Williams, J.J., P.D. Thorne, and A.D. Heathershaw, 1989a. Measurements of turbulence in a benthic boundary layer over a gravel bed. *Sedimentology* 36: 959-971.

Williams, J.J., P.D. Thorne, and A.D. Heathershaw, 1989b. Comparison between acoustic measurements and predictions of the bedload transport of marine gravels. *Sedimentology* 36: 973-979.

Williams, J.J., G.R. Butterfield, and D.G. Clark, 1990. Aerodynamic entrainment thresholds and dislodgement rates on impervious and permeable beds. *Earth Surface Processes and Landforms* 15: 255-264.

Yang, C.T., 1973. Formation of riffles and pools. *Water Resources Research* 7(6): 1567-1574.

Yang, C.T., C.S. Song and M.J. Woldenberg, 1981. Hydraulic geometry and minimum of energy dissipation. *Water Resources Research* 17(4): 1014-1018.

Yevjevich, V., 1972. *Stochastic Processes in Hydrology.* Water Resources Publications, Ft. Collins, CO.

Zanke, U., 1982. *Grundlagen der Sedimentbewegung.* [*The Basics of Sediment Movement.*] Springer Verlag, Berlin.

Zanke, U., 1990. Der Beginn der Sedimentbewegung als Wahrscheinlichkeitsproblem. [Initial sediment motion as a probability problem.] *Wasser und Boden* 1:40-43.

8. Appendix

Table 2. Squaw Creek 1986: discharge, total bedload transport rates, and fractional bedload transport rates for 3 grain size classes (sand, small gravels, and medium gravels) sampled with the Helley-Smith sampler.

Date	Time	No.	Q+ m³/s	Qb# g/m s	Sand (.25-1)* g/m·s	Gravels (2-16) g/m·s	Gravels (22-63) g/m·s
5-26	20:08-20:25	1	4.66	4.10	3.83	0.27	0.00
"	23:10-23:35	2	5.10	6.15	3.69	2.46	0.00
5-27	21:50-22:15	3	6.20	5.07	3.48	0.10	1.49
5-28	1:30-1:55	4	6.04	31.07	7.79	18.78	4.55
"	20:00-20:40	5	6.11	20.31	10.21	7.02	3.08
"	22:10-22:30	6	6.18	4.57	4.26	0.31	0.00
"	23:29-23:50	7	6.05	7.49	6.01	1.18	0.30
5-29	22:15-22:55	8	6.11	11.62	5.22	2.70	3.70
5-30	19:55-20:40	9	6.05	18.58	5.41	4.04	9.13
"	23:33-23:56	10	6.03	30.89	5.25	6.28	19.36
5-31	13:13-13:40	11	5.65	1.93	1.52	0.41	0.00
"	18:50-19:15	12	6.03	9.38	3.66	2.69	3.03
6- 2	9:50-10:15	13	5.51	2.06	1.35	0.71	0.00
"	19:05-20:05	14	5.99	5.74	3.01	0.72	2.01
6- 3	9:20- 9:45	15	5.33	4.27	1.81	1.49	0.97
6- 4	18:45-19:15	16	5.06	0.94	0.69	0.25	0.00
6- 6	17:15-17:35	17	5.57	4.89	2.08	1.10	1.71

+Discharge; #Total bedload transport rates; *Grain-size range in mm

Table 3a. Bedload samples from the net-sampler (1988): percentiles and grain-size parameters according to Folk and Ward (1957).

Date	Time	No.	φ95	φ84	φ75	φ50	φ25	φ16	φ5	D_{max} φ	sort* (Folk & Ward)	skew*	Qb# g/s·m	Q+ m³/s
5-20	18:53-19:05	3	-5.65	-5.53	-5.43	-5.04	-4.52	-4.37	-3.97	-5.5	0.54	0.21	1.18	4.74
5-22	21:01-21:30	4	-5.72	-5.62	-5.58	-5.30	-4.63	-4.26	-3.60	-5.5	0.66	0.57	0.43	4.92
5-23	19:43-20:45	5	-5.73	-5.60	-5.55	-5.13	-4.68	-4.15	-3.65	-5.5	0.68	0.39	0.29	5.00
"	21:05-22:05	6	-6.18	-6.07	-6.01	-5.42	-4.90	-4.52	-3.86	-6.0	0.74	0.25	1.47	5.09
"	22:32-00:00	7	-6.58	-6.05	-5.85	-5.50	-5.05	-4.80	-4.30	-6.5	0.66	0.07	6.80	5.26
5-24	00:50- 1:22	8	-6.58	-6.32	-6.15	-5.73	-5.15	-4.86	-4.29	-6.5	0.71	0.22	2.31	5.17
"	1:48- 2:37	9	-6.60	-6.42	-6.17	-5.66	-5.18	-4.93	-4.87	-6.5	0.73	0.09	9.25	5.17
"	19:53-20:05	10	-5.67	-5.56	-5.52	-4.91	-4.26	-3.95	-3.61	-5.5	0.71	0.23	8.10	5.66
"	22:18-22:34	11	-7.05	-6.32	-5.95	-5.43	-4.91	-4.65	-4.04	-7.0	0.87	0.07	41.7	5.73
5-25	1:15- 1:25	12	-7.08	-6.46	-6.16	-5.61	-5.11	-4.85	-4.29	-7.0	0.83	-0.05	50.5	5.73
"	2:54- 2:59	13	-6.65	-6.53	-6.44	-6.05	-5.34	-5.06	-4.52	-6.5	0.69	0.39	11.9	5.66
"	4:58- 5:04	14	-6.57	-6.19	-5.93	-5.58	-5.15	-4.91	-4.35	-6.5	0.66	0.08	45.2	5.66
"	7:14- 7:19	15	-5.58	-5.23	-4.95	-4.63	-4.18	-3.95	-3.47	-5.5	0.64	0.07	3.25	5.58
"	9:04- 9:09	16	-7.11	-6.83	-6.44	-5.58	-4.95	-4.60	-3.97	-7.0	1.03	-0.05	72.2	5.58
5-29	21:44-21:54	17	-6.43	-6.05	-5.86	-5.83	-4.40	-3.95	-3.64	-6.5	0.95	0.30	21.4	5.42
5-30	1:16 -1:32	18	-6.32	-6.08	-5.86	-5.34	-4.86	-4.58	-4.10	-6.5	0.71	0.07	28.2	5.26
"	15:04-15:09	19	-6.72	-6.22	-5.93	-5.47	-4.93	-4.68	-4.17	-7.0	0.77	0.02	187	5.58
5-31	18:44-18:54	20	-4.79	-4.78	-4.68	-4.60	-4.52	-4.25	-3.58	-4.5	0.30	0.58	0.15	4.47
6-1	11:10-11:38	21	-4.25	-4.17	-4.12	-4.02	-3.89	-3.80	-3.63	-4.0	0.18	0.19	0.04	4.29
"	22:36-23:07	22	-4.70	-4.60	-4.55	-4.42	-4.25	-4.17	-4.02	-4.5	0.21	0.27	0.04	4.29
6-5	21:40-21:58	23	-5.60	-5.44	-5.23	-4.75	-4.27	-4.07	-3.75	-5.5	0.62	0.04	1.36	5.17
6-7	15:31-15:57	24	-5.72	-5.62	-5.58	-5.48	-4.93	-4.63	-4.21	-5.5	0.48	0.70	0.72	4.29
6-8	17:36-17:58	25	-5.26	-5.18	-5.15	-5.06	-4.83	-4.58	-4.25	-5.0	0.30	0.60	0.26	3.90
	gravel bar		-7.60	-6.85	-6.30	-5.40	-4.40	-3.94	-3.00	-7.5	1.42	0.02	-	-
	channel bed		-7.89	-7.68	-7.57	-7.21	-6.45	-5.65	-3.97	-7.5	1.10	0.60	-	-

*+ Discharge; # Total bedload transport rates; * Sorting and skewness according to Folk and Ward (1957)*

Table 3b[1]. Particle transport rates (number of particles transported per meter width and minute), calculated for bedload samples from the net-sampler, 1988.

Date	Time	No.	11-16	16-22	22-32	32-45	45-64	64-90	90-125	125-180	Qb[#] g/s·m	Q[+] m³/s
					Grain-size classes (mm)							
5-20	18:53-19:05	3	0.912	0.927	0.479	0.240	0.062	-	-	-	1.18	4.74
5-22	21:01-21:30	4	0.479	0.181	0.121	0.058	0.043	-	-	-	0.43	4.92
5-23	19:43-20:45	5	0.397	0.090	0.128	0.029	0.026	-	-	-	0.29	5.00
"	21:05-22:05	6	1.163	0.520	0.318	0.253	0.068	0.034	-	-	1.47	5.09
"	22:32-00:00	7	1.748	1.998	1.709	1.182	0.521	0.055	0.025	-	6.80	5.26
5-24	00:50- 1:22	8	0.727	0.521	0.533	0.260	0.149	0.051	0.018	-	2.31	5.17
"	1:48- 2:37	9	3.112	1.856	1.728	1.381	0.568	0.150	0.590	-	9.25	5.17
"	19:53-20:05	10	14.987	6.168	2.848	1.206	0.435	-	-	-	8.10	5.66
"	22:18-22:34	11	22.224	14.089	11.232	6.704	2.338	0.416	0.101	0.059	41.7	5.73
5-25	1:15- 1:25	12	14.907	12.674	10.763	7.496	2.745	0.707	0.125	0.096	50.5	5.73
"	2:54- 2:59	13	1.505	1.451	1.659	1.064	0.345	0.261	0.101	-	11.9	5.66
"	4:58- 5:04	14	12.195	9.272	9.190	7.607	3.620	0.516	0.171	-	45.2	5.66
"	7:14- 7:19	15	5.334	3.386	2.151	0.214	0.089	-	-	-	3.25	5.58
"	9:04- 9:09	16	48.960	24.816	15.949	9.363	3.215	0.668	0.373	0.184	72.2	5.58
5-29	21:44-21:54	17	40.481	9.433	4.876	1.712	1.436	0.281	0.038	-	21.4	5.42
5-30	1:16 -1:32	18	13.078	12.336	8.418	5.283	1.290	0.465	0.025	-	28.2	5.26
"	15:04-15:09	19	60.311	68.160	55.465	28.609	11.511	1.988	0.743	0.061	187	5.58
5-31	18:44-18:54	20	0.205	0.073	0.204	-	-	-	-	-	0.15	4.47
6-1	11:10-11:38	21	0.184	0.092	-	-	-	-	-	-	0.04	4.29
"	22:36-23:07	22	0.022	0.094	0.024	-	-	-	-	-	0.04	4.29
6-5	21:40-21:58	23	2.051	1.156	0.785	0.182	0.046	-	-	-	1.36	5.17
6-7	15:31-15:57	24	0.189	0.344	0.172	0.109	0.081	-	-	-	0.72	4.29
6-8	17:36-17:58	25	0.037	0.132	0.108	0.108	-	-	-	-	0.26	3.90

+ Discharge; # Total bedload transport rates;

---

[1] *Table was added as a supplement during translation.*

Rocky Mountains

Southwest

Great Plains

U.S. Department of Agriculture
Forest Service

Rocky Mountain Forest and Range Experiment Station

The Rocky Mountain Station is one of seven regional experiment stations, plus the Forest Products Laboratory and the Washington Office Staff, that make up the Forest Service research organization.

RESEARCH FOCUS

Research programs at the Rocky Mountain Station are coordinated with area universities and with other institutions. Many studies are conducted on a cooperative basis to accelerate solutions to problems involving range, water, wildlife and fish habitat, human and community development, timber, recreation, protection, and multiresource evaluation.

RESEARCH LOCATIONS

Research Work Units of the Rocky Mountain Station are operated in cooperation with universities in the following cities:

Albuquerque, New Mexico
Flagstaff, Arizona
Fort Collins, Colorado*
Laramie, Wyoming
Lincoln, Nebraska
Rapid City, South Dakota

*Station Headquarters: 240 W. Prospect Rd., Fort Collins, CO 80526